Title
Maximum Fuel Utilization in Advanced Fast Reactors without Actinides Separation

Author
Heidet, Florent

Publication Date
2010

Peer reviewed|Thesis/dissertation

Maximum Fuel Utilization in Advanced Fast Reactors without Actinides Separation

By

Florent Heidet

A dissertation submitted in partial satisfaction of the

requirements for the degree of

Doctor of Philosophy

in

Engineering – Nuclear Engineering

in the

Graduate Division

of the

University of California, Berkeley

Committee in charge:

Professor Ehud Greenspan, Chair
Professor Brian Wirth
Professor Alice Agogino

Fall 2010

Maximum Fuel Utilization in Advanced Fast Reactors without Actinides Separation

Abstract

Maximum Fuel Utilization in Advanced Fast Reactors
without Actinides Separation

by

Florent Heidet

Doctor in Philosophy in Engineering – Nuclear Engineering

University of California, Berkeley

Professor Ehud Greenspan, Chair

The primary objective of this study was to estimate the maximum fuel utilization that is achievable using fast reactors that are designed to operate with fuel reconditioning when the fuel reaches its radiation damage constraint. The primary functions of the fuel reconditioning are to relieve the pressure of the gaseous fission products, replace the clad and reduce radiation induced defects in the fuel. That is, the fuel recycling processes considered cannot be used for the separation of actinides from most of the fission products and to extract plutonium or any other actinide from the fuel. Hence, these recycling processes are highly proliferation resistant and, hopefully, less expensive than processes traditionally considered for used fuel recycling. With the fuel reconditioning recycling, the maximum discharge burnup is dictated by the reactivity of the fuel and is not limited by the material damage constraints. A couple of fuel management strategies were examined: the conventional multi-batch fuel management and a breed-and-burn mode of operation. The two recycling processes examined are an AIROX-like process and the melt-refining process.

It is found that using fuel reconditioning it is possible to increase the fuel utilization by up to one order of magnitude with the conventional mode of operation and by two orders of magnitude using the breed and burn (B&B) mode of operation, relative to that achievable in once-trough LWRs. The conventional mode of operation, in which the fast reactor is constantly fed with enriched fuel, enables to achieve a discharge burnup ranging from 52.4% FIMA for a medium size 1200 MW_{th} fast reactor to 65.3% FIMA for a large 3000 MW_{th} fast reactor. With the innovative breed and burn mode of operation only depleted uranium is required for the fuel feed with the exception of the fissile fuel required for establishing the initial criticality. The achievable burnup is up to 57% FIMA in a 3000 MW_{th} B&B reactor and up to 44% FIMA in a 1200 MW_{th} B&B reactor. In order to sustain the breed and burn mode of operation it is necessary to accumulate in the depleted uranium feed an average burnup of at least 20% FIMA, when using metallic uranium fuel alloyed with 10 weight % zirconium in a tight-lattice core.

By discharging the fuel at this minimum required burnup and loading it, after reconditioning, into a new reactor along with fresh depleted uranium, it is possible to spawn additional B&B reactors without need for any additional fissile fuel. With this spawning mode of operation the achievable B&B reactor capacity growth rate is 3.85% per year, without need for uranium enrichment capability or actinides separation capability. The energy value of the depleted uranium currently accumulated in the USA, when used in the proposed breed-and-burn

fast reactors, is equivalent to at least seven centuries of the total 2009 USA supply of electricity, all sources included. Relative to LWR operating with the once-through fuel cycle, the fuel discharged from the B&B fast reactors at ~57% FIMA features, per unit of electricity generated: (a) ~40% the amount of TRU and Pu; (b) ~10% the inventory of ^{237}Np and its precursors; (c) ~12% of the decay heat from TRU; (d) ~28% of the radiotoxicity; (e) ~7% the neutron emission rate; the latter three are measured one year following discharge. The fraction of the fissile isotopes in the discharged plutonium is comparable but the decay heat and neutron emission rate per unit mass of discharged plutonium are nearly half as large.

The proposed modes of operation are expected to improve the economics and the proliferation resistance and, hence, may justify sooner deployment of fast reactors. The deployment of the suggested fast reactor system will constitute a significant step forward towards sustainable nuclear energy. However, technologies for fuel reconditioning need be developed and their economic viability need be established.

Table of Contents

List of figures

List of tables

List of symbols

Symbol	Meaning
ABR	Advanced Burner Reactor
AFCI	Advanced Fuel Cycle Initiative
ANL	Argonne National Laboratory
ASTRID	Advanced Sodium Technological Reactor for Industrial Demonstration
B&B	Breed and Burn
BNL	Brookhaven National Laboratory
BOEC	Beginning of Equilibrium Cycle
BOL	Beginning of Life
BU	Burnup
CEA	French Nuclear Agency (Commissariat a l'Energie Atomique)
DPA	Displacement Per Atom
EFPY	Effective Full Power Year
EM2	Energy Multiplier Module
ENHS	Encapsulated Nuclear Heat Source
EOC	End of Cycle
EOEC	End of Equilibrium Cycle
EOL	End of Life
EU	Enriched Uranium
FCC	Face Centered Cubic
FCMI	Fuel Cladding Mechanical Interaction
FIMA	Fission per Initial – heavy – Metal Atom
FP	Fission Product
GA	General Atomics
GE	General Electric
GEM	Gas Expansion Module
GFR	Gas-cooled Fast Reactor
HEU	High Enriched Uranium
HM	Heavy Metal
IMOCUP	Improved MCNP-ORIGEN2 Coupled Utility Program
INL	Idaho National Laboratory
k_{eff}	Effective multiplication factor

k_∞	Infinite multiplication factor
LANL	Los Alamos National Laboratory
LBE	Lead Bismuth Eutectic
LFR	Lead-cooled Fast Reactor
LWR	Light Water Reactor
MIT	Massachusetts Institute of Technology
MOCUP	MCNP-ORIGEN2 Coupled Utility Program
MOX	Mixed Oxide Fuel
NPP	Nuclear Power Plant
ODS	Oxide Dispersion Strengthened
OT	Once-Trough
P/D	Pitch to Diameter
SFR	Sodium-cooled Fast Reactor
SMA	Simple Moving Average
SWU	Separative Work Unit
TRU	Transuranics (Transuranium)
TWR	Traveling Wave Reactor
UN	Uranium Nitride
UNF	Used Nuclear Fuel
ULLR	Ultra Long Life Reactor

Acknowledgements

First and foremost I would like to express my deepest gratitude to Professor Ehud Greenspan, my advisor, for his guidance, help and support. I have benefited greatly from his tremendous knowledge and his insightful advices. I am also very thankful to Professor Brian Wirth for always being available to discuss and help me with the material related issues. Furthermore, I would like to acknowledge Doctors Massimiliano Fratoni and Francesco Ganda for their assistance getting me started with the various neutronics software I have been using throughout my work. I greatly benefited from their previous experience and the discussions we had together. I also would like to extend my sincere thanks to Lisa Zemelman, the Graduate Student Affairs Officer of the nuclear engineering department. She greatly helped me handling all the administrative matters, and always came up with a solution when the situation was complicated and uncertain. Finally, it has been a pleasure to be a graduate student in the department of nuclear engineering at UC Berkeley. It provided me with a motivating and friendly environment where I learnt greatly from both the Professors and other students. Last but not least, I would like to thank TerraPower LLC and its CEO, Dr. John Gilleland, for providing me most valuable and highly appreciated financial support as well as the DOE NEUP financial support during the last year of my Ph.D. work.

Chapter 1

Introduction

Over the past few years, production and distribution of energy has been a rising concern all over the world. Energy can be seen as one of the most fundamental needs of mankind since it enables producing electricity, drinkable water – by desalinating sea water, heat, goods, communication…It became so important that securing access to a sustainable and affordable source of energy is one of the main stakes of this century. Furthermore, due to growing concerns about global warming, many countries around the world have already or are currently proposing taxes on carbon emissions. Carbon-free sources of energy are becoming particularly attractive: even when including the carbon emission due to the construction of a nuclear power plant (NPP), nuclear energy is second to hydro-electric energy as the cleanest source of energy. In term of cost, disregarding a possible carbon tax, nuclear energy is second to coal as the cheapest source of energy. A recent IEA/NEA joint study [1] concluded that with a carbon tax of $30 per ton of CO_2 and with a financing cost of 5%, nuclear energy is the most competitive solution. In addition, the abundance of uranium and thorium resources, the extended experience in operating NPP, and the potential for achieving very large electrical generation capacity makes nuclear energy one of the main options for the upcoming centuries.

As of 2008, the installed nuclear energy capacity in the world is 372 GWe [2], out of which 100 GWe are generated in the United States [3]. This represents 17.2% of the world electricity production. According to a scenario developed by the International Institute for Applied System Analysis [4], the average annual growth rate from now to 2100 is forecasted to be 2.8% for the nuclear energy capacity, while the total energy growth rate is forecasted to be only 2%, as shown in Figure 1.1. In order to meet such a growth rate without dramatically depleting the mineable uranium resources and without producing excessive amount of radioactive waste, it is essential to develop a NPP and associated fuel cycle enabling extracting a significantly larger fraction of the energy content of the uranium ore than presently achieved. Most of the currently deployed commercial NPP are light water reactors (LWR) operating with enriched uranium at an average burnup of 50 GWd/tHM – i.e. 50 giga-watts-day per ton of heavy metal. Only 0.6% of the energy content of the natural uranium mined is extracted: 88% of uranium mined is left over as the tailings of the enrichment process that is not suitable for use in LWR, and 95% of the energy contained in the fuel loaded in the LWRs – the remaining 12% – is left in the used nuclear fuel (UNF) – the fuel discharged from the LWR. It is estimated that by

2009 approximately 570000 tons of depleted uranium were accumulated in the United States [5] and more than 1.5 million tons accumulated around the world [6].

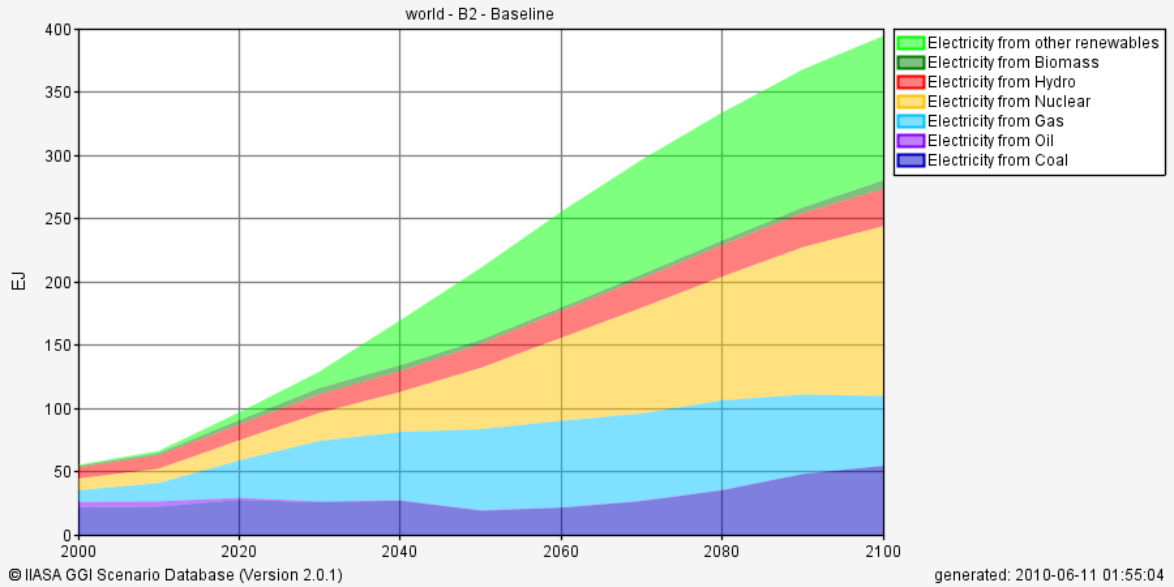

Figure 1.1: IIASA scenario energy growth rate [4]

Another challenge to be overcome to ensure a sustainable nuclear economy is the UNF management. The fuel is discharged from the NPP with a high level of radiotoxicity but also with a high energetic value. The two main options regarding the back end of the fuel cycle are the geological disposal of the UNF coming out from the once-through fuel cycle, and the recycling of the UNF. The present US administration cancelled the Yucca Mountain nuclear waste repository project and is assessing the feasibility of different UNF management options. Although no country has implemented geological disposal, mostly because of public acceptance, there is a scientific consensus that it is technically feasible. On the other hand, fuel reprocessing has been successfully used in several countries including France, Japan, United Kingdom and Russia, but the actinide separation process raises proliferation concerns. When chemically reprocessing the UNF, it is possible to extract plutonium that can be used to make nuclear weapons. It had been estimated [7, 8] that in 2010 there would be 560 tons of plutonium contained in the UNF in the United States, and more than 2100 tons in the world.

The development of Generation IV fast reactors can make a step forward toward improving uranium ore utilization while mitigating the nuclear waste issue. It is possible to use all the LWR UNF heavy metals (HM) as fuel for those fast reactors and greatly improve the waste characteristics while extracting additional energy. The Advanced Fuel Cycle Initiative (AFCI) program is part of the U.S. Department of Energy effort toward developing advanced fuel cycles that will enable reclaiming more energy from the UNF and decreasing the amount of nuclear waste to be disposed of.

1.1 Traditional fast reactor systems

The attractiveness of fast reactors over LWRs is because they have more excess neutrons beyond those required for maintaining the chain reaction. In fast reactors, neutrons are not moderated and about 60% of them have energy above 100 keV. For most of the heavy metal isotopes, the ratio between the fission cross-section and the capture cross-section is larger in a fast spectrum than in a thermal spectrum. In addition, the fast fission probability in ^{238}U is significantly larger in a fast than in a thermal spectrum. Furthermore, the average number of neutrons produced per fission is significantly larger when the fission is induced by a fast neutron than by a thermal neutron. Also, the ratio between the absorption cross-section of fission products and the absorption cross-section of heavy metal is smaller in a fast spectrum. All of these differences result in a larger number of excess neutrons available per fission in the fast spectrum core. These excess neutrons can be used to design the core to breed more fissile fuel than consumed, to extend the fuel burnup and to transmute nuclear waste. However, due to the lower fission cross-section, the initial fuel enrichment has to be more than twice the LWR fuel enrichment, and the core neutron flux amplitude is about two orders of magnitude larger than in LWR.

The first fast rector was built in the United States in 1948, a few years after the Chicago pile. Since then, only two commercial fast reactors, Super-Phenix and BN-600, have been built and operated. During the last 20 years most of the fast reactor programs have been stopped but due to the waste and resources consideration, most of those programs have been resumed. India, China and Russia recently announced plans to start the construction of several fast reactors in the next few years.

Out of the six core concepts selected for the Generation IV reactors, three, shown in Figure 1.2, are fast reactors: gas-cooled fast reactor (GFR), sodium-cooled fast reactor (SFR) and lead-cooled fast reactor (LFR). Fast reactors are compatible with a large variety of coolants, materials and type of fuels. Liquid metals are the coolants of choice for most of the fast reactors [9] due to their relatively high atomic mass, very large heat capacity, and low vapor pressure. All liquid metal coolants are opaque and make the fuel handling and maintenance more challenging. In addition, lead and sodium are not liquid at room temperature, requiring a heating system to keep the coolant liquid during reactor shutdown. On the other hand, gases such as helium or CO_2 can be used for the coolant but they have a very low heat capacity, requiring operation at very high pressure and flow rate and making it very challenging to come up with a safe economical viable design.

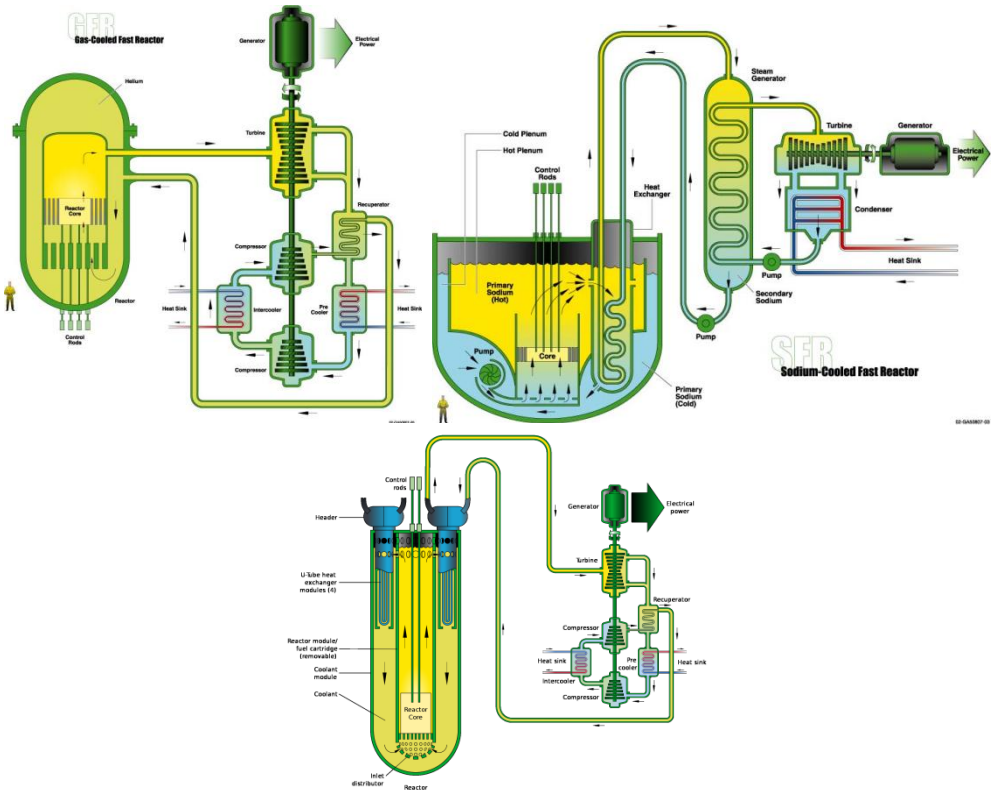

Figure 1.2: Scheme of the three fast reactor concepts selected as part of the Generation IV reactors

Although fast reactors can be operated with virtually any type of fuel, oxide and metallic fuels are usually preferred due to the experience already accumulated. The average target burnup of fast reactors currently being developed is in the vicinity of 10% FIMA [9] (Fission per Initial – heavy – Metal Atom). When reaching the target burnup the fuel is typically discharged from the reactor and stored until further decisions are made regarding the nuclear waste management. This burnup, while twice larger than the target burnup of advanced LWRs, is still far from the theoretical 100% FIMA achievable if the fuel was to be recycled after processing it to remove all the fission products. As the initial enrichment of the fuel is more than twice that required for LWRs, 10% FIMA does not offer higher natural uranium ore utilization than that of the once-through LWR.

To achieve a high conversion ratio, most of the fast reactor core designs include radial and/or axial blankets made of depleted uranium [9]. Those blankets are discharged with an average burnup that is smaller than of the enriched fuel and with a significant amount of fissile material. The traditional approach to fuel recycling for fast reactors was to recover the plutonium or transuranics (TRU) from the discharged fuel and use it as fissile material to fabricate the fuel to be used in the reactor for another cycle. This fuel processing is of proliferation concern and of economics concern. The proliferation concern is aggravated when using blankets as the fissile plutonium content of the plutonium extracted from the blanket elements can be very high.

1.2 Alternative approaches proposed

The idea is to design the core to generate the fissile fuel required for sustainable operation without relying on extraction of plutonium or TRU from the discharged fuel. By achieving significant breeding in the reactor blanket elements – made of natural uranium or depleted uranium, it is theoretically possible to produce sufficient fissile material to compensate for the fissile material consumed in the seed elements. Different approaches were proposed to achieve this objective, but few of them addressed the problem of the radiation damage sustainable in the presently available materials.

This breed and burn concept was first proposed by Feinberg [10] in 1958 and further studied by Atefi [11] and Fischer et al. of Brookhaven National Laboratory (BNL) [12] in 1979 and Feoktistov [13] in 1988. The concept studied by Fisher et al. was a complex core made of a central fast spectrum region radially surrounded by a moderated region. This initial feasibility study [12] estimated an achievable burnup of up to 15-20% FIMA; it also pointed out to the material damage issues associated with such a high burnup.

The mathematical modeling of the breed and burn mode was first provided by Goldin in 1995. In 1996 Teller et al. [14] proposed a traveling wave core concept in which the core was cylindrical and made of natural uranium or thorium with a centrally-positioned igniter moderately enriched in ^{235}U. In this concept the fissioning region is axially propagating above and below the igniter. When the core height is large enough, it was estimated that the fuel could be discharged at ~50% FIMA burnup without fuel reprocessing or refueling. Radiation damage and thermal-hydraulic issues were ignored.

In 1997 Toshinsky [15] proposed a breed and burn reactor concept the core layout of which is similar to that of a conventional fast reactor. The core is composed of several blanket and enriched fuel batches that are radially shuffled in an optimal sequence. At the end of a cycle, the highest burnup fuel batch is discharged and a fresh blanket batch is loaded in place of the blanket batch that has been shuffled to the higher fuel burnup location. The blanket fuel is made of uranium enriched with 1 wt% to 5 wt% ^{235}U. Toshinsky claimed that it is possible to sustain this mode of operation, without fuel reprocessing, with a discharge burnup of ~20% FIMA when a small pitch to diameter ratio and high heavy metal density are used.

Later, Sekimoto, , pursued Teller's idea and core geometry. In 2000, Sekimoto proposed the CANDLE reactor [16] in which the igniter region is located at an extremity of the cylindrical core and the axial propagation of the fission region is controlled by the core dimensions and fuel characteristics. It was estimated possible to achieve a burnup of up to 40.6% FIMA without fuel reprocessing or refueling.

Before proposing the CANDLE reactor, Sekimoto studied in 1993 the feasibility of ultra long life reactors (ULLR) [17]. The ULLR core is composed of an enriched fuel region and a blanket region, enabling operating the reactor for approximately 50 years and discharging the fuel the fuel with a burnup up to 20% FIMA. At the end of life the reactor is to reloaded with both enriched fuel and depleted uranium. With this mode of operation the uranium utilization is lower than the breed and burn mode. In 2006 Song et al. [18] proposed a similar ULLR design with an operating life of 35 years and in 2010 Kim & Taiwo proposed an updated version of this core [19] with a discharge burnup up to 30% FIMA, ignoring the radiation damage constraint.

In 2005, Driscoll (who was the advisor of Atefi [11]) et al. developed a breed and burn core concept [20] derived from the Gas cooled Fast Reactor (GFR). This core was designed to be fueled with uranium carbide rather than uranium oxide, cladded with an oxide dispersion

strengthened (ODS) steel cladding and cooled with helium. It was estimated possible to achieve a burnup of up to ~15% FIMA over 18 effective full power years (EFPY) when the reactor is fed with 5 wt% enriched uranium, without fuel reprocessing.

In 2008, the TerraPower LLC team, composed of several scientist who previously worked with Driscoll [20], announced the development of a traveling wave reactor (TWR) [21]. Two general design variants were developed by TerraPower LLC: a travelling-wave concept similar to that proposed by Teller et al., and a standing-wave concept somewhat similar to Toshinsky's concept. TerraPower LLC design uses depleted uranium for the feed fuel and sustains the breed-and-burn mode of operation with average discharge burnup close to 20% FIMA. This design relies on the development of materials able to sustain the radiation damage level corresponding to this burnup. With this approach, no fuel reprocessing is required.

The most recent breed and burn concept, the Energy Multiplier Module (EM2), has been proposed in 2010 by General Atomics (GA) [22]. The core is composed of bricks made of uranium carbide coated in a silicon carbide layer and is cooled with helium. The fission region is expanding in all directions and by removing at least 30% of the fission products from the fuel at the end of a cycle corresponding to ~15% FIMA, it was found possible to keep operating the core for unlimited number of cycles with depleted uranium feed. However, no technology is currently able to remove ~30% of all the fission products without complete separation of the actinides.

With the exception of the EM2, the breed and burn fuel managements mentioned above do not require fuel reprocessing or actinide separation. Therefore, the breed and burn fuel management is expected to be significantly more proliferation resistant and less expensive than the conventional approach. Apart from the initial enriched fuel required to "ignite" the reactor, no enriched fuel is required, and no actinide separation process needs to be implemented. However, this fuel management is facing a major challenge: the burnup required for sustainable operation is significantly exceeding the presently acceptable material constraints.

1.3 The UC Berkeley proposed approach

The approach proposed at UC Berkeley is reconditioning the fuel when it reaches its radiation damage limit. Fuel reconditioning in fast reactor was proposed by Greenspan [23] in 1998. Additional studies on fast reactor fuel cycle with multi-recycling have been performed by Monti [24] in 2005 and Ikegami [25] in 2006. The primary functions of the fuel reconditioning are to relieve the pressure of the gaseous fission products, replace the clad and reduce radiation induced defects in the fuel. That is, the fuel recycling processes considered cannot be used for the separation of actinides from most of the fission products and to extract plutonium or any other actinide from the fuel. Hence, these recycling processes are highly proliferation resistant and, hopefully, less expensive than processes traditionally considered for used fuel recycling. Two recycling processes are considered for the fuel reconditioning: an AIROX-like process and the melt-refining process. With the fuel reconditioning recycling, the maximum discharge burnup is dictated by the reactivity of the fuel and is not limited by the material damage constraints.

A couple of fuel management strategies for maximizing the uranium ore utilization without actinides separation are investigated: the conventional multi-batch fuel management and a breed-and-burn mode of operation. The breed and burn core design and fuel management studied at UC Berkeley are similar to those of the standing-wave cores proposed by TerraPower LLC [26]. However, in the UC Berkeley study when a fuel batch reaches its radiation damage constraint, it is reconditioned, as described above, and loaded back into the core. This fuel

reconditioning offers a practical solution to the problem often ignored in the early studies performed about breed and burn fuel cycles and it enables achieving the highest possible fuel utilization without actinide separation.

Another novel approach studied at UC Berkeley is the spawning mode of operation of breed and burn reactors; by discharging the fuel at the minimum burnup required to sustain the breed and burn mode of operation and loading it, after reconditioning, into a new reactor along with fresh depleted uranium, it is possible to spawn additional reactors without need for any additional fissile fuel. This spawning mode of operation enables expanding the installed capacity of breed-and-burn reactors at a high rate without the need for expanding the uranium enrichment capacity and without the need for actinides separation capability.

1.4 Objective of this study and organization

The main objective of this study is to assess the maximum fuel utilization that is achievable using fast reactors operating in either the conventional fuel cycle with multi-batch fuel management or with the innovative breed-and-burn mode of operation proposed above. The maximum discharge burnup is dictated by the reactivity of the fuel and not limited by the material damage constraints. This is achieved by reconditioning the fuel that reaches a radiation damage constraint. The minimum number of fuel reconditioning required to achieve the maximum attainable burnup are determined. The implications of the high burnup core designs on the core performance, resource utilization and waste characteristics are also assessed.

Another objective of this study is to estimate the minimum burnup required to sustain the breed and burn mode of operation in the core studied. The corresponding minimum doubling time required for spawning new breed and burn reactors using the fuel discharged from a preceding generation of breed and burn reactors at the minimum required burnup is also estimated, along with the installed capacity growth rate made possible by this spawning mode of operation.

The chapters of this dissertation are organized as follow:

- Chapter 2 discusses the core modeling, neutronics simulation, the fuel recycling process envisioned, the fuel behavior and thermal hydraulic methodologies used throughout this work;
- Chapter 3 presents preliminary results for simplified core models with fuel multi-recycling using enriched fuel feed. Uranium based oxide fuel and uranium and thorium based metallic fuels performances are analyzed with simplified conventional core models with a single- and multi-batch fuel management schemes;
- Chapter 4 focuses on the achievable fuel burnup for realistic cores fed with enriched fuel and operating with multi-recycling. The analysis is performed for both a large 3000 MW_{th} core and a smaller 1200 MW_{th} core, having the dimension of the General Electric S-PRISM reactor. The uranium utilization is estimated for core geometries with and without radial blanket;
- Chapter 5 addresses the conceptual design challenges of fast reactor cores using the breed-and-burn mode of operation. It focuses on the minimum required burnup to sustain the breed and burn mode of operation in several simplified systems: zero-dimensional, one-dimensional slab geometry and one-dimensional cylindrical geometry;

- Chapter 6 evaluates the performance of a large 3000 MW_{th} Breed & Burn (B&B) core that operates in the breed and burn mode. Both the transition period and the core at equilibrium are studied. The possibility of spawning additional fuel for a new core is also addressed;
- Chapter 7 evaluates the performance of an equilibrium S-PRISM size B&B that operates in the breed and burn mode. The control assembly systems performance is studied as well;
- Chapter 8 provides a succinct assessment of the performance of few alternative designs that use: lead based coolants, thorium based metallic fuel, silicon carbide cladding, gas coolant or nitride fuel.

Chapter 2

Methodology

The analysis of any nuclear reactor system is closely related to the fuel cycle it is to use. Many different fuel cycles can be envisioned: once-trough cycle, closed fuel cycles, fuel recycling process, type of fuel, batch management strategy… In order to assess the expected performance a new nuclear system it is necessary to simulate it. Being not possible to simulate a model that would perfectly represent reality, it is important to carefully explain and justify the assumptions made. With inadequate assumptions, the results might have no physical meaning, while with assumptions too conservative, it might become impossible to model the system with the tool currently available due to the complexity or simply because of the required computation time. The methodologies and main modeling assumptions used throughout the study are discussed in this section.

2.1 Fast reactor Cores Examined

During the preliminary assessment study described in Chapter 3 and during the conceptual study of the breed and burn mode of operation described in Chapter 5, many full core models and simplified core models are studied. However, in all the other chapters, only two different full core models are examined: a large fast reactor core and a small fast reactor core having approximately the size of the GE S-PRISM core. The general description of these two cores is provided below.

2.1.1 General considerations

The average neutron energy in a fast reactor system is in the vicinity of 1 MeV and the neutron mean free path is approximately 20 cm, about one order of magnitude above the neutron mean free path in thermal reactors. Therefore, the neutron leakage probability in a fast reactor is usually larger than for a same size thermal reactor. On the other hand, fast reactors are less sensitive to the level of heterogeneity. No significant spatial self-shielding is expected and the fuel, cladding and coolant materials can be mixed together, conserving their volume fraction.

This greatly simplifies the core model as there is no need for modeling each fuel pin or each fuel assembly.

For modeling, the core is split into several axial and radial zones of same volume in order to account for the variation of the axial and radial power distributions and the different burnup rates. Whereas the fuel shuffling is done fuel assembly by fuel assembly, the core is modeled in a coarser spatial resolution; instead of modeling the hexagonal fuel assemblies, the radial zones are modeled with concentric cylinders, each assumed to be of a uniform composition.

When fresh fuel is loaded into the core, the fuel occupies only a fraction of the volume available inside the cladding – this volume fraction is defined as the "smear density". The rest of the volume is occupied by the sodium bond that aims at limiting the mechanical and chemical interactions between fuel and cladding and at improving the heat conduction from the fuel to the clad. As the fuel burnup is increasing, the fuel swells, and the sodium is squeezed out of the fuel-cladding gap. This is occurring after only a few percent burnup. Since the objective of the study is to reach very high burnups, the period during which the fuel-clad gap contains sodium is significantly shorter than the period during which the fuel is swollen and occupies all the volume available inside the cladding. Therefore, the core is modeled assuming the fuel is already swollen and the sodium has been squeezed out to the fission gas plenum.

2.1.2 Large core

The large sodium cooled fast reactor core examined uses ternary metallic fuel U-Pu-Zr with 10 wt% zirconium, a fuel density of 15.85 g/cm^3 and a smear density of 75%, to accommodate the fuel swelling with burnup. In order to obtain an upper bound on the maximum attainable burnup, the fuel volume and gap fraction is taken to be 50%, corresponding to a pitch-to-diameter (P/D) of 1.122 – near the lower limit used in liquid sodium cooled reactors [9]. To simplify the core design and get upper bound estimates, no control assemblies, gas expansion modules (GEM), assembly ducts or inter-duct gaps are accounted for in calculating the volume fractions presented in Table 2.1. The cladding thickness has been assumed to be equal to 20.0% of the inner cladding diameter.

Table 2.1: Core Volume Fractions of the Large 3000 MW_{th} Core

Volume fractions	
Fuel	37.5%
Gap	12.5%
Clad	22.0%
Coolant	28.0%

The central radial part of the large sodium-cooled fast reactor is initially loaded with enriched fuel made of depleted uranium and TRU recovered from LWR Used Nuclear Fuel (UNF) that has been cooled for 10 years. Depending on the study being performed, this enriched fuel zone is radially surrounded by either (a) a thick reflector surrounded by a shield – Figure 2.1 – or (b) a depleted uranium blanket surrounded by a thin radial reflector followed by a shield – Figure 2.2. The dimensions, partially derived from the ANL ABR design [27], and material composition of the various components are given in Table 2.2. The shield dimensions and outer reflector radius are the same for both scenarios. The depleted uranium radial blanket volume is

equal to the enriched fuel volume and the reflector thickness is adjusted to maintain the radial shield dimensions identical. The active core height is 2.09 m and the active core diameter is 2.85 m for the model with a thick reflector and 4.03 m for the model with the radial blanket. The enriched fuel and radial blanket, when present, are divided each into four equal volume concentric burnup zones each of which is divided into three equal volume axial burnup zones.

A large core was selected since it has a relatively low neutron leakage probability and will therefore represent an upper bound on the burnup attainable from a finite core. The total core power is 3000 MW_{th}, corresponding to an average power density in the initial enriched fuel of 225 W/cm^3, yielding a peak power density within the imposed constraint of 450 W/cm^3. This constraint is based on existing fast reactor design database of the IAEA [9].

It is found that to get k_{eff} equal to unity at beginning-of-life (BOL) with a minimal radial power peaking factor, it is necessary to use 6.6%/11.7%/12.2%/15.3% TRU by weight in each of the four radial enriched fuel zones, from the innermost to the outermost. The radial blanket acting like a reflector at BOL, the required enrichment is the same for both scenarios: with and without radial blanket.

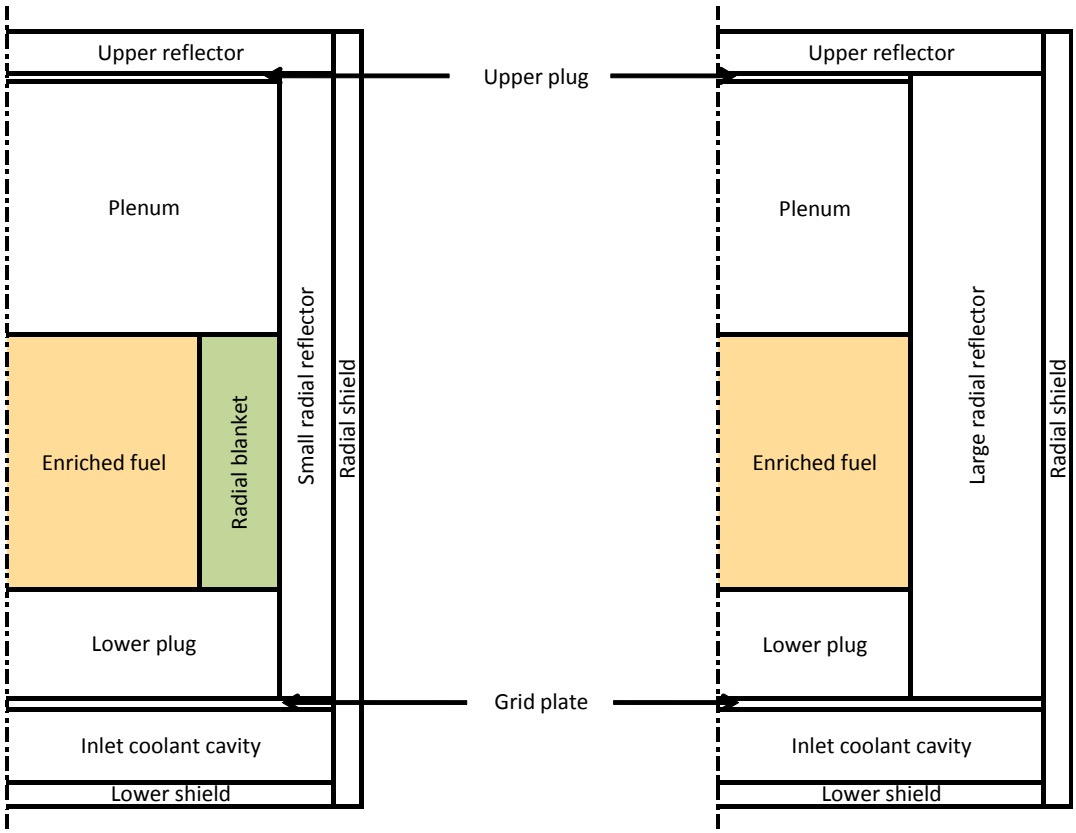

Figures 2.1 and 2.2: Layout of core and surrounding regions for the two large core scenarios simulated (Scenario (b) with the radial blanket on left; scenario (a) with the thick radial reflector on right)

Table 2.2: Dimensions and Composition of the Regions Modeled for the Two Large Core Scenarios (Blanket/Reflector)

Region	Height (cm)	Thickness (cm)	Material (Volume %)	T [K]
Upper reflector	34.93	242.2	50% HT9- 50% Na	783
Upper end plug	2.54	201.36 / 142.38	22% HT9 - 78% Na	783
Plenum	209.36	201.36 / 142.38	22% HT9 - 28% Na	783
Enriched fuel	209.36	142.38	37.5% Fuel - 22% HT9 - 28% Na	800
Blanket	209.36 / 0	58.98 / 0	37.5% Fuel - 22% HT9 - 28% Na	800
Lower end plug	90.42	201.36 / 142.38	22% HT9 - 78% Na	628
Grid plate	5.18	242.2	50% HT9 - 50% Na	628
Coolant inlet	60	242.2	22% HT9 - 78% Na	628
Lower shield	20	242.2	43.1% B_4C - 29.7% HT9 - 27.2% Na	628
Radial reflector	511.58	40.84 / 99.82	50% HT9 - 50% Na	628
Radial shield	631.79	20.5	43.1% B_4C - 29.7% HT9 - 27.2% Na	628

2.1.3 S-PRISM size core

The second core modeled corresponds to a relatively small sodium-cooled fast reactor, similar in size to the S-PRISM design developed by GE in the nineties [28]. This S-PRISM size core is also cooled with liquid sodium and the fuel used is the ternary alloy U-TRU-Zr with 6 wt% zirconium. It has been suggested by Hofman [29] that it is possible to manufacture metallic fuel with zirconium weight fraction as low as 6% without affecting the mechanical properties of the fuel. This enables loading a higher amount of heavy metal in the fuel, significantly improving the neutron economy. It is expected that the fuel with lower zirconium content will have a higher density than metallic fuel with 10 wt% zirconium. However, to be conservative, the same density and smear density of the 10 wt% zirconium fuel, 15.85 g/cm^3 and 75%, are used. The P/D ratio is equal to 1.106, the same as for one of the ABR designs[27]. The general core layout, shown in Figures 2.3 and 2.4, and the dimensions given in Table 2.3 are partially derived from the reference S-PRISM design.

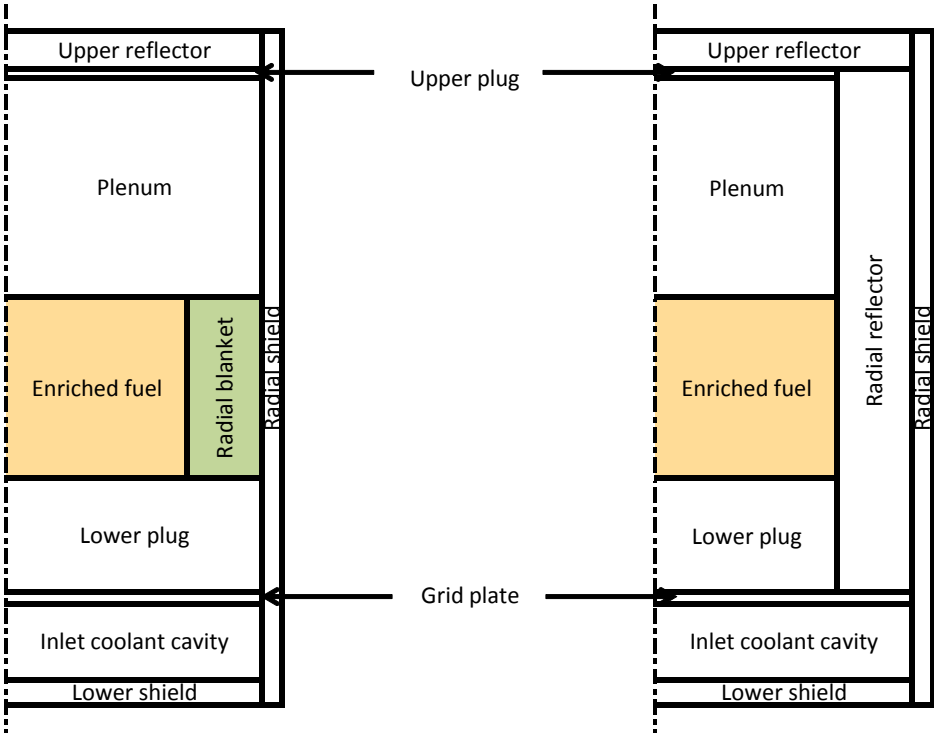

Figures 2.3 and 2.4: Layout of core and surrounding regions for the two S-PRISM size core scenarios simulated (Scenario (d) with the radial blanket on left; scenario (c) with the thick radial reflector on right)

The central part of the core is made of enriched fuel, while the surrounding zone is either made of (c) a thick reflector or of (d) a radial blanket, depending on the study performed. For both scenarios, the inner enriched fuel zone and the reflector outer diameter are the same and the surrounding shield is identical. The volume of the radial blanket, when used, equals the enriched fuel volume. The blanket and reflector volume in one scenario is equal to the large reflector volume of the other scenario. The active core height is 1.42 m and the active core diameter is 2.58 m for the model with a thick reflector and 3.65 m for the model with the radial blanket. In order to make this core model as realistic as possible, the core volume fractions given in Table 2.4 account for the GEMs, control systems, assemblies duct and inter-duct gap volumes. Despite a slightly smaller P/D ratio and lower zirconium weight fraction in the fuel, the heavy metal density in the S-PRISM size core is smaller than in the idealized large core because accounting for the GEMs & etc. volumes lower the core average fuel volume fraction to 5.08 g/cm^3 for the S-PRISM core (versus 5.35 g/cm^3 for the large core).

Table 2.3: Dimensions and Composition of the Regions Modeled for the Two S-PRISM Size Core Scenarios (Blanket/Reflector)

Region	Height (cm)	Thickness (cm)	Material (Volume %)	T [K]
Upper reflector	30.48	182.36	50% HT9- 50% Na	783
Upper end plug	2.54	182.36 / 142.24	22% HT9 - 78% Na	783
Plenum	171.83	182.36 / 142.24	22% HT9 - 28% Na	783
Enriched fuel	142.24	128.95	34.1% Fuel – 26.6% HT9 - 28% Na	800
Blanket	142.24 / 0	53.41 / 0	34.1% Fuel – 26.6% HT9 - 28% Na	800
Lower end plug	90.42	182.36 / 142.24	22% HT9 - 78% Na	628
Grid plate	5.18	182.36	50% HT9 - 50% Na	628
Coolant inlet	60	182.36	22% HT9 - 78% Na	628
Lower shield	20	182.36	43.1% B_4C - 29.7% HT9 - 27.2% Na	628
Radial reflector	0 / 407.03	0 / 53.41	50% HT9 - 50% Na	628
Radial shield	522.69	14.76	43.1% B_4C - 29.7% HT9 - 27.2% Na	628

Table 2.4: Core Volume Fraction of the S-PRISM Size Fast Core

Volume fractions	
Fuel	34.1%
Gap	11.4%
Clad	26.6%
Coolant	28.0%

Due to the shorter core, the axial neutron leakage is expected to be significantly larger for the S-PRISM size core, impeding the achievable burnup. This core is also expected to feature more favorable reactivity coefficients than the large core and a lower pressure drop across the core because of the shorter core height. The S-PRISM nuclear power plant design has already been performed by GE and was considered the most advanced and most promising fast reactor design of the USA; it was also considered to be licensable The initially guessed core power is assumed to be 1200 MWth slightly above the GE design value of 1000 MWth. The average power density in the enriched fuel at BOL is approximately 160 W/cm^3, almost 30% smaller than for the large core of Section 2.1.2.

It is found that to get k_{eff} equal to unity at BOL with a flat initial power distribution in the enriched fuel, it is necessary to use 11.0%/11.2%/13.5%/16.0% TRU by weight in each of the four radial enriched fuel zones, from the innermost to the outermost. On the average, the TRU enrichment is 12.8% larger than for the large core because of the larger axial neutron leakage and lower HM density. Due to the good reflective properties of the radial blanket, the required TRU enrichment at BOL for the S-PRISM size core is found to be the same for the both scenario (c) with the radial blanket but no radial reflector and scenario (d) with a radial reflector but no blanket.

2.2 Fuel recycling processes

The attainable burnup in fast reactors is limited by the mechanical integrity of the fuel rods that is constrained by, primarily, (a) radiation damage to the cladding; (b) gaseous fission products pressure buildup and (c) fuel-cladding mechanical interaction (FCMI) caused by fuel swelling due to accumulation of, primarily, rare earth solid fission products. With presently available structural materials that are compatible with liquid metal coolants the radiation limit constraint is approximately 200 displacements per atom (DPA). For relatively low fissile content metallic fuel cores, this corresponds to an average fuel burnup in the vicinity of 100 GWd/tHM ("giga-watts day per ton of heavy metals"). To enable achieving larger fuel burnup it is necessary to recondition the fuel by recycling it. In order to keep the fuel cycle as proliferation resistant as possible, the actinides separation processes are not appropriate and two simple fuel recycling processes are envisioned: an AIROX-like process and a melt-refining-like process. The objective of those two processes is to declad the discharged fuel, remove the gaseous and volatile fission products, relieve radiation and burnup induced defects in the fuel, add fuel makeup, refabricate the fuel and load it into a new cladding.

2.2.1 AIROX process

For oxide fuel the fuel de-cladding and gaseous plus volatile fission products removal can be achieved using the AIROX process [30] such as the DUPIC process [31] the feasibility of which was demonstrated by the Republic of Korea for recycling fuel from PWR to HWR. The AIROX process is a dry process that involves oxidation of the irradiated UO_2 fuel by O_2 atmosphere at 400°C to U_3O_8. The U_3O_8 is reduced back to UO_2 by exposure to H_2 at 600°C. When this process is repeated several times the fuel pellets decompose to a fine powder out from which it is possible to remove, in gaseous form, 100% of T, C, Kr, Xe and I, 90% of Cs and Ru and 75% of Te and Cd. As is, the AIROX process is not directly applicable to metallic fuel. In principle it is possible to first convert U-Zr to U_3O_8 by an oxidation process, apply the AIROX process, and then reduce it back to U-Zr. Alternatively, it may be possible to develop a voloxidation process that is directly applicable to metallic fuel to perform a similar function.

2.2.2 Melt-refining process

The melt-refining process has been developed for metallic fuel in the Experimental Breeder Reactor II project [32]. The melt-refining involves loading the decladded fuel into a zirconia crucible and melting the mixture at ~1300ºC for several hours under argon atmosphere. The gaseous and volatile fission products are released and certain solid fission products are partially removed by oxidation with the zirconia of the crucible. Based on [32] it is assumed that this process can remove nearly 100% of Br, Kr, Rb, Cd, I, Xe and Cs, and at least 95% of Sr, Y, Te, Ba and the rare earths (lanthanides). Thorium and americium are also oxidized with zirconia, and 95% of these two elements will be removed from the fuel.

The primary drawback of this process is that several percent of the plutonium and other actinides remain in the crud of the zirconia crucible. In addition the above-mentioned performance has been demonstrated for a fuel with a burnup level significantly smaller than the burnup targeted in the current study. If this study will indicate that such a process could provide

the nuclear program useful new options, a modified or different process that does not involve significant loss of actinides and cannot separate a specific or all of the actinides and, yet, can efficiently remove the gaseous and certain fraction of the volatile fission products could be developed.

2.2.3 Discussion

The above recycling processes cannot be used to partition plutonium from the uranium-based metallic fuel. For this reason, and also because the recycled fuel is seeded with relatively large amount of radioactive fission products in addition to all the actinides, this recycling approach is expected to be highly proliferation resistant. It is also expected to be less expensive than any of the chemistry-based recycling processes.

2.3 Fission gases release with burnup

The increasing burnup makes the fuel pin swell because of the accumulation of fission products in the fuel lattice. Depending on the crystalline structure of the fuel, the swelling can become very important, such as for pure uranium. For this reason, uranium based metallic fuel is alloyed with zirconium in order to change its crystalline structure, and decrease its swelling. For all types of fuel, the swelling is eventually constrained by the cladding, and therefore by the smear density. The smear factor is the fraction of the volume enclosed by the clad that is occupied by the un-irradiated fuel, if at nominal density. It has to be large enough to enable fission gases to diffuse out from the fuel into the fission gas plenum, thus limiting the fuel swelling and deferring the fuel-clad interaction. Obviously, it should be as small as acceptable in order to maximize the amount of fuel loaded in the core. Table 2.5 lists the smear density values usually used in this study for the different types of fuel considered.

Table 2.5: Basic Characteristics of the Fuels Studied [33-37]

Fuel	ρ [g/cm^3]	Smear factor	Melting temperature [°C]
U-TRU-Zr(10)	15.85	0.75	1240
(U,TRU)C	12.95	0.85	2400
(U,TRU)^{15}N	14.31	0.87	2650
(U,TRU)O_2[(c)]	11.5	0.85	2750
IMF[(d)]	19.98/7	0.85	1336
(Th,TRU)[(e)]	11.65	0.75	1842

(a)Inert Matrix Fuel is made of two phases: $(U,TRU)_2MoSi$ and Zr_8Fe_8Cu; (b)Smear factor is taken the same as U-based metallic fuel

After 3% to 4% FIMA burnup in metallic and oxide fuel, the fuel swelling becomes constrained by the cladding and the fraction of fission gases being released reaches a plateau value equal to approximately 75% [38-40]. For all simulations, apart for those of Chapter 3, 75% of the fission gases are being constantly released from the fuel. The release fraction variation during the first few burnup percents have a negligible effect due to the very high burnup reached during this study. The same gaseous fission products release fraction has been assumed for all

types of fuel because of the lack of data for fuel types less extensively studied. The elements removed are the noble elements and elements that are gaseous at the fuel operating temperature: H, He, N, O, F, Ne, Cl, Ar, Kr, Xe and Rn.

2.4 Fuel density change with fission products accumulation

The problem to be addressed in this section is the fuel density change with fission product accumulation. As the fission of each HM nucleus typically gives two fission products, the fission products accumulation in the fuel may decrease the fuel density and HM concentration per unit fuel volume. If the fuel density increases, make-up material such as depleted uranium can be added to conserve the nominal fuel volume. However, if the fuel density decreases, it will not be possible to reload all the HM in the core and the left over fuel will need to be dealt with.

The metallic fuel volume change with burnup has been addressed by Hofman in [41]. The gaseous fission products are all removed from the fuel when reconditioning it, but the non gaseous fission products are making the fuel density change by (a) decreasing its volume due to the heavy metal fissioned; (b) increasing its volume due to the increase of number of fission products that are soluble in the fuel matrix; and (c) increasing its volume due to accumulation of the non soluble fission products. Volume change induced by (a) and (b) have to be addressed together, since they are changing the crystalline structure parameters of metallic fuel.

The swelling due to non soluble fission products is obtained by using the same assumptions as in [41] regarding the partitioning and behavior of those fission products. Table 2.6 is providing the element groups, fission yields, assumptions made, average molar volume and volume change per percent burnup, before and after fuel recycling with the melt-refining. The fission yields are in fact the number of atoms in each element group per 100 fissions. Since 95% of the lanthanides are assumed removed by the melt refining process during fuel recycling, the fuel volume after recycling is significantly smaller than before. The fuel volume is increased by 1.36% per percent burnup before recycling and by only 0.54% per percent burnup after recycling. Hofman found that, with slightly different fission yields, the swelling was 1.18% per percent burnup.

Table 2.6: Volume Change Due to Non Soluble Fission Products

			Before recycling		After recycling	
Element group	State	Molar volume [cm3/mole]	Fission yields	%vol/% BU	Fission yields	%vol/% BU
Alkali (Cs, Rb)	70% in Na bond	21	20.3%	0.099	0.0%	0.000
Alkaline Earth (Sr, Ba)	20% in Na bond	16	11.1%	0.110	3.9%	0.038
Lanthanides + Pd	-	20	59.9%	0.929	18.0%	0.278
(Tc, Ru, Rh, Ag)	-	9	32.3%	0.226	31.7%	0.221
Total	-	-	-	1.364	-	0.538

The fuel matrix composition change can be estimated using the lattice parameter of U-Zr. It is assumed that all the soluble fission products – Zr, Nb and Mo – can be assimilated to Zr, and that all the actinides can be assimilated to uranium. For temperatures below 610°C, the U-Zr alloy is made of two phases: all the zirconium is found in the phase UZr_y, where y=1.778, and the rest of uranium is found as pure uranium. The atomic volume of the pure uranium phase is

v_1=0.02075 nm^3, and it is v_2=0.022567 nm^3 for the UZr_y phase. The U-Zr density can then be estimated at any burnup using Equation 1.1, where Na is the Avogadro number, M_X is the molar mass of element X and w_{Zr} is the weight fraction of zirconium – and associated elements – in the fuel.

$$\rho\left[\frac{g}{cm^3}\right] = \frac{10^{21}\left[\frac{cm^3}{nm^3}\right]}{N_a * \left(\left(\frac{1-w_{Zr}}{M_U} - \frac{36}{64}\frac{w_{Zr}}{M_{Zr}}\right) * v_1 + \frac{w_{Zr}}{M_{Zr}} * \left(1+\frac{36}{64}\right) * v_2\right)} \qquad (Eq.\,2.1)$$

The volume fraction change per percent burnup is then obtained using Equation 1.2, where m_{ini} and m_2 are the mass of both heavy metal and soluble fission products in the fresh fuel and in the fuel considered, respectively. It is found that for the fuel pertaining to Table 2.6 – after recycling – the soluble fission products and heavy metal consumptions are representing a volume change of -0.46% per percent burnup. The total volume change due to both soluble and non soluble fission products is then only 0.07% per percent burnup.

$$\Delta V[\%/\%BU] = \frac{\left(\frac{m_2 * \rho_{ini}}{m_{ini} * \rho_2} - 1\right)}{BU[\%]} \qquad (Eq.\,2.2)$$

It is concluded that using melt-refining for fuel reconditioning, the fuel density change per percent burnup is very small and therefore, there is no need for adding fuel make-up or for removing fuel during recycling.

2.5 Neutronic Analysis

2.5.1 MCNP5 1.40

MCNP5 is a Monte Carlo particle code, developed by Los Alamos National Laboratory (LANL). It can be used to simulate neutron, electron and photon transport. It is possible to combine the various types of surfaces available – plane, sphere, cone, torus… – to build the system geometry piece by piece and specify the isotopic material composition in each cell. The material definition is only restricted to the isotopes available in the nuclear database used by MCNP5. Among all the information that can be calculated by MCNP5, the most important for neutronics study are the spectra, effective one-group cross-sections, fluxes, displacement per atom (DPA) rates and leakage probabilities. The detailed capabilities of MCNP5 can be found in the MCNP5 manual [42].

The primary reason for using this software is its ability to directly use point-wise cross-section data without the need for generation of problem-dependent multi-group cross sections. The main drawback of the Monte Carlo technique, compared to the deterministic methods, is the very high computation time required to achieve acceptable statistics.

For all the simulations performed with MCNP5, the (n,f), (n,γ), (n,2n), (n,3n) and (n,α) one group cross-sections are generated for thirty-four actinide isotopes and ninety-nine fission product isotopes, given in Table 2.7. All the cross-section data used by MCNP5 for the present

study are based on the original ENDF/B-VI libraries. These libraries were previously generated for different temperatures using NJOY [43], to account for the temperature dependence of Doppler broadening of resonances.

Table 2.7: List of Isotopes Tracked in MCNP5

Element	Isotope number
Thorium	232, 233
Protactinium	233
Uranium	234, 235, 236, 237, 238, 239
Neptunium	236,237, 238, 239
Plutonium	236,237, 238, 239, 240, 241, 242, 243, 244
Americium	241, 241m, 242, 243, 244
Curium	242, 243, 244, 245, 246, 247, 248
Berkelium	249
Californium	249
Bromine	81
Krypton	83, 84
Rubidium	85, 87
Strontium	90
Yttrium	89
Zirconium	90, 91, 92, 93, 94, 96
Niobium	
Molybdenum	95, 96, 97, 98, 100
Technetium	99
Ruthenium	100, 101, 102, 103, 104, 105
Rhodium	103
Palladium	104, 105, 106, 107, 108, 110
Silver	109
Cadmium	110, 111, 112, 113, 114
Indium	115
Tin	117, 118
Antimony	121, 123, 125
Tellurium	125, 128, 130
Iodine	127, 129
Xenon	130, 131, 132, 134, 135
Caesium	133, 134, 135, 137
Barium	134, 137, 138
Lanthanum	139
Cerium	140, 142
Praseodymium	141
Neodymium	143, 144, 145, 146, 148, 150
Promethium	147
Samarium	147, 148, 149, 150, 151, 152, 154
Europium	151, 152, 153, 154, 155
Gadolinium	154, 155, 156, 157, 158
Terbium	159

2.5.2 ORIGEN 2.2

ORIGEN2.2 is a depletion code released in 2002 by Oak Ridge National Laboratory. The manual [44] describes ORIGEN2.2 as "a computer code system for calculating the buildup, decay, and processing of radioactive materials". It "uses matrix exponential method to solve a large system of coupled, linear, first-order ordinary differential equations with constant coefficients".

Practically, this code is used to estimate the reactor fuel composition as a function of time, using the effective one-group cross-sections and total flux values generated by MCNP5. For reactions for which cross-sections are not provided by MCNP5, cross-sections from the default ORIGEN2.2 library for liquid metal cooled cores with oxide fuel, "LMFBR recycle Pu/U", are used. Unfortunately, no default library representing a fast reactor operating with metallic fuel is available in ORIGEN2.2. Due to the spectral difference between oxide and metallic fueled cores, it is important that the data generated by MCNP5 for the thirty-four actinides isotopes and ninety-nine fission products isotopes represent at least 99% of the total fission and absorption cross-sections. When this is achieved, the discrepancy due to use of the cross-section values of ORIGEN2.2 default library for the other isotopes becomes insignificant. An extended composition of approximately 900 isotopes is used in ORIGEN2.2 for the depletion analysiss.

2.5.3 MOCUP and IMOCUP

MOCUP is the MCNP-ORIGEN2 Coupled Utility Program developed by Idaho National Laboratory (INL) in 1995 [45]. Its role is to interface ORIGEN2.2 with MCNP5. In particular, it provides ORIGEN2.2 with the initial fuel compositions, effective one-group cross-sections and total flux estimated by MCNP5 for each depletion zone, creates the ORIGEN2.2 input file, executes ORIGEN2.2 and generates the new input file for MCNP5 using the updated fuel composition.

MOCUP cannot handle the cross-sections for more than 123 isotopes from MCNP5, limiting the number of updated cross-sections it is possible to provide ORIGEN2.2. Furthermore, for each depletion zone two flux tallies ("track length estimate of cell flux", F4) need to be used in MCNP5 input file, limiting to 50 the number of zones that can be depleted as MCNP5 cannot handle more than 100 flux tallies. The isotope limitation is not a major issue for the present study: by properly selecting the important isotopes it is possible to get updated cross-section values representing more than 99% of the total macroscopic cross-sections. However, the number of depletion zones limitation is more problematic for this study as for many of the cores studied the desirable number of depletion zones exceeds 50.

During the course of this work, the MOCUP scripts have been re-written from scratch in order to remove those two limitations. The new scripts, provided in Appendix A, are named Improved MOCUP (IMOCUP) and are written using the basic UNIX commands. Using IMOCUP, it is possible to track and update with MCNP5 the cross-sections for any number of isotopes, and to deplete as many zones as wished, with only two flux tallies. The main drawback of IMOCUP compared to MOCUP is the slightly longer run-time it takes: a couple of minutes for IMOCUP, where it takes only a few seconds for MOCUP. These times are negligible as compared to the time it takes to run MCNP5 and ORIGEN2.2.

2.5.4 Additional modules

In addition to the software described above, several modules have been developed in order to simulate the proposed fuel cycle. The most important ones are:

- Shuffling module:
  This is used to shuffle the fuel between depletion zones accordingly to the user-defined pattern. It can be used to feed fresh material to the core and to discharge the high burnup fuel. This is particularly useful when simulating equilibrium core cycles, where at the end of a cycle some fuel elements are discharged, and fresh fuel elements are added.
- Recycling module:
  This is used to recycle a specific fuel batch. It can recycle the fuel using the AIROX or melt-refining processes, and will axially average the fuel composition. It can also be used to recycle several fuel batches if they are to be recycled together, yielding a single composition.
- Multi-batch module:
  This module allows to virtually subdividing a depletion zone into as many batches as wished, without altering the geometry. It uses an averaged material composition for the MCNP5 simulation, while it depletes the exact material composition using ORIGEN2.2 based on the average characteristics generated by MCNP5 – the fresh material composition needs to be provided by the user. Practically, it enables simulating a core with a finite number of batches, without modeling the batches separately, significantly simplifying the simulation. This approach is only valid for cores where the neutron mean free path is larger than the assembly pitch.
- Equilibrium module:
  This module iteratively determines the equilibrium core composition. It relies on an iterative process described by Figure 2.5, where the cross-sections and fluxes are obtained from an initially guessed cycle dependent core composition. These values are then used to estimate the new cycle-dependent core composition. The updated core composition is then used to refine the cycle-dependent cross-sections and fluxes. This iterative process is repeated until the cycle characteristics converge. This module can be associated to any of the above mentioned modules, and is using a running average method (called SMA method) in order to convergence faster.

2.6 Thermal hydraulic analysis

The main objective of the thermal hydraulic analysis is not to assess the full reactor cooling systems performance, but only to determine the maximum practical power that the core modeled can deliver When subjected to a number of constraints: the core pressure drop, the maximum core coolant velocity, the maximum coolant outlet temperature, the peak cladding temperature and the peak fuel temperature.

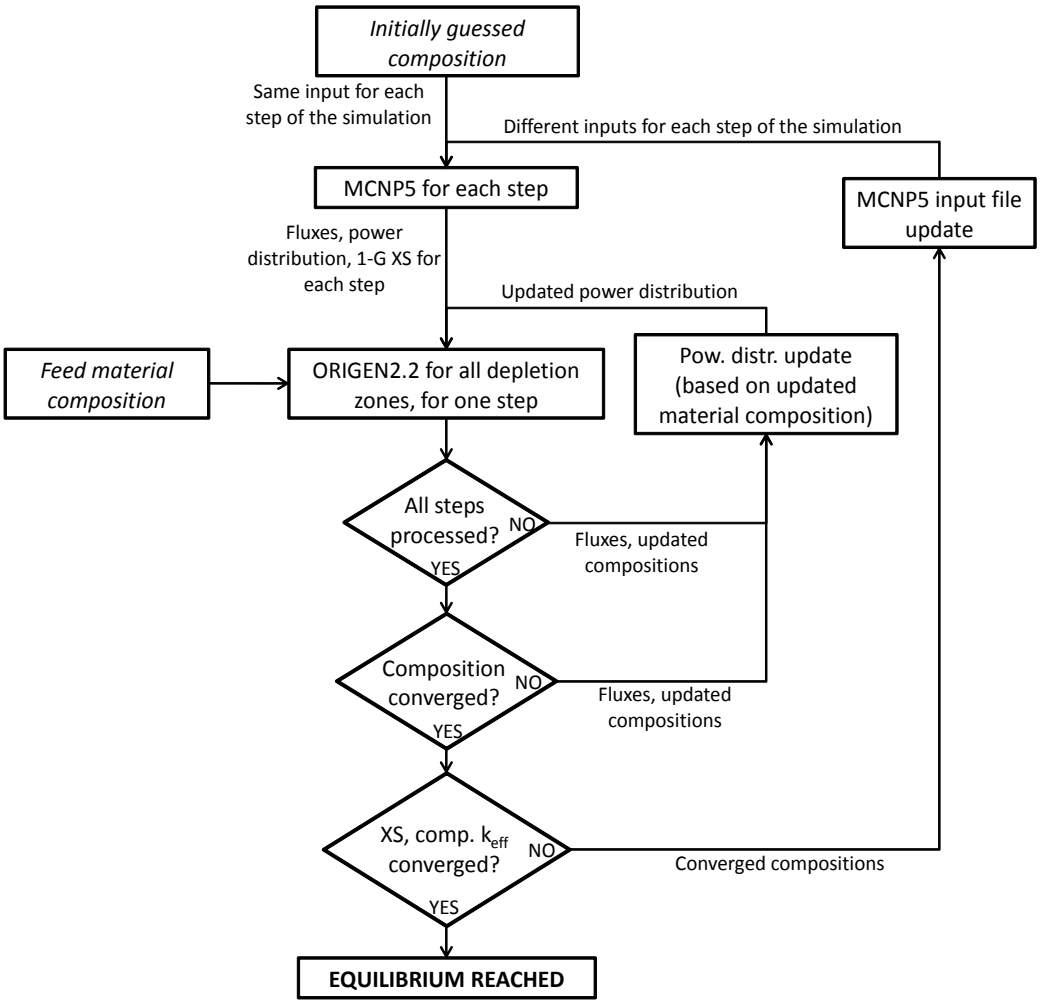

Figure 2.5: Process flow chart of the equilibrium module methodology

2.6.1 Constraints

- Maximum coolant velocity across the core:

Based on the IAEA database for fast reactors [9], the maximum velocity for sodium coolant is assumed to be 12 m/s in order to prevent structural damage due to fuel elements vibration. For reactors cooled with lead or lead-bismuth, the velocity is limited by the erosion rate of the protective oxide layer formed on the cladding in order to minimize the clad corrosion rate by the lead or lead-alloy. The commonly accepted velocity limit for lead based coolants is 2 to 3 m/s [46], but a new alloy is currently being developed by Prof. Ballinger et al. at the Massachusetts Institute of Technology (MIT) that may enable a velocity up to 6 m/s [47]. The limit used for this study is the later.

- Maximum pressure drop across the core:

The maximum acceptable power drop across the core is dictated by the pumping power requirement and pump technology. According to [9], fast reactors are usually designed with a core pressure drop not exceeding 1 MPa.

- Maximum cladding temperature:

The peak permissible cladding temperature is assumed to be 650°C, based upon fuel-cladding eutectic interaction. In addition, for the cladding to maintain its mechanical integrity at burnups exceeding 20% FIMA, the peak cladding temperature shall not exceed 550°C to prevent the cladding oxidation with the increasing fraction of lanthanides: the lanthanides isotopes tend to redistribute in the outer region of the fuel pin, limiting the maximum acceptable fuel-clad temperature [48]. If the burnup level is smaller than 20% FIMA, this constraint can be relaxed, and the 650°C constraint will be used.

- Maximum fuel temperature:

The peak fuel temperature must not exceed its melting temperature. The melting temperatures of the different types of fuel studied are provided above in Table 2.5.

2.6.2 Core pressure drop

The core pressure drop and the coolant velocity in the core are correlated and are obtained using the analytical approach described in [48]. The pressure drop across the core can be expressed as the sum of the pressure drops produced by (1) flow contraction at the inlet to the grid plate. (2) flow expansion after the grid plate, (3) flow contraction by the fuel rods, (4) the friction along the fuel rods, including the contribution of the wire wraps , (5) the friction in the upper support grid, (6) flow expansion at the outlet from the upper support and (7) flow expansion at the top of the core. The friction induced pressure drop represents more than 85% of the total core pressure drop. The detailed equations used for estimating each of those pressure drop components are provided in Appendix B.

The maximum coolant mass flow rate is then determined from the estimated core pressure drop, using the coolant characteristics provided in Appendix C for sodium, lead-bismuth and lead-lithium.

2.6.3 Maximum core power determination

The practical core power level is estimated using the maximum coolant mass flow rate obtained from the core pressure drop analysis described above. The analysis is performed for the fuel assembly generating the highest power by calculating the temperature gradient in the coolant, cladding and fuel, based on the axial power distribution obtained from MCNP5 and spatially meshing the fuel assembly. Depending on the choice of fuel rod diameter, the practical core power is limited by the coolant outlet temperature or peak cladding temperature. The calculation methodology and equations used are the same as those used in [48].

For the heat transfer analysis, the fuel-cladding gap is conservatively assumed being still filled up with sodium. As the fuel swells, the gap thickness is decreased, increasing the fuel volume. This is improving the heat transfer from the fuel to the clad and results in a decreased peak fuel temperature. Although this assumption is conservative, the build-up of fission products and actinides in the fuel will change its thermal conductivity. It was not possible to find reliable data regarding the evolution of the fuel thermal conductivity with burnup, and therefore the fresh fuel thermal conductivity [49] is used for this analysis.

Once the highest power generated by a fuel assembly is determined, the total core power is derived using the radial core power peaking factor and the total number of fuel assemblies.

Chapter 3

Preliminary Assessment of the Achievable Burnup in Fast Reactors without Actinide Separation

With once-trough (OT) fuel cycle, the core is initially loaded with enriched fuel and operated until it becomes subcritical. At this point, the highest burnup fuel is removed from the core and replaced with fresh enriched fuel, having the same composition as the enriched fuel initially loaded into the core. The discharged fuel is not reprocessed, and is stored until further decisions are made. It is possible to use a fuel management scheme with several batches in order to decrease the burnup reactivity swing of the reactor and increase the achievable burnup of the fuel. This mode of operation is commonly used in most of the countries for light water reactors (LWR), in which the core is traditionally split into four fuel batches.

As previously mentioned, the achievable burnup is limited in a fast reactor by the material integrity and not by the fuel reactivity. In order to model a fuel cycle for fast reactors, where the fuel is discarded when its reactivity becomes too low, it is necessary to multi-recycle the fuel with any of the two processes proposed in Section 0. It is assumed that the fuel recycling is occurring instantly, and the recycled fuel is immediately reloaded into the core. When the excess reactivity of the core becomes zero, the fuel has reached its maximum burnup and is discharged and stored. When acceptable full actinide separation processes will be available, it will be possible to remove all or most of the fission products and, possibly, certain actinides, and extract more energy from the stored fuel discharged from both LWRs and fast reactors.

In order to determine the theoretically maximum discharge fuel burnup in fast reactor with multi-recycling, a fuel management scheme with an infinite number of batches yielding a fixed multiplication factor, k_{eff}, equal to unity is assumed. It is assumed that the excess reactivity of the $k_\infty>1.0$ batches compensate for the reactivity deficiency of the subcritical ($k_\infty<1.0$) batches. The maximum achievable burnup is the burnup for which the average k_{eff} over all the batches equals unity.

3.1 Fast reactor cores examined

Two fast reactor core models are examined in order to bracket the range of the possible attainable burnup – a small core that is characterized by a relatively large neutron leakage probability, and an infinite core to provide an upper bound estimate.

The small core is based on a modular reactor core design – the Encapsulated Nuclear Heat Source (ENHS) [50]. The main core design parameters are provided in Table 3.1. It is composed of 9862 fuel rods having an active length equal to 125 cm and generating a total of 125 MW_{th}. The outside clad diameter is 1.56 cm and the clad thickness is 0.13 cm. The nominal P/D ratio is taken to be 1.1. This is somewhat smaller than the P/D sodium cooled cores are commonly designed with and is chosen for this study so as to obtain an upper bound on the breeding ratio and, hence, on the attainable burnup. For a similar reason, the reference coolant assumed is liquid lead; it provides an upper bound on the attainable burnup. A sensitivity of the attainable burnup to the P/D ratio as well as to the coolant type is performed in Section 3.4. The same fuel and core dimensions are used for both the oxide and metallic fuels.

Table 3.1: Core Design Parameters

Parameter	Value	Unit
Number of fuel rods	9862	-
Fuel rod diameter	1.56	cm
Clad thickness	0.13	cm
P/D	1.1	-
Active fuel length	125	cm
LHR	101.4	W/cm
Core average power density	39.8	W/cm^3
Fuel density (Oxide/Metallic)	10.8/15.85	g/cm^3
Smear density (Oxide/Metallic)	0.9/0.75	-

A simplified layout of the finite core and adjacent regions modeled is shown in Figure 3.1. The core is homogenized, as commonly done in fast reactor core analysis, by conserving the volume fractions of the fuel, clad and coolant materials. The burnup analysis is performed by dividing the core into nine equal volume depletion zones: three radial zones each divided into three axial zones. The initial composition assumed for all the core zones is identical, although it is common to use a smaller fissile content in the core inner zones and larger fissile content in the core outer zones in order to flatten the power distribution. No blanket assemblies are used for this analysis.

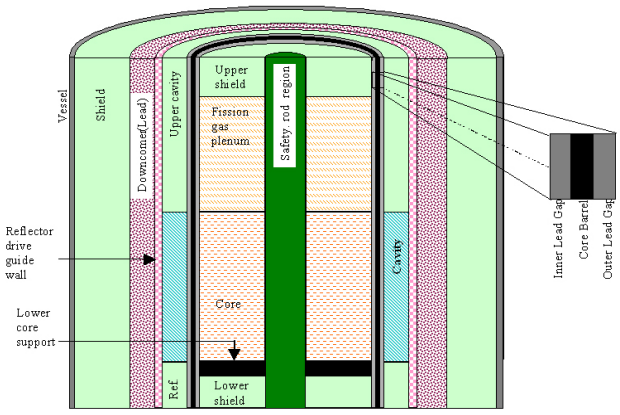

Figure 3.1: Schematic representation of the ENHS homogenous core model

The infinite core model is represented by a single heterogeneous ENHS unit cell with reflective radial and axial boundary conditions. The fuel rod dimensions and P/D ratio are the same as for the ENHS core described above. So are the materials used for the fuel, the clad and the coolant. A single depletion zone is used.

UO_2-$TRUO_2$ is assumed for the oxide fuelled core. Its density is 10.8 g/cm^3, corresponding to 95% of the theoretical density [51]. The smear density assumed is 90%. The metallic core is assumed to be a ternary metallic alloy U-TRU-Zr, with 10 wt% Zr. The metallic fuel density is taken as 15.85 g/cm^3 and its smear density is 75%, to accommodate its relatively large swelling. Table 3.2 summarizes the volume fractions of the oxide and metallic fuelled cores.

Table 3.2: Volume Fraction of the Constituents of Oxide and Metallic Fueled Cores

	Volume fraction – P/D=1.1	
	Oxide fuel	Metallic fuel
Fuel	46.84%	39.04%
Gap	5.20%	13.01%
Clad	22.90%	22.90%
Coolant	25.05%	25.05%

The heavy metal is composed of depleted uranium mixed with TRU recovered from LWR UNF that underwent 50 GWd/tHM and cooled for 10 years. The resulting TRU composition is given in Table 3.3.

Table 3.3: TRU Composition Obtained from LWR Fuel Discharged at 50 GWd/tHM and Cooled for 10 Years (Hong et al) [50]

LWR spent fuel composition	
Isotope	weight %
^{237}Np	6.641
^{238}Pu	2.749
^{239}Pu	48.652
^{240}Pu	22.98
^{241}Pu	6.926
^{242}Pu	5.033
^{241}Am	4.654
^{242}Am	0.019
^{243}Am	1.472
^{242}Cm	0
^{243}Cm	0.005
^{244}Cm	0.496
^{245}Cm	0.038
^{246}Cm	0.006

For both core models the fuel elements are recycled every 20 years, corresponding to an average core burnup of ~70 GWd/tHM for oxide fuel and ~50 GWd/tHM for metallic fuel. The fuel recycling consists in discharging all the fuel from the core, cooling it for three years, reconditioning it with the AIROX(-like) process and adding make-up material. For the small core, the fuel composition is also axially averaged as a result of the fuel recycling. The amount of make-up material – depleted uranium – added is determined by estimating the number of fission products atoms removed by the recycling process and dividing it by two (approximately two fission products are produced per fission). It has been later found that with the AIROX(-like) process, the fuel swelling does not enable for adding make-up material. During operation the gaseous fission products are continuously removed from the core.

3.2 Attainable single batch burnup

3.2.1 Uranium based oxide fuel

The heavy metal inventory at BOL in the small oxide core is 13.2 MT, the specific power density is 9.5 W/g and the average linear heat generation rate is 101.4 W/cm. The initial TRU concentration required for achieving criticality at BOL is 16.37 wt%. The neutron leakage probability from this core is approximately 15%. The infinite core BOL TRU critical concentration is 15.16%.

Figure 3.2 shows the k evolution with burnup for the two oxide cores examined. The maximum attainable burnup for a single-batch fuel management corresponds to the burnup for which the value of k drops below unity. For the small oxide core this maximum attainable burnup is limited to 7% FIMA. After each recycling the fuel composition across the core is assumed uniform; as a result there is a small decrease in the core reactivity from the end of one cycle to the beginning of the next one. It is found that after the first recycle, the core becomes subcritical. Various re-loading patterns featuring non-uniform fuel composition at the second cycle have been tried, but none enabled maintaining criticality for the second cycle.

For the infinite oxide core, the breeding ratio is initially significantly larger than one and, hence, the core multiplication factor keeps increasing up to the middle of the second cycle – corresponding to an average core burnup of ~110 GWd/tHM. The maximum attainable burnup in a single-batch fuel management scheme is close to 20% FIMA – corresponding to three cycles. The burnup accumulated during the second and third cycles is smaller than during the first cycle because heavy metal makeup is added in each recycle.

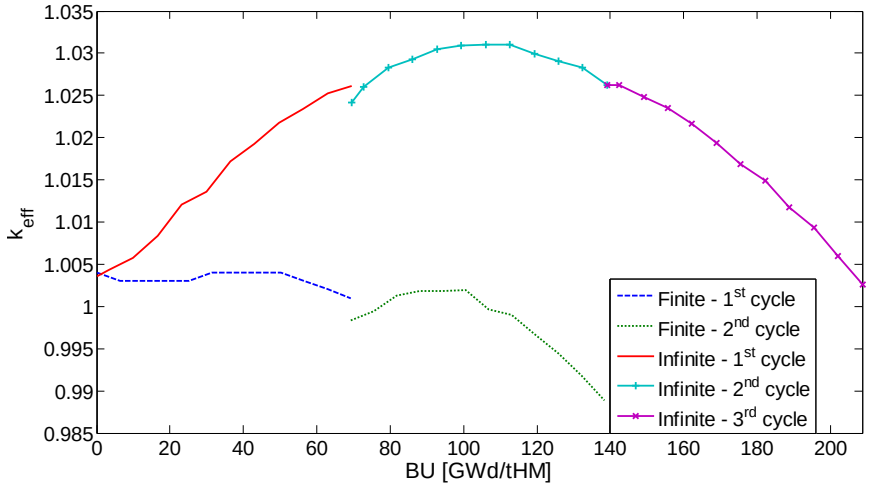

Figure 3.2: Reactivity evolution for the small and infinite oxide fuelled cores

3.2.2 Uranium based metallic fuel

The finite metallic fuelled core is loaded with 17.48 MT of heavy metal and has a specific power density of 7.15 W/g. The critical TRU concentration is 12.3% for the finite core and 9.67% for the infinite core. Figure 3.3 shows the multiplication factor evolution in these two cores. It is found that the maximum attainable burnup, using a single batch fuel management, is 24% FIMA and 41% FIMA for, respectively, the finite and infinite metallic core. The peak fast neutron fluence for the finite core is 3.7×10^{23} cm^{-2}; comfortably below the $4 \times 10^{23} cm^{-2}$ constraint assumed.

The maximum k_∞ value reached with the infinite metallic core is significantly larger than that reachable with oxide fuel, Figure 3.2, indicating that the metallic fuelled core has a significantly larger initial breeding ratio. This is consistent with the initial TRU loading required for the two core types – 9.67 wt% for the metallic fuelled core versus 15.16 wt% for the oxide fuelled core. This large difference in the initial TRU loading is due to the differences in the HM loading and in the spectra – the spectrum of the oxide fuelled core is softer. The number of

oxygen nuclei in the oxide core is significantly larger than the number of zirconium nuclei in the metallic fuelled core and the oxygen is more effective than zirconium in neutron slowing down.

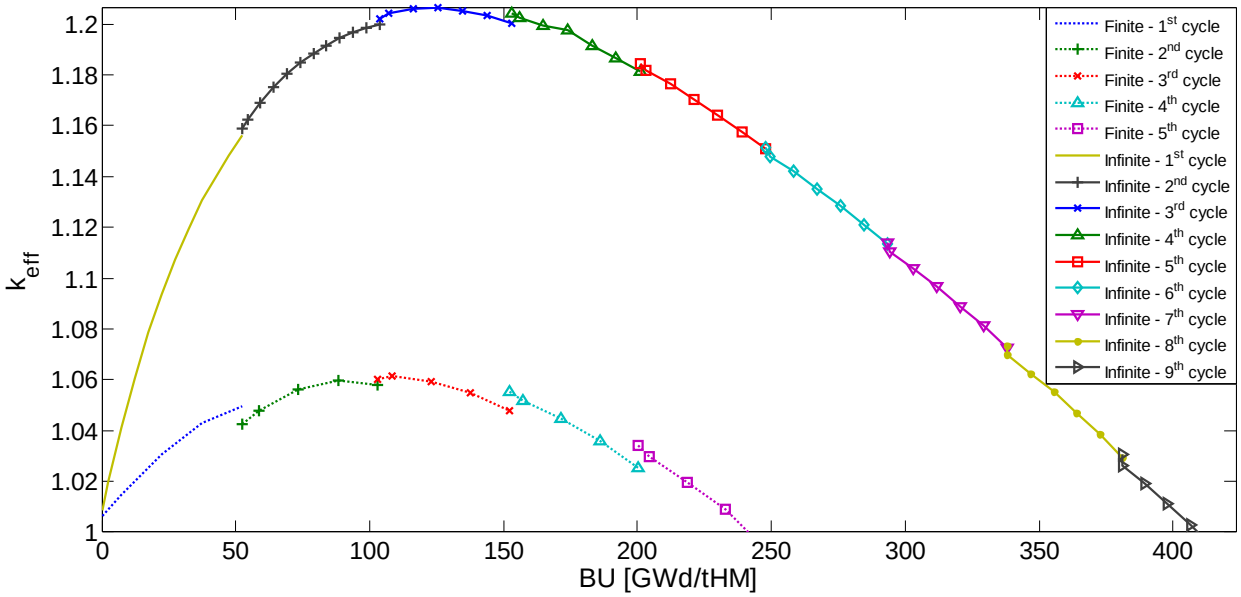

Figure 3.3: Reactivity evolution for the small and infinite metallic uranium fuelled cores

For the small metallic core, the first recycling decreases the core reactivity although the following recyclings are increasing more and more the core reactivity. These trends can be understood with the help of the data provided in Table 3.4. During the 3 years assumed for recycling, a fraction of the high η ^{241}Pu is decaying into the lower η ^{241}Am thus reducing reactivity. The addition of depleted uranium make-up also reduces the core reactivity; the combined effect is approximately 350 pcm. However, the removal of the volatile and gaseous fission products is increasing the reactivity by about 425 pcm. In addition, the axial averaging of the fuel composition before loading into the second core decreases the reactivity by 560 pcm because the fissile material is preferentially bred in the central part of the core in which the power density is larger and the reactivity worth is also larger. The net effect is a drop in reactivity from the end of the first cycle to the beginning of the second cycle. However, as the fission products concentration builds-up, averaging of the fuel composition during the recycling has the opposite effect – decreasing the amount of fission products at the central part of the core where their negative reactivity worth is the highest, and increasing the fission products concentration in the outer, low importance parts of the core. For the second to fourth recyclings, the composition averaging increases the core reactivity by, respectively, 110 pcm, 530 pcm and 795 pcm.

The infinite core model is a unit cell made of a single depletion zone. Therefore, there is no composition averaging. The fuel recycling reactivity shifts due to the fuel cooling, volatile and gaseous fission products removal and the fuel make-up is very small for the infinite core because all these term just about balance each other.

Table 3.4: Reactivity Changes due to Fuel Recycling for the Small Metallic Uranium Core

Reactivity changes [pcm]				
Recycling No.	1	2	3	4
Cooling [3 y]	-449	-175	-168	-240
Removal of gaseous and volatile FPs	461	505	380	409
Addition of depleted uranium makeup	-142	-215	-49	-95
Composition averaging	-560	113	529	795
Combined effect	-690	228	692	869

Tables 3.5 and 3.6 give information on the neutron balance in the infinite metallic fueled core and its variation from BOL to end-of-life (EOL). The fraction of neutrons absorbed in the fuel, clad and coolant stays approximately constant from BOL to EOL. However, at EOL, about 27% of the neutrons absorbed in the fuel are absorbed in the fission products (FP).

Table 3.5: Fraction of Neutrons Absorbed in the Core Constituents at BOL and EOL for the Infinite Metallic Uranium Fueled Core

Neutron absorption fraction		
Component	BOL	EOL
Fuel	96.32%	96.90%
Gap (Na)	0.37%	0.00%
Cladding	2.78%	2.60%
Coolant	0.53%	0.50%

Table 3.6: Fraction of Neutrons Absorbed in the Fuel Isotopes at BOL and EOL for the Infinite Metallic Uranium Fueled Core

	Neutron absorption fractions				
	^{238}U	^{239}Pu	^{241}Pu	FP	Other
BOL	59.16%	24.57%	4.36%	0.00%	11.91%
EOL	31.70%	30.73%	1.15%	27.22%	9.21%

3.2.3 Thorium based metallic fuel

Figure 3.4 shows the multiplication factor evolution for an infinite thorium-based core. The initial fuel composition is natural thorium plus the critical amount – 13.0 weight %, of TRU from fuel discharged from LWR at 50 GWd/tHM. As the crystalline structure of thorium is face-centered cubic (FCC), it is more stable than pure uranium and does not need to be alloyed with zirconium. The thorium density assumed is 11.65 g/cm^3; somewhat smaller than that of the metallic uranium fuel. The smear density assumed is 75%. There is only 1.45 kg of heavy metal (HM) loaded in the thorium fuel rod versus 1.77 kg for the metallic uranium fuel rod. The maximum value k_∞ gets to with burnup is 1.16 versus 1.21 for the metallic uranium fuel, as shown in Figure 3.3. This is because the η value of ^{233}U is smaller than that of, primarily, ^{239}Pu, in the hard spectrum of the systems examined.

The scenario examined for the thorium fuelled core uses the same assumptions than for the uranium fuelled infinite core: the gaseous fission products are continuously removed during operation and the fuel is recycled with an AIROX-like process every 20 years. In this scenario, thorium make-up fuel is added, corresponding to approximately 2% of the initial mass. This approach is only theoretical since it conserves the fuel mass, but not the fuel volume. The maximum burnup attainable is found to be 38% FIMA. This value is 8.2% lower than for the metallic uranium fuel under the same conditions. Adding the make-up fuel increases the amount of heavy metal consumed and the time required to achieve the maximum burnup. The core average fast neutron fluence accumulated during the 20 EFPY cycle is approximately $2.3x10^{23}cm^{-2}$ for the infinite thorium core versus $2.44x10^{23}cm^{-2}$ for the metallic uranium core.

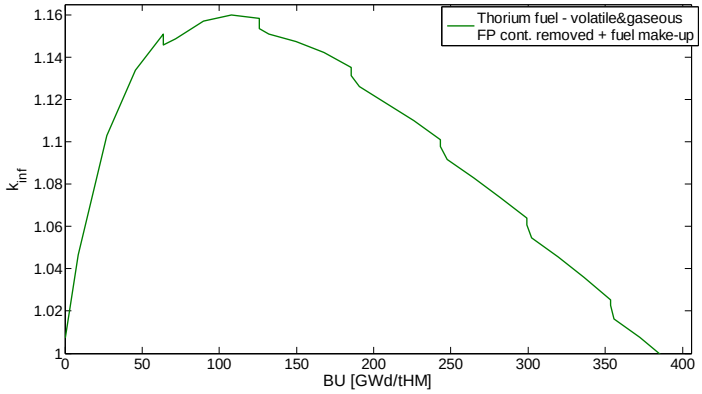

Figure 3.4: Reactivity evolution with burnup of the infinite thorium fuelled core with fuel make-up

Table 3.7: Comparison of the Fractional Neutron Absorption in the Fuel Isotopes for the Infinite Metallic Uranium and Metallic Thorium Cores; Volatile & Gaseous FP are Continuously Removed

	Metallic uranium			Metallic thorium	
	BOL	BU=38%	BU=42%	BOL	BU=38%
^{232}Th	-	-	-	53.74%	35.38%
^{233}Pa	-	-	-	0%	0.08%
^{233}U	-	-	-	0%	37.10%
^{238}U	59.20%	33.30%	31.30%	0%	0%
^{239}Pu	24.60%	32.80%	31.10%	28.73%	0.97%
^{240}Pu	4.20%	5.30%	5.30%	4.83%	2.01%
^{241}Pu	4.40%	1.20%	1.30%	5.07%	0.55%
Other HM	7.60%	4.20%	4.00%	7.63%	7.45%
FP	0%	23.20%	27.00%	0%	16.46%

Table 3.7 compares the neutron balance in the thorium and uranium based metallic fuelled cores. A much larger fraction of neutrons are absorbed, at EOL, in the fission products of the metallic uranium fuel than of the thorium fuel, even for a comparable burnup – BU=38% FIMA. At this burnup the macroscopic absorption cross-section of the heavy metal of the thorium fuel is only 7% smaller than that for the metallic uranium fuel. On the other hand, the macroscopic absorption cross-section of the fission products is 43% smaller for the thorium fuel than for the metallic uranium fuel. This difference is primarily due to the different fission products yield; ^{233}U fissions yield significantly fewer non-volatile isotopes having a large effect on the neutron capture, than the fission of ^{239}Pu: Tc, Ru, Rh Pd and Ag isotopic densities are about 2.5 times smaller in the thorium based core than in the uranium based core. The fraction of neutrons absorbed in each fission product isotope is compared in Figures 3.5 and 3.6 for the uranium fueled core and the thorium fueled core at 38% FIMA burnup.

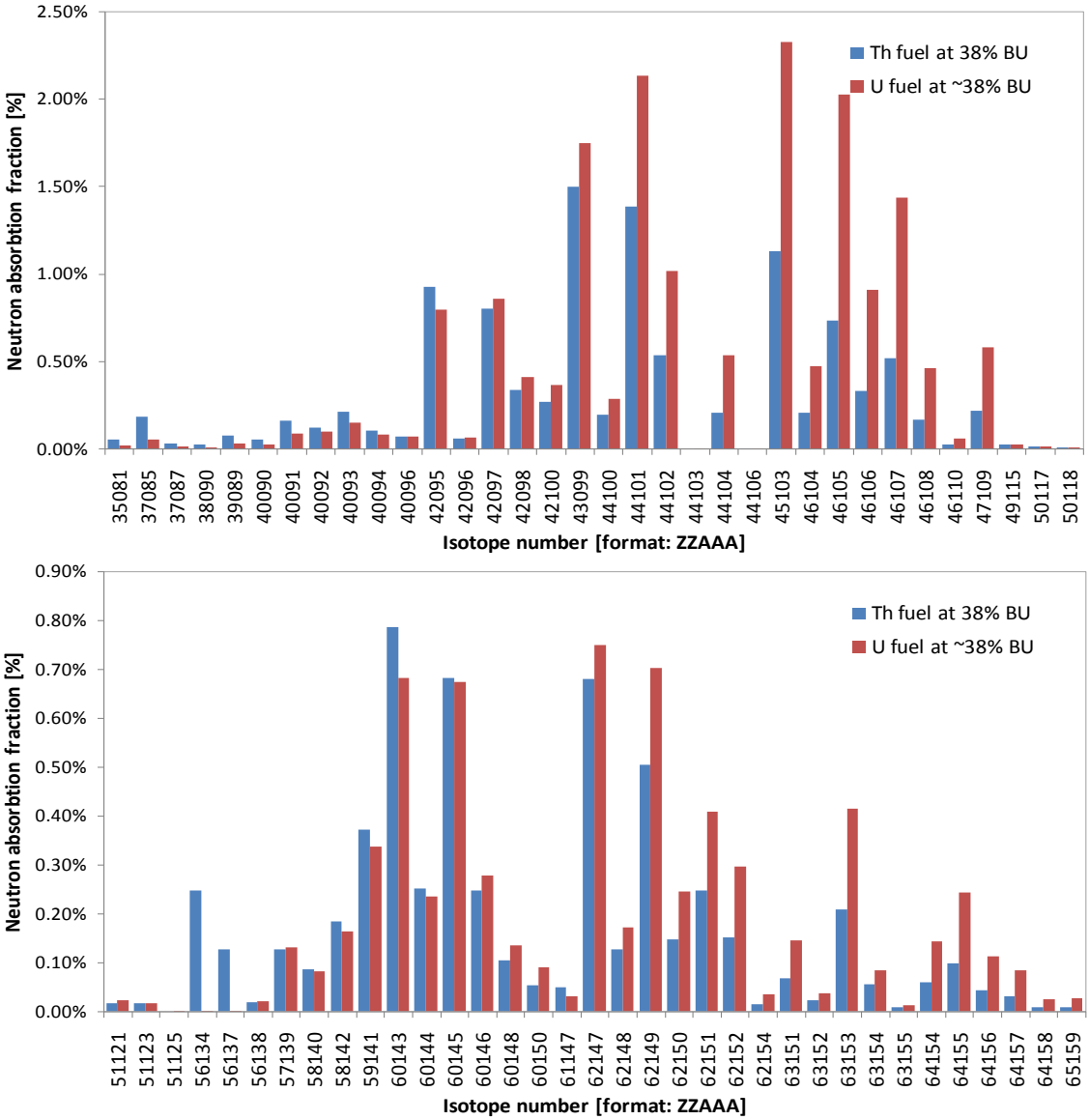

Figures 3.5 and 3.6: Comparison of the neutron capture fraction in the fission products of the uranium fueled core and thorium fueled core

3.3 Attainable multi-batch burnup

The discharge burnup of any of the cores examined above can be significantly increased by using multi- rather than single- batch fuel management – as commonly done in all commercial reactors. Figure 3.7 gives the upper bound on the attainable burnup using multi-recycling with limited processing in metallic uranium fueled core – with initial TRU loading. This upper bound is obtained by considering an infinite system and assuming a fuel management scheme having "infinite" number of batches; that is, by averaging the burnup-dependent k_∞ plots (continuous and diamond lines) over the burnup, thus obtaining the dotted line and "+" line of Figure 3.7. The upper bound on the attainable burnup is the burnup value at which the batch average k_∞, described by Equation 3.1, equals 1.0; it is found to be 725 GWd/tHM – a 73% increase over the single-batch burnup. The corresponding attainable burnup for the infinite metallic thorium fuelled core, inferred from Figure 3.8, is 672 GWd/tHM – a 77% increase over the corresponding single-batch burnup. The amount of HM the quoted burnup values pertain to is the summation of the initial HM load and the depleted uranium or thorium makeup added each recycling.

$$\frac{1}{k_\infty^{ave}} = \frac{1}{BU}\int_0^{BU} \frac{1}{k_\infty(BU)}\, dBU \qquad \text{(Eq. 3.1)}$$

The "bullet" and "diamond" lines in Figures 3.7 and 3.8 pertain to a mode of operation without any fuel processing. Although not realistic, the results are displayed to show that the recycling with limited processing mode-of-operation examined in this study provides some benefits also in terms of the amount of energy that can be generated per reactor, before the fuel has to be completely replaced.

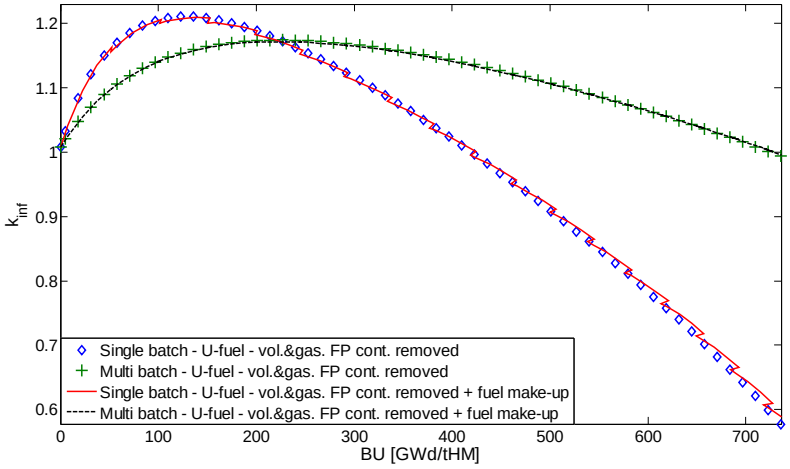

Figure 3.7: k_∞ evolution in infinite metallic uranium fuelled fast reactor cores operating in a single-batch mode (continuous and diamond lines) versus infinite-batch mode (dotted and "+" lines). "+" and "diamond" lines correspond to continuous core operation without recycling of any kind

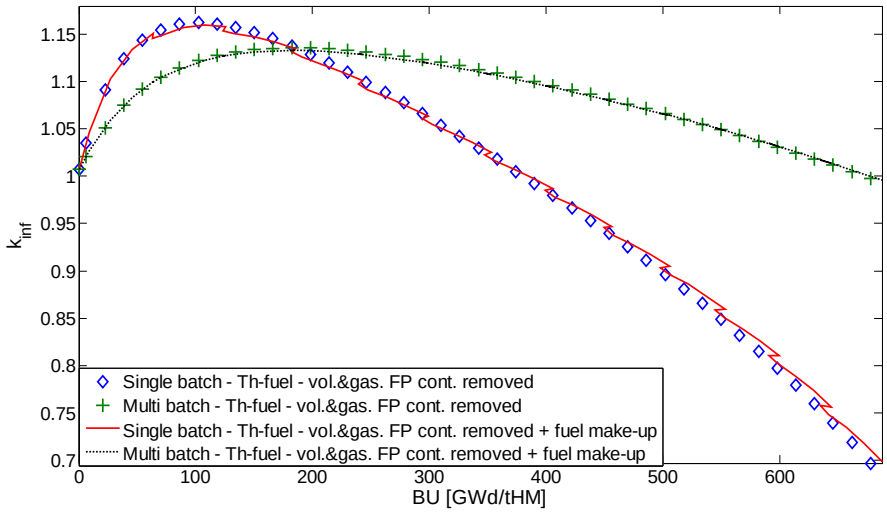

Figure 3.8: k_∞ evolution in infinite metallic thorium fuelled fast reactor cores operating in a single-batch mode (continuous and diamond lines) versus infinite-batch mode (dotted and "+" lines). "+" and "diamond" lines correspond to continuous core operation without recycling of any kind

3.4 Sensitivity analysis

The sensitivity of the attainable burnup to a number of the design parameters is studied for the infinite metallic core without any recycling. Although not realistic from the radiation damage perspective, this approach was adopted in order to save computational time. What are looked for are the relative changes. The reference case, Case 1 in Table 3.8, is the infinite metallic core, mentioned above, in which the attainable single-batch burnup is 39% FIMA. The reference parameters include lead bismuth eutectic (LBE) coolant, a P/D ratio of 1.1 and removal of no fission products. Following is a brief discussion of the results obtained.

When the initial fissile fuel is enriched with ^{235}U (Case 2) rather than with TRU, the attainable burnup is reduced by 2.6%. This is because the average η value of ^{235}U is smaller than that of the fissile plutonium isotopes.

Increasing the P/D ratio from 1.1 to 1.3 (Case 3) reduces the attainable burnup by 6.2%. This is due to increased parasitic neutron losses in the coolant and to the softening of the neutron spectrum.

Replacing lead-bismuth eutectic by sodium coolant (Case 4) does not result in any notable change. The neutron capture probability in LBE is larger than in sodium resulting in slightly decreased parasitic neutron losses in the coolant. It also has a significantly larger scattering macroscopic cross-section; it is more than twice larger than sodium. Using LBE instead of sodium in a finite core will decrease the neutron leakage probability, enabling achieving a larger maximum discharge burnup.

Continuously removing the volatile and gaseous fission products (Case 5) increases the attainable burnup by 9.2%. It is assumed that these gaseous fission products leak from the metallic fuel into the fission gas plenum during the reactor operation. They are modeled as being released from the fuel, but are not added to the plenum composition; their effect on the axial neutron leakage is ignored.

Increasing the core power density by a factor of 5 (Case 6) results in a 1.3% increase in the attainable burnup. This is due, primarily, to an increase in the fraction of the ^{241}Pu that fissions before decaying to ^{241}Am.

Table 3.8: Attainable Burnup Sensitivity to Coolant Type, P/D Ratio, Fissile Material, Volatile FP Removal and Power Density

Parameters						Achievable performances		
Case #	Fissile	P/D	Coolant	TRU %	Other	BU [GWd/tHM]	BU [%]	Relative length
1 (ref.)	TRU	1.1	Pb-Bi	9.67	-	383.5	38.9%	1
2	U235	1.1	Pb-Bi	8.51	-	371.2	38.0%	0.97
3	TRU	1.3	Pb-Bi	10.6	-	359.8	36.6%	0.94
4	TRU	1.1	Na	9.64	-	385.5	39.1%	1.01
5	TRU	1.1	Pb-Bi	9.67	Partial FP removal	419.5	42.6%	1.09
6	TRU	1.1	Pb-Bi	9.67	Power dens. increased	388.4	39.4%	0.2

3.5 Fuel resources implications

3.5.1 Fuel utilization

Table 3.9 compares the upper-bound estimates of fuel resource utilization and selected waste characteristics of the infinite metallic U and Th systems addressed in Figures 3.7 and 3.8 with that of a light water reactor that operates to 50 GWd/tHM. If realistic systems will perform even half-as well, the proposed multi-recycling with limited processing mode of operation will offer significant advantages over LWR operating on the OT fuel cycle in terms of U (Th) ore utilization and actinides waste minimization. That is, multi-recycling in fast reactors with limited processing as hereby proposed is expected to increase six fold the natural uranium ore utilization and reduce fivefold the amount of TRU that need be disposed of per unit of electricity generated, as compared to those attainable from LWR that operate on the once-through fuel cycle.

Table 3.9: Fuel Cycle Characteristics of Multi-recycling with no Chemical Separation Versus Once-trough LWR

Characteristic	LWR	Infinite U core	Infinite Th core
Initial fissile fuel type	U	TRU	TRU
Fissile fuel wt. %	4.5	9.67	13
Discharge burnup (GWD/tHM)	50	725	677
Fraction of initial TRU left (%)		56.6	5.1
TRU discharged per GWD generated (g/GWD)	300	75.5	9.7
^{233}U discharged per GWD (g/GWD)	-	-	42.4
Relative TRU discharged per GW_eD (%)	100	20.8	2.7
Relative U_{nat} consumption per GW_eD with enriched U(%)	100	15.6	--
Fraction of initial Pu left (%)	--	61.5	4.3
Fraction of fissile Pu left (%)	--	56.4	0.7
Fissile/total Pu at BOL/EOL (%)	-/64.5	64.5/66.0	64.5/15.7
^{238}Pu/total Pu at BOL/EOL (%)	-/3.2	3.2/2	3.2/11.0
^{237}Np+^{241}Pu+^{241}Am+^{245}Cm discharged (g/GWD)	58.6	5.2	1.8
Fraction of initial ^{237}Np+^{241}Pu+^{241}Am+^{245}Cm left (%)	--	21.5	5.2

3.5.2 Actinides discharged composition

Tables 3.10 and 3.11 compare the isotopic composition of, respectively, the U and TRU discharged from each of the reactors inter-compared in Table 3.9. The plutonium discharged from the thorium fuelled reactor has, as expected, the smallest fraction of fissile isotopes and the largest concentration of ^{238}Pu and other even isotopes. The fraction of ^{239}Pu plus ^{241}Pu in the plutonium discharged from the uranium-fuelled fast reactor is smaller than that discharged from the LWR. The concentration of ^{237}Np and its precursors – ^{241}Pu, ^{241}Am and ^{245}Cm – is the largest in the LWR, followed by the thorium-fuelled fast reactor; the uranium-based fast reactor has significantly smaller concentration.

Table 3.10: Concentration, in Weight Percent, of the Uranium Isotopes Discharged from the Reactors Inter-compared

	LWR	Infinite U core	Infinite Th core
BU [GWd/tHM]	50	725	672
wt% of TRU	1.57	20.55	2.19
U-232	-	-	0.17%
U-233	-	-	61.85%
U-234	-	0.27%	26.60%
U-235	1.37%	0.08%	6.21%
U-236	0.69%	0.23%	5.17%
U-238	97.95%	99.42%	-

Table 3.11: Concentration, in Weight Percent, of the Transuranium Isotopes Discharged from Two of the Fast Reactors Versus that of the Fuel Discharged from LWR[a]

	LWR	Infinite U core	Infinite Th core
BU [GWd/tHM	50	725	672
wt% of TRU	1.57	20.55	2.19
Np-237	5.03%	0.61%	7.60%
Np-239	0.62%	0.03%	-
Pu-238	2.25%	2.22%	9.24%
Pu-239	52.21%	52.08%	3.34%
Pu-240	18.86%	32.55%	36.22%
Pu-241	13.98%	3.38%	4.21%
Pu-242	4.51%	3.85%	19.82%
Am-241	0.53%	3.11%	5.69%
Am-242m	0.01%	0.22%	0.47%
Am-243	0.91%	1.05%	6.77%
Cm-242	0.17%	0.07%	0.14%
Cm-244	0.83%	0.63%	4.72%
Cm-245	0.08%	0.12%	1.01%
Cm-246	0.01%	0.07%	0.68%
Cm-247	-	0.01%	0.07%
Cm-248	-	-	0.03%

[a] The concentration of all TRU isotopes not given in this table is smaller than 0.01 weight %

3.5.3 Waste characteristics

Figures 3.9 through 3.12 compare, respectively, the radio-toxicity of the actinides and of the fission products, the decay heat from the actinides and the spontaneous neutrons emission as a function of time after discharge from each one of the three reactors compared in Tables 3.9 through 3.11. The results are normalized per unit of electricity generated. The fast reactors energy conversion efficiency is assumed being 40% versus 33% of the reference LWR due to the higher coolant operating temperature.

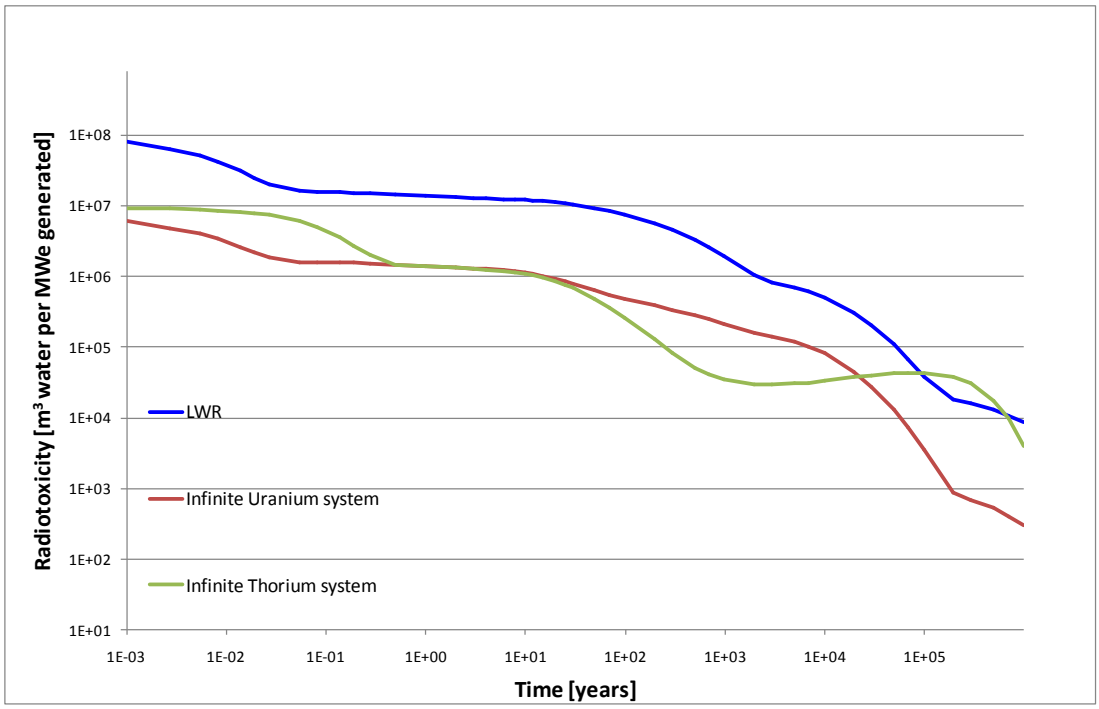

Figure 3.9: Radio-toxicity of the actinides discharged from the fast reactors versus LWR, normalized per unit of electric energy generated, as a function of time after discharge.

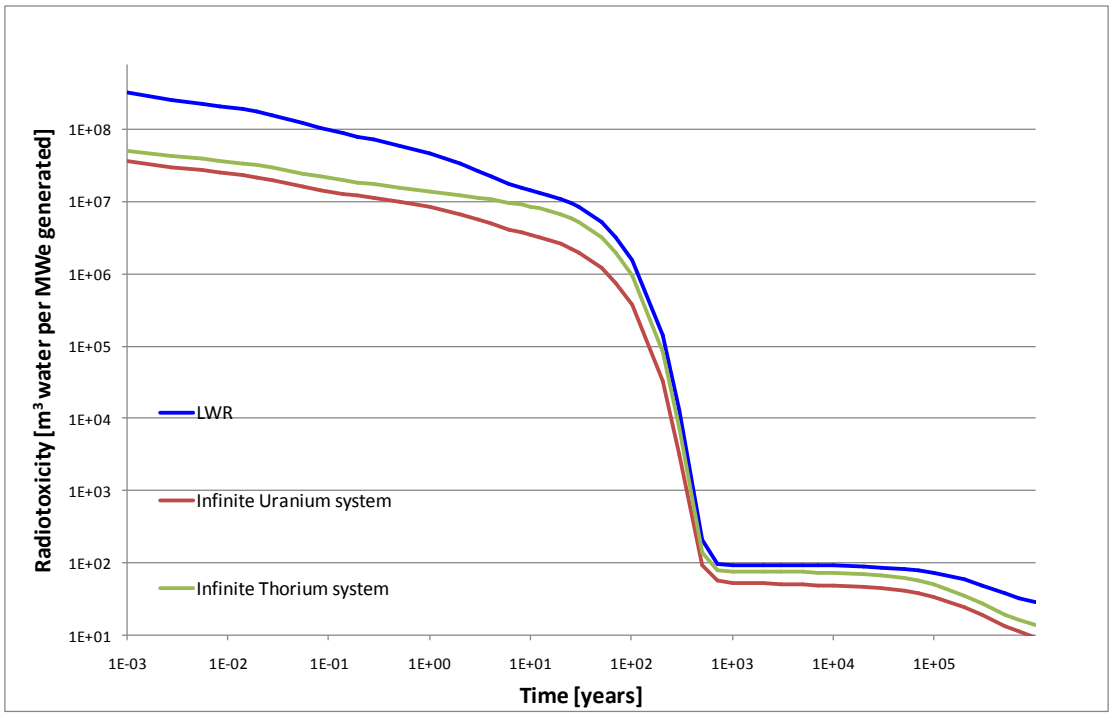

Figure 3.10: Radio-toxicity of the fission products discharged from the fast reactors versus LWR, normalized per unit of electric energy generated, as a function of time after discharge.

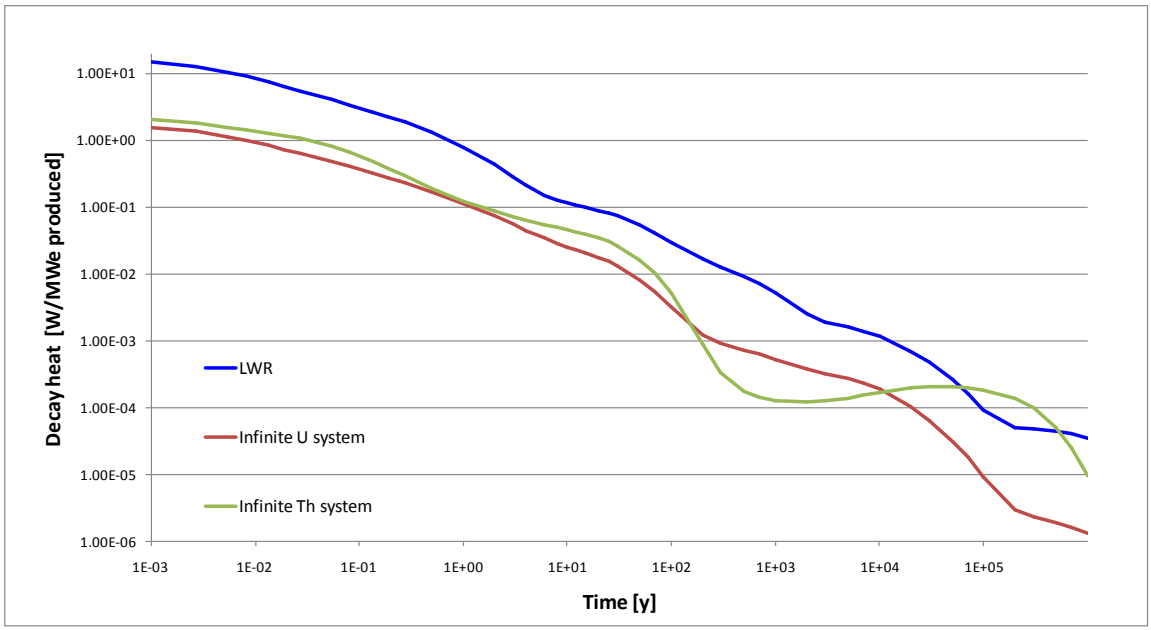

Figure 3.11: Decay heat from the fuel discharged from the fast reactors versus LWR, normalized per unit of electric energy generated, as a function of time after discharge.

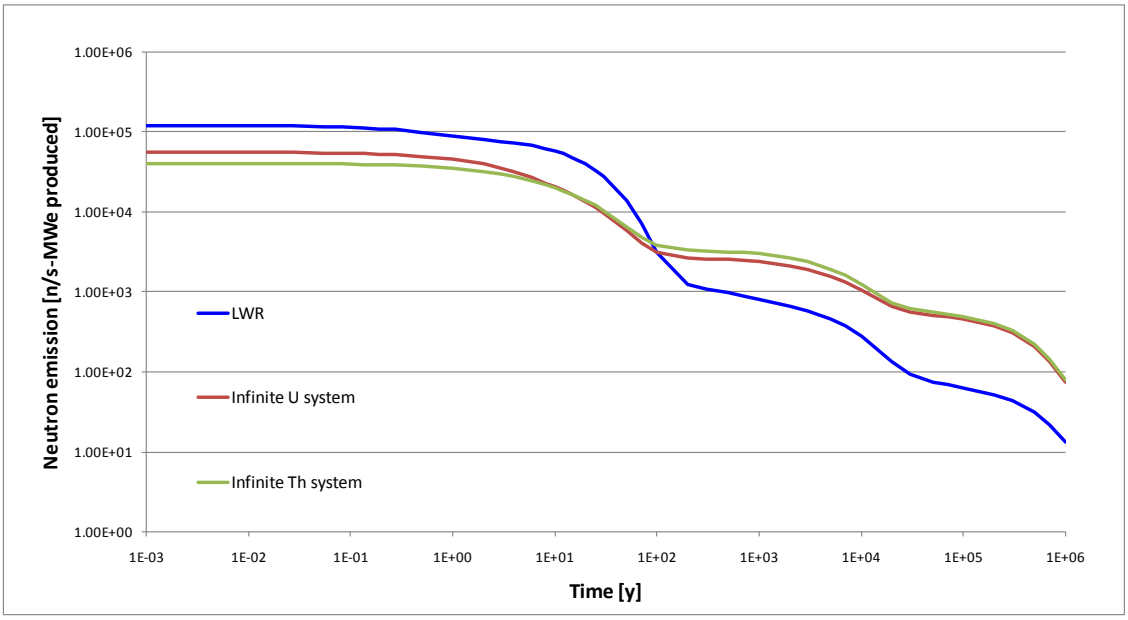

Figure 3.12: Spontaneous neutrons emission from the fuel discharged from the fast reactors versus LWR, normalized per unit of electric energy generated, as a function of time after discharge. Including primarily spontaneous fission neutrons and (α,n) neutrons.

It is observed that the radio-toxicity of the fission products from the fast reactors is initially one order of magnitude smaller than from the LWR until ~500 years following the fuel discharge, at which time most of the unstable fission products decayed. Thereafter, the differences in the radio-toxicity level become small. The radio-toxicity of the heavy metal discharged from the fast reactors is always ~4-5 times smaller than for the LWR discharged heavy metals except for the thorium fuelled fast reactor following ~10^5 years after discharge. The

larger radio-toxicity at that time is mostly due to the build-up of ^{229}Th from the decay of ^{233}U the half-life of which is 1.59E+5 years.

In the decay heat evolution shown in Figure 3.11, the deviation between the Th curve and the other curves is due to the same isotopes buildup mentioned above. However, the decay heat in the long time range is of no practical significance. Initially and for the first 10^4 years, the decay heat of the fuel discharged from the fast reactors is one order of magnitude smaller than the value for the LWR discharged fuel.

The neutron emission rate evolution from the discharged fuels displayed in Figure 3.12 exhibits a different behavior. The main contributors to spontaneous neutron emission are the curium and even plutonium isotopes. The three humps in the plots correspond each to the half-life of a major neutron emitter. The first hump is due to the decay of ^{244}Cm (18.1 y), the second to the decay of ^{240}Pu (6564 y) and ^{246}Cm (4730 y) and the last to the decay of ^{242}Pu (3.733E+5 y). Being rich in ^{244}Cm, the LWR has initially a higher spontaneous neutrons yield, but after ~100 years it drops to a level smaller than that of the other fuels because of the lower amount of the other primary spontaneous neutron emitters.

3.6 Conclusions and Discussion

In this chapter, it has been found that the maximum achievable burnup in an infinite core, with a single batch fuel management scheme, is 20% FIMA for uranium based oxide fuel, 41% FIMA for uranium based metallic fuel and 38% FIMA for thorium based metallic fuel. With an infinite-batch fuel management scheme it is theoretically possible to achieve burnup as high as 74% FIMA with uranium based metallic fuel, corresponding to a uranium utilization factor of 4.0%. Per unit of energy generated, the infinite cores fueled with uranium or thorium based metallic fuel are featuring a radiotoxicity and decay heat almost one order of magnitude smaller than for a once-trough LWR operating at 50 GWd/tHM and a spontaneous neutron emission approximately five times smaller during 100 years after discharge.

The burnup and, correspondingly, uranium ore utilization and waste minimization achievable in a real system is expected to be significantly smaller because of neutron leakage and neutron loss to reactivity control elements that are required to compensate for the burnup reactivity swing. By designing a very large core, it is theoretically possible to achieve a nearly zero neutron leakage probability, but that would result in a significantly positive coolant void reactivity coefficient due to spectrum hardening. It is possible to partially mitigate the positive reactivity effect of spectrum hardening by increasing of the neutron leakage probability from a finite but not from an infinite core.

Concerning the burnup reactivity swing, it has been found that for the infinite core fueled with uranium based metallic fuel, the multiplication factor becomes as high as 1.20. In order to maintain k_{eff} close to unity in a finite core without the help of the control systems, it is necessary to design a shuffling scheme resulting in a small burnup reactivity swing. The more fuel batches in a reactor, the easier it is to achieve this goal. However, with many fuel batches, the time between two cycles will be very short, and the time required for fuel shuffling may become significant, strongly decreasing the capacity factor of the reactor.

Finally, after designing an acceptable core geometry and fuel shuffling scheme, it will be necessary to validate the core concept by calculating the reactivity coefficients to insure the proper behavior of the core in case of basic accidents.

Chapter 4

Achievable Burnup in Fast Reactors Using Conventional Fuel Management

In Chapter 3, the maximum achievable burnup with metallic fuel has been assessed for an infinite core model and a small, very leaky core, both operating at low power density. The mode of operation consisted in loading the core with enriched fuel, operating it until it becomes subcritical and then replacing the burnt fuel with fresh enriched fuel. The infinite core model is a convenient approach for a quick determination of an upper bound of the maximum achievable burnup but does not yield practical results, while the small core yields practical results but is not a typical core design enabling achieving very high burnup due to the significant amount of neutrons lost by leakage. In order to obtain practical estimates of the maximum burnup in fast reactors, it is necessary to use a finite core model that accounts for a reasonable neutron leakage probability and that operates at a power level consistent with that of commercial fast reactors.

In this chapter, the maximum achievable burnup is assessed for both the large 3000 MW_{th} core and for the S-PRISM size 1200 MW_{th} core, the details of which have been discussed in Section 2.1.2 and 2.1.3. The performances of those two core designs are estimated for a single- and infinite-batch fuel management schemes for a scenario where no radial blanket is used and for a scenario for a large radial blanket is used instead of the radial reflector.

The achievement of the maximum burnup that is limited by the lack of reactivity requires multi-recycling of the fuel. When a fuel element reaches 20% FIMA burnup, corresponding to approximately 400 DPA accumulated in the cladding, all the fuel elements are recycled using the melt-refining process described in Section 1.2.2. In order to simplify the fuel cycle simulation, the fuel recycling is assumed to occur instantaneously. This does not account for the decay of certain isotopes, in particular ^{241}Pu, during the fuel recycling and therefore very slightly overestimates the k_{eff} value of the reactor. After being reconditioned, the fuel elements are reloaded in the core at the same location as they have been discharged from. The initial fissile fuel loaded in the core is made of TRU mixed with depleted uranium having 0.2 wt% ^{235}U. The TRU is recovered from fuel discharged from LWR after 50 GWd/tHM and being cooled for 10 years. The structural material extensively used during this study is the ferritic martensitic stainless steel HT-9.

4.1 Fast reactor cores examined

The two fast reactor cores studied have been described in Section 2.1.2 for the large core and in Section 2.1.3 for the S-PRISM size core. The four scenarios studied in this section with a single and infinite-batch fuel management scheme are:

- Scenario (a): large 3000 MW_{th} core with a large radial reflector and no blanket;
- Scenario (b): large 3000 MW_{th} core with a radial blanket but no radial reflector;
- Scenario (c): S-PRISM size core with a radial reflector and no blanket;
- Scenario (d): S-PRISM size core with a radial blanket but no radial reflector.

For scenario (b), the small radial reflector described in Section 2.1.2 is removed in order to be consistent with the core model used for scenario (d), where no radial reflector is used. The radial reflector on Figure 2.1 is replaced with the radial shield, conserving its thickness, 20.5 cm. The outer shield diameter is decreased from 5.35 m to 4.44 m.

A design similar to scenario (b), the Ultra-long Life Fast Reactor (ULFR), has recently been proposed by Kim & Taiwo [19]. In the ULFR design the radiation limit constraint is released and no fuel recycling is envisioned. In addition, the ULFR core volume is 3.6 times larger than the 3000 MW_{th} core volume and the fuel used is U-Pu-Mo. Despite those differences, the total core power is the same, 3000 MW_{th} and the core is also composed of enriched fuel elements and blanket elements. They found that this ULFR design can achieve a burnup up to 303 GWd/tHM in the enriched fuel regions and less than half this value in the blanket because of the significantly larger blanket to enriched fuel volume fraction than in Scenario (b).

The fuel management approach assumed for the present analysis is the same for both the large core and the S-PRISM size core. The initial cycle is stopped when a fuel element reaches the burnup limit. For HT-9, experiments have shown good performance up to 200 DPA [52], but no experiment has been performed at higher DPA. This corresponds to approximately 100 GWd/tHM (~10% FIMA). It is however assumed that by the time this reactor concept will be fully developed and ready for deployment the cladding material will be able to withstand about 400 DPA. Therefore, the burnup limit used for this study is 20% FIMA. When this limit is reached in a fuel element, all the fuel and blanket elements are recycled using the melt-refining process described in Section 1.2.2. All the fuel elements discharged from a batch are recycled together, yielding a single fuel composition per batch after recycling. After the melt-refining, the fuel is refabricated and all the fuel elements are reloaded in the core at the same location as they have been discharged from. There is no fuel shuffling occurring.

The full core recycling done whenever a fuel element reaches its radiation damage limit is not a practical way to manage the fuel: most of the fuel elements can reside in the core for at least two consecutive cycles without exceeding the clad damage limit. Recycling of only the fuel elements that reached and are closing to reach the clad damage limit will enable decreasing the cost and time of fuel recycling. However, doing a partial fuel recycling will result in a larger amount of fission products in the core, and thus, larger neutron capture, slightly decreasing the achievable burnup. The achievable burnups obtained in this section are slightly larger than the burnups achievable with partial fuel recycling.

4.2 Large 3000 MW_{th} fast reactor

The performance of the large 3000 MW_{th} core is analyzed both with – scenario (b) – and without radial blanket – scenario (a), for both a single- and infinite-batch fuel management schemes. The maximum achievable burnup with a single-batch fuel management scheme is reached when k_{eff} becomes smaller than unity. With a large number of batches, the maximum achievable burnup is reached when the average $k_{eff} - k_{ave}$ defined by Equation 4.1 becomes unity. This assumes that the core multiplication factor is maintained equal to unity by shuffling the batches.

$$\frac{1}{k_{\text{ave}}} = \frac{1}{BU}\int_0^{BU} \frac{1}{k_{\text{eff}}\,(\text{BU})}\,dBU \qquad \text{(Eq. 4.1)}$$

When the reactor is started, the uncontrolled core multiplication factor increases because the breeding ratio is larger than unity due to the tight P/D ratio and large fraction of fertile material. As the fission products accumulate in the fissile zones of the core, the parasitic neutron capture increases, making the breeding ratio smaller than unity, and reducing the uncontrolled multiplication factor. The evolution of k_{eff} and k_{ave} for the two scenarios considered is presented in Figure 4.1. It is found that for scenario (a) the achievable burnup is 35.0% FIMA (339 GWd/tHM, blue curve) for the single-batch fuel management scheme and 58.0% FIMA (561.5 GWd/tHM, red curve) for the infinite-batch fuel management scheme. When replacing the large radial reflector by a blanket having the same volume as the enriched fuel zone, plus a smaller radial reflector, scenario (b), the achievable burnups in the enriched fuel zone increase to 47.0% FIMA (green curve) and 65.3% FIMA (orange curve) for the single- and infinite-batch fuel management schemes, respectively. This represents an improvement of +34% for the single-batch burnup and +12.6% for the infinite-batch burnup.

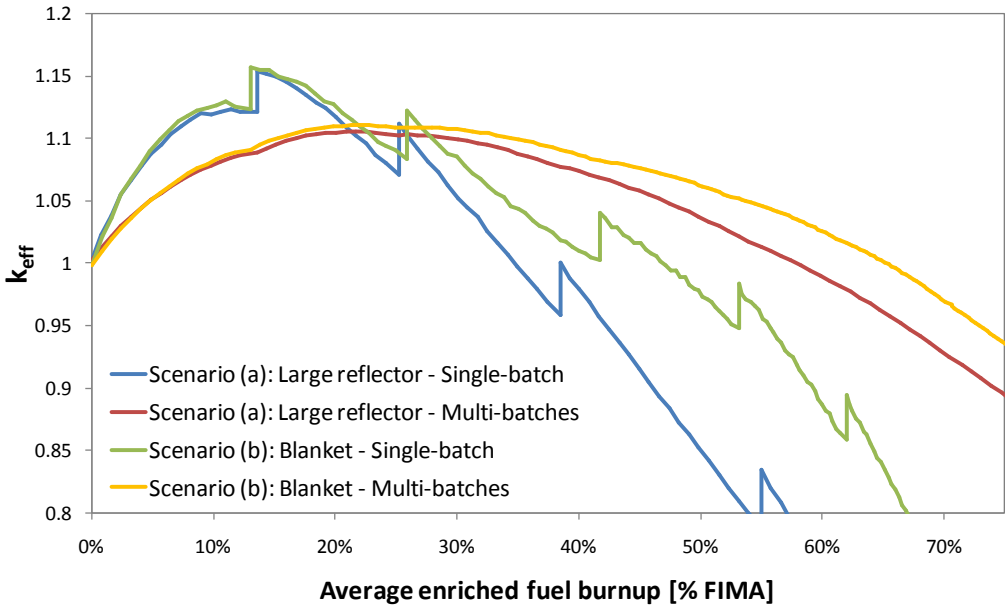

Figure 4.1: Single- and infinite-batch multiplication factor evolution for scenario (a) and (b) – large 3000 MW_{th} core

The discontinuities occurring in the k_{eff} evolution for the single-batch fuel management schemes correspond to the occurrence of fuel recycling. The radiation damage limit is not reached at the same time for the two scenarios studied. For scenario (b), the radial blanket produces some power, slightly decreasing the power fraction generated in the enriched fuel and its damage accumulation rate. The fuel recycling for scenario (b) is occurring at longer time intervals than scenario (a) where 100% of the power is produced in the enriched fuel. The burnup accumulation in the enriched fuel of the scenario (b) is slower, but when reaching high burnup, the fissile material bred in the radial blanket enables sustaining the chain reaction for a longer period of time, resulting in a larger achievable burnup for both the single- and infinite-batch fuel management schemes. The average blanket burnups corresponding to the single- and infinite-batch fuel management schemes are 11.7% FIMA and 39.7% FIMA, respectively.

The evolution of the neutron leakage probability from the active core is shown in Figure 4.2 and the radial power density distribution at three different burnups is given in Figure 4.3 for scenario (a) and Figure 4.4 for scenario (b). The axial neutron leakage probability, not shown in Figure 4.2, is probability is approximately constant at 4% for both scenarios. At BOL the radial neutron leakage probability is 10.2% for scenario (a) and only 0.6% for scenario (b) because most of the neutrons leaking radially are captured in the blanket by ^{238}U and the power peaks away from the core center due to the non-uniform fissile fuel loading (See Section 2.1.2). At 13.6% FIMA the power peaks at the core center, thereby decreasing the radial neutron leakage probability for scenario (a) due to the larger distance between the neutron production site and the outer core boundary. The same effect is observed for scenario (b), but the radial leakage probability is initially very small due to the large radial blanket, and thus, does not significantly decrease. Towards the EOL the power peaking shifts radially away from the core center as the central core zone has the highest concentration of fission products. As a consequence the radial neutron leakage probability is increased.

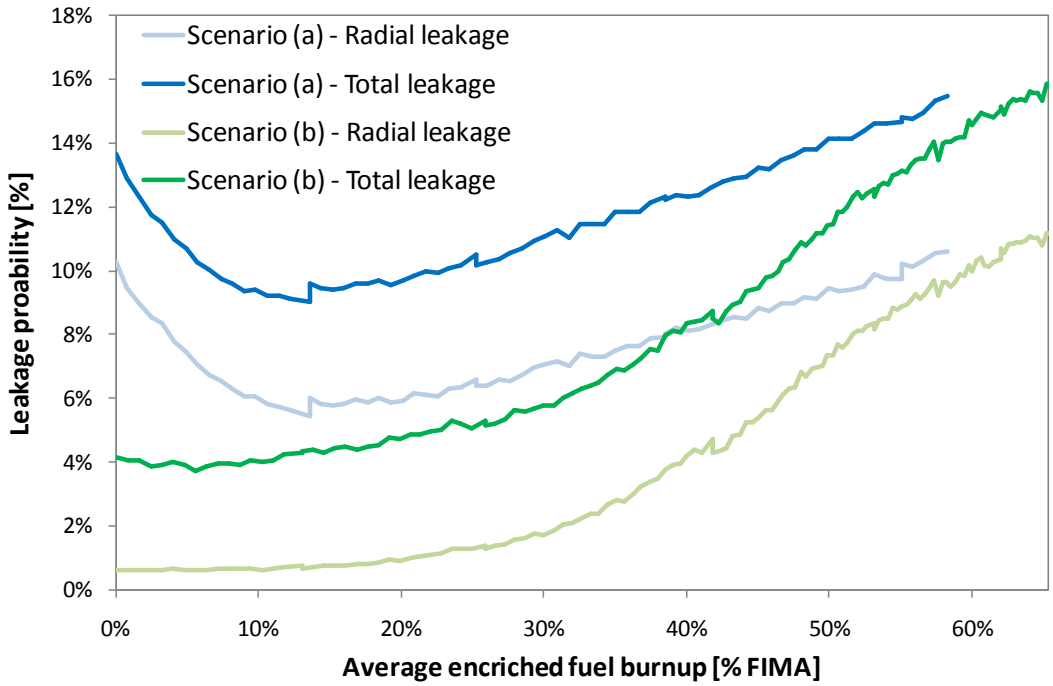

Figure 4.2: Radial and total neutron leakage probability evolution for scenarios (a) and (b)

As shown by Figure 4.5, the peak power density of scenario (b) is decreasing from 370 W/cm^3 to 200W/cm^3, while for scenario (a) it slightly increases up to 420 W/cm^3 before decreasing to 260 W/cm^3. The initial TRU enrichments had been chosen such as to minimize the initial increase of the peak power fraction. The optimization had been performed for the core for scenario (b). This explains why the peak power density slightly increases for scenario (a) and not for scenario (b). The presence of the radial blanket enables smearing the power over a larger volume thus decreasing the peak power density but increasing the radial power peaking factor: from 2.58 at BOL it drops to 1.34 by EOL for scenario (b) while for scenario (a) it stays between 1.44 and 1.03. The axial power peaking factor is similar for both scenarios and varies from 1.34 at BOL to 1.15 at EOL. End-of-life corresponds to the maximum achievable burnup with the infinite-batch fuel management scheme.

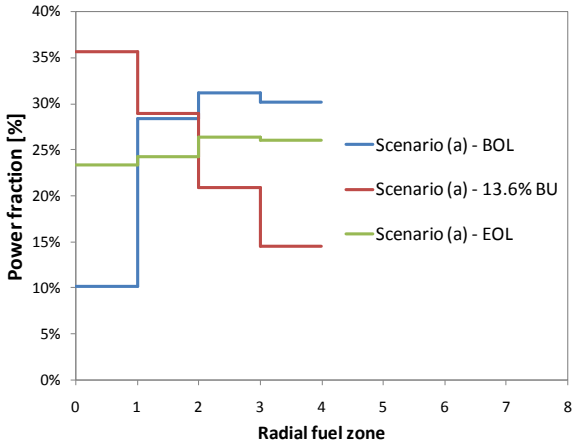

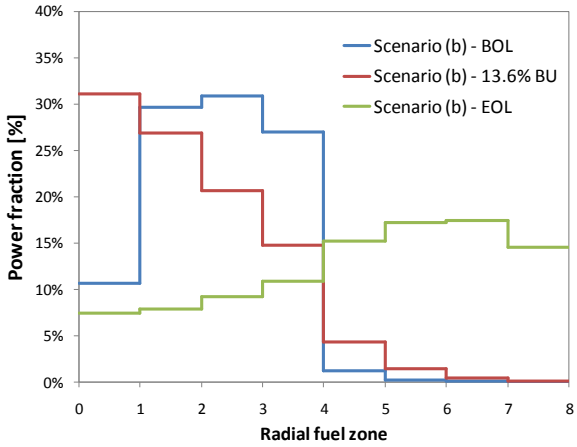

Figures 4.3 and 4.4: Radial power distribution at BOL, 13.6% FIMA in enriched fuel and EOL for the large 3000 MW_{th} core: scenario (a) on left; scenario (b) on right

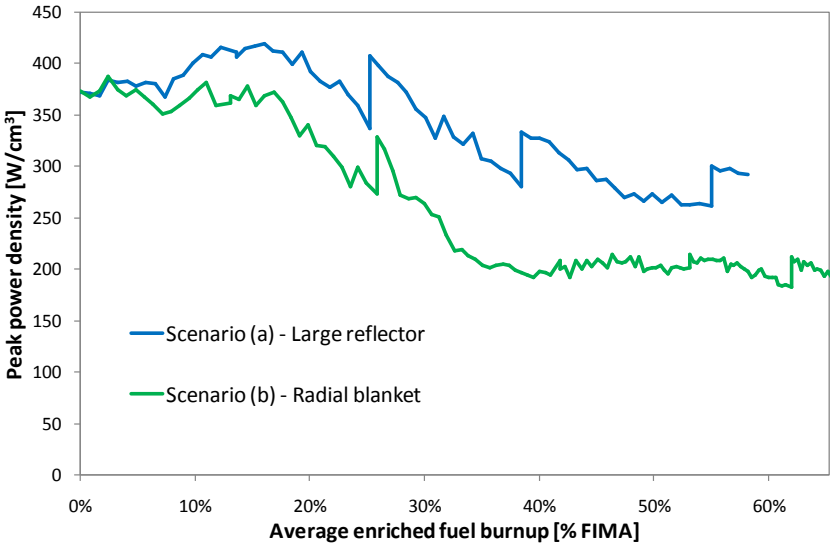

Figure 4.5: Peak power density evolution with average enriched fuel burnup for scenarios (a) and (b)

The HM inventory and HM and TRU vectors composition of the fuel discharged from the large 3000 MW_{th} fast reactor core using an infinite-batch fuel management scheme are summarized in Table 4.1. Due to the larger breeding gain achieved by using a radial blanket, the total mass of fissile plutonium isotopes in the core of scenario (b) is approximately twice larger than in the core of scenario (a). The mass of ^{237}Np and its precursors is also found to be almost twice larger in the core of scenario (b) than in the core of scenario (a). The TRU vector composition in the enriched fuel is also more favorable with scenario (a) since the fissile plutonium bred in the core has been consumed while in scenario (b) the plutonium bred in the blanket has not been much consumed. The fissile plutonium represents 61.7 wt% of the TRU for scenario (a) and 67 wt% in scenario (b). In the blanket, it represents 72 wt% of the TRU. At EOL, the blanket is made of 14.8 wt% TRU and could be used as the startup fuel for a new core if one could partially separate the fission products: the minimum average TRU enrichment to make the core critical is 11.45 wt%, when no fission products are present. Due to the high fissile content of the blanket and the impossibility to separate the fission products from the heavy metal with a highly proliferation resistant process, scenario (b) is perceived less proliferation resistant than scenario (a), despite the larger burnup achieved in the enriched fuel.

Table 4.1: Heavy Metal and TRU Vectors of the Fuel Discharged for Scenario (a) and (b) at EOL

	U and TRU discharge composition at EOL								
	Scenario (a)			Scenario (b) - Enriched fuel			Scenario (b) - Blanket		
Isotope	Mass [kg]	HM wt%	TRU wt%	Mass [kg]	HM wt%	TRU wt%	Mass [kg]	HM wt%	TRU wt%
^{234}U	10.5	0.0%	-	11.7	0.0%	-	3.8	0.0%	-
^{235}U	3.6	0.0%	-	3.6	0.0%	-	3.6	0.0%	-
^{236}U	13.7	0.0%	-	15	0.1%	-	17.1	0.0%	-
^{238}U	24233.9	81.5%	-	19829.3	80.7%	-	36509.2	85.2%	-
^{237}Np	31.9	0.1%	0.6%	22.2	0.1%	0.5%	41.1	0.1%	0.7%
^{239}Np	7.7	0.0%	0.1%	2.8	0.0%	0.1%	5.2	0.0%	0.1%
^{238}Pu	53.3	0.2%	1.0%	43.5	0.2%	0.9%	38.5	0.1%	0.6%
^{239}Pu	3135.4	10.5%	57.3%	2667.9	10.9%	56.4%	4369.1	10.2%	69.3%
^{240}Pu	1729.9	5.8%	31.6%	1549.5	6.3%	32.8%	1574.5	3.7%	25.0%
^{241}Pu	242.8	0.8%	4.4%	190.4	0.8%	4.0%	170.9	0.4%	2.7%
^{242}Pu	195.8	0.7%	3.6%	163.3	0.7%	3.5%	57.5	0.1%	0.9%
^{241}Am	21.3	0.1%	0.4%	45.2	0.2%	1.0%	37.1	0.1%	0.6%
^{242}Am	0.7	0.0%	0.0%	1.6	0.0%	0.0%	1.3	0.0%	0.0%
^{243}Am	18.6	0.1%	0.3%	18.7	0.1%	0.4%	6.2	0.0%	0.1%
^{242}Cm	1.4	0.0%	0.0%	1.6	0.0%	0.0%	1.4	0.0%	0.0%
^{244}Cm	25	0.1%	0.5%	14	0.1%	0.3%	2.6	0.0%	0.0%
^{245}Cm	5.7	0.0%	0.1%	3.3	0.0%	0.1%	0.4	0.0%	0.0%
^{246}Cm	3.3	0.0%	0.1%	2.7	0.0%	0.1%	0.1	0.0%	0.0%
All TRU	5472.9	18.4%	-	4726.7	19.2%	-	6305.8	14.7%	-

With an infinite-batch fuel management scheme in the large 3000 MW_{th} core, it has been found possible to achieve a burnup up to 58% FIMA when the enriched fuel is surrounded with a reflector (a), and up to 65.3% in the enriched fuel and 39.7% in the blanket when the enriched

fuel is surrounded with a blanket of same volume (b). When the enriched fuel is fabricated with the TRU recovered from the LWR UNF and the depleted uranium generated when enriching the fuel for LWR, it is possible to multiply the amount of electricity generated by the LWR, per ton of uranium mined, by 2.81 and 4.27 with scenarios (a) and (b), respectively.

It is assumed that when using enriched uranium instead of TRU based fuel, the required ^{235}U enrichment is equal to the TRU enrichment found to be 11.45% in Section 2.1.2. In reality, the ^{235}U enrichment will be slightly smaller. With this assumption, the above mentioned achievable burnup corresponds to a uranium utilization factor – not accounting for the thermal efficiency – of 2.63% for scenario (a) and 4.76% for scenario (b). For comparison, the uranium utilization factor of the ULFR is estimated to be approximately 2.3%, significantly smaller than for scenario (b).

4.3 S-PRISM size 1200 MW_{th} fast reactor performance

The study performed for the large 3000 MW_{th} fast reactor is replicated for the S-PRISM size 1200 MW_{th} fast reactor described in Section 2.1.3. Two similar scenarios are studied for this core: (c) the enriched fuel is surrounded by a large radial reflector without radial blanket; and (d) the enriched fuel is surrounded by an equal volume radial blanket without radial reflector. Due to the smaller dimensions and lower power density (see Section 2.1) of this reactor, it is expected that its neutron economy and attainable burnup will be inferior to those of the large core. On the other hand, this core is similar in dimensions to the S-PRISM and the Advanced Liquid Metal Reactor [53] cores and is expected to feature more acceptable reactivity coefficients.

Figure 4.6 shows that the maximum single- and infinite-batch achievable burnups are, respectively, 28.7% FIMA (274 GWd/tHM, blue curve) and 45.9% FIMA (442 GWd/tHM, red curve) for scenario (c) and are 32.7% FIMA (green curve) and 52.4% FIMA (orange curve) for scenario (d). The average blanket burnup corresponding to the single- and infinite-batch mode of operation are, respectively, 3.4% FIMA and 16.7% FIMA. Similarly to the large 3000 MW_{th} fast reactor previously studied, the achievable burnup is larger when there is a radial blanket because the neutrons radially leak out of the enriched fuel zone into the blanket where they are breeding plutonium. When the fissile to fission products atom ratio in the enriched fuel zone becomes low, the reactor is maintained critical thanks to the fissile material bred in the blanket.

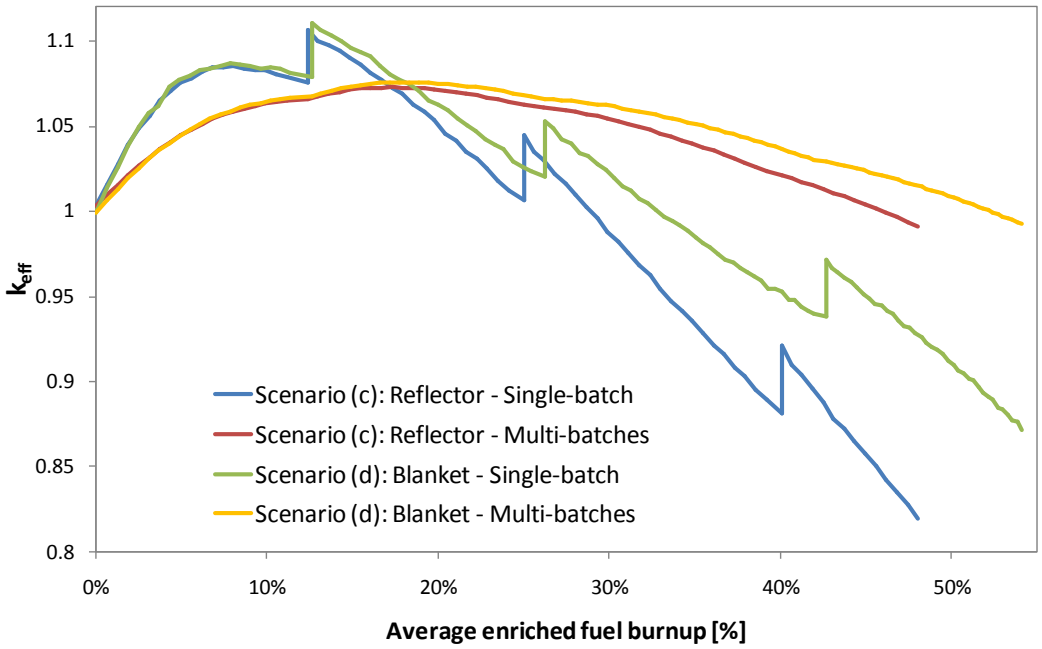

Figure 4.6: Single- and infinite-batch multiplication factor evolution for scenarios (c) and (d) – S-PRISM size core

The use of a radial blanket enables extending the enriched fuel burnup by +13.9% and +14.1% for the single- and infinite-batch fuel management schemes, respectively. The gain for the infinite-batch management scheme is similar to the gain found for the large 3000 MW_{th} core, but the gain for the single-batch management scheme is significantly smaller – it was +34% for the large core. This difference is explained by the fact that, for the large core, a fuel recycling occurs at 41.8% FIMA burnup, right before k_{eff} becomes smaller than unity. If this recycling was to occur slightly later, the single-batch burnup for the large core would then be limited to this burnup, 41.8% FIMA, instead of 47.0% FIMA. Furthermore, as shown by Figure 4.7, the use of a radial blanket decreases the neutron leakage probability at BOL by approximately 8%: approximately 50% of all the neutrons leaking out from the enriched fuel zone are absorbed in the blanket and the other 50% are mostly lost due to axial leakage. In the large core, the blanket decreases the neutron leakage probability by approximately 10%; approximately 73% of all the neutrons leaking out of the enriched fuel zone are absorbed in the blanket and the other 27% are mostly lost due to axial leakage. As burnup is increasing, the radial neutron leakage probabilities of scenarios (b) and (d) are increasing. For the large core, the radial leakage probability becomes as large as for scenario (a).

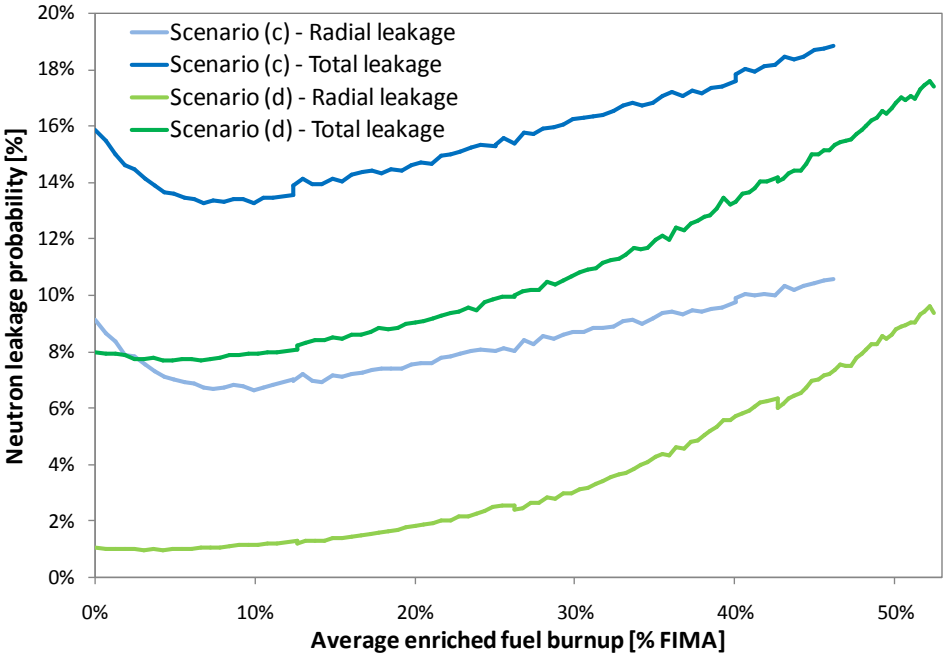

Figure 4.7: Radial and total neutron leakage probability evolution for scenarios (c) and (d)

The initial decrease in the neutron leakage probability for scenario (c) corresponds to the same phenomena described in Section 4.2 for the large 3000 MW_{th} core: the power distribution first moves inward, decreasing the radial leakage probability. The radial power distribution is given in Figures 4.8 and 4.9 at BOL, at the minimum leakage probability (6.8% FIMA burnup) and at EOL for the S-PRISM size reactor, for scenarios (c) and (d).

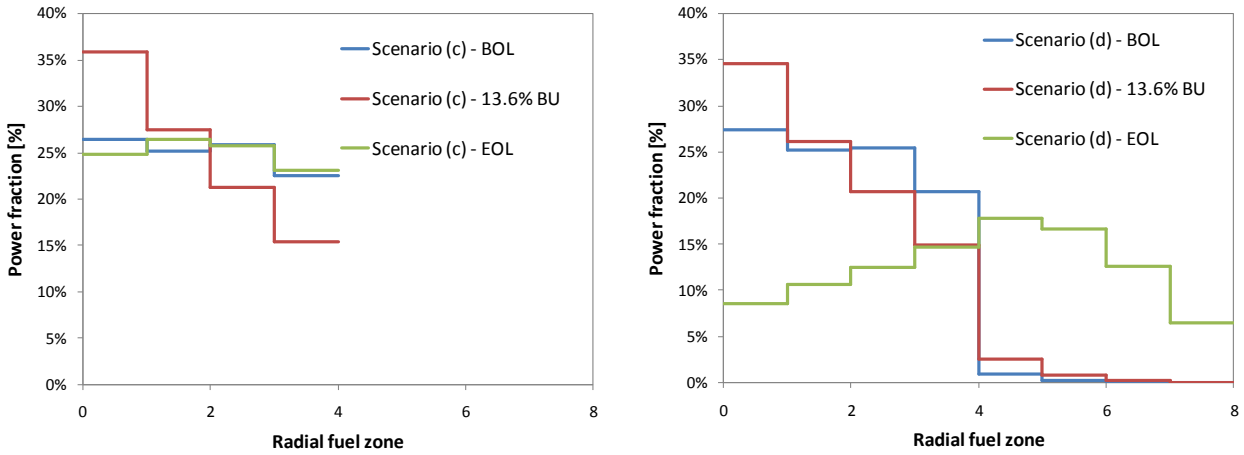

Figures 4.8 and 4.9: Radial power distribution at BOL, 6.8% FIMA burnup – in enriched fuel – and EOL for the S-PRISM size core: scenario (c) on left, scenario (d) on right.

The initial TRU enrichment has been chosen to flatten the radial power profile at BOL, and therefore the peak power density, shown in Figure 4.10, occurs at the burnup corresponding to the minimum leakage probability, 6.8% FIMA. Despite a peaking factor of 1.87 and 3.57 for scenario (c) and (d), respectively, the peak power density does not exceed 300 W/cm^3 in both cases, comfortably below the commonly used value of 450W/cm^3 [9]. From the thermal

hydraulics standpoint, the key characteristic is the radial power peaking factor: for scenario (c) and (d) it is equal to 1.47 and 2.78, respectively. When approaching EOL, the radial power peaking factor becomes approximately 1.06 for scenario (c) and 1.42 for scenario (d). The same total power being generated by a volume twice larger, the radial power peaking factor is always larger for scenario (d) than for scenario (c), but the peak power density is always larger or equal for scenario (c) than for scenario (d).

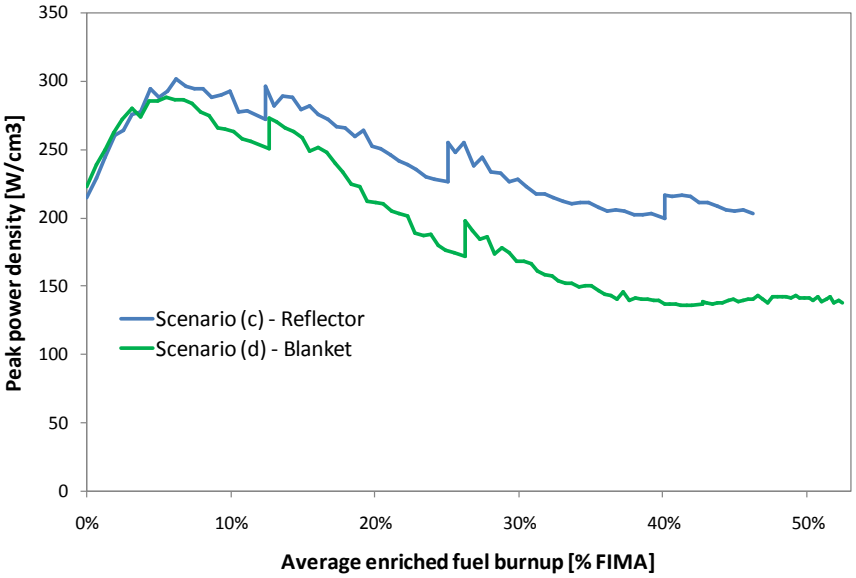

Figure 4.10: Peak power density evolution with average enriched fuel burnup for scenarios (c) and (d)

The heavy metal inventories and TRU vector compositions of the fuel discharged from the infinite-batch fuel management scheme for scenarios (c) and (d) are presented in Table 4.2. At EOL there is twice more TRU, fissile plutonium and ^{237}Np and its precursor left in the core of scenario (d) than in the core of scenario (c). With only 11 wt% TRU in the blanket, even by removing all the fission products, it is not possible to use it to start a new reactor: the average minimum required TRU enrichment to make the S-PRISM size reactor critical is 12.9 wt%, with no fission products. At EOL, the discharged fuel TRU contains 62.2 wt% of fissile plutonium for scenario (c) and 71.5 wt% for scenario (d). In the blanket of scenario (d), the fissile plutonium represents 82.0 wt% of the TRU and 9.0 wt% of all the heavy metals. Due the very high fissile plutonium content in the blanket, the small burnup (16.7% FIMA) and the impossibility to use the blanket to start another S-PRISM size core, scenario (d) is significantly less proliferation resistant than scenario (c).

Table 4.2: Heavy Metal and TRU Vectors of the Fuel Discharged for Scenarios (c) and (d)

	U and TRU discharge composition								
	Scenario (c)			Scenario (d) - Enriched fuel			Scenario (d) - Blanket		
Isotope	Mass [kg]	HM wt%	TRU wt%	Mass [kg]	HM wt%	TRU wt%	Mass [kg]	HM wt%	TRU wt%
^{234}U	12.2	0.1%	-	12.7	0.1%	-	1	0.0%	-
^{235}U	4.3	0.0%	-	3.9	0.0%	-	12.1	0.0%	-
^{236}U	11	0.1%	-	11.5	0.1%	-	10.9	0.0%	-
^{238}U	16656	82.1%	-	14702.3	81.6%	-	28033.6	88.9%	-
^{237}Np	29	0.1%	0.8%	21.3	0.1%	0.6%	19.9	0.1%	0.6%
^{239}Np	3.1	0.0%	0.1%	1.5	0.0%	0.0%	2	0.0%	0.1%
^{238}Pu	49.3	0.2%	1.4%	41.3	0.2%	1.3%	12	0.0%	0.3%
^{239}Pu	2100.6	10.4%	58.4%	1898.9	10.5%	57.7%	2800	8.9%	80.7%
^{240}Pu	1084.7	5.3%	30.2%	1008	5.6%	30.6%	564.8	1.8%	16.3%
^{241}Pu	137.5	0.7%	3.8%	113.1	0.6%	3.4%	45.1	0.1%	1.3%
^{242}Pu	130.6	0.6%	3.6%	114.7	0.6%	3.5%	8.5	0.0%	0.2%
^{241}Am	25.9	0.1%	0.7%	51.6	0.3%	1.6%	16.4	0.1%	0.5%
^{242}Am	1	0.0%	0.0%	2.4	0.0%	0.1%	0.6	0.0%	0.0%
^{243}Am	16.1	0.1%	0.4%	19.9	0.1%	0.6%	0.9	0.0%	0.0%
^{242}Cm	1.2	0.0%	0.0%	1.4	0.0%	0.0%	0.4	0.0%	0.0%
^{244}Cm	13.1	0.1%	0.4%	11.1	0.1%	0.3%	0.2	0.0%	0.0%
^{245}Cm	3.1	0.0%	0.1%	2.4	0.0%	0.1%	0	0.0%	0.0%
^{246}Cm	1.8	0.0%	0.1%	1.7	0.0%	0.1%	0	0.0%	0.0%
All TRU	3596.9	17.7%	-	3289.3	18.3%	-	3470.8	11.0%	-

When the enriched fuel used to feed the S-PRISM size core design is made with the TRU recovered from the LWR UNF and the depleted uranium generated by the LWR fuel enrichment process, it is found possible to multiply the amount of electricity generated by unit uranium mined by 2.23 for scenario (c) and 2.86 for scenario (d). Alternately, the feed fuel can be directly made of enriched uranium, assuming that the average enrichment level is 12.93%, identical to the required TRU enrichment found in Section 2.1.3. For scenario (c) and (d), the S-PRISM size reactor fed with enriched uranium enables extracting, respectively, 61% and 89% more energy per unit uranium mined than when the enriched uranium is loaded in LWR and reprocessed to fabricate TRU based fuel for the S-PRISM size reactor. The uranium utilization factors (not including the thermal efficiency) are then 1.84% for scenario (c) and 2.77% for scenario (d). Those values are smaller than for the large 3000 MW_{th} reactor because of the lower discharge burnup and higher enrichment required.

4.4 Conclusions and discussion

In order to make the k_{eff} of the large 3000 MW_{th} fast reactor core equal to unity at BOL with both scenarios (a) and (b), it is necessary to use an average TRU fuel enrichment of 11.45 wt%, corresponding to 8.16 tons of TRU. The maximum achievable burnup, assuming shuffling a large number of fuel batches, is estimated to be:

- 58.0% FIMA, when the enriched fuel is surrounded by a large reflector;
- 65.3% FIMA, when the enriched fuel is surrounded by a radial blanket plus a small reflector.

For a S-PRISM size fast reactor core, the required average initial TRU enrichment for scenario (c) and (d) is 12.93 wt%, corresponding to 4.86 tons of TRU. It is found that the maximum achievable burnup with an ideal infinite-batch fuel management scheme is:

- 45.9% FIMA, when the enriched fuel is surrounded by a large reflector;
- 52.4% FIMA, when the enriched fuel is surrounded by a radial blanket without reflector.

These results are to be compared with the theoretical maximum achievable burnup with no neutron leakage of 74% FIMA, obtained in Section 3.3. This value has been determined with a rather low power density, about three times smaller than in the two finite cores studied in this chapter. Using larger power density enables reaching slightly larger burnups and therefore it is expected that the theoretical maximum achievable burnup with the same power density as used in this chapter will be a few percent larger. Nevertheless, without use of a radial blanket it is possible to achieve ~78% and ~62% of the maximum theoretical burnup in the large 3000 MW_{th} core and the S-PRISM size core, respectively. When using a radial blanket in the two full core models, it is possible to achieve a discharge burnup – in the enriched fuel – representing ~88% and ~71% of the maximum theoretical value.

For the four scenarios studied in this chapter, the peak power density is below the maximum acceptable value. When the reactors are fed with enriched uranium, it has been found possible to achieve uranium utilization factors up to 2.63%, 4.76% for scenarios (a) and (b) in the large reactor and up to 1.84% and 2.77% for scenarios (c) and (d) in the S-PRISM size reactor. The values for the large reactor are than the value estimated for the ULFR because of the higher discharge burnup and lower required enrichment. In order to achieve larger uranium utilization factors, it would be required to decrease the required fuel enrichment since the uranium utilization factor varies with its inverse. From proliferation resistance point of view, the discharged fuel characteristics are improved when achieving larger burnup. However, while the radial blanket enables achieving larger discharge burnup in the enriched fuel, it makes the system less proliferation resistant because of the large amount of TRU and plutonium built-up at EOL in the blanket and the significant fraction of fissile plutonium: 72 wt% for the large reactor and 82 wt% for the S-PRISM size reactor. Development of a fuel cycle in which the blanket material would be used to make a new core, eventually adding some TRU to it, could make the blanket system more proliferation resistant than the system without blanket and increase the uranium utilization.

Chapter 5

Feasibility Study of Fast Reactor Cores using a Breed and Burn Mode of Operation

In the previous chapter it has been found that to achieve very high uranium utilization, it is necessary to decrease the fuel enrichment while maintaining a very high discharge burnup. The breed and burn mode of operation described in this chapter enables to use all the uranium mined to produce energy and is therefore offering a uranium utilization factor equal to the discharge burnup. Terra Power, LLC is presently pursuing [21] the vision of Edward Teller et al. of a Travelling Wave Reactor [14] in which the fuel is not recycled. Except for the initial critical fissile fuel loading (i.e. the igniter, also called starter or driver), this reactor type is to be fuelled with fertile material. The breeding gain needs to be sufficiently high to build up the fissile concentration in feed fuel elements fast enough to enable them to sustain the chain reaction before the fuel reaches its radiation damage limit. If this principle can be achieved, it will be possible to operate such breed and burn fast reactors on fertile fuel feed without need for fuel recycling. In this chapter, the minimum required burnup to sustain the breed and burn mode of operation is assessed for several simplified core models. First, the performance of a zero-dimensional unit cell is assessed in order to determine the theoretical minimum required burnup with metallic fuel to sustain the breed and burn mode. Then, in Section 5.2 and 5.3, a one-dimensional unit cell made of several slabs is used to determine the minimum required burnup when the fuel is shuffling for various core dimensions and assess the performance of different types of fuel. Finally, a one-dimensional cylindrical model having more practical characteristics is studied.

A number of studies have quantified the burnup required for propagating a “fission-wave” in fast reactors. Design studies of the CANDLE reactor concept by Sekimoto et al. [16, 54] reported that the burnup required for the fission wave to propagate in fast reactor cores fed with depleted or natural uranium is in the vicinity of 40%. Toshinsky proposed [15] a core design and multi-batch fuel management strategy in which a breed-and-burn mode of operation could be established with the fuel discharged at approximately 20% average burnup. However, in order to

be able to breed-and-burn with this relatively small discharge burnup, Toshinsky had to assume that the metallic fuel occupies 60% of the core volume; this is nearly 50% higher fuel volume fraction than in typical fast reactor core designs [9].

5.1 Theoretical minimum required burnup – 0-D system

5.1.1 Methodology

The first phase in a breed-and-burn mode of operation consists in building up the fissile content in fertile feed element until its $k_\infty * P_{NL}$ reaches unity where P_{NL} is the neutron non-leakage probability from the core. For the unit cells studied in Sections 5.1, 5.2 and 5.3, the neutron leakage probability is equal to zero, making $P_{NL}=1$. As k_∞ keeps increasing beyond unity, the feed element becomes a driver element – it produces more neutrons than required for sustaining a chain reaction. These excess neutrons can then be used to build up the fissile inventory (and k_∞) in other fertile feed elements. The theoretical minimum burnup required for establishing the breed-and-burn mode of operation is the burnup at which the total number of excess neutrons generated is equal to the total number of external neutrons that need to be absorbed in the feed element in order to bring its $k_\infty * P_{NL}$ to unity.

The simplest model used for estimating the theoretical minimum burnup required for establishing the breed-and-burn mode of operation is a zero-dimensional unit cell initially loaded with depleted uranium. The fuel is made of the metallic alloy U-Zr, with 7.5 wt% Zr. The metallic fuel density is taken to be 15.85 g/cm^3 and its smear density is 75%, to accommodate the fuel swelling with burnup. The feed fuel is assumed to be pure ^{238}U. Not accounting for the 0.2 wt% ^{235}U left in the depleted uranium is a conservative assumption since the presence of some ^{235}U will slightly increase the core k_{eff} and therefore the number of neutron available in the core. The structural and cladding material is HT-9 and both liquid sodium and lead-bismuth coolants are examined. The power density of the core is 300 W/cm^3 as is commonly used for liquid metal cooled fast reactors [9].

To simplify the analysis, the clad, gap, coolant and fuel are mixed conserving their volume. The volume fractions of this metallic fuelled core, corresponding to a small pitch-to-diameter ratio and large fuel rod diameter, are summarized in Table 5.1.

Table 5.1: Initial Volume Fractions of the Unit Cell Models

Core component	Volume fraction
Fuel - U(92.5)-Zr(7.5)	40.50%
HT-9	19.35%
Coolant Na/LBE	26.65%
Gap Na	13.50%

5.1.2 Minimum required burnup in a 0-D infinite unit cell

Figure 5.1 shows the evolution of k_∞ for the 0-D unit cell. For burnups smaller than the value marked by the orange vertical line (<33 GWd/tHM), the unit cell has a deficit of neutrons, and past this line, it is producing excess neutrons. The green vertical line marks the burnup (~130 GWd/tHM) beyond which the unit cell becomes a net producer of neutrons. The theoretical

minimum burnup is the burnup for which the total neutron production since beginning-of-life (BOL) is equal to the total neutron absorption. This condition is represented by Equation 5.1, where P_{CR} is the fraction of neutrons not lost in the reactivity control systems. The neutron production and absorption rates are expressed by Equations 5.2 and 5.3, where N_{HM} is heavy metal atomic density at BOL and ν is the average number of neutrons emitted per fission. The neutron production from the (n,2n) and (n,3n) has been assumed null. The magnitude of the theoretical minimum required burnup, BU_{th}, is finally obtained by Equation 5.4. When an infinite-batch fuel management scheme is assumed, it means that the uncontrolled k_{eff}=1 and therefore P_{CR}=1.

$$\int_0^{BU_{th}} P_{NL} * P_{CR} * n.prod.rate(\mathrm{BU}) = \int_0^{BU_{th}} n.abs.rate(\mathrm{BU}) \qquad \text{Eq. (5.1)}$$

$$n.prod.rate(\mathrm{BU}) = N_{HM} * \nu(\mathrm{BU}) * d\mathrm{BU} \qquad \text{Eq. (5.2)}$$

$$n.abs.rate(\mathrm{BU}) = n.prod.rate(\mathrm{BU})/\mathrm{k}_{\infty}(\mathrm{BU}) \qquad \text{Eq. (5.3)}$$

$$\int_0^{BU_{th}} \left[\frac{1}{k_{\infty}(\mathrm{BU})} - P_{NL} * P_{CR}\right] \nu(\mathrm{BU}) d\mathrm{BU} = 0 \qquad \text{Eq. (5.4)}$$

The minimum theoretical required burnup for this 0-D infinite unit cell (P_{NL}=P_{CR}=1) is found to be 13.1% FIMA both when using sodium coolant and lead-bismuth coolant.

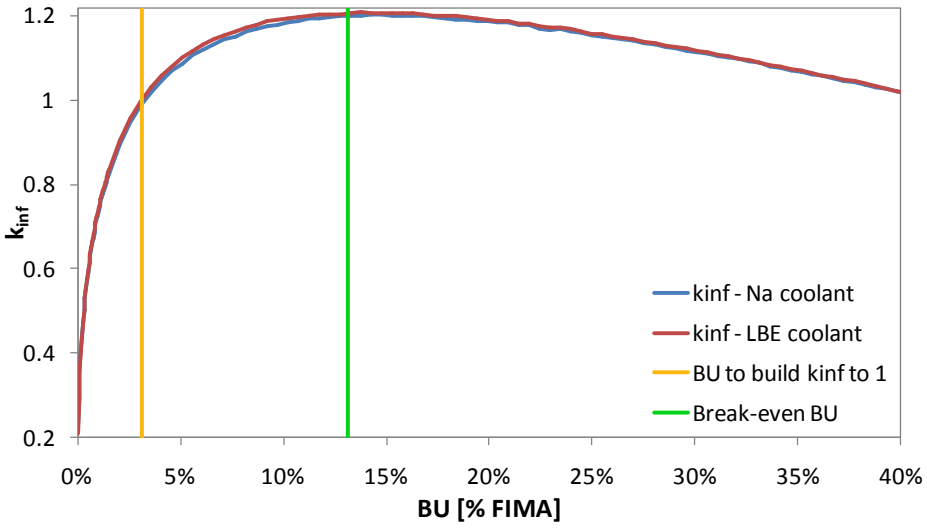

Figure 5.1: k_{∞} evolution for the 0-D unit cell with sodium and lead-bismuth coolant

The 0-D system examined above does not accurately represent the physics of the actual breed-and-burn core because, primarily, of spectral differences. The initial neutron spectrum in the system – depleted U – is harder than the spectrum expected in the low fissile content feed fuel elements that are segregated from the high fissile content fuel elements in which most of the fissions occur – and vice versa for the spectra in the high fissile content fuel elements. The spatial-dependent spectral effects are explored in the following section. Improved formulation of the 0-D approximation is presented by Petroski in [33].

5.2 Theoretical minimum required burnup – 2 zone unit cells

5.2.1 Methodology

The model used is a one-dimensional infinite unit cell made of two slabs of equal volume with reflective boundary conditions applied to the outer surfaces. Initially, one of the slabs is the igniter; it is made of depleted uranium and TRU. The other slab is the blanket or feed fuel; it is made of depleted uranium having 0.2 wt% ^{235}U. The core is assumed to operate in equal length cycles; at the end of a cycle the high-burnup slab is removed, the other is shuffled into its place, and a fresh depleted uranium feed is loaded into the blanket zone. This shuffling process followed by burnup analysis is continued until an equilibrium composition is reached. When equilibrium is reached, a neutron balance is done similarly to that reported in Section 5.1.2. If the left hand side of Equation 5.1 gives a positive value, there are excess neutrons in the system and the cycle length is decreased. This iterative process is continued until Equation 5.1 is satisfied.

The numerical analysis is done for metallic fuel of the specifications of Section 5.1.1. The initially loaded TRU is recovered from used fuel LWR that was discharged at 50 GWd/tHM and cooled for 10 years. The initial TRU composition does not affect the equilibrium cycle. The structural and cladding material is HT-9 and the coolant is liquid sodium. The core volume fractions are given in Table 5.1 and the total average power density assumed is 150 W/cm^3.

5.2.2 Minimum required burnup dependence on slab thickness

The minimum burnup required for a break-even neutron balance is determined for thicknesses ranging from 1 cm to 100 cm per slab – 2 cm to 200 cm for the total unit cell thickness. Table 5.2 summarizes the results obtained along with the maximum and minimum values of k_∞, at beginning and end of equilibrium cycle (BOEC and EOEC).

Table 5.2: Break-even Discharge Burnup, Minimum k_∞ and Maximum k_∞ for the 1-D Infinite Cell

Case #	Slab thickness [cm]	Break-even BU	Cycle length [yr]	k_∞ BEOC	k_∞ EOEC
1	1	14.31%	7	0.71817	1.14686
2	5	14.31%	7	0.72559	1.14753
3	10	14.30%	7	0.74066	1.14361
4	20	14.19%	7	0.7902	1.13469
5	40	13.50%	6.61	0.78568	1.09873
6	100	12.80%	6.26	0.47226	1.16091

The minimum required burnup found is 14.3% FIMA for any slab thickness up to 10 cm (20 cm total thickness). This value is somewhat larger than the 13.1% FIMA obtained for the 0-D system due to spectral differences between the 0-D and 1-D systems. For thicknesses below 10 cm the system dimensions are smaller than the neutron mean free path and despite the very small spectral differences the minimum required burnup stays approximately constant. When increasing the thickness above 10 cm, the system dimensions become similar or larger than the neutron

mean free path, resulting in more important spectral differences and decreased minimum required burnup. More surprising are the results obtained for the thick unit cells – the minimum required burnup for, say, the 100 cm thick slab system (case 6) – 12.8%, is smaller than that predicted for the thinner slab 1-D system (14.3% FIMA) and for the 0-D system (13.1% FIMA; Section 5.1.1). This difference also results from the spectral differences illustrated in Figures 5.2 and 5.3. The thick system blanket spectrum is significantly softer than of the 0-D system and of the thin 1-D system blankets (not shown in the figures) due to enhanced slowing-down of mostly driver-originated neutrons that leak into the blanket. The softer blanket spectrum enhances the capture-to-fission probability in ^{238}U. As a result, for a given concentration of ^{239}Pu built up in the blanket, the blanket burnup is smaller for the thicker system. Likewise, the thick 1-D driver region spectrum is slightly harder than of the thin 1-D systems and of the 0-D system as the effect of the blanket region on neutron slowing down reduces with increase in the driver zone thickness. A harder spectrum implies improved neutron economy – more excess neutrons per fission.

However, the use of a single burnup zone for the thick slab systems is inaccurate because it does not properly account for the spatial variation of the neutron flux and fuel composition. In order to ensure that the results obtained for the unit cell made of two 100cm thick slabs are accurate, each slab has been subdivided into 10 slabs 10 cm thick. At EOEC, 10 (out of 20) slabs are discharged, the other 10 slabs shuffled inward and 10 slabs made of depleted uranium are added to the core. It has been found that the minimum required burnup is increased from 12.80% FIMA to 12.87% FIMA and that the maximum and minimum k_{inf} values reach by the system are slightly smaller than when modeling only two slabs of 100 cm. Moreover, shuffling regions as thick as 100 cm is not practical because it will result in a large peak-to-average discharge burnup and in a large burnup reactivity swing.

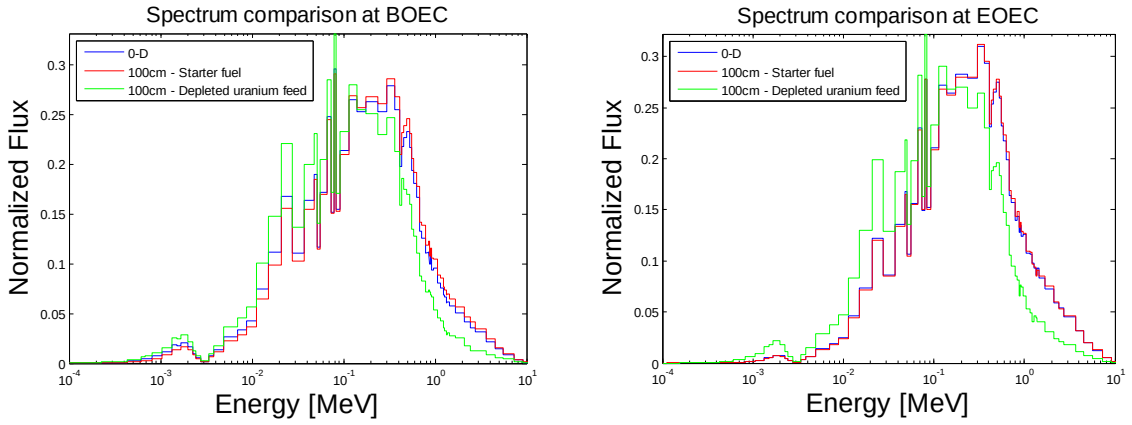

Figures 5.2 and 5.3: Spectrum comparison at BOEC (left) and EOEC (right) for the 2x100 cm 1-D cell against the 0-D unit cell (starter fuel = igniter = driver)

It is observed that for all scenarios studied in this section the minimum value of k_∞ is significantly smaller than unity. In order to maintain k_∞ above unity during all the cycle, it would be necessary to use a large number of fuel batches and progressively shuffle them. Such a system is not practical because of the assumed zero burnup reactivity swing. By increasing the number of slabs and the discharge burnup, it is possible to maintain the unit cell critical at equilibrium by progressively discharging the slabs rather than discharging half of them. This is discussed in Section 5.3, where the criticality constraint is imposed: k_∞ must stay larger than unity during the equilibrium cycle. To compensate for the $k_\infty<1$ at the BOEC with the $k_\infty>1$ at EOEC and

minimize the burnup reactivity swing and minimum discharge burnup, it will be necessary to use a more complex shuffling scheme.

5.3 Minimum required burnup for infinite multi-zone 1-D slab lattice

5.3.1 Methodology

The systems studied are made of an infinite array of 1-D unit cells each consisting of 2 to 40 equal thickness slabs. A reflective boundary condition is applied at the outermost boundaries of the unit cell. Initially half of the unit cell volume is loaded with the igniter fuel and the other half with feed fuel. The igniter and feed slabs are initially fully segregated. The feed fuel is depleted uranium and the igniter fuel is made of depleted uranium with TRU from LWR UNF. The composition of the metallic fuel, materials used, volume fractions and core power density are the same as in Section 5.2. The core is operating in cycles of equal length with fuel shuffling as illustrated in Figure 5.4.

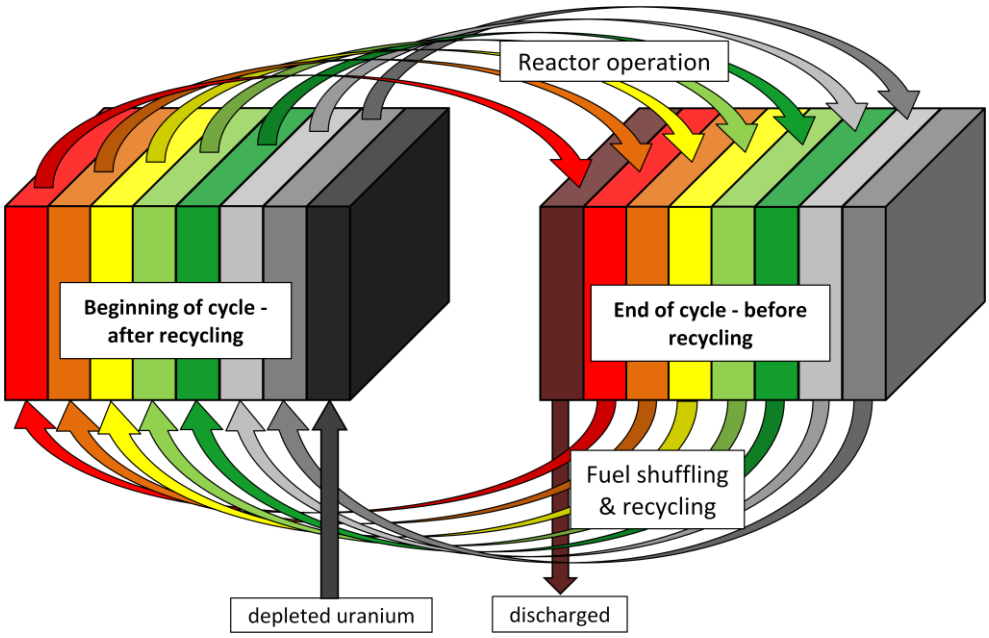

Figure 5.4: Scheme of the shuffling process for an eight-zone 1-D unit cell

At the end of a cycle, the leftmost zone fuel (Figure 5.4 right) is removed, the fuel from each of the other zones is shuffled leftward, and fresh depleted uranium fuel is loaded into the right-most zone. This shuffling process followed by burnup analysis is continued until an equilibrium composition is reached. If the minimum k_∞ over the equilibrium cycle is smaller than 1.0, the cycle length is reduced and this shuffling/burning process is repeated. The minimum required burnup is that burnup for which the minimum equilibrium cycle k_∞ is 1.0.

5.3.2 Dependence on unit cell thickness

The sensitivity of the minimum required burnup to the unit cell thickness is studied for 10 zone unit cells. The results of a parametric study that covers zone thickness ranging from 2 to 20 cm – corresponding to unit cell thickness ranging from 20 to 200 cm – are summarized in Table 5.3.

Table 5.3: Discharge Durnup and Minimum k_∞ for 10 Zones 1-D Infinite Unit Cells

Slab thickness [cm]	Discharge BU	Cycle length [y]	k_{inf} at BOEC	BU reactivity gain
2	18.4%	1.8	0.99962	7.3%
6	16.3%	1.6	1.00718	4.5%
8	16.3%	1.6	1.01214	3.8%
10	16.4%	1.6	1.00885	4.6%
20	18.3%	1.8	0.99001	8.4%

The minimum required burnup, 16.3% FIMA, is obtained for an 8 cm thick zone; i.e., for an 80 cm thick unit cell. The table shows the same discharge burnup for 6, 8 and 10 cm thick slabs, but the minimum BOEC k_∞ is the largest for the 8 cm thick zones system, implying that refining the convergence of k_∞ will result in smaller minimum required burnup for the 8 cm zones system. The minimum required burnup corresponding to k_∞=1.000 is estimated to be 16% FIMA. The net leakage out of each zone and the zone power fraction at BOEC and EOEC are presented in Figures 5.5 and 5.6. There is no net leakage from the unit cell.

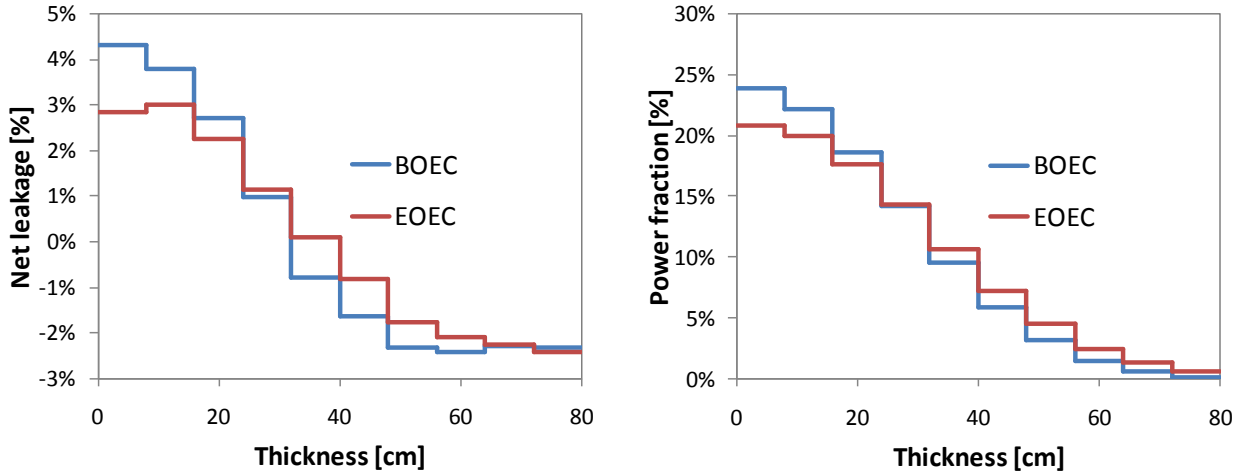

Figures 5.5 and 5.6: Net neutron leakage (left) and power fraction distribution (right) at BOEC and EOEC for the 1-D unit cell with 10 slabs of 8cm. EFPY=1.6y and discharge burnup=16.3% FIMA

5.3.3 Dependence on number of zones in unit cell

The sensitivity of the minimum required burnup to the number of burnup/shuffling zones in a unit cell of a given thickness is studied for a 80 cm thick slab-geometry unit cell. Table 5.4

summarizes the results obtained and Figure 5.7 shows the evolution of k_∞ at the equilibrium cycle for the four cases presented.

Table 5.4: Minimum Required Burnup Sensitivity to Number of Zones in the 80 cm Thick 1-D Infinite Unit Cell

Slab #	Slab thickness [cm]	Min. BU	Cycle length [y]	k_{inf} at BOEC	BU reactivity gain
2	40	28.6%	14	0.996	12.6%
10	8	16.3%	1.6	1.01214	4.4%
20	4	14.2%	0.7	1.00896	2.2%
40	2	13.4%	0.325	1.0026	1.3%

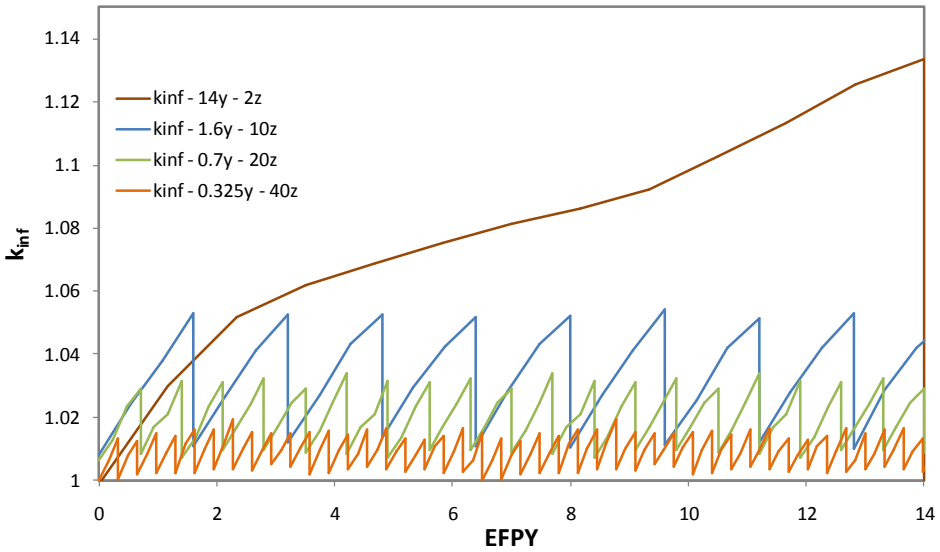

Figure 5.7: Evolution of k_∞ corresponding to the minimum required burnup for an 80 cm thick unit cell divided into different number of depletion zones

As expected, as the number of burnup zones is increased, the required cycle length is decreased and the reactivity swing becomes smaller. The minimum burnup required for sustainable breed and burn operation is found decreasing with increasing number of burnup zones; it converges towards approximately 13% FIMA – close to the minimum values obtained in Sections 5.1.2 and 5.2.2. However, as the cycle length acceptable to utilities is probably at least one year, the practical minimum required burnup for leakage-free cores is close to 15% FIMA.

5.3.4 Dependence on fuel type and density

The sensitivity of the minimum required burnup to the fuel type used is analyzed using the 1-D infinite unit cell and the search methodology described in Section 5.1. The analysis is performed for a unit cell made of ten 8 cm thick slabs. The fuels studied and their characteristics are summarized in Table 5.5. The volume fraction does not include the gap volume and the theoretical densities are use for all fuels, while it is only possible to approach the theoretical density with metallic fuels. The inert matrix fuel volume fraction, 45.2%, is split among the $(U,TRU)_2MoSi$ phase, 76.1% and the Zr_8Fe_8Cu phase, 23.9%.

Table 5.6 summarizes the minimum required burnup obtained and the corresponding accumulated fast flux fraction, fast neutron fluence and DPA. The fast flux fraction and fast neutron fluence pertain to neutrons of energy larger than 0.1 MeV. The three last lines given in Table 5.6 pertain to systems that could not meet the criticality constraint (Equation 5.1).

Table 5.5: Characteristics of the Fuels Studied

Fuel	ρ [g/cm^3]	Smear factor	Volume fraction	HM density [g/cm^3]
U-TRU-Zr(7.5)	15.85	0.75	40.5%	5.94
(U,TRU)C[(a)]	12.95	0.85	45.9%	5.66
(U,TRU)^{15}N[(b)]	14.31	0.87	47.0%	6.33
(U,TRU)O_2[(c)]	11.5	0.85	45.9%	4.65
IMF[(d)]	19.98/7	0.85	34.4%/10.8%	5.48
(Th,TRU)[(e)]	11.65	0.75	40.5%	4.72

[(a)][(b)][(c)]Data taken from [33-36]; [(b)] data taken from [8, 9]; [(d)]Inert Matrix Fuel is made of two phases: $(U,TRU)_2MoSi$ and Zr_8Fe_8Cu; [(e)]Smear factor is taken the same as U-based metallic fuel

Table 5.6: Sensitivity of the Performance to the Fuel Type, at Equilibrium

Fuel	Minimum Burnup	k_∞ at BOEC	Cycle length [y]	Fast flux fraction	Fast fluence [n/cm^2]	DPA
U-TRU-Zr	16.3%	1.01214	1.6	61.0%	7.97E+23	299
(U,TRU)C	23.6%	0.99678	2.2	53.5%	8.17E+23	345
(U,TRU)^{15}N	18.8%	0.99591	2	52.9%	7.27E+23	301
(U,TRU)O_2	*31.3%*	*0.97378*	*2.4*	*50.9%*	*9.25E+23*	*403*
IMF	*22.2%*	*0.89951*	*2*	*55.9%*	*9.57E+23*	*362*
(Th,TRU)	*28.7%*	*0.93775*	*2.2*	*65.1%*	*1.26E+24*	*461*

Following are several observations:

- Although nitride fuel has a larger heavy metal density than uranium-based metallic fuel, the concentration of nitrogen atoms is higher than of zirconium atoms, and the slowing-down power of nitrogen is larger causing the nitride fuel spectrum to be somewhat softer than that of the metallic fuel. As a result the minimum required burnup is smaller for uranium based metallic fuel than for nitride fuel. However, due to its softer spectrum, the DPA accumulated in nitride fuel is practically the same, and the fast neutron fluence is smaller.
- As the heavy metal density of carbide fuel is 6% smaller than that of nitride fuel and as C atoms slow down neutrons more effectively than N atoms, the minimum required burnup is larger for carbide fuel. The DPA and fast fluence are larger in carbide fuel because of the longer required cycle length.
- Thorium based metallic fuel and oxide fuel are penalized by their heavy metal density that is about 21% smaller than that of nitride and uranium based metallic fuels. Moreover, the fast fission cross section of thorium is significantly smaller than that of ^{238}U and the η value of ^{233}U for fast neutrons is significantly smaller than that of ^{239}Pu and of ^{241}Pu. As a result it was found impossible to achieve critical equilibrium composition in the range of design variables examined.

- The inert matrix fuel has a heavy metal density close to that of the carbide fuel but has a significantly larger amount of structural elements and, hence, enhanced parasitic neutron absorption. No critical equilibrium composition could be achieved in the range of design variables examined.

5.4 Minimum required burnup for a 1-D semi-finite cylindrical core

The objective of this part of the study is to determine the minimum required burnup considering a more realistic finite one-dimensional system in which the neutron leakage probability is accounted for. Instead of the multi-slabs unit cell studied in the previous section, a one dimensional cylindrical core with realistic dimensions is studied.

5.4.1 Methodology

The system examined for this study is a one-dimensional cylindrical core that is surrounded by a radial shield. The shield is made of 43.1 volume % boron carbide (B_4C; natural boron), 29.7% HT-9 and 27.2% void. The ABR core developed by ANL [27] is used as a reference for this 1-D model. In order to get a lower-bound estimate on the minimum required burnup the system spectrum is made somewhat harder than practical by reducing the pitch-to-diameter ratio from 1.18 (ANL) to 1.10 and using lead-bismuth rather than sodium for the coolant (although thermal-hydraulic analysis calls for a lead-cooled system P/D > ~1.30). The TRU concentration yielding k_{eff}=1 at BOL of the ANL design is found to be 13.8 wt%. The one-dimensional variant of this core is illustrated in Figure 5.8. The central part of the core is initially loaded with depleted uranium with TRU starter fuel and is surrounded with depleted uranium feed fuel that is surrounded by a shield that is 350 cm in outer diameter. The starter fuel region diameter was set at 130 cm so as to obtain k_{eff}=1 using the same 13.8 wt% TRU concentration. The initial feed fuel volume is four times the starter fuel volume. The average power density in the initial TRU-loaded zone is 326 W/cm^3; it corresponds to a peak power density of 450 W/cm^3. This value is a commonly used design limit for liquid metal cooled reactors [9]; no thermal-hydraulics study has been performed for this system, and the power density value would need to be updated based on detailed thermal-hydraulics analysis.

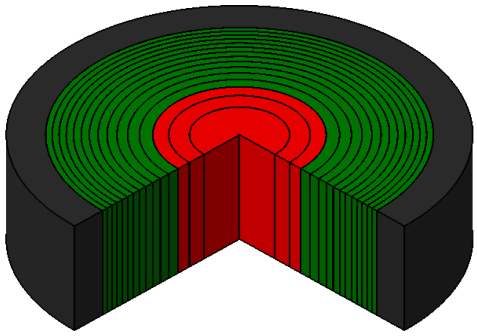

Figure 5.8: Layout of an axially infinite cylindrical core; initial blanket (green) volume is 4 times the initial starter (red) volume. The black part is the shield.

The core is divided into 15 equal volume concentric burnup zones. The reactor is assumed to operate in equal length cycles; at the end of a cycle the inner-most fuel zone is removed, each of the other equal-volume fuel zones is shuffled inward, and fresh depleted uranium feed fuel is loaded into the outer-most zone. This shuffling process followed by burnup analysis is continued until an equilibrium composition is reached. If the minimum k_{eff} over the equilibrium cycle is smaller than 1.0, the cycle length is reduced and this shuffling/burning process is repeated. The minimum required burnup is that burnup for which the minimum equilibrium cycle k_{eff} is 1.0. It is assumed that 75% of the gaseous fission-products instantaneously leave the fuel and accumulate in the fission gas plenum. This phenomenon has been discussed in Section1.3.

The igniter fuel is the same as described in Section 5.2, but with 10 wt% Zr. The depleted uranium fuel is the binary alloy U-Zr, with 10 wt% Zr, where the uranium is made of 0.2 wt% ^{235}U and 99.8 wt% ^{238}U. The structural and cladding material is HT-9. Table 5.7 summarizes the volume fractions of this metallic fuelled core. The shield is made of 43.1 volume % boron carbide (B_4C; natural boron), 29.7% HT-9 and 27.2 % void.

Table 5.7: Initial Volume Fractions of the 1-D Cylindrical Core Model

	Material	P/D=1.10
Control rods	empty (coolant)	9.55%
Fuel	U-TRU-Zr	31.17%
Fuel-clad gap	Na	10.39%
Clad	HT-9	14.41%
Coolant	LBE (Pb-Bi)	21.33%
Assembly duct	HT-9	8.38%
Assembly gap	LBE (Pb-Bi)	4.78%

5.4.2 Minimum required burnup

The minimum burnup required to sustain the breed and burn mode of operation for this 1-D semi-finite model is 20% FIMA. This corresponds to a 2.5 years cycle length. The burnup reactivity swing is approximately 2%. The net leakage out of each zone and the zone power fraction at BOEC and EOEC are presented in Figures 5.9 and 5.10. A zone having a positive net leakage probability (R<~70cm) is a net producer of neutrons whereas a zone having a negative net leakage probability is a net sink of neutrons. The radial neutron leakage probability out of the core is 0.63% at BOEC and 0.83% at EOEC.

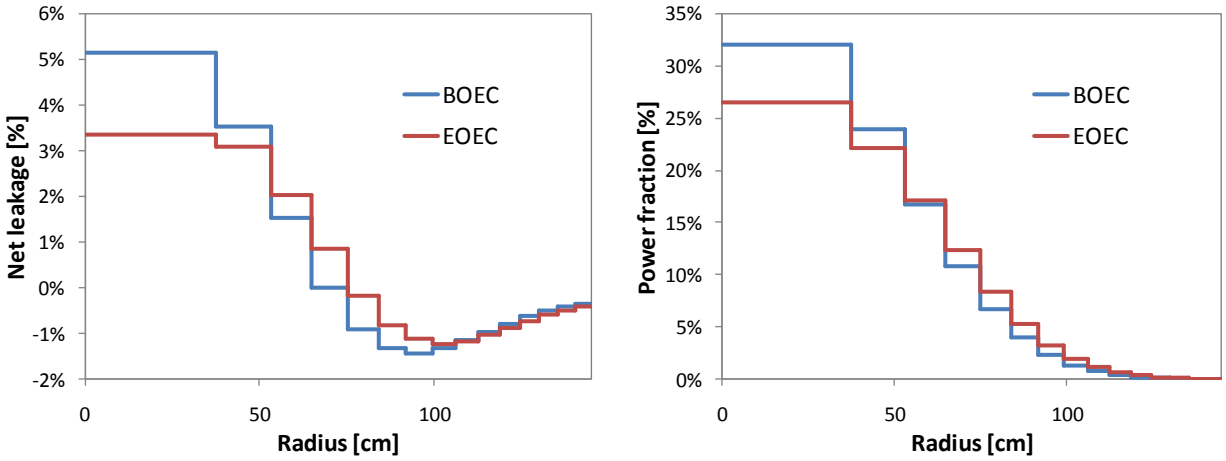

Figures 5.9 and 5.10: Net neutron leakage (left) and power fraction distribution (right) at BOEC and EOEC for the 1-D core with 15 burnup zones. EFPY=2.5y and discharge burnup=20% FIMA. The x-axis corresponds to the core radius.

Table 5.8 gives selected characteristics of this 20% burnup equilibrium core. The "breeding ratio" given in the table is the ratio between the number of heavy metal atoms, excluding ^{238}U atoms, in the entire core at the end and beginning of an equilibrium cycle. The radiation damage to the cladding is 341 DPA corresponding to a fast neutron fluence (fluence for which the neutron energy is above 0.1 MeV) is 9.5E+23 n/cm^2. These values are about twice larger than the currently acceptable values for HT-9 – 200 DPA and 4.0E+23 n/cm^2. This is consistent with previous experience [50] that the presently accepted HT-9 radiation damage limit in a low fissile fuel content hard spectrum fast reactor core is reached at, approximately, 10% burnup FIMA.

Table 5.8: Selected Characteristics of the 1-D Cylindrical Breed and Burn Core

Parameter	Value
Average core power density [W/cm^3]	65.2
Average specific power [W/g HM]	14.7
Breeding ratio	1.15
HM/TRU mass at BOEC [tons]	66.5/2.7
HM/TRU mass at EOEC [tons]	65.6/3.2
Discharge burnup [GWd/tHM]	198
Fast fluence [10^{23}n/cm^2]	9.5
DPA	341
Burnup reactivity gain [% Δk]	1.8
Core average flux [10^{15}n/cm^2-s]	1.24
Fast flux fraction > 0.1 MeV [%]	64.5

5.5 Discussion

The 20% minimum required burnup obtained for the 1-D cylindrical core using 15-batch fuel shuffling scheme is similar to the value obtained by Toshinsky for a 14-batch finite core [15] that used a larger fuel volume fraction. Since all the mined uranium is eventually fed to the core operating with the breed and burn mode of operation, the uranium utilization is equal to the fuel discharge burnup, 20%. Compared to the values achieved in the previous chapter for fast reactors in which the fuel is multi-recycled, the breed and burn mode of operation without fuel recycling enables achieving 4 to 10 times larger uranium utilization.

The minimum required burnup for the 1-D cylindrical core can be somewhat reduced by increasing the number of batches and shortening the cycle length. The axial leakage from a realistic core design will tend to increase the minimum required burnup as will the non-uniform axial power distribution of a finite core. On the other hand, if the average HM density in the core could be increased say, by decreasing the mass fraction of zirconium in the metallic fuel or increasing the fuel volume fraction, the minimum required burnup could be reduced. Recently, Petroski reported [55] that the theoretical minimum burnup required for sustaining a breed-and-burn operation in a large fast reactor core is approximately 15%; this value refers to a somewhat different composition core. Decreasing the discharge burnup will decrease the uranium utilization by as much. When the breed and burn mode can be achieved without exceeding the radiation damage limit, the discharge burnup should be as large as acceptable in order to maximize the uranium utilization.

The results obtained in our analysis indicate that the radiation damage to be imparted to the cladding in a core designed to operate in a sustainable breed-and-burn mode and that uses depleted uranium as the feed fuel will be higher than the 200 DPA presently acceptable design limit of HT-9. In order to establish a sustainable breed-and-burn mode of operation in practical cores it will be necessary to resort to one, or a combination of a number of measures including the following: (a) extension of the DPA constraint of HT-9 clad based on improved knowledge about its behavior at higher than so far tested fluence levels; (b) development of advanced structural materials that can withstand higher DPA levels; (c) increase in the average uranium density in the core; (d) improvements in the fuel and core design. Another option is to recycle the fuel to replace the clad and remove the gaseous fission products. If recycling the fuel, it is no longer necessary to design for the minimum required burnup. The following chapters investigate the maximum burnup that is possible to achieve in a breed-and-burn mode of operation in which depleted uranium is used for the feed fuel when using fuel recycling without actinide separation.

5.6 Conclusions

The minimum burnup required for establishing a sustainable breed-and-burn mode of operation in a liquid-metal cooled fast reactor that uses depleted uranium for its feed is found to be ~13% FIMA. This limit pertains to zero-leakage core fuelled with HT-9 clad U-Zr metallic fuel having 7.5 wt% Zr and 75% smear density arranged in a tight P/D=1.112 lattice. The minimum burnup required to establish the breed-and-burn mode of operation using alternative fuel types was found to be slightly higher for nitride fuel and carbide fuel and significantly higher for oxide fuel, inert matrix fuel and thorium based metallic fuel. It is estimated that neutron leakage from a practical core design will increase the minimum required average burnup of metallic fuelled cores to approximately 20% FIMA and the uranium utilization to 20%. The

corresponding accumulated radiation damage levels exceed the 200 DPA or 4E+23 n/cm^2 presently acceptable constraints on HT-9 clad. It is possible that improvements in the state of knowledge of the performance of HT-9 and/or development of improved structural materials and/or improvements in the fuel and core design will enable attaining the breed-and-burn mode of operation without exceeding the radiation damage constraints. Otherwise, it will be necessary to recycle the fuel to replace the clad and remove the gaseous fission products, or to use for the feed slightly enriched uranium rather than depleted or natural uranium.

Chapter 6

Performance of a Large B&B Core

It has not been found possible, in Chapter 5, to establish and sustain the breed and burn mode of operation without exceeding the currently acceptable radiation damage limits for the HT-9 cladding. When the fuel is reconditioned to operate with the breed and burn mode, it is no longer necessary to design for the minimum burnup. To maximize the uranium utilization, maximizing the discharge burnup is the objective. The performance of a large fast reactor operating with the breed and burn mode, described in Chapter 5, is analyzed in this section. The performances of this core are assessed in the two first sections of this chapter during the transition period, when it is started with enriched fuel, and at equilibrium for the maximum achievable discharge burnup. The expected performance of this core, when operated at the minimum required discharge, is discussed in Section 6.3. By discharging the fuel when it reaches its minimum required burnup, it is possible to reload it in a new core in order to ignite a new breed and burn reactor. This spawning mode of operation is analyzed in Section 6.5 for the transition and the equilibrium periods. A neutron balance analysis, similar to the one of Section 5.1, is performed for this large B&B core in Section 6.4 and a thermal hydraulic validation is performed in Section 6.6.

The core model studied in this chapter, referred to as the "large B&B core", is the large 3000 MW_{th} fast reactor core with the large radial blanket that was described in Section 2.1.2 and analyzed in Chapter 4 assuming a infinite-batch fuel management scheme with conventional refueling. The highest achievable burnup for B&B cores will be obtained with this large core model because of its large size, low neutron leakage and high power density. The core dimensions, total power, P/D ratio and constituents volume fractions are as defined in Section 2.1.2. The fuel management scheme is modified to be the breed and burn mode. The maximum radiation damage constraint assumed for this study is taken to be 400 DPA, corresponding to approximately 20% FIMA. This is about twice larger than the currently accepted limit for HT-9. When a fuel element reaches this limit, all the fuel in the core is recycled with the melt-refining process described in Section 1.2.2. In order to simplify the fuel cycle simulation, the fuel recycling is assumed to occur instantaneously (same assumption as in Chapter 4).

6.1 Transition period

The core is initially started using an igniter made of enriched fuel. The excess neutrons are used to build-up plutonium in the radial blanket elements and when the k_∞ of these elements becomes larger than unity use them to drive the core, without addition of fissile material from an external source. Two options are envisioned for providing the initial enriched fuel loading: (a) enriched uranium (EU) or (b) TRU from LWR UNF. The enriched uranium can be provided by existing enrichment plants (or surplus weapons uranium); the required enrichment level is smaller than the currently accepted limit of 20 wt% ^{235}U. However, the fabrication of EU igniters will increase the natural uranium mining requirement. On the other hand, recovering the TRU from the LWR UNF requires no supply of natural uranium but the US lack the UNF separation capability. The TRU vector composition assumed is that given in Table 3.3; it corresponds to a discharge burnup of 50 GWD/tHM and 10 years of cooling time. At the time of this study, it is has been estimated that there are at least 560 tons of TRU available in the UNF already discharged from the US reactors [56]. It could provide the enriched fuel for at least 83 GWe of B&B reactors. The objective of the work performed in this section is to find out whether it is practically feasible to ignite the large B&B core using either TRU based fuel or EU fuel. At first, the maximum excess reactivity, power peaking factor and cycle length constraints are not considered. When the fuel recycling is occurring, no fuel is discharged, no shuffling is performed and no fresh fuel is added. This scenario is similar to scenario (b) studied in Section 4.2 with the exception of the small radial reflector used in the current scenario. When the reactor becomes subcritical, the fuel will need to be shuffled and/or discharged and replaced with fresh depleted uranium fuel. This is discussed in Section 6.2.

6.1.1 TRU based igniter

The initially loaded igniter fuel is depleted uranium mixed with that concentration of TRU that will provide criticality at BOL along with radial power flattening. The required TRU concentration in each of the four radial zones composing the igniter is 6.6%/11.7%/12.2%/15.3% TRU by weight, from the innermost zone to the outermost zone. Those are the same values as in Section 2.1.2.

The evolution of the multiplication factor with respect to the average core burnup – including both the heavy metal in the igniter and the blanket – is shown in Figure 6.1. The uncontrolled k_{eff} reaches values above 1.15, and becomes smaller than unity after 30.4 years. At this time, the average core burnup is 303 GWd/tHM but the igniter average burnup is 467 GWd/tHM (48.15% FIMA) and the blanket average burnup is only 139 GWd/tHM (14.28% FIMA). The axially averaged burnup in the igniter zone reaching the highest burnup is 500 GWd/tHM. By shuffling the eight radial zones it would be possible to decrease the excess reactivity during the transition period and increase the achievable igniter burnup. In Section 4.2, it was found that for scenario (b), the achievable igniter burnup with a single-batch fuel management scheme was 47% FIMA, slightly smaller than the value found in the current study because no radial reflector was used between the blanket and the radial shield.

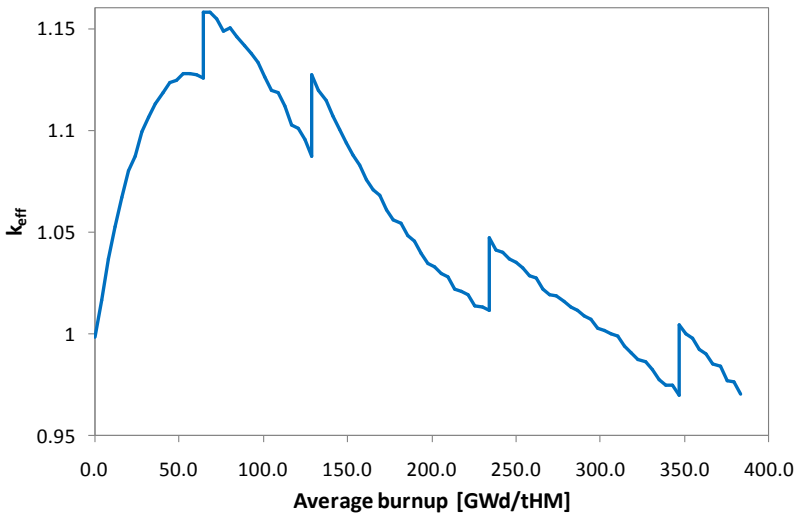

Figure 6.1: k_{eff} evolution for the large B&B core using TRU igniter and melt-refining recycling

The power peaking, shown in Figure 6.2, is occurring in the innermost radial zone when k_{eff} reaches its maximum value. When the reactor is started, the neutron flux is larger in the innermost part of the reactor that features a relatively high breeding ratio (due to low TRU concentration), and thus, the plutonium buildup rate is the largest in this zone. As plutonium is building up near the core center, the multiplication factor of the reactor and the power fraction in the core center are increasing. The power density distribution at BOL and at 303 GWd/tHM are given in Figures 6.3 and 6.4. When the reactor becomes subcritical at 300 GWd/tHM, the igniter is producing only 40% of the total power – the blanket is producing 60%, and the radial power peaking factor, that reached 2.62 at 69 GWd/tHM, is only 1.42.

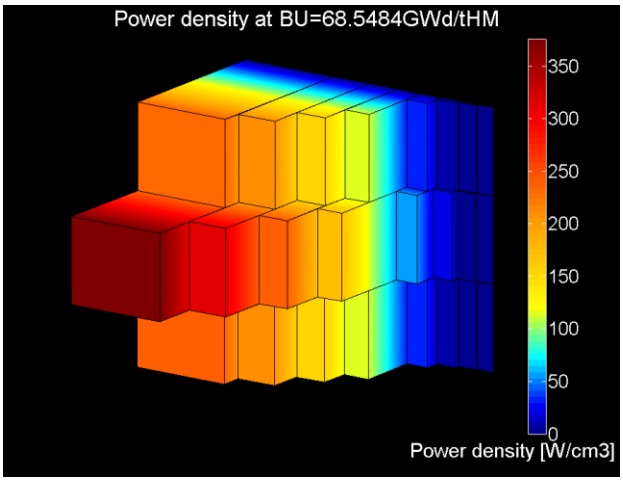

Figure 6.2: Power density distribution in the large B&B core with TRU igniter when the power peaking is occurring at 69 GWd/tHM

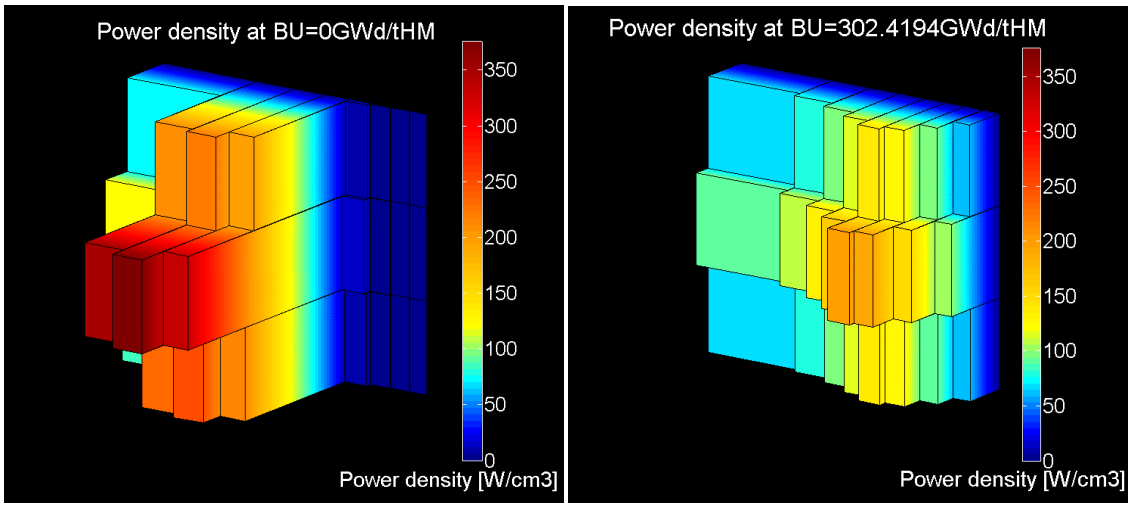

Figures 6.3 and 6.4: Power density distribution in the large B&B core with TRU igniter at BOL and EOL (~300 GWd/tHM)

The zone-wise DPA accumulation in the cladding is shown in Figure 6.5. The decreasing rate of DPA accumulation with the zone distance from the core center is due to a reduction in the neutron flux amplitude and, for the blanket zones, also to spectrum softening, as illustrated in Figure 6.6.

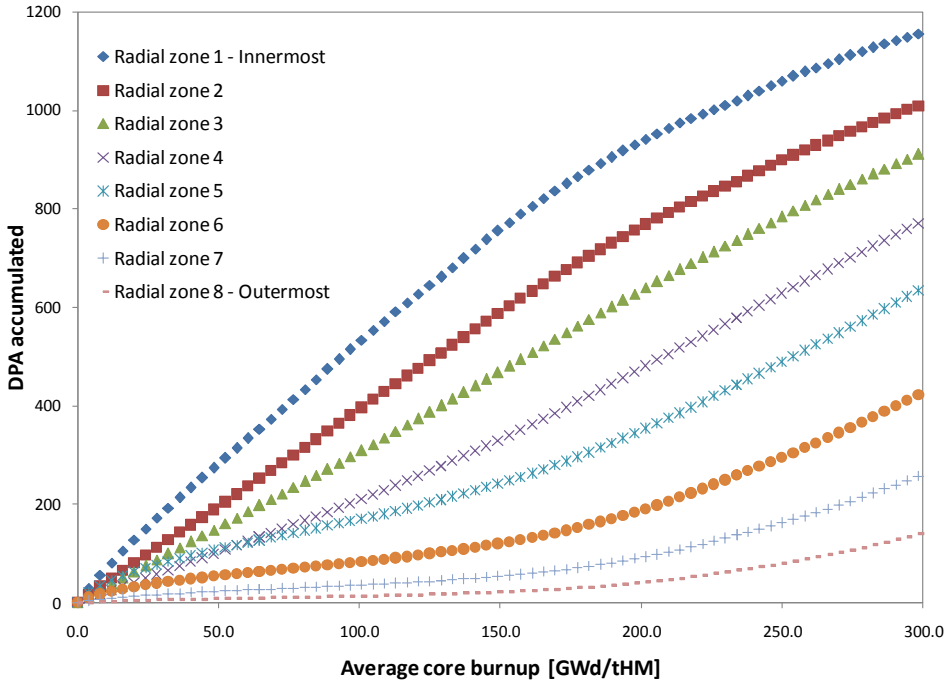

Figure 6.5: Peak DPA accumulation for the different radial zones for the large B&B core

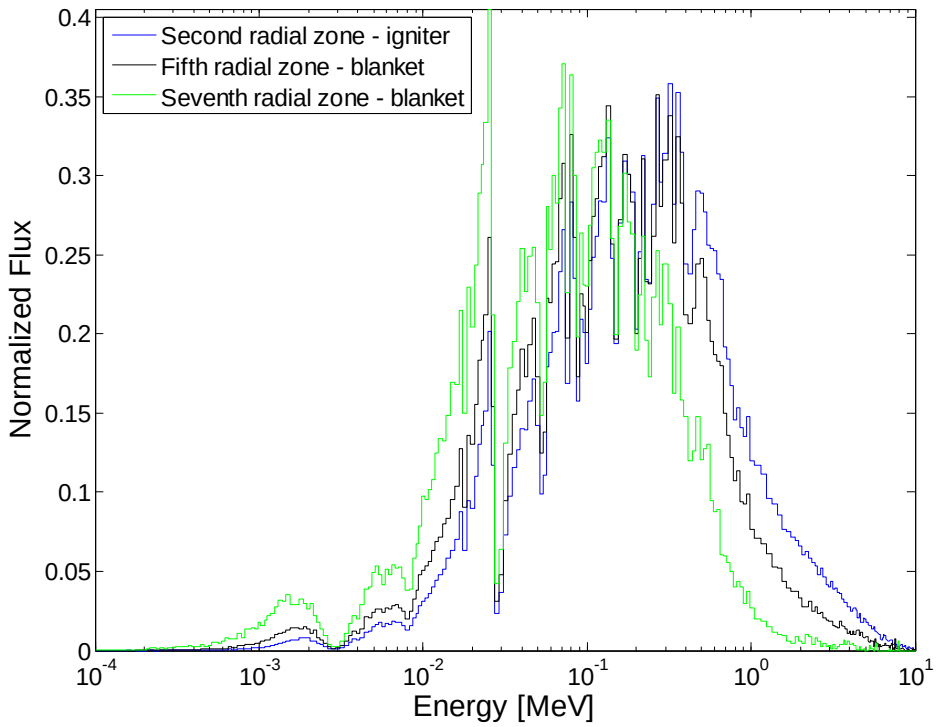

Figure 6.6: Neutron spectra at BOL for the second inner most igniter radial zone, and two of the blanket radial zones – out of four.

The infinite multiplication factor of the various radial zones of the reactor is estimated using the one-group cross-sections generated by MCNP5, assuming that every zone have the same average number of neutrons emitted per fission – 2.92. k_∞ is an important measure of the reactivity worth of each zone and is useful to determine when the blanket has sufficient fissile material to drive the core in lieu of the igniter. The axially averaged values for the eight radial zones are provided in Figure 6.7. It is observed that the k_∞ value of the innermost fuel zone is increasing until the average core burnup is ~70 GWd/tHM, confirming that the power fraction in the central core zone is increasing from BOL to 70 GWd/tHM and peaks around this burnup. At ~180 GWd/tHM, the innermost blanket zone reactivity is similar to that of the most reactive igniter zone (#4).

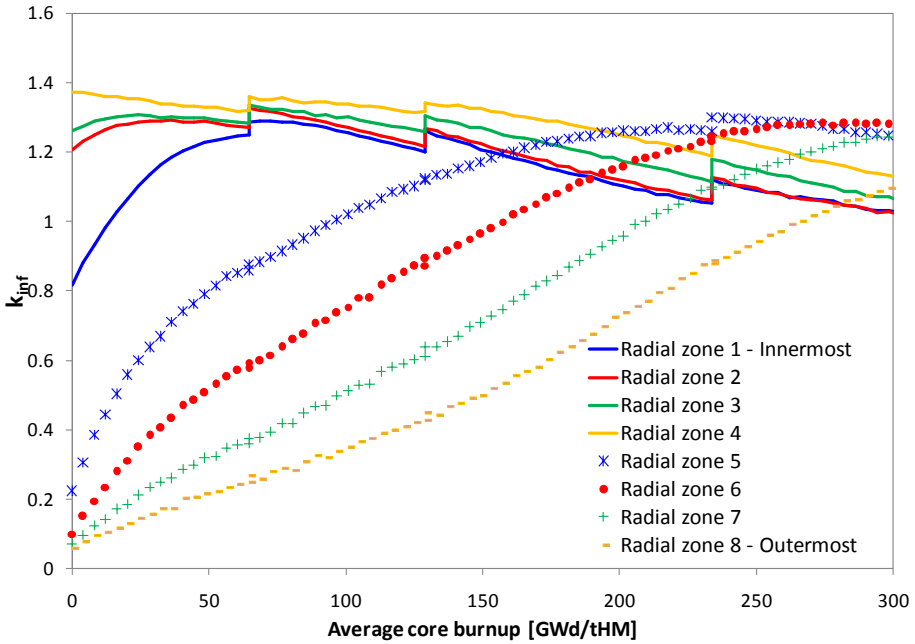

Figure 6.7: Evolution of the infinite multiplication factor for the eight radial zones of the large B&B core with the TRU igniter

When the core becomes subcritical at 303 GWd/tHM, the reactivity of the blanket zones is sufficiently high to enable propagating the fission wave to a new depleted uranium blanket, by removing the igniter, shuffling the blanket and adding fresh depleted uranium elements. This scenario is examined in Sections 6.5.1 and 6.5.2.

6.1.2 Enriched uranium igniter

The same large B&B core is studied with an igniter made of enriched uranium. Although ^{235}U has a smaller reproduction factor, η, than the fissile plutonium isotopes in a fast spectrum, the required ^{235}U enrichment is smaller than the TRU enrichment because the fissile isotopes represent only 70% of the TRU. It is found that to achieve k_{eff}=1 and a similar power distribution at BOL as with the TRU igniter, the required ^{235}U enrichments are 6.1%/10.8%/11.3%/14.8% by weight. To start the large B&B core with an EU igniter (not optimized), 7.66 tons of ^{235}U are required.

The evolution of the multiplication factor, with the fuel being recycled with the melt-refining, is shown in Figure 6.8. The reproduction factor of ^{235}U being smaller than for fissile plutonium, the maximum value reached by k_{eff} is smaller. As the igniter burnup increases, the initially loaded ^{235}U is consumed and ^{239}Pu is bred in both the igniter and the blanket. At high burnup the EU igniter core behaves the same way as the TRU igniter core. Their behaviors become similar before the cores become subcritical and therefore, the average achievable burnup with the EU igniter without fuel shuffling is 306 GWd/tHM, approximately the same as for the TRU igniter core (303 GWd/tHM). The average EU igniter and blanket burnup are also the same as for the TRU igniter core: 468 GWd/tHM (47.88% FIMA) for the igniter and 145 GWd/tHM (14.87% FIMA) for the blanket. The peak radial burnup in the igniter is 501 GWd/tHM.

The lower value reached by k_{eff} for the EU igniter core shows that there are fewer excess neutrons available for breeding when using the EU igniter rather than the TRU igniter. With an

optimized shuffling scheme, it is theoretically possible to discharge the TRU igniter at a larger burnup than the EU igniter. This is due to the larger number of neutrons emitted per fission in the fissile plutonium isotopes, 2.91, than in ^{235}U, 2.51.

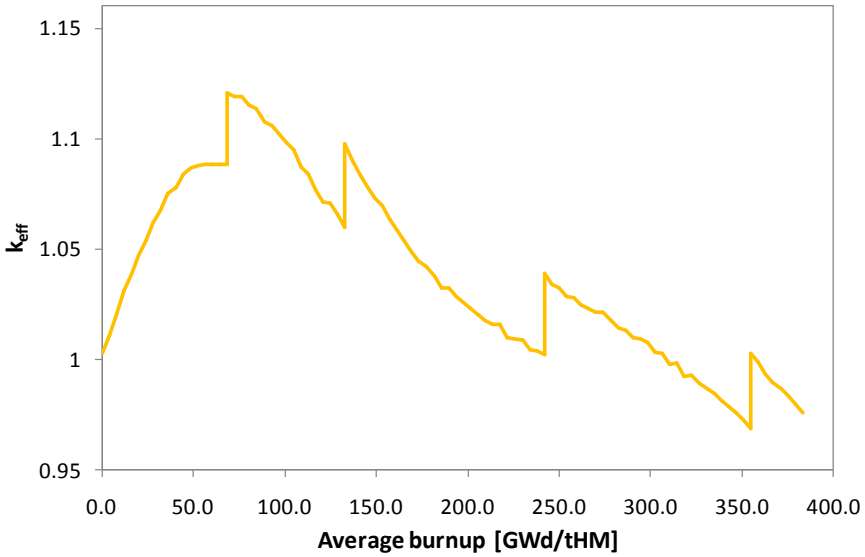

Figure 6.8: k_{eff} evolution for the large B&B core using EU igniter and melt-refining

Despite the slightly smaller peak value of k_{eff}, the EU igniter core behavior is very similar to the TRU igniter core:

- The power distribution is almost identical to the ones presented on Figures 6.2, 6.3 and 6.4 – the power peaking factor is 2.56 instead of 2.62;
- At EOL, the radial burnup distribution are identical;
- The neutron spectrum at BOL and at ~300 GWd/tHM are the same for both systems, as presented in Figures 6.9 and 6.10;
- DPA accumulation is the same as shown in Figure 6.5. It is sensitive to the spectrum and power fraction; therefore it is similar to the TRU igniter core accumulation.
- The infinite multiplication factors of the radial zones, given in Figure 6.11, are almost the same. At BOL, the k_∞ values in the EU igniter are larger than in the TRU igniter, but when the first recycling occurs, around 65 GWd/tHM, the k_∞ of all the radial zones of the two systems are almost equal.

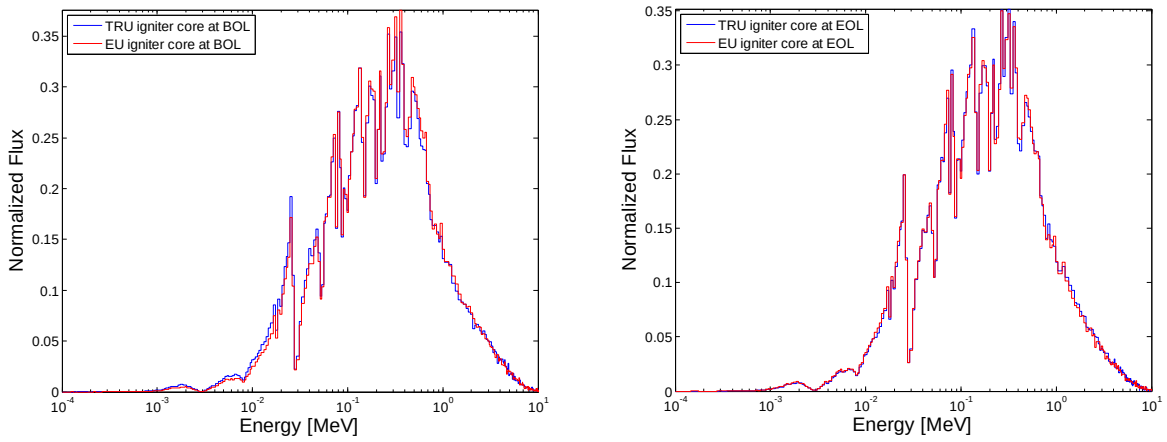

Figures 6.9 and 6.10: Spectra comparison at BOL (left) and EOL (right) for the fourth radial fuel zone of the large B&B core with EU igniter and TRU igniter

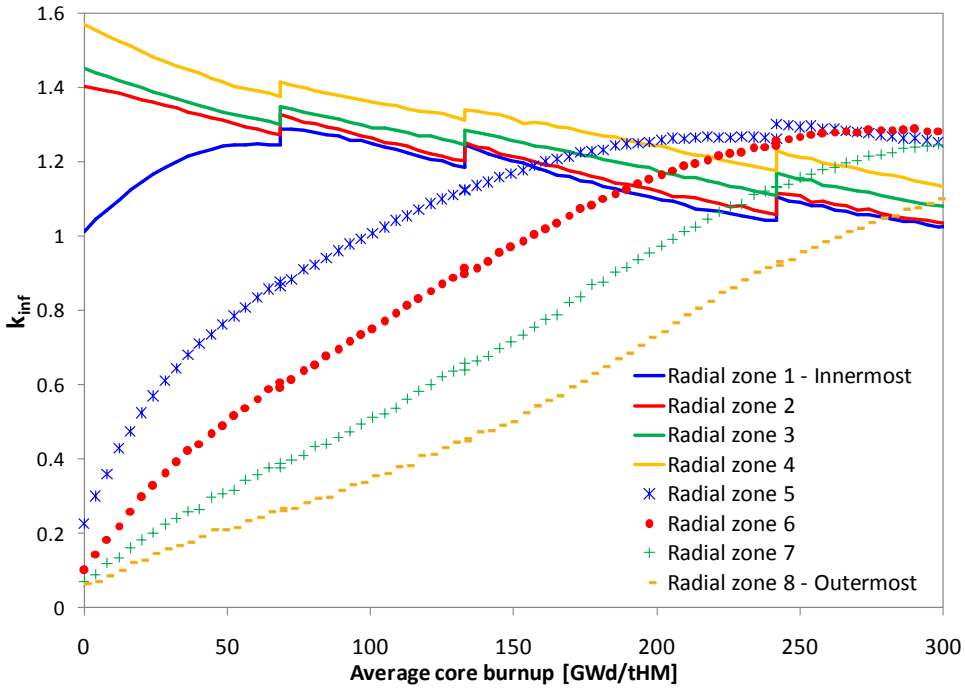

Figure 6.11: Evolution of the infinite multiplication factor for the eight radial zones of the large B&B core with the EU igniter

6.1.3 Results validation with an assembly-level core model

The results presented in Sections 6.1.1 and 6.1.2 pertain to a simplified core model, where the eight radial fuel batches are represented by concentric cylinders, each made of only three different axial fuel compositions. In reality, each cylindrical zone represents more than 70, usually hexagonal, fuel assemblies. In order to ensure that the above results calculated assuming the approximate core representation are not biased, the core is re-modeled with a higher level of detail.

Due to the limited computation capability available at UC Berkeley for neutronics simulations, it is not possible to model every single fuel pin with their own fuel vector. All the fuel assemblies are modeled individually, assuming uniform composition across each fuel assembly. Each assembly is split in three axial zones having different compositions. The assembly pitch is assumed to be the same as the one of S-PRISM [28] and of the ANL ABR concept [27], 16.142 cm. The volume fractions used in each assembly are the same as described in Table 2.1 for the cylindrical core model. In order to conserve approximately the same total core volume, the core is composed of 571 fuel assemblies. Unfortunately, the total core volume is slightly increased since the number of fuel assemblies needs to be an integer. Considering the core symmetries, it is possible to model only 1/12 of the core. As shown in Figure 6.12, only 58 assemblies or partial assemblies need to be modeled, each with three axial zones: there are a total of 174 different fuel compositions and, correspondingly, 174 depletion zones. The igniter used for this comparison is the TRU igniter. The same TRU enrichments as in Section 6.1.1 are used.

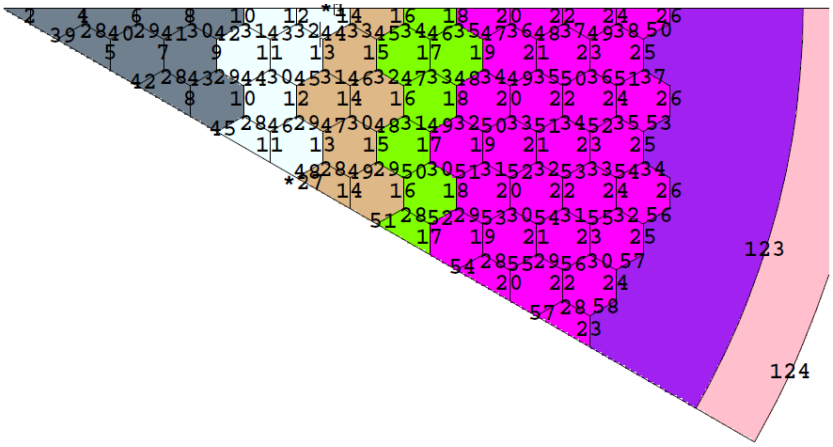

Figure 6.12: Plot of the geometry used in MCNP5. The four igniter enrichments are represented in grey, white brown and green, and the blanket is in pink. Note that the reflector assemblies, in purple, are not modeled individually. The shield is the rightmost section

It is not possible to have the same number of assemblies in each of the eight fuel batches (i.e. radial zones) because of the total number of fuel assemblies in the core. Therefore, the number of assemblies in each batch is not the same for each of the eight fuel batches. Despite this small difference with the cylindrical model previously studied, the evolution of the multiplication factor with the average core burnup is identical, as shown by Figure 6.13. The fuel recycling do not occur at the same time: with the cylindrical model, the accumulated burnup in a radial zone corresponds to the average burnup of 70 assemblies; with the assembly-level model, the burnup is accumulated faster in the lead assembly than in the rest of the batch, forcing the fuel recycling to occur slightly earlier than for the cylindrical model.

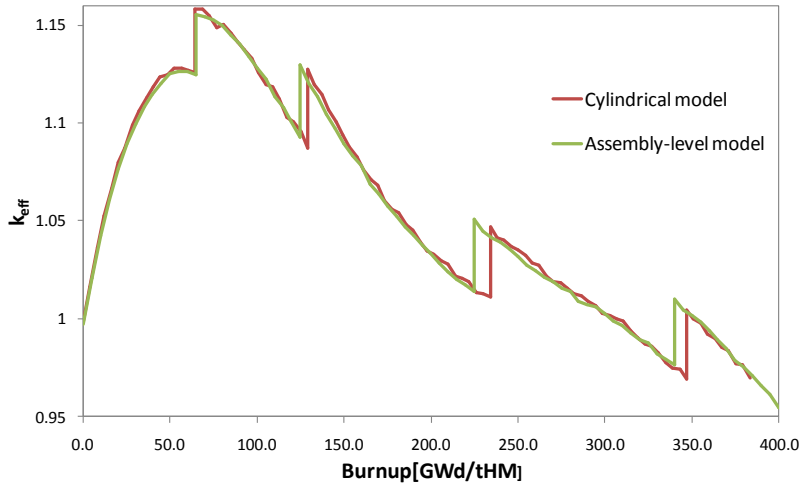

Figure 6.13: Multiplication factor evolution for the assembly-level and cylindrical models representing the large B&B core with melt-refining

The plutonium, TRU, ^{238}U and FP inventories at BOL, and EOL – when the core becomes subcritical, are compared in Table 6.1 along with additional characteristics. As previously mentioned, the assembly-level model has a slightly larger core volume in order to accommodate all the fuel assemblies. Despite this difference, the igniter average burnup and isotope inventory show a good agreement among the two models: with 1.2% volume difference, there is a 1.2% initial ^{238}U mass difference, which corresponds to 1.6 extra tons of ^{238}U. The two models being simulated with the same total power and during the same time period, there still are 1.6 extra tons of ^{238}U after 39.4 EFPY in the assembly-level model. All the plutonium, TRU and fission products inventories are within 1% difference. The main difference arises from the radial power peaking factor. It is found to be ~15% larger at BOL with the assembly-level model because of the larger number of radial compositions and, hence, finer spatial resolution. At EOL, which is at 39.4 EFPY, it is only 6% larger.

Table 6.1: Characteristics Comparison Between Cylindrical Model and Assembly-level Model at BOL and After 39.4 EFPY – ~300 GWd/tHM

	BOL		39.4 EFPY	
Model	CY	AL	CY	AL
Igniter volume [m^3]	13.333	13.37	-	-
Blanket volume [m^3]	13.333	13.606	-	-
Average igniter BU [% FIMA]	-	-	48.15%	47.81%
Total ^{238}U [tons]	134.2	135.8	84.9	86.5
Total ^{239}Pu+^{241}Pu [tons]	4.556	4.560	9.662	9.690
Total TRU [tons]	8.184	8.190	13.172	13.22
Total FP [tons]	-	-	22.19	22.39
Radial power peaking factor	2.497	2.880	1.422	1.510

*CY=Cylindrical; AL=Assembly-level

The performance achieved with the assembly-level model shows a reasonably good agreement with the performance achieved with the cylindrical model. However, the simulation took twice longer for the assembly-level model. For the large B&B core it is acceptable and sufficient to use the simple cylindrical model to get a preliminary assessment of the core performance with acceptable accuracy.

It is possible to establish the breed and burn mode of operation in a large 3000 MW_{th} B&B core with an igniter made of enriched uranium or an igniter enriched with the TRU recovered from the LWR UNF. For both igniters the maximum achievable burnup in the igniter with a single-batch fuel management scheme is ~48% FIMA, but the peak core k_{eff} is larger with the TRU igniter than the EU igniter because of the larger number of neutron per fission with ^{239}Pu than with ^{235}U. This burnup corresponds to ~15% FIMA in the blanket; all four blanket batches have k_∞ larger than unity and are able to sustain the breed and burn mode after removing the igniter and adding depleted uranium batches. This is discussed in Sections 6.2.1 and 6.5.2.

6.2 Equilibrium cycle maximum achievable burnup

In Section 6.1 that was shown possible to ignite the large B&B core using enriched fuel, and breed sufficient fissile material in the blanket to bring its k_∞ above the igniter's k_∞ while keeping the core critical. When the core becomes subcritical, the blanket characteristics are the same for both the TRU and EU igniters. In this section, the large B&B core equilibrium composition, achieved after multiple fuel shufflings, is determined and the equilibrium core performance is quantified.

6.2.1 Preliminary results for simple shuffling schemes

Once the initial core made of an enriched igniter and a blanket becomes subcritical at ~300 GWd/tHM, several fuel shuffling schemes, described below, are tried. The resulting k_{eff} evolutions with burnup are shown in Figure 6.14 and the attainable burnups are given below. For all of the shuffling schemes discussed in this section (Section 6.2.1 only), there is no fuel recycling taking place, but 75% of the gaseous and volatiles fission products are assumed to be continuously removed during operation.

Scenario 1: The location of the fuel initially loaded in the seed and in the blanket is interchanged. With this shuffling, there is no fresh fuel added and this mode of operation is not "breed-and-burn". The overall core average burnup achieved is 40% (intersection of the yellow curve with the k_{eff}=1.0 line). This shuffling scheme does not enable a sustainable operation.

Scenario 2: The fuel located at the inner half of the core is discharged in its entirety, the fuel in the outer half of the core is shuffled into the inner half of the core, and a fresh feed fuel made of depleted uranium is loaded into the outer half of the core. Equilibrium is reached after two fuel shuffling and the average discharge burnup of the fuel is 48% (green curves). This shuffling scheme is very coarse as 50% of the core volume is replaced at each cycle and the corresponding burnup reactivity swing is very large – over 8%.

Scenario 3: When k_{eff}=1, the innermost radial zone fuel is removed, the fuel in all the other zones is shuffled inward, and depleted uranium feed fuel is loaded at the outermost

zone. It takes many cycles to reach equilibrium using this approach because the cycle length is not constant. The average discharge burnup is 55% (red curves) and the burnup reactivity swing is only about 4%; approximately one half that of the previous shuffling scheme.

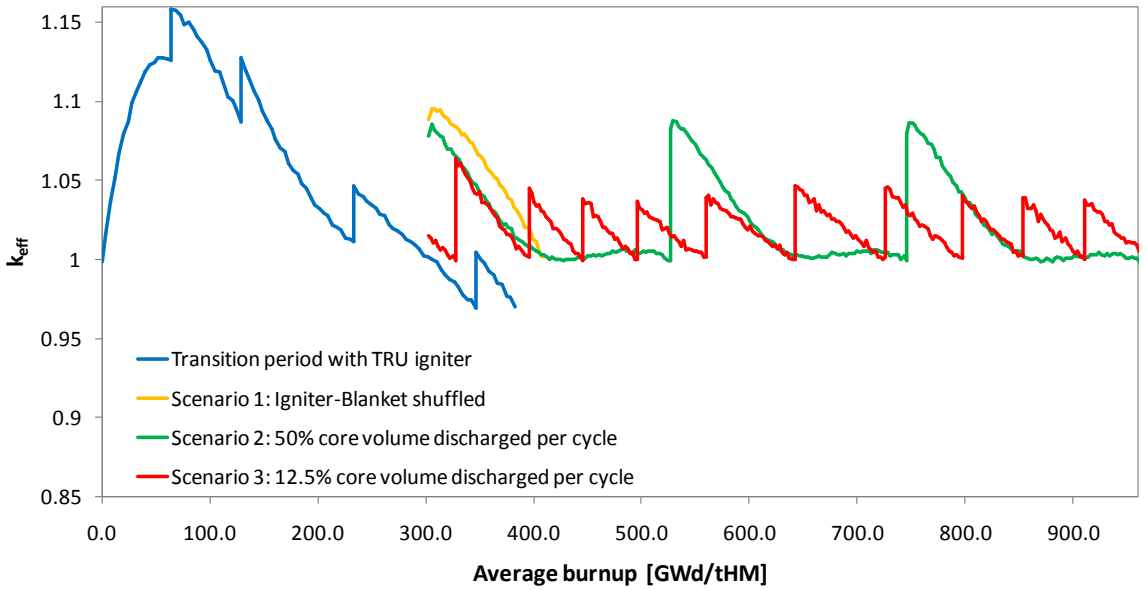

Figure 6.14: Multiplication factor evolution for different shuffling strategies in the large B&B core

6.2.2 Simple progressive shuffling scheme

Using the progressive shuffling scheme proposed in scenario 3, it takes several cycles to achieve equilibrium because the cycle length is not kept constant. When the core becomes subcritical, all the fuel is recycled with the melt-refining process and shuffled; the highest burnup zone is discharged and a fresh depleted uranium zone is added to the core. During operation, 75% of the gaseous fission products are continuously removed from the fuel. In order to determine the performance of the core at equilibrium an iterative approach is used to determine the equilibrium core characteristics. The equilibrium module used, developed at UC Berkeley, has been briefly described in Section 2.5.4. The equilibrium characteristics are independent of the type of igniter used.

Once equilibrium is reached, the maximum fuel discharge burnup is 55% FIMA, corresponding to cycles 8.80 years long. The evolution of k_{eff} for several equilibrium cycles is shown in Figure 6.15.

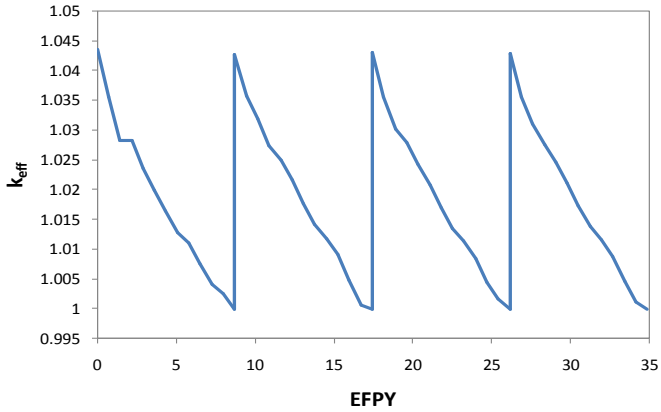

Figure 6.15: Multiplication factor evolution with burnup for four equilibrium cycles at 55% FIMA burnup for the large B&B core

The reactivity gain of ~4.5% with recycling is mostly due to the axial mixing of the fuel composition: most of the fissions are occurring in the central axial part, where the EOEC fission products content is the largest and the heavy-metal content is the lowest. The reactivity gain due to fuel recycling and shuffling is larger as compared with the preliminary analysis (Figure 6.14, red). The burnup reactivity loss is larger in this case because (1) no volatile fission products are removed during operation, whereas in the preliminary study 75% of them are removed, in addition to the gaseous fission products, during operation; and (2) no fuel recycling is applied in the preliminary study.

Figures 6.16 and 6.17 show, respectively, the net neutron total leakage probability out of each radial zone and the radial power distribution at the BOEC and EOEC. The resulting equilibrium radial power distribution is quite favorable; the radial peak-to-average axially integrated power ratio is 1.66. As the peak power density is 248 W/cm^3, the equilibrium core could possibly be operated at higher power than assumed – 3000 MW_{th}. It is observed that over the equilibrium cycle the power density distribution shifts radially outward. Correspondingly, the radial leakage probability increases from 1.9% at BOEC to 4.1 % at EOEC. The equilibrium core axial leakage probability is 4.1%, as at BOL.

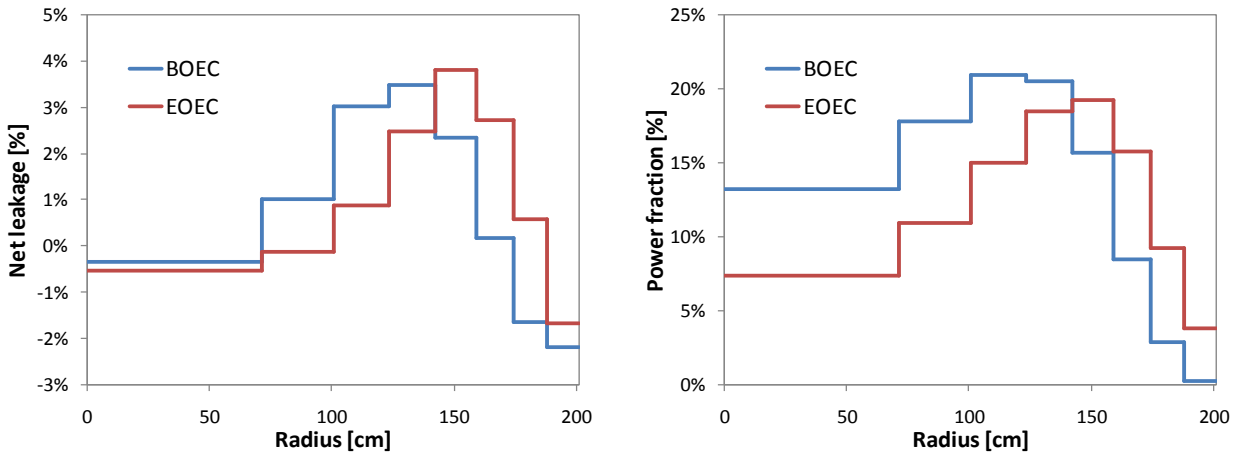

Figures 6.16 and 6.17: Zone-wise net neutron total leakage – left – and power fraction distributon – right – at BOEC and EOEC for the large B&B core having a discharge burnup of 55% FIMA.

Table 6.2 summarizes selected design and performance parameters of the equilibrium core. The "conversion ratio" provided in the table is the ratio between the number of transuranium atoms in the entire core at the end and beginning of an equilibrium cycle. The EOEC zone-wise concentration of the important actinides is given in Figure 6.18. The concentration of ^{239}Pu peaks after the third shuffling – in the third zone from the outer core boundary. Thereafter it is slightly decreasing as the ^{238}U concentration is depleted when approaching the central zone.

Table 6.2: Core Design and Performance Parameters at Equilibrium for the 8 Radial Zones Large B&B Core

Parameters	Value
Fuel/Gap/Clad/Coolant volume fractions [%]	37.5/12.5/22/28
Average power density [W/cm^3]	112.5
Peak power density [W/cm^3]	248
Average specific power density [W/g HM]	21.0
Cycle length [y]	8.8
Average core burnup at BOEC/EOEC [% FIMA]	19.9/26.9
HM mass at BOEC/EOEC [tons]	114.4/104.5
TRU mass at BOEC/EOEC [tons]	10.2/11.5
Conversion ratio	1.15
Discharge burnup [GWd/tHM]	540.8
Burnup reactivity loss [% Δk]	4.4
Core average flux [10^{15}n/cm^2-s]	1.8
Fast flux fraction > 0.1 MeV [%]	65.0
Axial neutron leakage at BOEC/EOEC [%]	4.1/4.1
Radial neutron leakage at BOEC/EOEC [%]	1.9/4.1

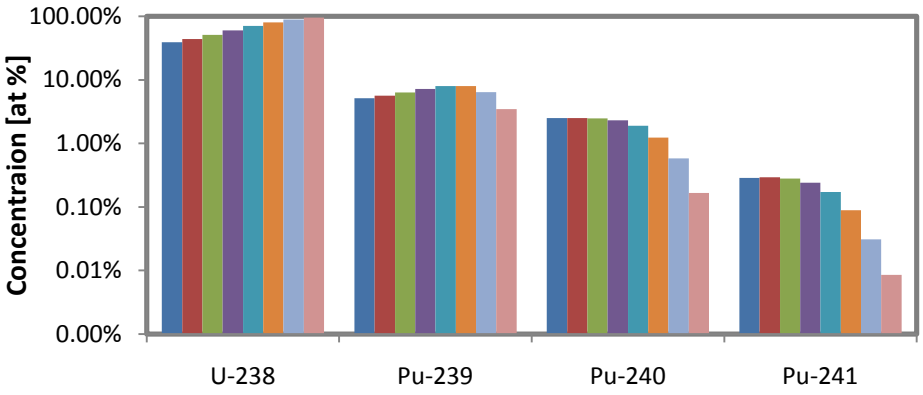

Figure 6.18: Fuel composition at EOEC, accross the core, from the center (left) to the outer (right). The concentration is given as the atomic fraction among the heavy metal and fission products

Table 6.3 compares selected characteristics of the fuel discharged at 55% FIMA burnup from the large B&B core and of the fuel discharged at 50 GWd/tHM from a once-through LWR. The uranium ore utilization is measured in several ways, both assuming that the initial starter fuel is made of 11% enriched uranium, and that the large B&B core is being fed only with the depleted uranium left over from the uranium enrichment process: (1) Per unit weight of natural uranium ore.; (2) Per separative work unit (SWU) required. It is found that the large B&B core and fuel cycle hereby proposed offers two orders of magnitude increase in the uranium ore utilization and nearly two orders of magnitude reduction in the SWU requirement without resorting to actinides separation. The restriction to use the depleted uranium left-over from the natural uranium used for making the enriched uranium for the starter fuel is artificial; the same core could continue fissioning depleted uranium – as well as used fuel discharged from LWRs, huge quantities of which has been accumulated. It is assumed that at the end of life of the reactor hardware, the equilibrium core will be transferred to a new reactor and no fissile fuel will have to be added to achieve criticality – as is required in the first reactor. Also given in Table 6.3 is the total energy value of the 1.5 million tons of depleted uranium accumulated in the world so far [6], if all this depleted uranium was to be fed into the breed-and-burn reactors – 3000 times the world present annual generation of nuclear electricity. The current rate of depleted uranium being generated in the uranium enrichment plants in the world could support a breed-and-burn based power reactor capacity that is 100 times higher than the capacity of the presently operating nuclear power reactors, worldwide.

It is also observed in Table 6.3 that, relative to LWR operating with the once-through fuel cycle, the fuel discharged from the large B&B core under consideration features, per unit of electricity generated: (a) ~40% the amount of TRU and Pu; (b) ~10% the inventory of ^{237}Np and its precursors; (c) ~12% of the decay heat from TRU one year following discharge; (d) ~28% of the radiotoxicity of TRU and fission products one year following discharge; (e) ~7% the neutron emission rate one year following discharge. The fraction of the fissile isotopes in the discharged plutonium is comparable but the decay heat and neutron emission rate per unit mass of discharged plutonium are nearly half as large.

Table 6.3: Selected Fuel Cycle Characteristics of Breed and Burn Core Operating with Multi-Recycling with No Actinides Separation Versus Once-through LWR

Characteristic	LWR	Breed & Burn
Feed fuel type	Enriched U	Depleted U
^{235}U wt. %	4.5	0.2
Discharge burnup ($GW_{th}D$/tHM)	50	541
Natural uranium utilization		
1. GW_eD generated per ton U_{nat}; FR uses same amount of U_{nat}	1	109
2. GW_eD generated per SWU; FR uses enriched U starter fuel + leftover U_{dep}	1	>90
GW_eY generated by all U_{dep} in world / GW_eY presently generated in world	1	3000
GW_eY generated by U_{dep} made per year / GW_eY presently generated in world	1	100
Discharged fuel		
TRU per $GW_{th}D$ ($g/GW_{th}D$)	300	142.9
Relative amount of TRU per GW_eD (%)	100	39.7
Relative amount of Pu per GW_eD (%)	100	43.1
Fissile/total Pu at EOEC (%)	64.5	66.7
^{238}Pu/total Pu at EOEC (%)	3.2	0.8
^{237}Np+^{241}Pu+^{241}Am+^{245}Cm ($g/GW_{th}D$)	58.6	5.9
^{99}Tc/^{129}I/^{135}Cs ($g/GW_{th}D$)	23.1/5.2/15.3	14.1/7.6/40.1
Decay heat 1 year after discharge (W/kg Pu)	16.8	7.9
Neutron emission 1 year after discharge (n/s/kg Pu)	4.58E+05	2.09E+05
Radio-toxicity (m^3 of water/GW_eD)		
HM 1 year after discharge	1.36E+10	2.42E+09
HM 30 years after discharge	1.03E+10	2.14E+09
FP 1 year after discharge	4.71E+10	1.43E+10
FP 30 years after discharge	8.54E+09	6.52E+09
Relative radio-toxicity per GW_eD (%)		
HM 1 year after discharge	100	17.8
HM 30 years after discharge	100	20.8
FP 1 year after discharge	100	30.4
FP 30 years after discharge	100	76.3
Relative decay heat per GW_eD (%)		
1 year after discharge	100	12.2
30 years after discharge	100	49.1
Relative spontaneous neutron yield per GW_eD (%)		
1 year after discharge	100	7.2
30 years after discharge	100	8.1

6.2.3 Improved shuffling schemes

The shuffling scheme studied in Section 6.2.2 consists of a simple inward promotion. Although this is simple to simulate, a different choice of shuffling scheme can enable achieving larger discharge burnup and smaller burnup reactivity swing. While it is moderately difficult to define a shuffling scheme enabling larger discharge burnup, it becomes more challenging when trying not to excessively increase the peak power density. The choice of the improved shuffling pattern is made based on the following considerations:

- The two outermost fuel zones, being almost pure depleted uranium, should remain located at the outermost radial core location in order to minimize the fraction of neutrons radially leaking out of the core;
- A low burnup – low fissile material – fuel zone should be loaded near the core center in order to decrease k_{eff} at BOEC and reduce the power peaking;
- A medium burnup fuel should not be located at the innermost location. This is the fuel with the highest reactivity worth, and if located at the innermost location, will result into a very large power peaking;
- The high burnup fuel contains many fission products, and its reactivity worth is decreasing with increasing burnup. In order to extend its burnup, it should be located in a zone with a hard neutron spectrum, for instance near the core center. This will slightly penalize the core reactivity.

After studying several shuffling schemes, it is found possible to extend the burnup by +2% FIMA while decreasing the burnup reactivity swing to about 2% by using the pattern schematically showed in Figure 6.19 and recycling the fuel with the melt-refining process. As a result of this improved shuffling, the peak power density increases by +18% to 293 W/cm^3. This corresponds to a radial power peaking factor of 2.02. This is still significantly smaller than the radial power peaking factor achieved during the transition period, and thus will not be limiting the core power level.

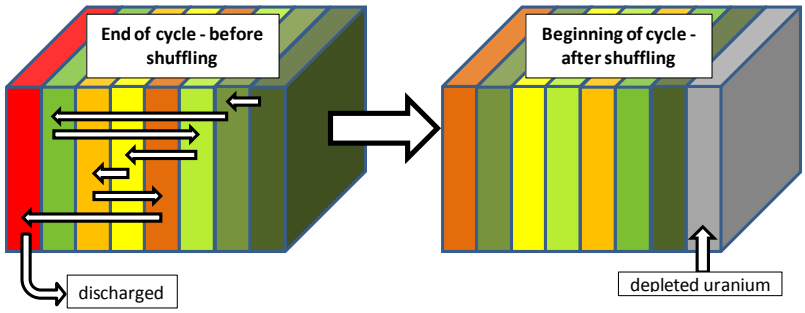

Figure 6.19: Schematic of the improved shuffling scheme used for the large B&B core

Due to the larger discharge fuel burnup, the cycle length is increased to 9.04 years. The radial power and burnup distributions at BOEC and EOEC are given in Figure 6.20 and 6.21, below. Compared to the simple shuffling scheme previously studied, the power distribution change from BOEC to EOEC is very different. For the simple shuffling, the power distribution was shifting toward the outer zones, where the burnup was smaller. For improved shuffling scheme, the radial zones having a burnup larger than 15% FIMA at BOEC see their power fraction decreasing, while for the other zones it is increasing. This phenomenon is particularly

important for the second innermost radial zone. At EOEC, the burnup of this zone is about 15% FIMA, corresponding to the maximum k_∞ value – shown in Figure 5.1 and discussed in Chapter 5. The power peaking is occurring in this zone at EOEC due to its central location. It also makes the power density in the innermost radial zone slightly increase at EOEC despite having a burnup above 50% FIMA. Perhaps the primary advantage of the improved shuffling scheme is that it offers a relatively small shift in the radial power distribution with burnup. This will simplify the design of the core cooling system.

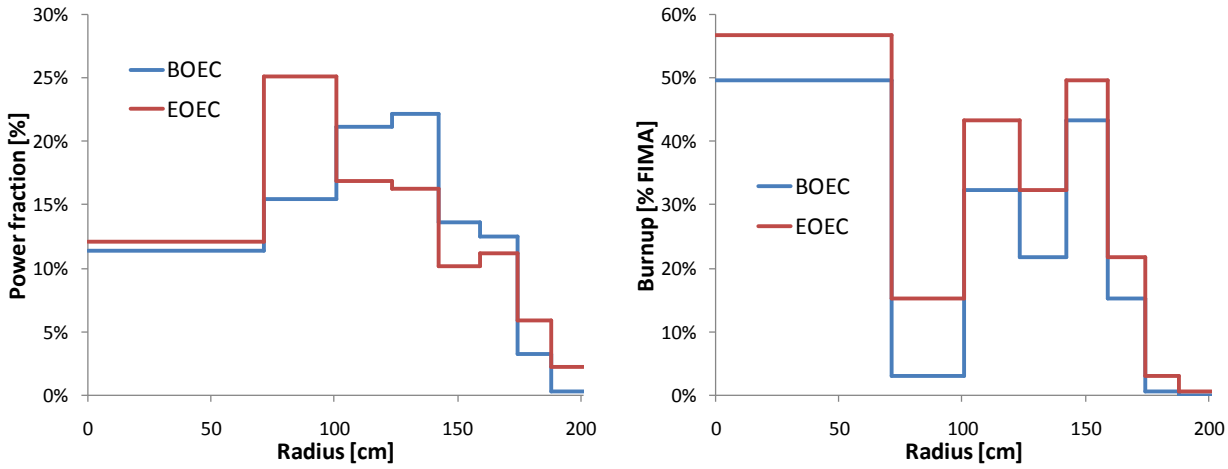

Figure 6.20 and 6.21: Radial power – left – and burnup – right – distributions at BOEC and EOEC for the improved shuffling scheme for the large B&B core

6.3 Equilibrium cycle minimum required burnup

For the maximum burnup, 57% FIMA, achieved with the improved shuffling in Section 6.2.3, the amount of plutonium bred during a cycle is larger than the minimum required for sustaining the breed and burning mode of operation. In Section 5.4 it was found that the minimum required burnup for sustaining the breed and burn mode in a 1-D cylindrical model is approximately 20%. When the minimum discharge burnup is small enough, the discharged fuel k_∞ is larger than unity and it can be used to establish the breed and burn mode in another reactor. The objective of this section is to quantify the minimum required burnup in the large B&B core. The possibility to spawn additional B&B cores is discussed in Section 6.5.

The fuel being discharged with a small burnup, only a small fraction of the fuel elements remaining in the core have k_∞ above unity, resulting in a large peak power density. In order to minimize the amplitude of the reactivity swing between two cycles, and to have a larger choice of shuffling schemes to deal with the large peak power density, the number of radial fuel zones modeled in large B&B core model is increased from 8 to 12. The zone thickness is decreased to conserve the core dimensions. The same fuel management assumptions as in Sections 6.2.2 and 6.2.3 are used: (a) 75% of the gaseous fission products is continuously removed from the fuel; (b) at EOEC all the fuel is recycled with the melt-refining process, (c) the highest burnup zone is discharged and (d) a fresh depleted uranium zone is added to the core.

6.3.1 Simple shuffling scheme

The results presented here pertains to the same simple shuffling scheme used in Section 6.2.2: at EOEC the innermost fuel zone is removed, all the other fuel zones are shuffled inward, and fresh depleted uranium fuel is added at the outermost location.

For a discharge burnup of 199.8 GWd/tHM – 20.4% FIMA, the multiplication factor, shown in Figure 6.22, is equal to unity at BOEC and increasing up to 1.035 at EOEC. Decreasing the discharge fuel burnup makes the core subcritical at BOEC, while increasing it makes it larger because of the larger amount of fissile material in the core. At BOEC, the multiplication factor is increasing due to the increase of fissile material in all the radial zones. When approaching the middle of the equilibrium cycle, the overall mass of fissile material is increasing in the core but the mass of fissile material is decreasing in the innermost radial zone that features the highest burnup and highest fission products concentration. This effect, along with the increasing radial leakage probability due to the power distribution shifting outward, reduces the rate of increase of the multiplication factor and eventually causes it to start to decrease at EOEC. The power distribution at BOEC and EOEC is shown in Figure 6.23. The burnup reactivity swing is 3.5%, and approximately 2.5% of the total number of neutrons generated need to be absorbed by the control systems to maintain k_{eff} equal to unity.

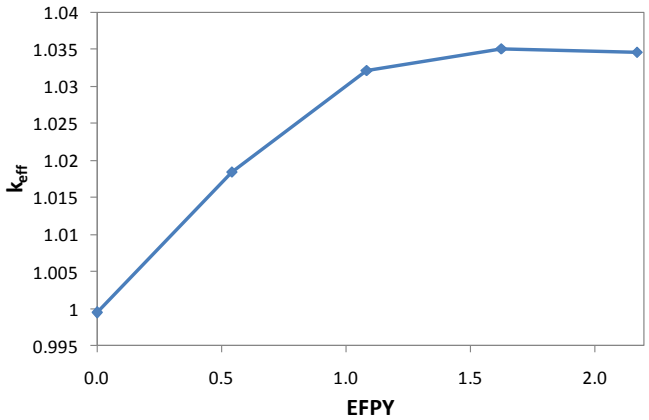

Figure 6.22: Multiplication factor evolution for the large B&B core operating with the minimum discharge burnup for the simple shuffling scheme

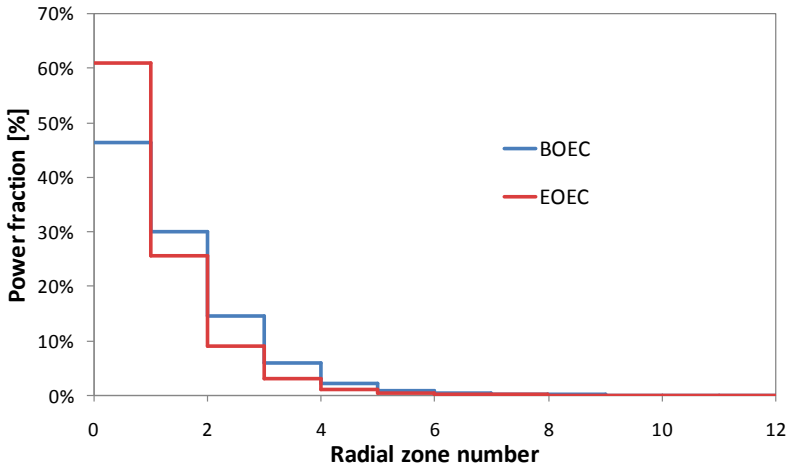

Figure 6.23: Power distribution at BOEC and EOEC for the large B&B core operating with the minimum discharge burnup for the simple shuffling scheme

The power peaking is occurring in the innermost radial zone at EOEC. For a discharge burnup of 20.4% FIMA, the k_∞ value of the discharged fuel elements is close to its maximum. Therefore, when the highest k_∞ fuel is loaded in the innermost zone of the core where the neutron flux is the highest, its fission rate is very high so that the innermost zone produces more than 60% of the total core power in less than 8.5% of the core volume. At BOEC, the innermost zone has a burnup of 9.1% FIMA and its k_∞ is 1.28, the highest of all the fuel zones. Then, it accumulates +10.3% burnup FIMA during a single cycle, and at EOEC its k_∞ is still 1.25, but is decreasing. The k_∞ and burnup distributions are both shown in Figure 6.24 for the 12 radial zones.

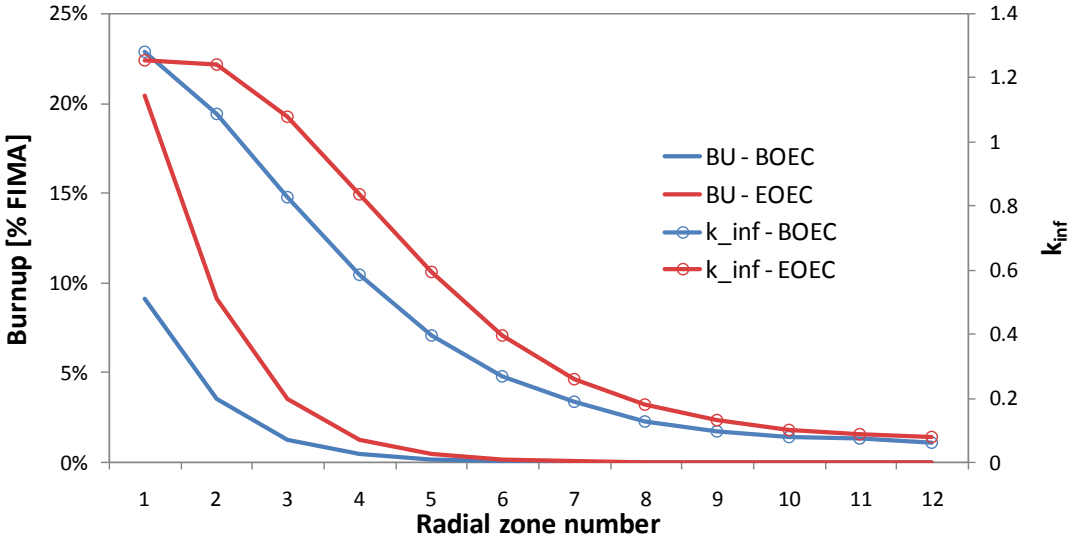

Figure 6.24: Burnup and k_∞ distribution at BOEC and EOEC for the large B&B core operating with the minimum discharge burnup for the simple shuffling scheme

The outer half of the core is producing no power and accumulates almost no burnup because of the shuffling scheme used: most of the neutrons are generated near the center of the core, and are absorbed before reaching the outermost fuel regions. The axial neutron leakage

probability is constant from BOEC to EOEC and equals to 3.8%; the radial leakage is practically zero. The axially averaged radial power peaking factor of this core at EOEC is 7.32. It is difficult to efficiently cool such a core and its average power density level will be very low.

6.3.2 Improved shuffling schemes

The objective of the study reported in the present section is to investigate possibilities for reducing the power peaking factor by using alternative shuffling schemes and to quantify the implications of these shuffling schemes on the minimum required burnup. The main idea pursued is to increase the volume fraction of the core producing power by building up fissile material in the fed fuel sooner. A potential disadvantage of power flattening is an increase in the radial neutron leakage probability that may result in a larger minimum required burnup.

The best of the improved shuffling schemes identified is described in Table 6.4. The fresh depleted uranium fuel is loaded at the outermost location, and then shuffled back and forth toward the core center a couple times. When it reaches location #5 – fifth radial zone, it is discarded. Location #1 is the innermost location, while location #12 is the outermost. The multiplication factor is linearly increasing from 1.00 at BOEC to 1.04 at EOEC. While the fissile material content of the highest burnup zones – locations #4 and #5 – is decreasing during the cycle, the fissile content of the inner zones is increasing, resulting in an overall increase of k_{eff}. The infinite multiplication factor is given, in Figure 6.25, at BOEC and EOEC for each radial zone along with their burnup. The minimum discharge burnup required to maintain the breed and burn mode with this shuffling scheme is found to be 189.3 GWd/tHM (19.4% FIMA) and only 2.1% of the neutrons are to be absorbed by the control systems to maintain k_{eff} equal to unity.

Table 6.4: Improved Shuffling Scheme Pattern

Radial zone…	is moved to radial location…
12	11
11	10
10	9
9	8
8	1
1	7
7	6
6	2
2	3
3	4
4	5
5	discarded

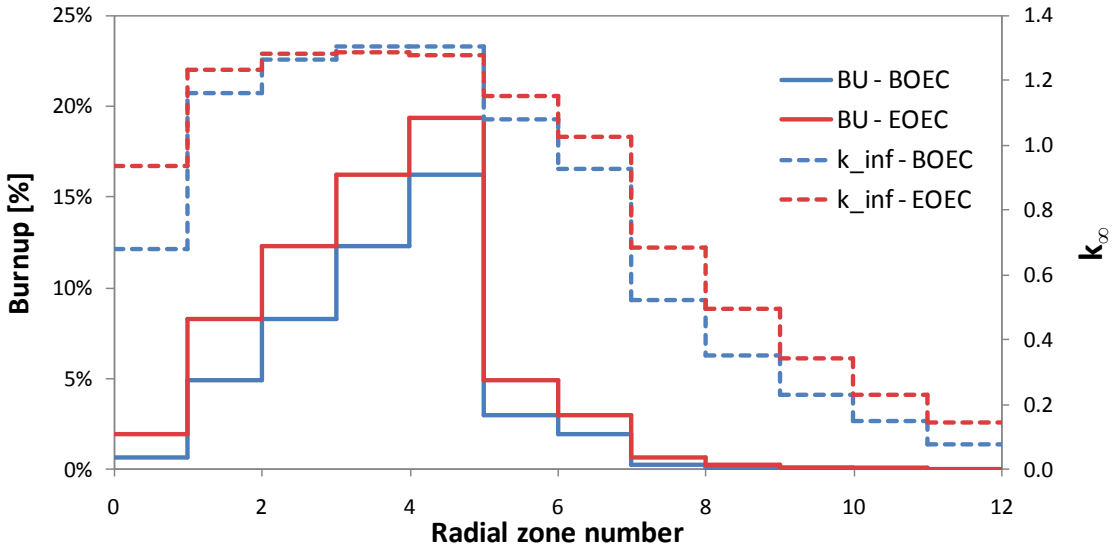

Figure 6.25: Burnup and k_∞ radial distribution at BOEC and EOEC for the large B&B core with the improved shuffling scheme for minimum discharge burnup

The infinite multiplication factor is larger than unity at BOEC for 5 out the 12 radial zones; all located in the innermost half of the core. The radial power distribution of Figure 6.26 shows that no power is generated by the outermost radial fuel zone. The five outermost radial zones have the lowest burnup and lowest power fraction, producing very few neutrons. Most of the neutron flux observed in these zones is due to neutrons leaking from the inner half of the core to the outer half; most of these neutrons are absorbed in the outer blanket elements. The radial neutron leakage probability resulting from this improved shuffling scheme is constant and equal to 0.7%, not significantly larger than for the simple shuffling scheme. The total neutron leakage probability is 4.5% at BOEC and decreases to 4.3% at EOEC.

The radial power distribution change between BOEC and EOEC is much smaller than for the simple shuffling scheme. The power distribution variation is only occurring in the five innermost radial zones, and stays almost constant in the seven outermost radial zones. The axially averaged radial power peaking factor is found to be 2.58, occurring at BOEC. This peaking factor, while still large, is only ~1/3 of the simple shuffling scheme, and is similar to the radial power peaking factor found in Section 6.1 for the large B&B core during the transition period.

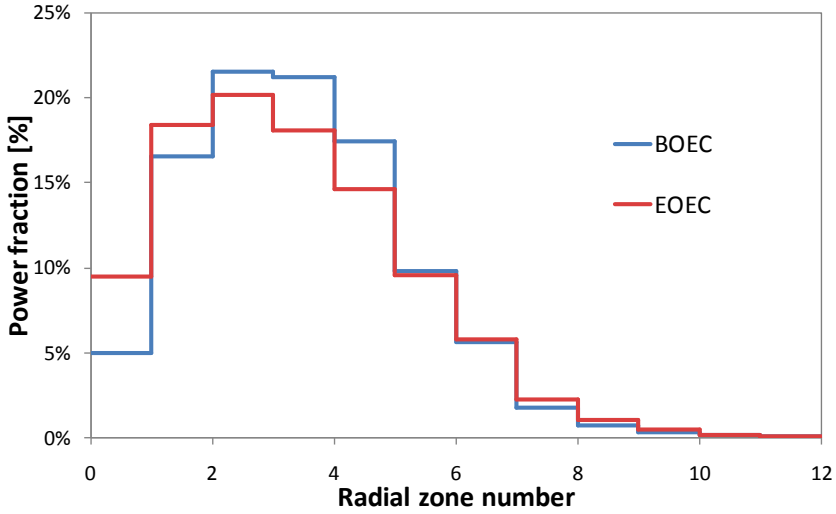

Figure 6.26: Radial power distribution at BOEC and EOEC for the large B&B core with the improved shuffling scheme for the minimum discharge burnup

The data presented above suggest that while the improved shuffling scheme provides an acceptable radial power distribution, the neutron losses by leakage and in the control systems is slightly increased and that the required burnup is expected be larger than for the simple shuffling scheme while it is found smaller. For the simple shuffling scheme 6.3% of the neutrons are lost: 2.5% are lost in the control systems and 3.8% by leakage. For the improved shuffling scheme 6.6% of the neutrons are lost: 2.2% are lost in the control systems and 4.4% by leakage.

The smaller minimum required burnup found for the improved shuffling scheme, despite the larger neutron loss, is explained by looking at the fuel recycling, which is occurring for all the fuel zones at EOEC for both shuffling schemes. For the simple one, the innermost fuel zone is accumulating more than 55% of the discharge burnup in a single cycle before being discharged. None of the solid or volatile fission products generated in this zone are removed from the fuel, resulting in a large parasitic neutron capture. For the improved shuffling scheme, the burnup is somewhat evenly accumulated in the different radial zones and a fraction of the fission products is removed at every EOEC by the melt-refining process, yielding a smaller parasitic neutron capture. Overall, about 5.2% of the neutrons are captured in the fission products for the simple shuffling scheme, while this fraction is only 4.5% for the improved shuffling scheme.

While this results in a better neutron economy for the improved shuffling, it is strongly dependant on the frequency of the fuel recycling. If the cladding can sustain 400 DPA (~20% FIMA), no fuel recycling is required and the minimum required burnup for the improved shuffling scheme would be around 21% FIMA, while still ~20.4% FIMA for the simple shuffling scheme.

Using this improved shuffling scheme it is possible to maintain the minimum required burnup in the range of 20% FIMA while decreasing the radial power peaking factor from 7.32 to 2.58 and reducing the power distribution variation with burnup and the burnup reactivity swing. It is possible to decrease the burnup reactivity swing even more by increasing the number of fuel batches and reducing the cycle length. Compared to the same large B&B core at equilibrium with the maximum discharge burnup, the peak power density is 28% larger because of the fewer fuel elements having k_∞ above unity.

6.4 Neutron balance

The neutron balance approach described in Section 5.1 can be used for the large B&B core to confirm the minimum required burnup and maximum achievable for establishing and sustaining the breed and burn mode in the large B&B core. It can also be used to estimate the number of neutrons that need to be absorbed in the fuel to sustain the breed and burn mode and the number of excess neutrons that could still be produced by the fuel when it is discharged.

Although it is convenient and less computational intensive to perform the neutron balance using a zero dimension unit cell, it is not as reliable as doing it for the finite core model studied in this chapter: (i) the neutron spectrum is significantly changing with burnup for the unit cell while for the finite core the neutron spectrum does not significantly change, because the average core burnup increases only slightly during a cycle; (ii) the neutron leakage probability cannot be estimated using the unit cell model; (iii) the excess reactivity that needs to be mitigated with control systems cannot be estimated using the unit cell model.

In Section 6.4.1 the neutron balance of the large B&B core model is compared to the neutron balance of a zero dimensional unit cell for which the neutron leakage probability and fraction of neutrons lost in the control systems are identical to the large B&B core values. This comparison is performed for the large B&B core operating both with the maximum achievable burnup and with the minimum required burnup. Section 6.4.2 compares the neutron balance performed with the large B&B core model for the TRU igniter and EU igniters discussed in Section 6.1

6.4.1 Finite core compared to unit cell at equilibrium

The neutron balance is performed for several equilibrium cores:

Scenario 1: An infinite unit cell initially composed of depleted uranium, accounting for the neutron leakage probability and the fraction of neutrons absorbed in control systems obtained for the large B&B core at 19.4% FIMA in Section 6.3.2. The fuel is recycled with the melt-refining process every ~9% FIMA.

Scenario 2: An infinite unit cell initially composed of depleted uranium, accounting for the neutron leakage probability and the fraction of neutrons absorbed in control systems obtained for the large B&B core at 55% FIMA in Section 6.2.2. The fuel is recycled with the melt-refining process every ~9% FIMA.

Scenario 3: The large B&B core at equilibrium of Section 6.2.2 operating at 55% FIMA. The average neutron leakage probability is 6.95% and the average fraction of neutrons absorbed in the control systems is 2.1%. The fuel is recycled at every EOEC.

Scenario 4: The large B&B core at equilibrium of Section 6.3.2 operating at the minimum discharge burnup of 19.4% FIMA. The average neutron leakage probability is 4.4% and the fraction of neutrons absorbed in the control systems is 2.2%. The fuel is recycled at every EOEC.

In order to perform the neutron balance for the finite core models, the axially averaged characteristics of each of the radial fuel zones are first estimated at each burnup step of an equilibrium cycle. The axially averaged infinite multiplication factor for each radial zone is obtained using Equation 6.1. The reactions rates are summed up for the three axial zones (“i”

varies from1 to 3). The average number of neutron emitted per fission is assumed to be constant in all the zones and equal to 2.92.

$$k_\infty = \frac{\nu * \sum_{i=1}^{i=3} [\phi_i * \Sigma_{F,i}^{HM}]}{\sum_{i=1}^{i=3} [\phi_i * (\Sigma_{A,i}^{HM} + \Sigma_{A,i}^{FP} + \Sigma_{A,i}^{Zr} + \Sigma_{A,i}^{Na} + \Sigma_{A,i}^{HT-9})]} \qquad \text{(Eq. 6.1)}$$

The evolution of k_∞ with burnup is given for the four scenarios in Figure 6.27. The evolution of k_∞ is the same for the two unit cell scenarios (1&2) and only one curve is shown for both of them: the difference between these scenarios is the different neutron leakage probability and fraction of neutrons absorbed in the control systems assumed for the neutron balance. After a few percent burnup, the k_∞ for scenario (4) is larger than for scenario (3), which is itself larger than for scenarios (1&2). For scenario (4), there are eight fuel recyclings occurring over a 19.4% FIMA burnup range, while for scenario (3) the eight fuel recyclings are occurring over a 55% FIMA burnup range. For scenarios (1&2), when the fuel reaches 55% burnup, only five fuel recycling occurred.

Despite the fuel recycling differences, the evolution of k_∞ for the three models shows a very good agreement for burnup above 0.5% FIMA. Below 0.5% FIMA burnup, the unit cell displays a significantly higher k_∞ than the two large B&B core scenarios. This behavior is due to the harder spectrum achieved in the unit cell at very low burnup. The unit cell is initially made of pure depleted uranium and the spectrum is very hard because there are no fission products to slow down the neutrons. For the large B&B core models, the spectrum is dictated by the whole core, and the neutrons are slowed down by the fuel elements having a larger burnup – and more fission products – before reaching the very low burnup zones, resulting in a softer spectrum in those zones. With a harder spectrum, the fission cross-section of ^{238}U is larger, yielding a larger k_∞ for the unit cell model.

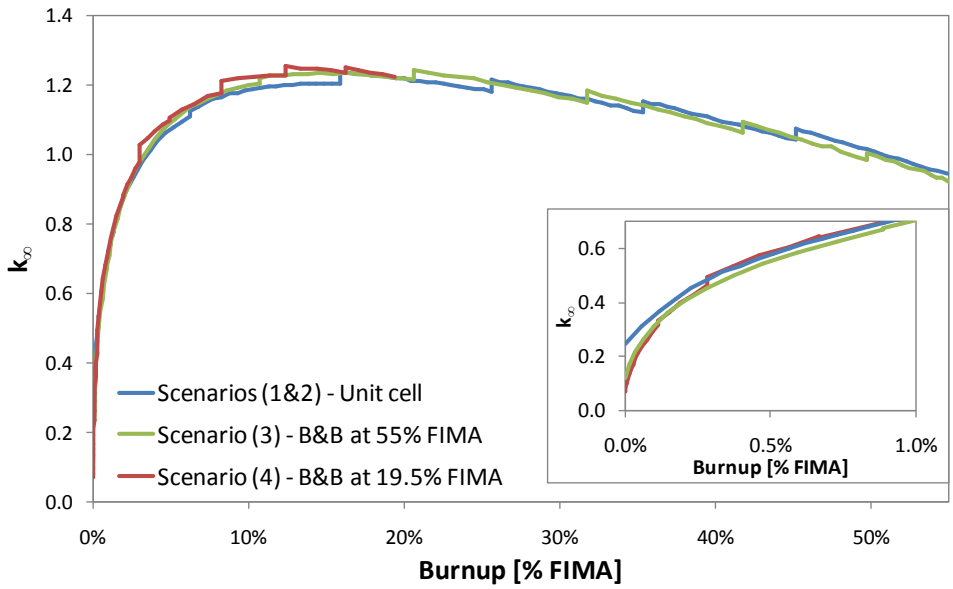

Figure 6.27: k_∞ evolution with burnup for the four scenarios studied

The neutron balance, in neutron per cm^3 of fuel (not core), is performed using the k_∞ evolution and the estimated neutron losses. The balance obtained for the high burnup, high neutron loss scenarios – (2) and (3), and for the low burnup, low neutron loss scenarios – (1) and (4) – are presented in Figures 6.28 and 6.29, respectively.

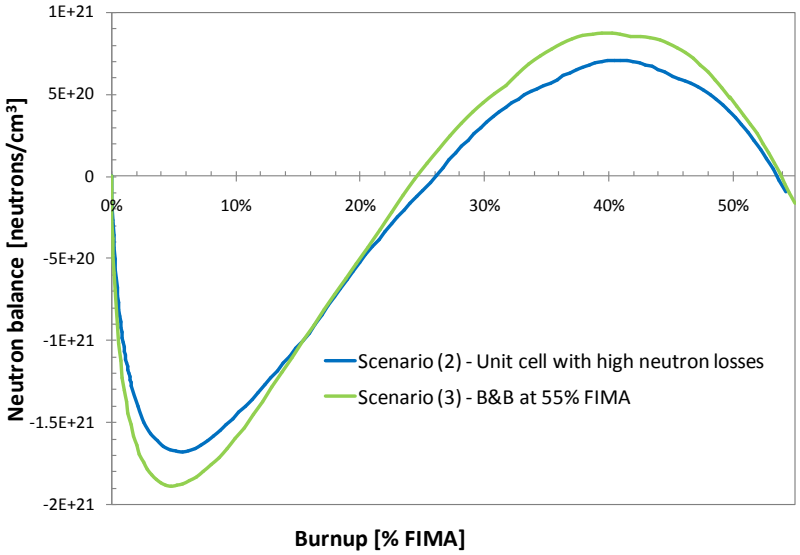

Figure 6.28: Neutron balance for scenarios (2) and (3) – High burnup and high neutron losses

For scenario (3), approximately 1.8E+21 neutrons need to be absorbed per cm^3 of fuel to bring the multiplication factor of a depleted uranium assembly above unity. From 0% to 5% FIMA the assembly lacks neutrons and from 5% to 24% FIMA it provides excess neutrons to breed plutonium in other subcritical assemblies. This fuel assembly can maintain $P_{CR}*P_{NL}*k_\infty$ (P_{NL}=probability of non-leakage; P_{CR}=fraction of neutrons not absorbed in the control systems) above unity up to 42% FIMA and features an additional neutron excess of approximately 8.7E+20 neutrons/cm^3 of fuel, sufficient to extend the fuel burnup up to ~54% FIMA. The neutron balance obtained with the unit cell – scenario (2) – features similar attainable burnup, but the number of required neutrons and number of excess neutrons, per unit of fuel, are 10% smaller than with the neutron balance of scenario (3).

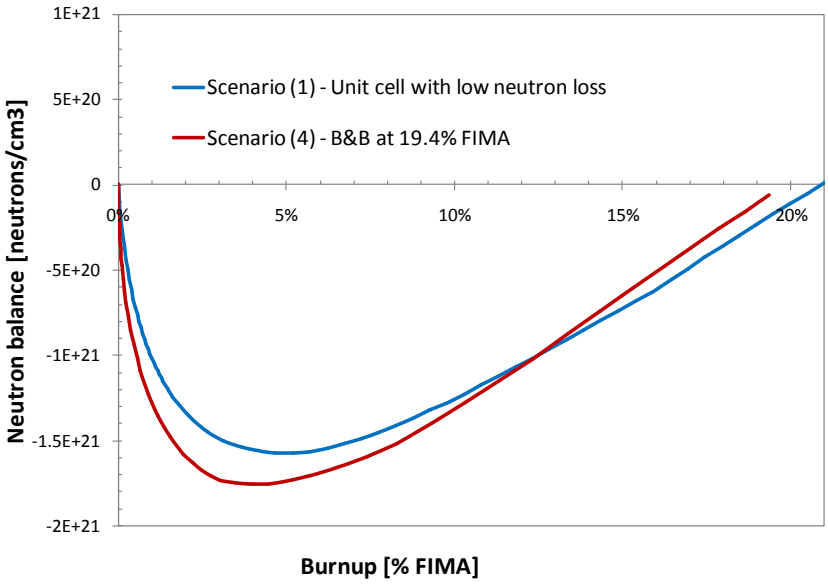

Figure 6.29: Neutron balance for scenarios (1) and (4) – Low burnup and low neutron losses

For scenario (4), approximately 1.75E+21 neutrons need to be absorbed per cm^3 of fuel to bring the multiplication factor of a depleted uranium assembly to unity. The neutron leakage probability being low, this occurs at 3.5% FIMA. At 20% FIMA, the depleted uranium assembly restituted as many excess neutrons as have been provided to it. This is the minimum required burnup for sustaining the breed and burn mode of operation. In Figure 6.29, the neutron balance for scenario (1) shows a minimum burnup of 21% FIMA and features ~10% smaller number of required neutrons per unit of fuel than for the finite core model – scenario (4). When discharging the fuel at 20% FIMA, the number of excess neutrons that could still be produced by the fuel is approximately 1.80E+21 neutrons per cm^3 of fuel. This is sufficient to start a new large B&B core using the fuel discharged at ~20% FIMA. This slight discrepancy between the finite core models and the unit cell models is due to the spectra difference at low burnup, and fuel recycling difference at burnups above 5% FIMA. Those small k_∞ differences represent up to 10% difference in the neutron balance.

The neutron balance performed for an infinite unit cell yielded minimum required burnup and maximum achievable burnup values reasonably similar to those obtained by the neutron balance performed for the finite core model. However, due to the spectral differences between the two systems, it has been found that the infinite cell method does not provide accurate results for the number of neutrons that need to be absorbed in the fuel and the number of excess neutrons that can be produced by the fuel.

6.4.2 Neutron balance for TRU and EU igniters

A neutron balance similar to that performed in Section 6.4.1 for the large B&B core at equilibrium is performed for the large B&B core when initially started with TRU igniter or EU igniter. The core geometry and igniters compositions are described in Section 6.1. During the transition period there is no fuel shuffling and therefore, the estimation of the igniter characteristics is performed for innermost half core volume corresponding to the whole igniter volume. The k_∞ values are obtained using Equation 5.1, summing the reaction rates over the three

axial and four radial fuel zones composing the igniter – twelve zones. It is assumed that 3% of the neutrons are absorbed by the reactivity control systems, corresponding to 6% reactivity swing. Based on the studies previously performed, the average neutron leakage probability is assumed 3.85% for the TRU igniter and 4.05% for the EU igniter.

The evolution of k_∞ for the two igniters is shown in Figure 6.30. Although the enrichments of each igniter is chosen such as to get $k_{eff}=1$ at BOL, the neutron leakage probability from the EU igniter is larger than from the TRU igniter. At BOL the EU igniter initially has a larger amount of fissile material and its k_∞ is larger than for the TRU igniter. ^{235}U producing fewer neutrons than ^{239}Pu per fission, more neutrons are available for breeding in the TRU igniter. The initial conversion ratio of the TRU igniter is larger than for the EU igniter, making the TRU igniter k_∞ increase more rapidly with burnup. As the ^{235}U of the EU igniter is being consumed, the EU igniter k_∞ converges toward the TRU igniter k_∞.

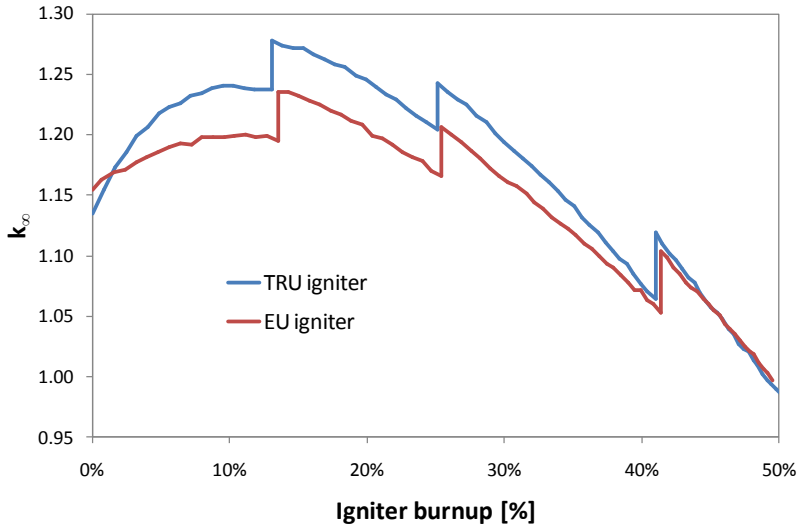

Figure 6.30: k_∞ evolution for the TRU and EU igniters of the large B&B core

The neutron balance, presented in Figure 6.31, shows that the excess neutron density of the TRU igniter is to 4.27E+21 neutrons per cm^3 of fuel and is 3.17E+21 neutrons per cm^3 of fuel for the EU igniter. It was previously found that for the large B&B core operating at the minimum required burnup, 1.75E+21 neutrons per cm^3 of fuel are required to make the k_∞ of a depleted uranium element equal to unity. Based on the neutron balance, it takes only 14% FIMA burnup with the TRU igniter and 19.5% FIMA burnup with the EU igniter to provide this number of neutrons to the depleted uranium elements. Using a single TRU igniter, it is theoretically possible to initiate a breed-and-burn mode of operation in two large B&B cores, while using a single EU igniter it is only possible to initiate it in a single large B&B core.

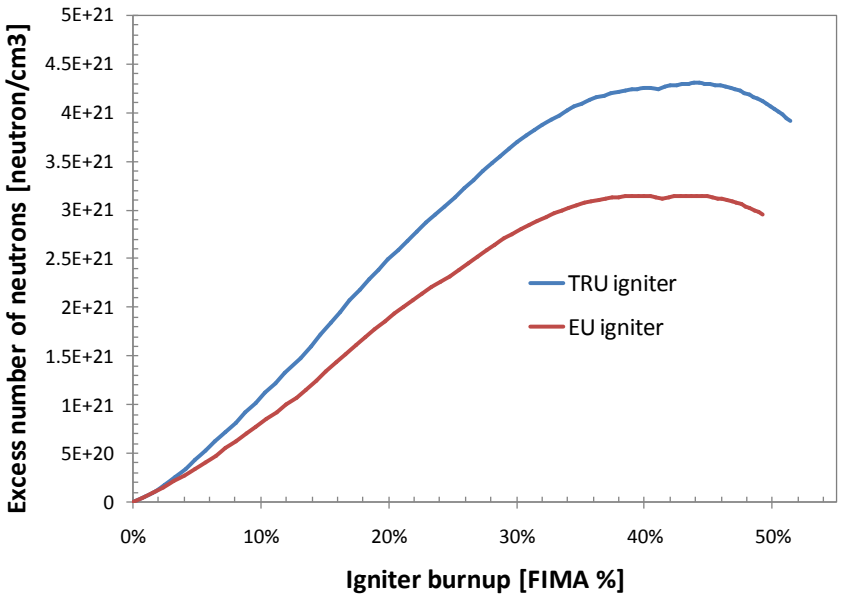

Figure 6.31: Excess number of neutrons in the large B&B for the TRU and EU igniters with 3% of neutrons absorbed in the control systems

For the above analysis it has been assumed that 3% of the neutrons are lost to the control systems, corresponding to a burnup reactivity swing of about 6%. It is possible to design a shuffling scheme that yields a burnup reactivity swing no larger than 3%. With this modified assumption, a single EU igniter is theoretically able to establish a breed-and-burn mode of operation in two cores, while two TRU igniters would be able to establish it in five cores.

6.5 Feasibility of spawning new cores

The neutron balance analysis performed in the previous section showed that if the TRU/EU igniter is discharged right after initiating a breed and burn mode of operation in the first core, is loaded as the igniter into another core (of a new reactor) it can establish a breed and burn mode of operation in this second core and, possible, even in a third core. Moreover, the fuel discharged from an equilibrium large B&B core at the minimum required burnup – ~20% FIMA – has sufficient excess reactivity to establish a B&B mode of operation in a new large core. As a result, many B&B reactors could be initiated, or spawned, from the first generation, or "Mother" B&B reactor. Enriched fuel need be purchased only for the Mother reactor core. Only depleted uranium feed is required for fueling this fleet of B&B reactors thereafter. In the following analysis it is assumed that EU is used for the Mother igniter. Although neutronically TRU is the preferred igniter, EU is assumed because of the existence of enrichment plants that make it possible to implement the breed and burn scenario relatively soon.

The purpose of the following study is to prove that it is practically feasible to spawn two large B&B cores using the same EU igniter. The model used is the cylindrical finite core model made of 12 radial depletion zones first described in Section 6.3. Section 6.1.2 found that 7.66 tons of ^{235}U are required to make the reactor critical, with an igniter occupying 50% of the core volume. The neutron balance of Section 6.4 showed that in order to start two large B&B cores from the same EU igniter, it is necessary to decrease the burnup reactivity swing below 4%. The

main constraints used for the current study are (1) acceptable radial power distribution; (2) burnup reactivity swing no larger than 4%; and (3) cycle length not shorter than one year.

When the core multiplication factor becomes too large or too small, different shuffling schemes are tried, and the one yielding the best performance is used. With more time and larger computational capability it would have been possible to compare more shuffling schemes and fully optimize the transition period. The same process is repeated until it is possible to discharge the igniter – while maintaining the core critical with the bred depleted uranium fuel elements – or when 20% FIMA average burnup is reached in any of the fuel elements. During the depletion, 75% of the fission gases are continuously removed and when the burnup limit is reached – 20% FIMA, only the fuel batches with the highest burnup are recycled using the melt-refining. Melt-refining is assumed to occur instantly.

6.5.1 Initial core, first generation: startup with EU igniter

The large B&B core is initially composed of five radial zones made of enriched uranium and seven radial zones made of depleted uranium, as shown in upper left corner of Figure 6.33. The innermost zone is loaded with depleted uranium as are the outermost 6 zones. From the innermost to the outermost EU zones, the ^{235}U enrichments are 11.2 wt%, 12.3 wt%, 12.3 wt%, 11 wt% and 8.5 wt%, respectively. The total mass of ^{235}U required is 6.57 tons, 14% smaller than for the initial design discussed in Section 6.1.2, because of the smaller volume of enriched fuel despite the larger enrichments.

During the first core generation (0 to ~10 EFPY), the conversion ratio is always larger than unity, making the multiplication factor constantly increasing, even after several shufflings. Since the limiting constraint is the maximum k_{eff} value, the shuffling schemes used are designed such as to yield k_{eff}=1 at the beginning of the next cycle. The evolution of the multiplication factor is shown in Figure 6.32. The five sharp shifts correspond to the five fuel shufflings it is necessary to perform to propagate the fission wave to the depleted uranium elements. These shufflings are schematically shown in Figure 6.33.

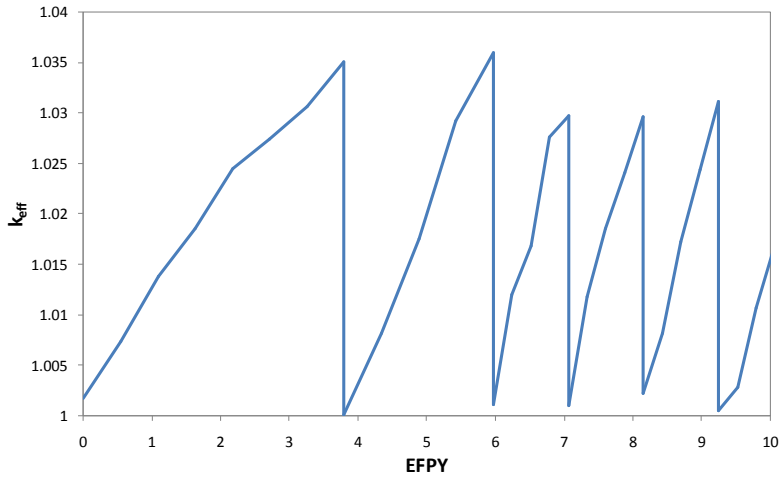

Figure 6.32: k_{eff} evolution for the initial large B&B core, first generation

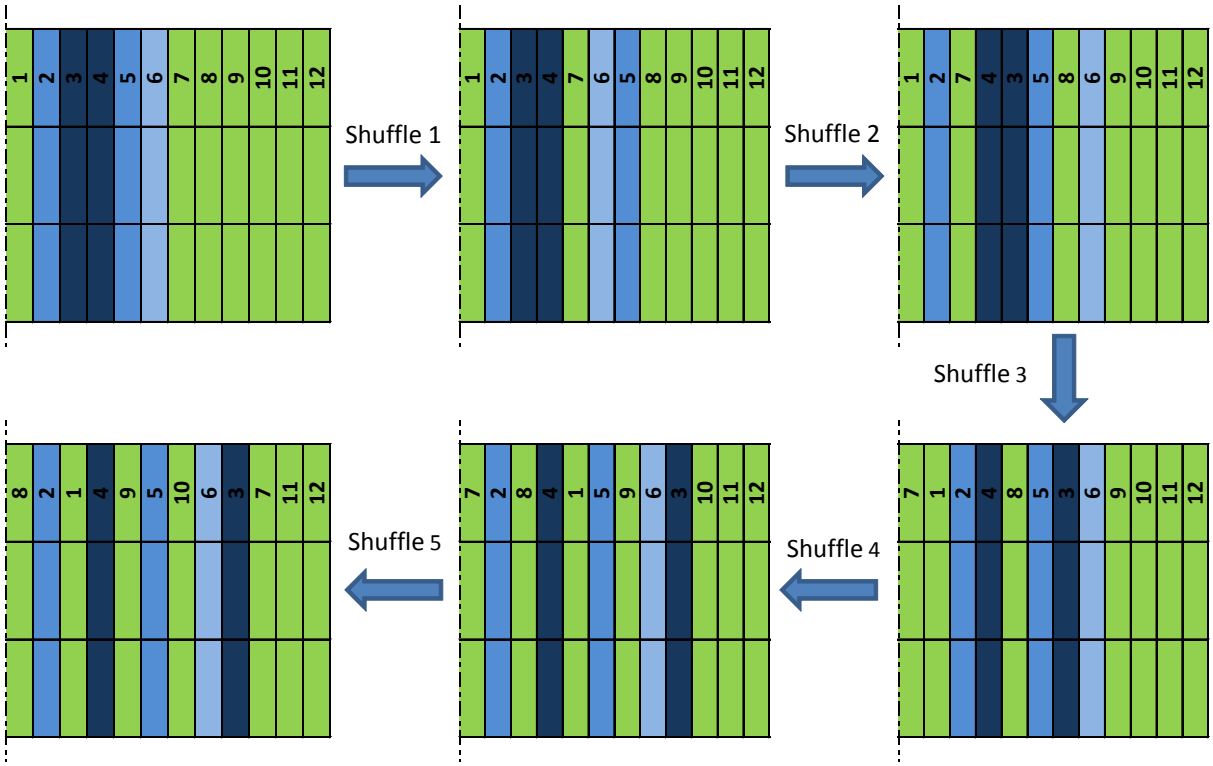

Figure 6.33: Schematics of the five shufflings performed in the initial large B&B core before removing the igniter. Blue zones are made of EU; green zones are made of DU

The shufflings chosen are successful in making k_{eff}=1 at the BOC by changing the core layout to a less reactive configuration:

- The high fissile material zones are relocated further away from the core center, increasing the radial neutron leakage;
- The low fissile material zones are placed in-between the high fissile material zones, decreasing the fission probability, but increasing the conversion ratio.

Due to the increased conversion ratio, the k_{eff} increase is made faster for the subsequent cycles: the first cycle lasts 3.8 years, while the second only 2.2 years and the following cycles only 1.1 years. This information is summarized in Table 6.5.

Table 6.5: Summary of the Five Shufflings for the Initial Large B&B Core; First Generation

Shuffling #	1	2	3	4	5
# of zones shuffled	2	5	5	5	5
Time since BOC [y]	3.8	2.2	1.1	1.1	1.1
k_{eff} before shuffling	1.03509	1.03599	1.02973	1.02966	1.03112
k_{eff} after shuffling	1.00012	1.00115	1.00099	1.00225	1.00055

After 10.1 effective full power years – EFPY, 20.4% FIMA burnup is reached in the second innermost radial zone, and the igniter fuel elements need to be recycled. The average igniter burnup is 15.0% FIMA, while the burnup of the seven depleted uranium radial zones ranges from 0.1% FIMA to 8.8% FIMA with an average of 2.9% FIMA. The radial power

peaking factor is shown in Figure 6.34. It is 3.2 at BOL and slightly decreases to 2.5 by EOL. The initial value is higher than for the reference case studied in Section 6.1.2 because of the smaller igniter volume, initially producing 98% of the total core power in only 42% of the core volume.

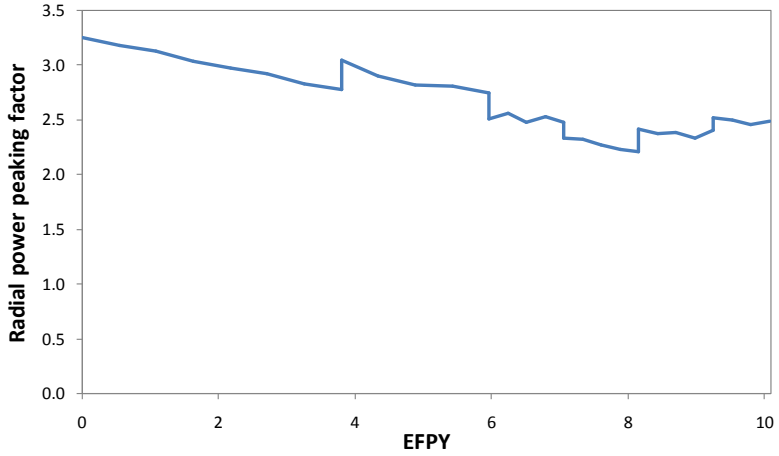

Figure 6.34: Radial power peaking factor evolution the initial B&B core, first generation

6.5.2 Initial core, second generation: breed and burn mode establishment

After operating the first large B&B core for 10.1 EFPY, the initial igniter fuel zones are discharged along with the highest burnup depleted uranium zone and are replaced by the same volume of fresh depleted uranium fuel. The once-burnt depleted uranium fuel elements are shuffled in the initial B&B core such as to make it critical. Their average burnup is 3.4%, and only three out of the twelve zones have an infinite multiplication factor above unity. It is found possible to make the reactor critical, with k_{eff}=1.00094±0.00076 at beginning of cycle, but the radial power peaking factor is as high as 5.3 because only 25% of the core volume is producing power. This power peaking factor is not practical, but the first objective being to prove the neutronics feasibility of spawning two cores from the same igniter, the study is still performed: the igniter is discharged from the initial B&B core as early as neutronically possible (i.e. 10.1 EFPY), in order to conserve as many excess neutrons as possible to start the second core. This is discussed in Section 6.5.3.

The depletion of the initial core, second generation, made of six once-burnt and six fresh depleted uranium zones is performed. When k_{eff} becomes close to 1.04, different shuffling schemes are explored. The evolution of the multiplication factor is shown in Figure 6.35, and the shuffling schemes are summarized in Table 6.6Table 6.6. The first fuel recycling is occurring 3.3 EFPY after the beginning of the second generation – 13.4 EFPY since the first startup of the initial core. When this recycling is occurring, the four fuel zones with the highest burnup are recycled.

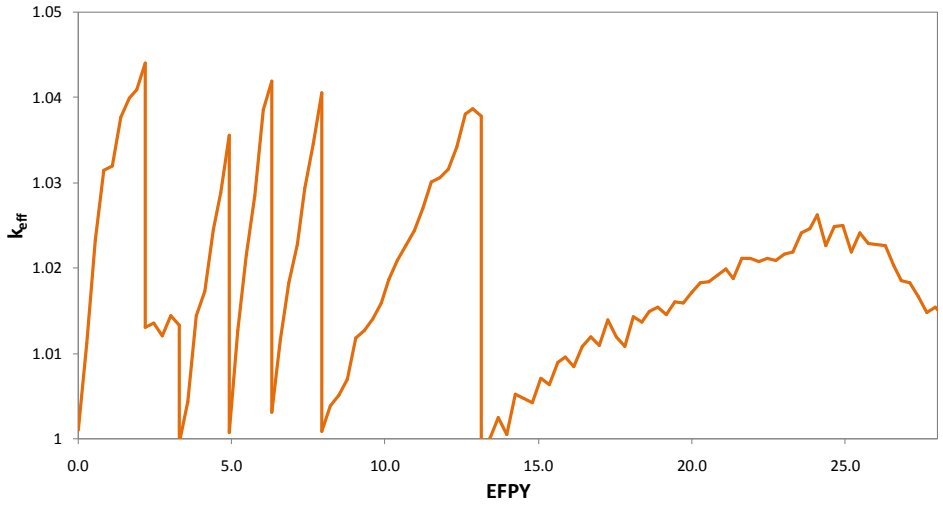

Figure 6.35: k_{eff} evolution for the first core, second generation, driven by the once-burnt fuel

Table 6.6: Summary Table of the Shufflings and Recycling – Initial Core; Second Generation

Shuffling #	1	2	3	4	5	6
# of zones shuffled	3	4	4	6	4	4
Time since BOL [yr]	2.2	3.3	4.9	6.3	7.9	13.1
k_{eff} before shuffling	1.04407	1.01328	1.03565	1.042	1.04058	1.03784
k_{eff} after shuffling	1.01304	0.99946	1.00067	1.00305	1.00079	0.99939
# of zones recycled	-	4	-	-	-	-

During the last cycle shown in Figure 6.35, the maximum burnup accumulation is reached in several depletion zones, and it would be necessary to recycle the fuel one more time at 17 EFPY. The main fuel recycling effect is to increase the k_{∞} of the fuel recycled due to the partial removal of fission products, improving the neutron economy. If the fuel was to be recycled at 17 EFPY, the core performance will be slightly improved. However, at this point the average burnup of the once-burnt depleted uranium elements is 4% FIMA, and their k_{inf} is already larger than 1.0. It is possible to discharge the twice-burnt fuel elements and use their remaining excess neutrons to assist starting another core, or it is possible to keep them in the current core to extend their burnup before discharging them. At 17 EFPY the twice-burnt depleted uranium elements have an average burnup of 26% FIMA.

It is concluded that, from the neutron economy standpoint, it is feasible to establish the breed and burn mode of operation in the first core using once-burnt depleted uranium fuel elements with an average burnup of only 3.5%. However, such a small burnup will only ensure the reactor to be critical, yielding a very large radial power peaking factor. In order to decrease this excessive radial power peaking factor, it is necessary to increase the depleted uranium elements burnup above 4% FIMA before discharging the igniter or twice-burnt fuel elements.

6.5.3 New core: once-burnt EU igniter

It is assumed that the igniter fuel elements discharged from the initial core, first generation, after 10.1 EFPY are recycled. As the igniter occupies only 42% of the core volume, the outermost depleted uranium radial zone, having the smallest burnup, is also discharged from the initial core and loaded into the new core along with the recycled igniter and six additional fresh depleted uranium zones. The once-burnt igniter average burnup is 15% FIMA. This is lower than the minimum value predicted by the neutron balance in section 6.4.2 because:

- During the first generation in the initial core, fewer neutrons are absorbed in the control systems than it was assumed for the neutron balance because of the lower burnup reactivity swing: only ~1.5% of the neutron are absorbed in the control systems versus 3% assumed;
- The neutron leakage probability is approximately 9% smaller. At BOL it is 3.78% while it was assumed to be 4.05% for the neutron balance;
- The depleted uranium elements that reached a burnup larger than 3.4% FIMA have k_∞ larger than unity and are already providing excess neutrons to other subcritical fuel elements. The same behavior is occurring for the finite cores previously studied in this chapter but does not apply to the neutron balance where a single fuel zone is analyzed.

Out of the twelve radial fuel zones, five have k_∞ above unity, making it possible to achieve radial power peaking factor similar to the value (~3) achieved in Section 6.5.1 for the initial core, first generation. With the configuration shown in Figure 6.36, k_{eff} is equal to 1.00442±0.00076 at BOL and the radial power peaking factor is 3.12. The same shuffling approach as performed in Sections 6.5.1 and 6.5.2 is used until sufficient fissile material has been bred in the depleted uranium elements, enabling discharging the twice-burnt igniter fuel elements. The k_{eff} evolution is shown in Figure 6.37, and the shuffling scheme is summarized in Table 6.7.

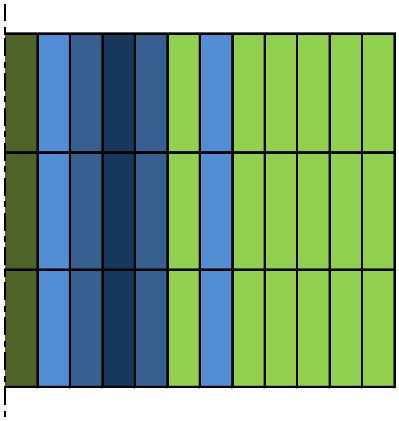

Figure 6.36: Second core initial loading pattern– blue=once burnt igniter; light green=fresh DU; dark green=once burnt DU

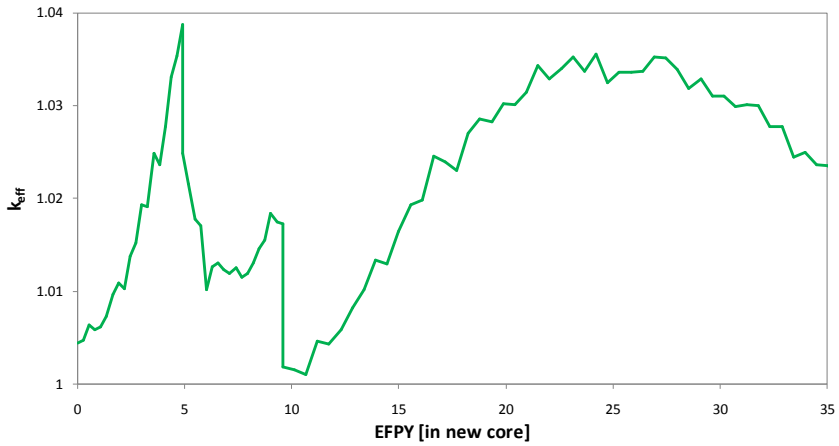

Figure 6.37: k_{eff} evolution for the new core, first generation, driven by the once-burnt igniter

Table 6.7: Summary of the Shufflings Scheme and Recycling for New Core; First Generation

Shuffling #	1	2
# of zones shuffled	5	5
Time since BOL [yr]	4.9	9.6
k_{eff} before shuffling	1.03876	1.01728
k_{eff} after shuffling	1.02491	1.00191
# of zones recycled	-	6

After 9.6 EFPY and one fuel shuffling, the maximum permissible burnup accumulation is reached in the second innermost fuel zone and the reactor is stopped for fuel recycling. The six twice-burnt fuel zones are recycled and reloaded. The third cycle in the new core, first generation, can then be sustained for more than 20 years without exceeding the multiplication factor, peak power density or accumulated burnup constraints.

When the simulation is stopped after 36.1 EFPY, the average igniter burnup is 42.1% FIMA, and the average burnup of the six once-burnt depleted uranium zones is 9.6% FIMA. It is preferable to stop the reactor earlier: when the average burnup of the depleted uranium elements reaches ~5% FIMA at 19.9 EFPY, for which the breed and burn mode can be sustained in the core using only the fuel elements initially loaded as depleted uranium. The twice-burnt igniter elements could be discharged with an average burnup of 31.5% FIMA and used as the igniter for a third core.

These results, although preliminary and not representing optimal fuel management scenarios, confirm that the amount of excess reactivity left in the EU igniter discharged from the Mother core is significantly larger than the minimum required for establishing a B&B mode of operation in a new reactor core, and therefore it is possible to keep the igniter in the Mother core longer. This will enable achieving a burnup larger than 3.4% FIMA in the depleted uranium elements of the initial core and will enable decreasing the radial power peaking factor of the initial core , discussed in Section 6.5.2, in which the breed and burn mode is being established.

6.5.4 Feasibility of reducing EU inventory by shortening igniter fuel rods

The igniters examined so far had initially axially uniform fissile fuel content extending over the full length of the active core. The feasibility of reducing the amount of ^{235}U for the igniter by using higher enrichment levels concentrated in the axial central part of the core is explored in this section. The idea is to maximize the fraction of the igniter generating excess neutrons that are captured in the ^{238}U of the blanket (initially depleted uranium) elements while minimizing the fraction of the igniter generated excess neutrons that either axially leak out from the core or are captured in the ^{238}U of the igniter fuel elements. The possible drawbacks of this approach are that the amount of separative work units for a same ^{235}U mass is slightly larger when the enrichment is higher and that the peak fuel and cladding temperatures may increase because of the larger specific power in the igniter.

The EU igniter fuel zones height and location are searched so as to (a) maintain the reactor critical (b) minimize the mass of ^{235}U required; and (c) achieve a flat power distribution at BOL. The ^{235}U enrichment is taken to be 20% by weight, the highest presently acceptable because of proliferation concerns. A number of igniter architectures, shown in Figure 6.38, were examined. The green represents the depleted uranium batches, the blue the reduced length EU assemblies and the grey the emptied fuel rods filled with sodium due to the enriched fuel length reduction. The initial core layout yielding the best performance was found to be the layout #3, also presented on left side of Figure 6.39. The green zones are made of depleted uranium, the blue zones are made of 20% enriched uranium and the grey zones are made of fuel rods sections filled with sodium. The active igniter fuel lengths and ^{235}U masses are given in Table 6.8.

The mass of ^{235}U required for the optimal design is 5.68 tons, 13.5% smaller than for the reference igniter studied in the previous section, despite of using a larger enrichment level and a larger number of EU fuel assemblies. The total HM inventory at BOL is 99.7 tons instead of 142.6 tons, and with a core power of 3000 MW_{th}, the average specific power increases from 21.2 W/g of HM for the previously studied igniter to 30.1 W/g of HM for this igniter. The peak specific power at BOL is ~85.8 W/g of HM versus 52.6 W/g of HM but the BOL radial power peaking factor is 1.93 versus 3.25 for the igniter of Section 6.5.1.

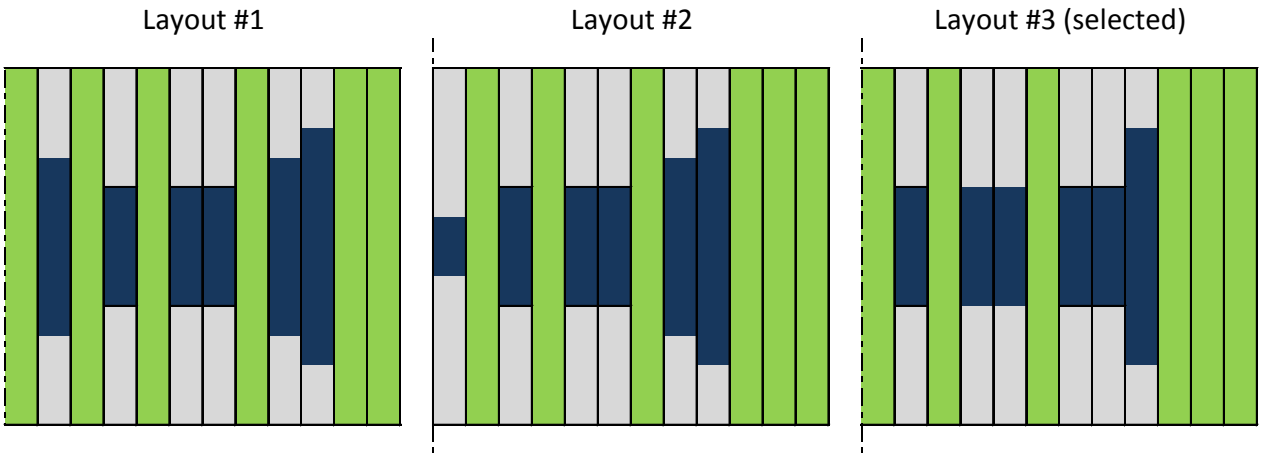

Figure 6.38: Different core layout at BOL analyzed with reduced length EU assemblies. The lengths represented on these schemes are approximate.

Table 6.8: Active Fuel Length and ^{235}U Mass at BOL

Radial zone	1	2	3	4	5	6	7	8	9	10	11	12
Fuel length [cm]	209.4	99.8	209.4	66.4	65.3	209.4	72.5	82	115	209.4	209.4	209.4
^{235}U wt%	0%	20%	0%	20%	20%	0%	20%	20%	20%	0%	0%	0%
^{235}U mass [tons]	0	1.13	0	0.75	1	0	0.82	1	1.3	0	0	0

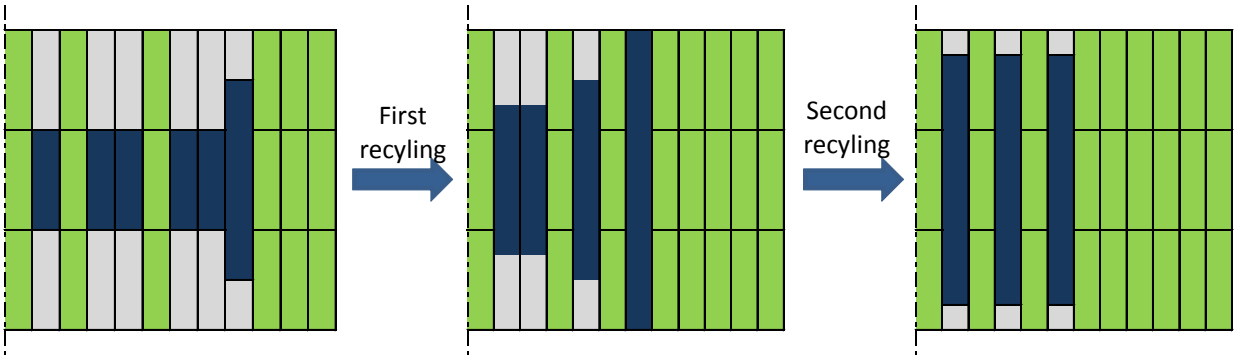

Figure 6.39: Optimized core layout with reduce length EU fuel assemblies at BOL – left, after the first recycling – middle, and after the second recycling – right

The same shuffling approach as described in the previous sections is applied. After 5.2 EFPY, corresponding to an average core burnup of 57.2 GWd/tHM, the igniter fuel elements need to be recycled because they reached burnups between 11.38% and 19.90% FIMA. All the igniter fuel elements are reprocessed together, using the melt-refining process. It is decided to reprocess the igniter fuel elements altogether in order to obtain a single fuel composition and to simplify the fuel recycling management. The single fuel composition resulting from the igniter fuel recycled features an average burnup of 16.08% FIMA.

The recycled fuel is reloaded in the core, occupying only four radial zones, as shown in the middle scheme of Figure 6.39, by increasing the active fuel rod length. The two emptied radial zones are filled with fresh depleted uranium. The length of fuel in the igniter fuel assemblies recycled is determined such as to flatten the radial power distribution at beginning of the second cycle. The main advantage of reloading the recycled fuel this way – filling fewer radial zones – is the ability to start introducing additional fresh depleted uranium fuel elements, without discharging any igniter fuel. The core heavy metal inventory is increased, and the specific power is decreased, resulting is a slower burnup accumulation during the second cycle.

After an additional 4.7 EFPY – 9.9 EFPY since BOL, the fuel would need to be shuffled to prevent the radial power peaking factor from becoming larger than 2. The average burnup of the eight depleted uranium zones is 4.04% FIMA and is 5.23% FIMA for the six depleted uranium zones having the highest burnup: this burnup is sufficient to maintain the core critical when discharging all the igniter fuel elements, the average burnup of which is 25.5% FIMA.

In a scenario where the igniter is kept in the initial core until it becomes subcritical, the fuel is shuffled when the radial power peaking factor becomes too large. When the fuel needs to be recycled, the igniter fuel is reloaded in only three radial zones as shown on the right side of Figure 6.39, and fresh depleted uranium is introduced to complete the core. After ~23 EFPY, when the core becomes subcritical, the average igniter burnup is 42.5% FIMA, while the depleted uranium fuel elements burnup ranges from 0.99% to 21.52% FIMA with an average at 12.83% FIMA. The evolution of k_{eff}, the radial power peaking factor and the leakage probabilities is presented in Figures 6.40 and 6.41, from BOL to 23 EFPY.

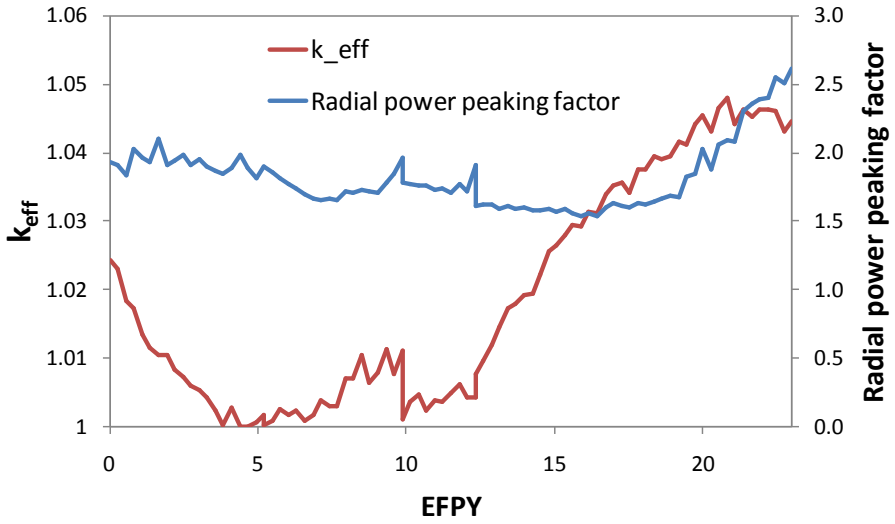

Figure 6.40: Evolution of k_{eff} and radial power peaking factor for the large B&B core driven by shortened EU igniter assemblies – shuffling occurs at 5.2, 9.9 and 12.3 EFPY; recycling occurs at 5.2 and 12.3 EFPY

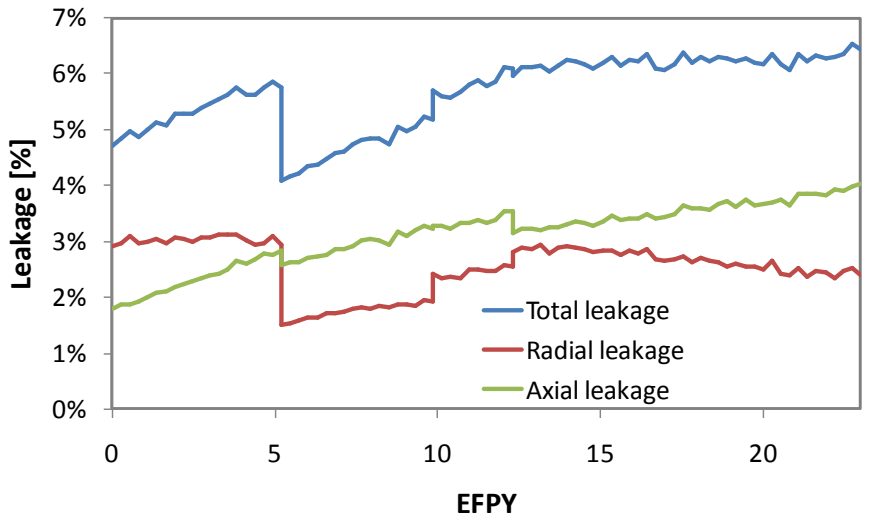

Figure 6.41: Evolution of the leakage probability for a core driven by shortened EU igniter assemblies

The feasibility of establishing the breed and burn mode in a new core, first generation, using the discharge igniter at 16.08% FIMA burnup has not been studied. The propagation of the fission wave in the initial core, second generation, has already been studied in Section 6.5.2 with depleted uranium fuel elements having an average burnup of 3.4% FIMA. In this section, the average burnup of the depleted uranium fuel elements is ~5.0% FIMA. With this higher burnup it will be possible to achieve smaller radial power peaking factor than the one obtained in Section 6.5.2 for the initial core, second generation. Assuming the igniter fuel is discharged at 9.9 EFPY

with 16.08% FIMA, based on the studies presented in the previous sections, some comments can be made:

- The igniter volume being small, it might not have enough excess neutrons to establish a B&B mode of operation in a second core just by itself;
- It is possible to discharge one of the depleted uranium zones having $k_{\infty} \approx 1$ from the first core along with the igniter, in order to assist it providing excess neutrons to the new core;
- In order to maintain a favorable radial power distribution in the first core, second generation, it may be preferable to recycle the two highest burnup depleted uranium zones – average burnup is 8.13% FIMA, and reload them in three or four radial zones with shorter active fuel length. This will also decrease the axial leakage probability, improving the neutron economy.

It is concluded that by decreasing the enriched fuel rod length, it is possible to establish the breed and burn mode of operation in the large B&B core while decreasing the ^{235}U required to start the core by 13.5% compared to the scenario studied in Section 6.5.1 and by 26% compared to the reference scenario discussed in Section 6.1.1. Furthermore, when the shortened enriched fuel rods are recycled, it is possible to re-fabricate fewer of them but having an increased length and add depleted uranium fuel batches without discharging any fuel. This enables maintaining the radial power peaking factor approximately equal to 2.0 for all the cycle length. If it is found possible to start a second core from the same igniter, the doubling time of the first generation of large B&B core will be 9.9 EFPY, similar to the 10.1 EFPY found for the scenario presented in Section 6.5.1. The doubling time is the time during which the fissile material loaded in a reactor doubles. Practically, it is the time required for a reactor to generate sufficient fissile material to sustain the reaction chain in the current core and start an additional core in another reactor without fissile material from another source. However, the current scenario will enable decreasing by almost 14% the ^{235}U requirement, and simplify the fuel management while featuring a very acceptable radial power peaking factor. A thermal hydraulic analysis of the shortened fuel rods must be performed to ensure that at the nominal core power, the maximum fuel and cladding temperatures are not exceeded.

6.5.5 Spawning feasibility of equilibrium core

The feasibility of spawning new cores from the large B&B core operating at equilibrium as described in Section 6.3.2 is assessed in this section. The core is composed of 12 radial depletion zones, all having an active fuel length of 209.36 cm. One equilibrium cycle lasts 2.05 years and at EOEC the fuel is discharged at 19.4% FIMA burnup and is recycled using the melt-refining process. The discharged fuel elements are stored until accumulating 50% of the core volume; the core being made of 12 fuel batches, this is achieved after 12.3 EFPY (6 cycles). Then, they are loaded into a new core along with the same volume of fresh depleted uranium fuel elements. This is schematically represented in Figure 6.42. The shuffling pattern of the equilibrium core – left side of the figure – is not representative of the improved shuffling scheme used for the simulation. The two innermost and four outermost fuel zones of the new core are initially made of depleted uranium. The six zones of fuel at 19.4% FIMA burnup are loaded between the depleted uranium fuel elements.

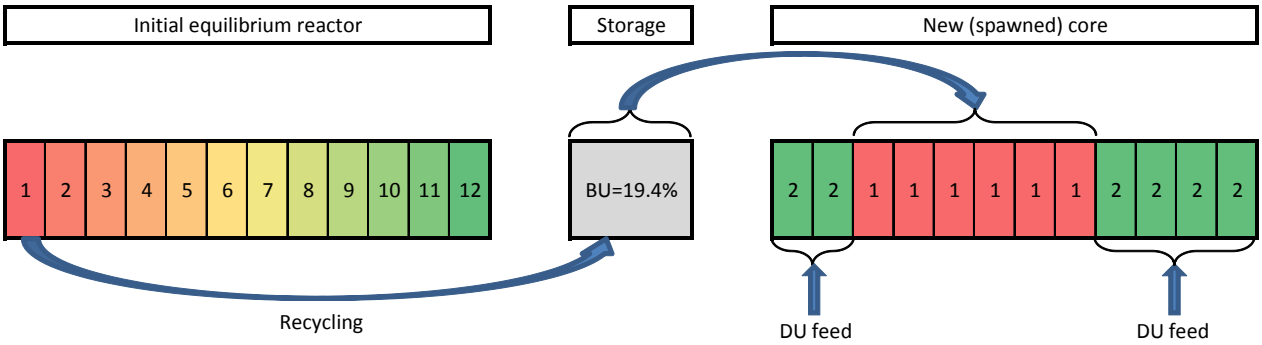

Figure 6.42: Schematic of core spawning from large B&B core at equilibrium operating at 19.4% FIMA burnup

The new core is depleted until 20% FIMA burnup is accumulated in any of the fuel elements, or until k_{eff} becomes too large or too small. At BOL of the new core, the radial power peaking factor is 2.38. This is smaller than the value for the equilibrium core, 2.58, obtained in Section 6.3.2. The new core can be operated for 14.8 EFPY without shuffling before 20% FIMA burnup is accumulated in a fuel element. At 14.8 EFPY, the average burnup of the six "19.4% burnup" fuel zones is 36.2% FIMA and the average burnup of the depleted uranium elements is 6.3% FIMA. This burnup is high enough to enable removing the "19.4% burnup" elements, replacing them with fresh depleted uranium elements, and to propagate the fission wave. The evolution of k_{eff} and of the radial power peaking factor is shown in Figure 6.43, from BOL to 14.8 EFPY.

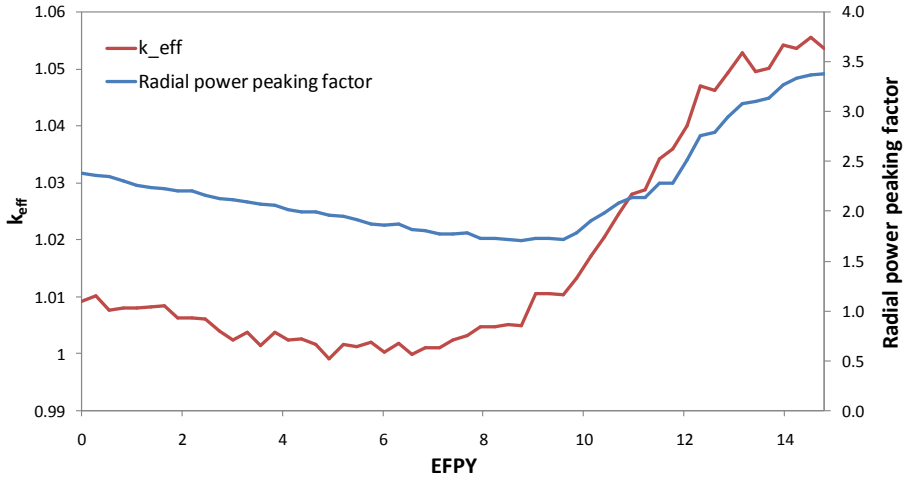

Figure 6.43: Evolution of k_{eff} and the radial power peaking factor for the new large B&B core driven by the fuel discharged from the equilibrium B&B core

At BOL, k_{eff} is slightly decreasing because k_∞ is decreasing in the "19.4% burnup" fuel elements, and the fissile material build-up in the depleted uranium elements is not sufficient to overweight it. After ~8 EFPY, the k_∞ of the two innermost depleted uranium fuel zones is larger than unity, and due to their favorable location near the center of the core, it causes the core k_{eff} to strongly increase. As the fission rate becomes very large in those two zones, the radial power

peaking factor is also strongly increasing: it reaches 3.37 at 14.8 EFPY. By shuffling the fuel around 11 EFPY, it is possible to maintain k_{eff} close to unity and the peaking factor around 2.

At EOL, the "19.4% burnup" fuel elements that reached 36.2% FIMA are left with a significant reserve of excess reactivity. Based on the study performed in the previous section for the EU igniter during the transition period with shortened fuel rods, a similar approach should be used for the equilibrium core spawning. The neutron balance performed in Section 6.4.1 and the results obtained in the current section suggest it is theoretically possible to start the new core by using only one third (33%) instead of 50% of the equilibrium core volume. However, due to practical reactivity and power peaking constraints it is likely that approximately 40% of the equilibrium core volume will be required for spawning a new core. The large B&B core doubling time at equilibrium would then be 10.2 EFPY instead of 12.3 EFPY.

It is concluded that it is possible to spawn additional B&B core from a core at equilibrium with a doubling time in the vicinity of 10.2 EFPY when the fuel is discharged from the equilibrium core at 19.4% FIMA. The core spawned features more favorable radial power distribution and similar burnup reactivity swing than the equilibrium core.

6.5.6 Breed and burn reactors annual capacity growth rate

In every social-economic and technical development scenarios examined by the IIASA [4], it is forecasted that the world nuclear capacity will increase during the next century. Depending on the specificities of the scenario, the growth rate is estimated to be somewhere between 2.4% and 3.6%. With the large B&B reactor studied in this chapter, it is possible to discharge the fuel at the minimum required burnup to sustain the breed and burn mode, ~20% FIMA, and use it to start a new large B&B reactor core. This spawning mode of operation is feasible during both the transition period and the equilibrium. It is schematically illustrated by Figure 6.44. No EU or TRU enriched fuel is required for starting-up of the second and following generations of B&B reactors.

Assuming a capacity factor of 90% and two years to transfer the fuel and fabricate the new cores, the doubling time is approximately 13.3 years. With the igniter and equilibrium core performance found in Sections 6.5.1 trough 6.5.5, the number of large B&B cores at a generation "i" is equal to the number of large B&B cores at generation "i-1" plus the number at generation "i-2". This deployment scenario, represented in Figure 6.44, enables reaching an average B&B capacity growth rate of 3.85% per year. If a single 3000 MW_{th} B&B core is started in 2020 and operated with this spawning mode, the electrical B&B capacity evolution is compared in Figure 6.45 with the theoretical growth rate of 3.85%/year. In 2100 the electrical B&B capacity will be 25.2 GW_e and by 2120 it will be 40.8 GW_e.

It is concluded that with the large B&B core operating with the spawning mode, it is possible achieve an electrical capacity growth rate larger than in any of the scenarios forecasted for nuclear energy by the IIASA, only using depleted or natural uranium, with the exception of the Mother core initial enriched fuel loading.

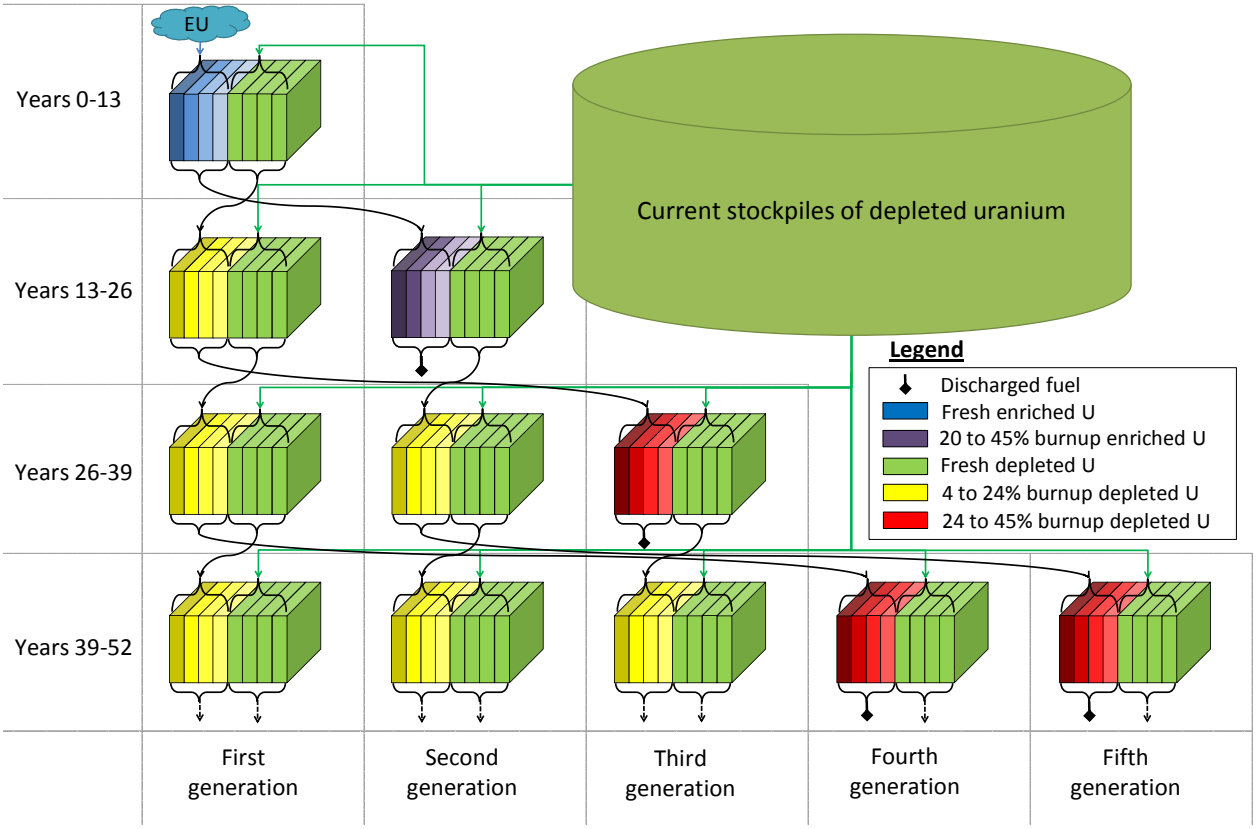

Figure 6.44: Spawning schematic of the large B&B Core

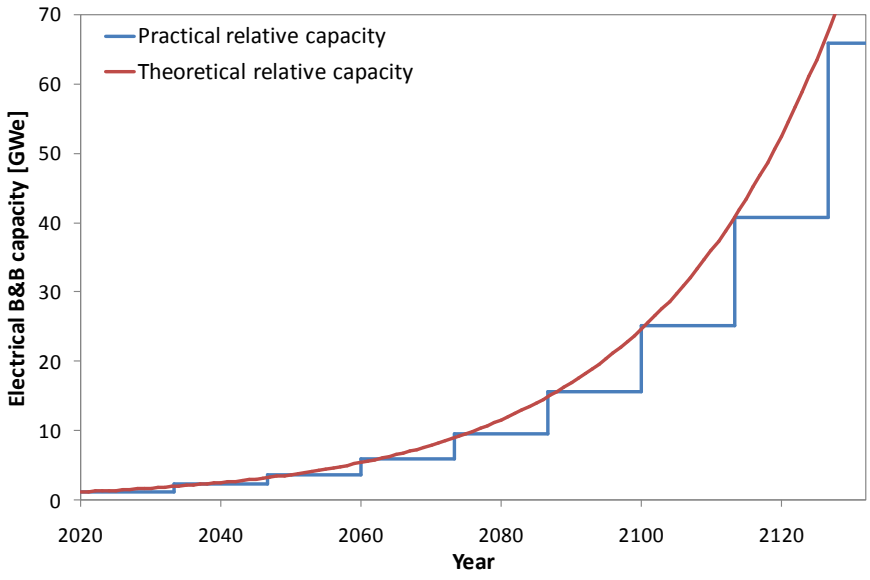

Figure 6.45: Large B&B reactor electrical capacity evolution for one large B&B reactor deployed in 2020 and operated in the spawning mode

6.6 Thermal hydraulic validation

Throughout this chapter it was assumed that the large B&B core is operating at 3000 MW_{th} without exceeding any of the thermal hydraulic constraints. The objective of this section is to assess the maximum achievable power for the large B&B core, based on the power peaking factors obtained from the neutronics analysis in the previous sections. The thermal hydraulic constraints have been described in Section 2.6.1, and are summarized here:

- maximum pressure drop: 1 MPa;
- maximum sodium velocity across the core: 12 m/s
- maximum fuel-cladding interface temperature: 650°C
- maximum fuel temperature: 1240°C

The inlet coolant temperature is assumed to be 395°C and the target outlet coolant temperature is taken to be 580°C. The coolant volume fraction used for this thermal hydraulic study is different from the fraction used for the neutronics study. For the neutronics analysis, the coolant volume fraction corresponds to all the coolant in the core, relatively to the total core volume. For the thermal hydraulic analysis, the coolant volume fraction represents the volume of coolant inside a fuel assembly, relatively to the total volume inside the assembly. This assumes that the coolant circulating in-between the assembly ducts does not participate in the heat removal. The inner assembly coolant volume fraction is 26.59% for a P/D ratio 1.111. The fuel rod diameter and cladding thickness are depending on the number of fuel rod per assembly and are provided in the result tables for each scenario studied. All the results presented in this section are constrained by the maximum pressure drop constraint and not the maximum coolant velocity constraint. The main component of the pressure drop is the friction along the fuel rod, including the plenum section. The total fuel rods length is 418.72 cm. The fuel assembly pitch is taken to be 161.42 mm with an inter duct gap of 4.32 mm and a duct thickness of 3.94 mm. These are the values chosen for the S-PRISM core design by GE [28], and by ANL in their recent studies on ABR [27].

6.6.1 Equilibrium core

The thermal hydraulic analysis detailed in section 2.3 is performed for the large B&B core at equilibrium studied in Section 6.2.2, operating with the simple shuffling scheme. For this core, the radial power peaking factor is 1.67. The results obtained for various fuel rod dimensions and numbers of fuel rods per assembly, all using the same volume fractions, are presented in Table 6.9.

Table 6.9: Thermal Hydraulic Performance of the Large B&B Core for a Radial Power Peaking Factor of 1.67

Parameters	Case 1	Case 2	Case 3	Case 4
p/d	1.111	1.111	1.111	1.111
Fuel rod pitch [mm]	9.06	11.48	13.24	15.64
Fuel rod diameter [mm]	8.16	10.33	11.91	14.07
Fuel rods per assembly	**271**	**169**	**127**	**91**
Clad thickness [mm]	0.667	0.845	0.974	1.151
Coolant volume fraction	26.6%	26.6%	26.6%	26.6%
Reynolds number	8.39E+04	1.18E+05	1.44E+05	1.80E+05
Pressure drop [MPa]	1.00	1.00	1.00	1.00
Coolant velocity [m/s]	8.75	9.91	10.61	11.40
Maximum core power [MW_{th}]	**3020.7**	**3421.2**	**3662.9**	**3935.6**
Max. inner cladding temp. [°C]	596.7	610.9	624.1	645.7
Max. fuel temperature [°C]	644.6	714.0	792.5	923.5

When using no more than 271 fuel rods per fuel assembly, it is possible to achieve 3000 MW_{th} in the large B&B core at equilibrium without exceeding any of the constraints. Decreasing the number of fuel rods to 91 rods per assembly, it is even possible to reach 3900 MW_{th}. For this power, the peak cladding temperature and maximum coolant velocity are close to their design limit. When decreasing the number of fuel rods per fuel assembly, keeping the assembly dimension constant, the fuel pin diameter is increased and the hydraulic diameter is increased. In order to sustain the same pressure build-up due to fission gas release inside the fuel rod, the cladding thickness is also increased. This makes the temperature gradient in the cladding larger. However, a larger hydraulic diameter decreases the coolant friction along the fuel rods, yielding a smaller core pressure drop. The coolant velocity can be increased, and the attainable core power is increased.

The achievable power for a different radial power peaking factor can simply be obtained by multiplying the attainable power presented in Table 6.9 by the ratio of the radial power peaking factors. For the improved shuffling scheme presented in Section 6.2.3, the radial power peaking factor has been found to be 2.02. For case 3 of Table 6.9, the maximum core power is found to be 3042 MW_{th} instead of 3663 MW_{th}, yielding the same cladding and fuel peak temperatures. The maximum achievable power, corresponding to case 4, is 3270 MW_{th}.

For the large B&B core studied in Section 6.3.2 operating at the minimum discharge burnup of 19.4% FIMA, the radial power peaking factor has been found to be 2.58. The maximum core power, for case 4, is approximately 2550 MW_{th}. This is smaller than the 3000 MW_{th} assumed for the neutronics study. It is possible to decrease the reactor power level to 2500 MW_{th} in order to meet the thermal hydraulic constraints. This smaller core power may slightly affect the neutronics performance of the core because of the enhanced loss of certain short-lived actinides – in particular ^{241}Pu that has a half-life of 14.3 years, to radioactive decay. It is found that decreasing the power from 3000 MW_{th} to 2500 MW_{th} does not affect the neutronics performance of the core. The main difference is the doubling time of the core that is increased by 17%. An alternate solution to meet the thermal hydraulic constraints is to slightly increase the P/D ratio from 1.111 to 1.133. With this new P/D ratio, it is possible to achieve approximately 3000 MW_{th} with a core pressure drop of 1 MPa and a coolant velocity equal to 12 m/s. The peak

cladding temperature is equal to the design limit. A neutronics study needs to be performed in order to assess the core performance with increased neutron leakage probability due to the larger P/D ratio.

The thermal hydraulic study of the large B&B core showed that when the radial power peaking factor is smaller than ~ 2.2, it is possible to generate at least 3000 MW_{th} with the large B&B core by using 91 fuel rods per assembly. For the core at equilibrium with a discharge burnup of 55% FIMA, it is possible to achieve 3900 MW_{th}. To achieve 3000 MW_{th} with the minimum required burnup shuffling scheme studied in Section 6.3.2 it is necessary to increase the P/D ratio to 1.133 because of the larger radial power peaking factor – 2.58.

6.6.2 Transition period

During the transition period the attainable core power can also be obtained using the data provided in Table 6.9 and the radial power peaking factor. It has been found in Section 6.1, that for the TRU and EU igniters without shuffling, the radial power peaking factors are as high as 2.62 and 2.56, respectively. Those peaking factors are limiting the core power level to 2510 MW_{th} for the TRU igniter and to 2570 MW_{th} for the EU igniter. Although these power levels are significantly lower than the 3000 MW_{th} assumed, it has been shown in Section 6.5 that with a good fuel management scheme it is possible to maintain the radial power peaking factor around 2.0 or lower.

With shorten fuel rods, it has been found that the radial power peaking factor is consistently lower than 2.00. The challenge with these fuel rods is the peak fuel and cladding temperatures because at BOL the full power is produced by a smaller fuel volume. In this case, it is favorable to use a larger number of thinner fuel pins, despite the larger pressure drop, in order to decrease the cladding thickness and fuel rods diameter. For the fuel rod dimensions of case 1, it is found possible to achieve 2550 MW_{th} without exceeding any constraint. For the shortest fuel rod presented in Table 6.8 – the length of which is 65.3 cm, the peak cladding temperature is 638°C and the peak fuel temperature is 860°C. Despite the necessity of decreasing the core power when using shorten fuel rods, the specific power density is still larger than for the regular core operating at 3000 MW_{th}: 25.6 W/g of HM instead of 21.2 W/g of HM.

6.7 Conclusions

In this chapter, it was found possible to sustain the breed and burn mode of operation in the large B&B core. This core can deliver up to 3000 MW_{th} with a power density approximately half the value used for conventional fast reactors [9] because of the large radial blanket. At equilibrium the maximum achievable burnup with the improved shuffling scheme has been found to be 57% FIMA with the melt-refining process. This burnup is approximately equal to the maximum achievable burnup in a conventional large fast reactor – 58% FIMA – without blanket and operating with an infinite-batch fuel management, studied in Section 4.2. This is also ~13% smaller than the maximum achievable burnup for the same conventional large fast reactor having a radial blanket – 65.3% FIMA, operating with an infinite-batch fuel management, also studied in Section 4.2. The maximum uranium utilization factor for the large B&B core, 57%, is more than one order of magnitude larger than for the conventional large fast reactors. Furthermore, it has been found that the minimum required burnup at equilibrium to sustain the breed and burn mode

in this large B&B core is in the vicinity of 20% FIMA and that it is possible to achieve a radial power peaking factor around 2.0 by using an improved shuffling scheme.

It was also found possible to establish the breed and burn mode of operation in the large B&B core by using either an EU igniter or a TRU igniter. For the EU igniter a shuffling scheme was design in order to establish the breed and burn mode without reaching too high radial power peaking factor or too large burnup reactivity swing. By decreasing the enriched uranium fuel rods length, the mass of ^{235}U required to establish the breed and burn mode can be decreased by more than 25% and enables improving the radial power distribution.

When the fuel is discharged from the core when it reaches the minimum required burnup to sustain or establish the breed and burn mode, it is left with a significant excess reactivity and can be used to establish a breed and burn mode in another reactor core. This is feasible both during the transition period, with a doubling time of approximately 9.9 EFPY, and at equilibrium with a doubling time of 12.3 EFPY that can possibly decreased to 10.1 EFPY. By spawning large B&B cores with an effective doubling time of 14 years, it is found possible to achieve a B&B reactor capacity growth rate of 3.85% per year without needing enriched fuel or enrichment capability but for the Mother cores. With this mode of operation, in addition of achieving a uranium utilization factor above 45%, it is possible to meet the highest nuclear energy growth forecasted by the IIASA scenarios while decreasing the uranium enrichment capacity currently existing.

For the deployment of those large B&B reactors to be possible a number of technical challenges need to be overcome. To improve the economics and simplify the fuel management, it is important (a) to develop fuel cladding able to sustain DPA significantly higher than the currently limit – 200 DPA – for HT-9. Several ferritic martensitic steels and ODS alloys are being developed but due to the lack of irradiation facility able to achieve very high DPA irradiation in a short time, it will takes several years before any of those materials can qualify for such a use. (b) The second important issue is the feasibility of the fuel reconditioning process. During this study it has been assumed that the melt-refining process would be able to perform identically with fuel having a burnup as high as 50% FIMA than with fuel having 10% FIMA burnup, for which it has been demonstrated during the EBR-II project [32]. Because of the higher concentration of fission product in very high burnup fuel it is possible that the performance of the process will be impaired. (c) Another issue is the feasibility to re-fabricate the fuel with very high burnup for which the element inventory is very different from the fresh fuel or low burnup fuel for which fabrication process has already been demonstrated. Lastly, (d) the core cooling feasibility needs to be demonstrated for core having a power distribution shifting during a cycle. At EOEC, the power distribution is different from BOEC and the coolant flow rate must be adjusted during the cycle.

Chapter 7

Performance of a S-PRISM Size B&B Core

The previous section analyzed the performance of a large B&B core, generating 3000 MW_{th}, for which it has been found possible to achieve up to 57% FIMA with the breed and burn mode of operation. In order to assess the performance of a medium-size reactor, the S-PRISM size core using the breed and burn mode of operation is presented in this section. The S-PRISM size core has already been described and studied in Section 4.3 for a single- and an infinite-batch fuel management schemes, with a conventional mode of fueling (with enriched fuel). The current section focuses on the equilibrium performance of the S-PRISM size B&B core. The maximum achievable burnup with the breed and burn mode is assessed for a cylindrical core model and is compared to the results obtained for an assembly-level core model and the achievable burnup forecasted by the neutron balance. The control systems performance of the core at equilibrium is estimated in Section 7.5 and the thermal hydraulics validation is presented in Section 7.7. The final design performance with improved model and fuel cycle assumptions is presented in Section 7.8.

The S-PRISM size core, compared to the large B&B core, features a reduced core height, lowered zirconium weight fraction in the fuel – 6 wt% instead of 10 wt% – and a smaller fuel volume fraction, given in Table 2.4. The heavy metal density in the S-PRISM size B&B core is 5% smaller than in the large B&B core. All of the S-PRISM size B&B core parameters are identical to those described in Section 2.1.3 for the S-PRISM size core with a radial blanket, apart from the number of radial zones used. The model used in the current chapter is made of 15 or 16 radial depletion zones and 3 axial depletion zones; the total core volume is conserved. Increasing the number of radial zones (fuel batches) enables minimizing the burnup reactivity swing and increasing the achievable burnup. The initial S-PRISM size B&B core design contains 445 fuel/blanket assemblies, 6 gas expansion modules – GEMs – and 12 control rods assemblies. Unless specified differently, all the fuel elements are recycled with the melt-refining process at the EOEC and 75% of the gaseous fission products are continuously removed from the fuel during operation. The highest burnup batch is discharged and a fresh depleted uranium batch is added to the core.

7.1 Equilibrium cycle maximum achievable burnup

Equilibrium cycles characteristics are determined for the S-PRISM size B&B core by applying the iterative equilibrium method described in Section 2.5.4 and already used in Chapter 6 for the large B&B core. The equilibrium core performance has been assessed for several shuffling schemes. The results obtained for a simple shuffling scheme and for the best improved shuffling scheme are presented in this section.

7.1.1 Simple shuffling scheme

The power density is initially assumed to be the same as for the large B&B core previously studied, 112.5 W/cm^3. The core having a volume of 14.86 m^3, the chosen power density yields a total core power of 1672 MW_{th} and a specific power density of 22.16 W/g of HM – the density of HM in the core is 5.08 g/cm^3. The fuel shuffling scheme consists in progressively moving the radial fuel zones inward as their burnup is increasing. The advantages of this shuffling scheme are that (a) the fresh depleted uranium, loaded at the outermost location, is acting like a reflector, minimizing the radial neutron leakage probability; the highest burnup fuel being located at the core center where the neutron flux is larger, it (b) mitigates the power peaking in the core center while (c) enabling increasing its burnup.

It is found that with this simple shuffling scheme, the maximum achievable burnup at equilibrium is 398 GWd/tHM – 40.9% FIMA, yielding a minimum k_{eff} value equal to 1.0023 at EOEC, shown in Figure 7.1. The core k_{eff} is decreasing during the cycle because the infinite multiplication factor, k_∞, of the high burnup fuel elements located near the core center is decreasing with burnup and the radial neutron leakage probability, shown in Figure 7.3, is increasing during the cycle. Each cycle lasts 3.15 years. The reactivity gain with recycling, ~2.3%, is due to the high k_∞ fuel elements being moved closer from the core center where the flux is larger and to the axial mixing of the fuel composition: most of the fissions are occurring in the central axial part, where the EOEC fission products content is the largest and the heavy-metal content is the lowest. This reactivity gain is about twice smaller than for the large B&B core with the simple shuffling scheme because of the larger number of radial fuel zones.

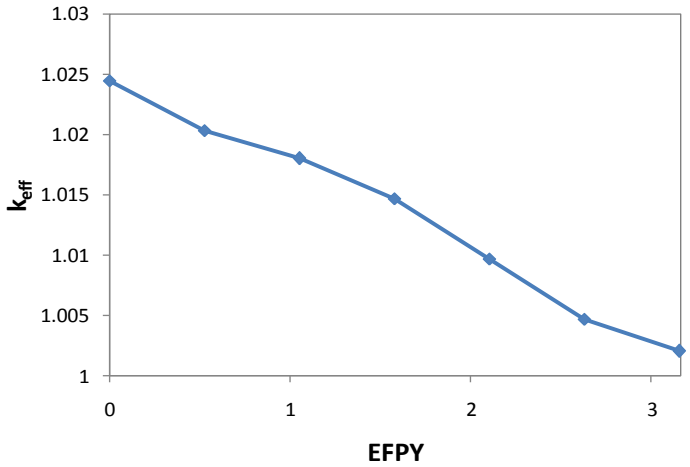

Figure 7.1: Evolution of k_{eff} at equilibrium for the S-PRISM size B&B core with fuel discharged at 40.9% FIMA with the simple shuffling scheme

Figures 7.2, 7.3 and 7.4 show, respectively, the net total neutron leakage probability out of each radial zone, the power fraction distribution and the radial burnup distribution at BOEC and EOEC. It is observed that the power peaking at BOEC is occurring in the innermost fuel zone. The power distribution is slightly shifting outward during the cycle. The axially averaged radial power peaking factor is 2.38 at BOEC and the local peak power density is 324 W/cm^3. This radial power peaking factor is significantly larger than for the large B&B core at equilibrium, and the thermal hydraulics analysis of Section 7.7 needs to confirm that the thermal hydraulics constraints are met.

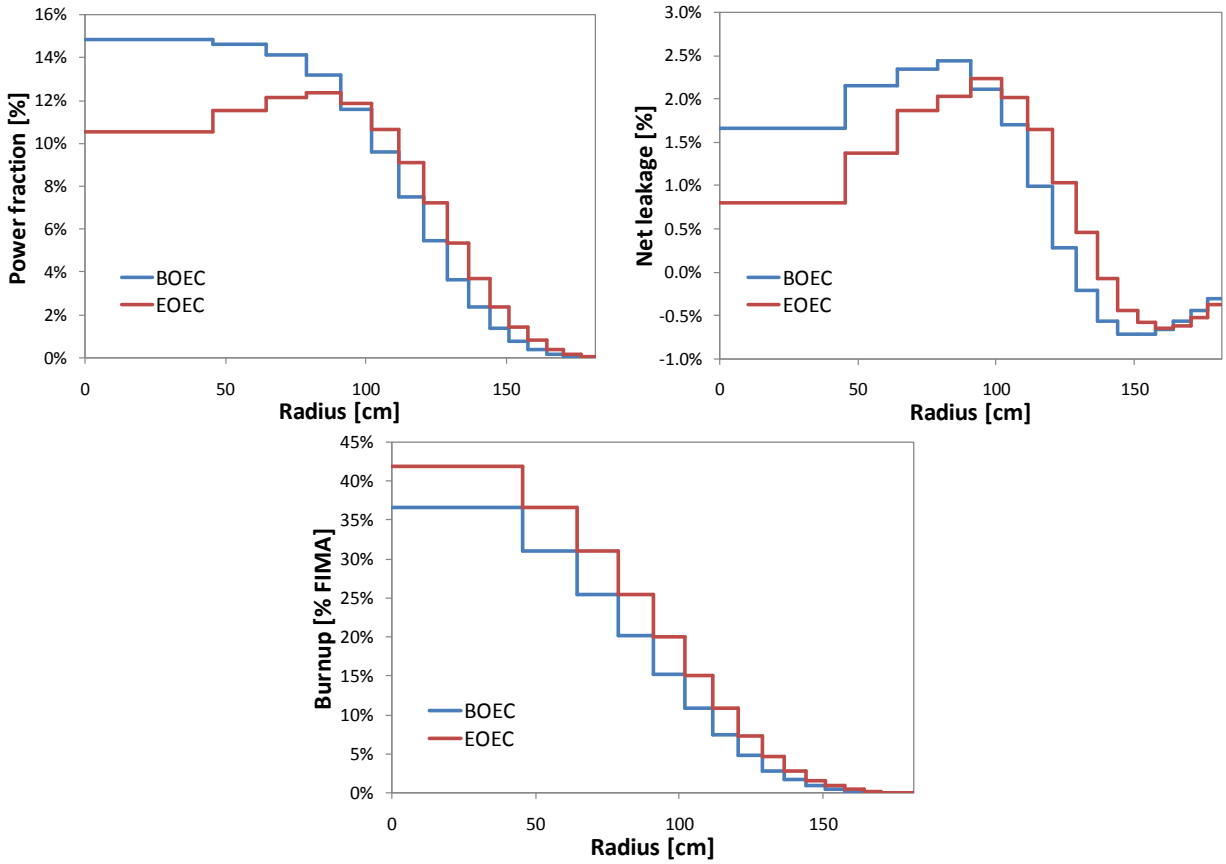

Figures 7.2, 7.3 and 7.4: Zone-wise net neutron radial leakage (left), power fraction distributon (right) and burnup distribution (bottom) at BOEC and EOEC for the S-PRISM size B&B core having a discharge burnup of 40.9% FIMA.

Table 7.1 summarizes selected design and performance characteristics of the S-PRISM size core at equilibrium. The "conversion ratio" provided in this table is the ratio between the number of transuranium atoms in the entire core, at the EOEC and BOEC. The total neutron leakage probability is slightly increasing from 9.55% at BOEC to 10.27% at EOEC because the radial power distribution shifts outward. The axial neutron leakage probability stays constant and equal to 7.87%. On average, the neutron leakage probability is 42% larger than in the large B&B core. The average S-PRISM size B&B core burnup is only 9.9% FIMA at BOEC, twice smaller than for the large B&B core – 19.0% FIMA; as a consequence, ~11% fewer neutrons are captured in the fission products in the S-PRISM size B&B core.

Table 7.1: Core Design and Performance Parameters at Equilibrium for the 16 Radial Zones S-PRISM Size B&B Core

Parameters	Value
Fuel/Gap/Clad/Coolant volume fractions [%]	34.1/11.4/26.6/28
Average power density [W/cm^3]	112.5
Peak power density [W/cm^3]	324
Average specific power density [W/g HM]	22.2
Cycle length [y]	3.15
Average core burnup at BOEC/EOEC [% FIMA]	9.9/12.5
HM mass at BOEC/EOEC [tons]	68.1/66.1
TRU mass at BOEC/EOEC [tons]	4.5/5.0
Conversion ratio	1.09
Discharge burnup [GWd/tHM]	397.8
Burnup reactivity loss [% Δk]	2.25
Core average flux [10^{15}n/cm^2-s]	1.79
Fast flux (E>0.1MeV) fraction > 0.1 MeV [%]	67.3
Axial neutron leakage at BOEC/EOEC [%]	7.9/7.9
Radial neutron leakage at BOEC/EOEC [%]	1.7/2.4

7.1.2 Improved shuffling scheme

The simple shuffling scheme discussed in the previous section is improved in order to increase the maximum achievable burnup and decrease the burnup reactivity swing. With 16 radial zones, many shuffling schemes can be envisioned, several of which have been tried. Most of the shuffling schemes studied enabled increasing the discharge burnup, but the radial power peaking factor was found to be significantly larger than for the simple shuffling scheme.

Due to the larger radial power peaking factor, the total core power is decreased to 1000 MW_{th}, the same as of the reference S-PRISM design by GE [28]. The average power density is 67.3 W/cm^3, and the specific power is 13.2 W/g of HM. The best shuffling scheme identified is schematically described in Table 7.2. The freshly loaded depleted uranium, initially loaded at the outermost core location, is progressively shuffled inward six times before being loaded at the 4th radial core location and shuffled inward two times. It is then moved to the 5th radial core location and shuffled outward four times. Finally, it is loaded for its last cycle at the innermost core location.

Table 7.2: Improved Shuffling Scheme Pattern for Melt-refining in the S-PRISM Size B&B Core

Radial zone…	is moved to radial location…
16	15
15	14
14	13
13	12
12	11
11	10
10	4
4	3
3	2
2	5
5	6
6	7
7	8
8	9
9	1
1	discarded

With this improved shuffling scheme, the maximum achievable burnup is found to be 440 GWd/tHM – 45.2% FIMA – for the S-PRISM size B&B core. This is a 10.5% improvement over the simple shuffling scheme, despite using a power density 40% smaller. The evolution of k_{eff}, shown in Figure 7.5, is initially increasing but is decreasing when approaching EOEC. At BOEC, the burnup of most of the fuel elements loaded in the inner half of the core is above 15% FIMA. With increasing burnup, the k_∞ of the inner fuel elements is slightly decreasing. However, the third and fourth radial zones see their k_∞ increasing with burnup because it is below 15% FIMA. At EOEC this k_∞ increase is overweighting the k_∞ decrease of the other zones, making the core k_{eff} slightly increase. After ~3 EFPY, the k_∞ increase in the third and fourth radial zones become less significant, and due to the radial leakage probability increase – due to outward shift of the power distribution, k_{eff} is decreasing. The k_∞ and burnup radial distributions at BOEC and EOEC are shown in Figure 7.6. The burnup reactivity swing with the improved shuffling scheme is only 0.47%, slightly larger than the delay neutron fraction of the reactor, β_{eff}. With such a small burnup reactivity swing, the reactor excess reactivity control is simplified and the reactivity worth required of the control rods is smaller.

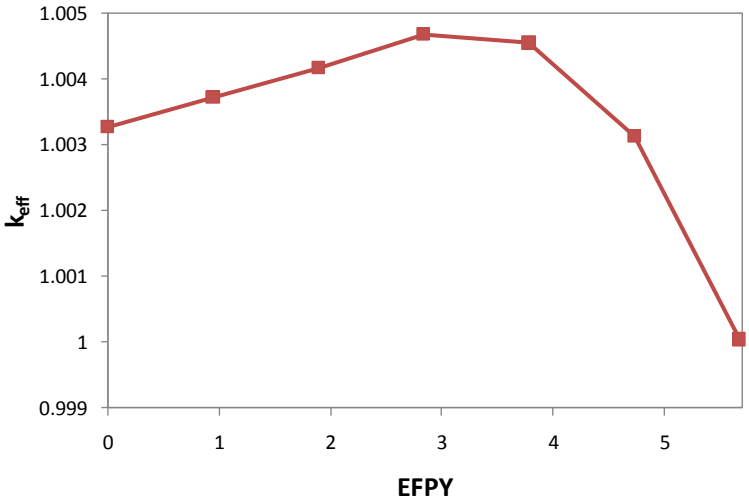

Figure 7.5: Evolution of k_{eff} at equilibrium for the S-PRISM size B&B core operating at 45.2% FIMA with the improved shuffling scheme

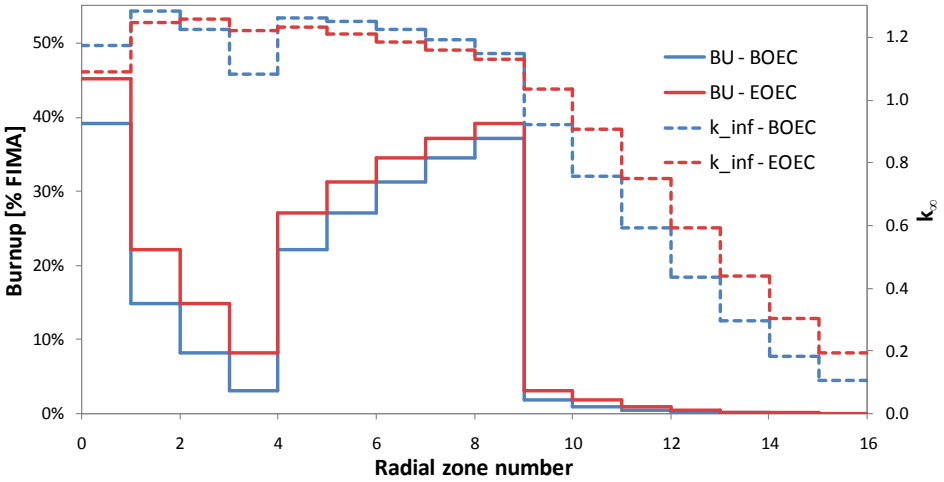

Figure 7.6: Burnup and k_∞ radial distribution at BOEC and EOEC for the S-PRISM size B&B core with the improved shuffling scheme

At BOEC, the axial and radial neutron leakage probabilities are 7.7% and 1.7%, respectively. During the cycle, the radial power distribution shown in Figure 7.7 is slightly shifting outward, making the radial neutron probability increase to 2.0% by EOEC; the axial neutron leakage probability is constant during the cycle. The leakage probability change represents 78% of the burnup reactivity swing and along with the HM depletion is responsible for the k_{eff} decrease near EOEC.

The axially averaged radial power peaking factor is 2.76 and is occurring at BOEC in the second innermost radial zone. Due to the low core power density, the local peak power density is only 231 W/cm^3. Despite the larger radial power peaking factor, the power distribution stays approximately constant during the cycle. The largest power fraction change is occurring in the innermost fourth radial zones, but overall it is significantly smaller than in the simple shuffling scheme of Section 7.1.1.

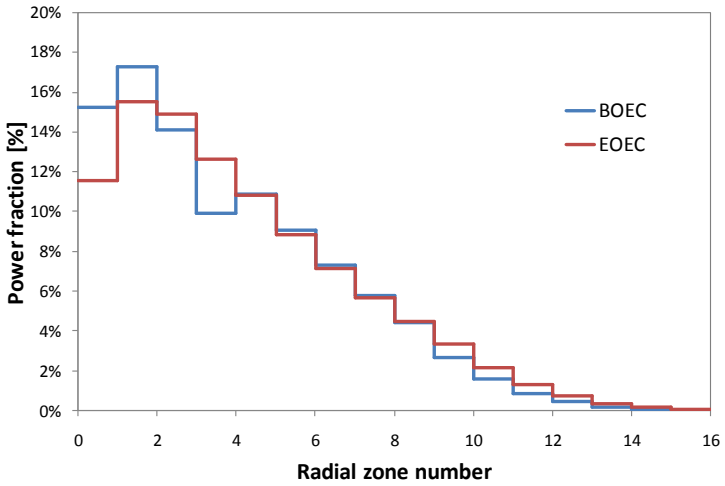

Figure 7.7: Radial power distribution at BOEC and EOEC for the S-PRISM size B&B core with the improved shuffling scheme

Overall, the proposed improved shuffling scheme enables increasing the maximum discharge burnup by +4.3% FIMA, to 45.2% FIMA, and makes the core significantly easier to control due to the very small burnup reactivity swing and makes it easier to cool due to the small radial power distribution change during the cycle. The main drawback is the radial power peaking factor that is ~16% larger than for the simple shuffling scheme and is decreasing the achievable core power.

7.2 Neutron balance

The same neutron balance analysis performed for the large B&B core at equilibrium in Section 6.4 is performed in this section for the S-PRISM size B&B core. The volume fractions, neutron leakage probability and fraction of neutrons absorbed in the control systems assumed for the S-PRISM size B&B core being different than those used for the large B&B core, none of the previous 0-D neutron balance is valid for the S-PRISM size B&B core. The neutron balance is performed for both the finite core and for a 0-D unit cell. The fuel k_∞ for the finite core is calculated using Equation 6.1, and its evolution with burnup is obtained using the improved shuffling scheme described in Table 7.2. The 0-D unit cell having no neutron leakage and only one depletion zone, the infinite multiplication factor is equal to the MCNP5 eigenvalue (k_{eff}). The average neutron leakage probability and fraction of neutron being absorbed in the control systems have been calculated in Section 7.1.2: 9.6% and 0.35%, respectively. Those values are used for the 0-D unit cell neutron balance in order to match the S-PRISM size B&B core practical behavior.

The evolution of k_∞ for the two models is shown in Figure 7.8. For burnups below 3% FIMA, corresponding to the seven outermost radial zones, the k_∞ values show a good agreement between the two models. When the fuel is shuffled toward the core center, at 3% FIMA, the spectrum is significantly harder, and its k_∞ is suddenly increased and becomes larger than in the 0-D unit cell. For burnups above 15% FIMA, this difference is less important. As the fuel is shuffled outward, it experiences a softer spectrum than in the 0-D unit cell at the same burnup. Above 35% FIMA, k_∞ is slightly larger in the 0-D unit cell. However, at 39% FIMA the fuel is

finally shuffled to the core center, where the spectrum is similar to the 0-D unit cell spectrum, yielding similar k_∞ values.

The differences in k_∞ between the two models studied are small, but have a significant effect on the neutron balance. The neutron balances are presented in Figure 7.9, using the same neutron leakage probability and fraction of neutrons absorbed in the control systems for both models. The 0-D unit cell shows it is not possible to sustain a breed and burn mode of operation in the S-PRISM size B&B core unless the neutron leakage probability is decreased – for instance by using an efficient reflector. This result does not agree with the result obtained with the finite core model because of the spectral differences discussed in the previous paragraph. The neutron balance for the finite core model confirms that the maximum discharge burnup is 45% FIMA. In Section 7.1.2 it has been found that the maximum discharge burnup for the improved shuffling scheme is 45.2% FIMA.

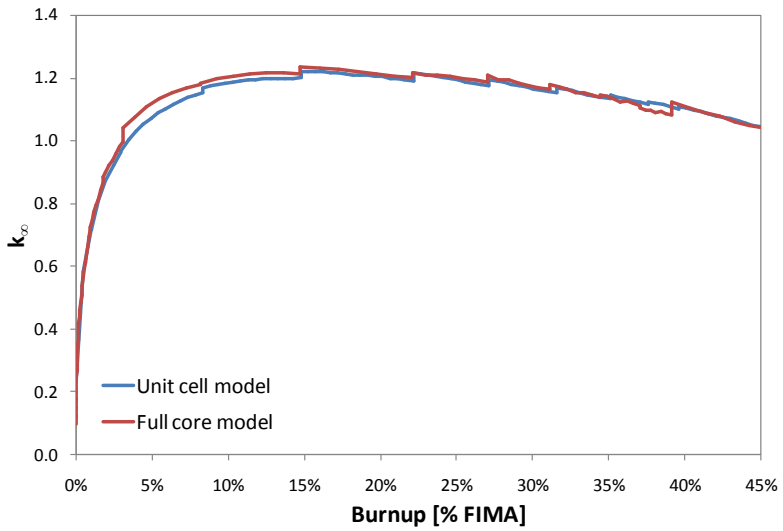

Figure 7.8: Evolution of k_∞ for the finite core model and the 0-D unit cell

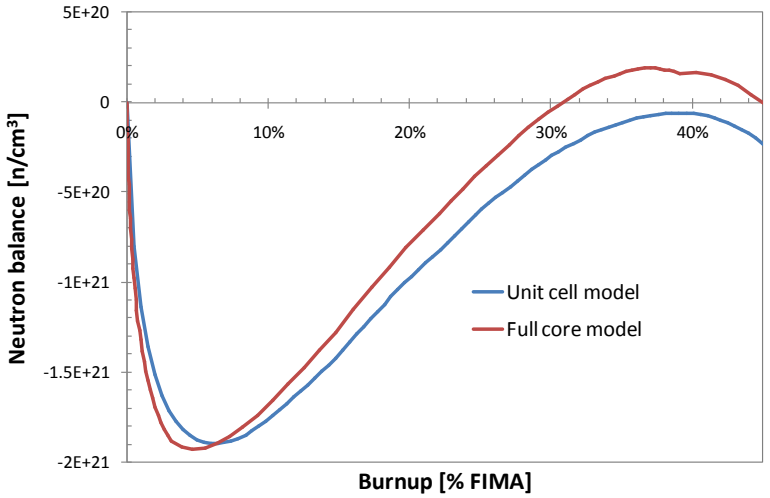

Figure 7.9: Neutron balance for the unit cell and finite core models – S-PRISM size B&B core

The minimum burnup required to sustain the breed and burn mode of operation in the S-PRISM size B&B core is in the vicinity of 31% FIMA. This is 50% larger than the value found for the large B&B core due to the larger neutron leakage probability and lower HM fraction. The effect of the lower HM fraction can be assessed by performing the neutron balance with the same fraction of neutron lost (6.6%) than in the large B&B core. It is found that with this fraction of neutron lost, the minimum discharge burnup for the S-PRISM size B&B core is about 22.5% FIMA, larger than for the large B&B core by 2.5% FIMA. Therefore, the increased leakage probability in the S-PRISM size B&B core accounts for more than 75% of the minimum required burnup increase, compared to the large B&B core.

This neutron balance shows that the maximum discharge burnup for a S-PRISM size B&B core is 45% FIMA and that the minimum required burnup to sustain the breed and burn mode of operation is ~31% FIMA. Furthermore, it was found that the 0-D unit cell model cannot accurately predict the maximum and minimum discharge burnup for complex shuffling schemes because of the spectral differences.

7.3 Sensitivity analysis

In Sections 7.1 and 7.2, it has been found possible to sustain the breed and burn mode in a S-PRISM size B&B core, with a discharge burnup up to 40.9% FIMA with the simple shuffling scheme and up to 45.2% FIMA with the improved shuffling scheme. Among the assumptions made to simulate the S-PRISM core the most important are that (a) the core power is 1672 MW_{th} for the simple shuffling scheme and 1000 MW_{th} for the improved shuffling, (b) the heavy metal density in the core is 5.08 g/cm^3, and (c) the fuel is recycled with the melt-refining process. The sensitivity of the S-PRISM size B&B core performance to those three parameters is assessed in this section.

7.3.1 Core power

The first parameter studied is the total core power. By changing the core power, the equilibrium core composition is changed due to the decay of the short-lived isotopes, in particular ^{241}Pu and some fission products. ^{241}Pu being an important fissile isotope, it can significantly modify the maximum achievable burnup. The fission products will affect the waste characteristics: with a small core power, a large fraction of the short-lived fission products will decay before EOEC. The radiotoxicity of the discharged fuel is expected to be smaller with a lower power density. Although the waste characteristics are very important for the attractiveness of the fuel cycle, this section only focuses on the neutron economy issue.

The S-PRISM size B&B core is studied with increased power density. For the simple shuffling scheme, the core power density is doubled and set at 225 W/cm^3, corresponding to a total core power of 3344 MW_{th}. For the improved shuffling scheme, two different core powers are used: 3344 MW_{th}, corresponding to the increased power level of the simple shuffling scheme, and 1600 MW_{th}, which is a more practical value. The corresponding power densities are 225 W/cm^3 and 107.7 W/cm^3, respectively. The results obtained are presented in Table 7.3.

Table 7.3: S-PRISM size B&B Core Power Density Sensitivity Results

Shuffling	Simple	Simple	Improved	Improved	Improved
Total power [MW_{th}]	1672	3344	1000	1600	3344
Power density [W/cm^3]	112.5	225	67.3	107.7	225
Discharge burnup [GWd/tHM]	397.8	415.1	439.6	445.4	452.1
Fractional burnup increase	-	4.35%	-	1.33%	2.86%
Minimum k_{eff}	1.00309 ±0.00071	1.00098 ±0.00069	1.00004 ±0.00054	0.99938 ±0.00049	0.99968 ±0.00059
Burnup reactivity swing $\%\Delta k_{eff}$	2.25	2.4	0.47	0.57	0.6

By increasing the power density, the ^{241}Pu fission to decay atom ratio is increased and the maximum achievable burnup is increased. When doubling the power for the simple shuffling scheme, it is found possible to increase the maximum discharge burnup by ~4.35%. This burnup gain is overestimated because for the lower power level, 1672 MWth, there is an excess reactivity of ~300 pcm, making it possible to slightly increase the discharge burnup without increasing the power. For the improved shuffling scheme, when the power is increased by +60%, the discharge burnup is increased by ~1.3%, and when the power is increased by +234%, the discharge burnup is increased by ~2.9%. The discharge burnup gain is not proportional to the power change. It is also observed that when increasing the power density, the burnup reactivity swing is slightly increased – more excess neutrons are available in the core.

It is concluded that the attainable discharge burnup only slightly depends on the core power density. The burnup tends to increase with increased power density.

7.3.2 Heavy metal density

The heavy metal density is a critical parameter for the core performance. With a high HM density, it is possible to harden the neutron spectrum, increase the core average η, increase the fraction of neutrons absorbed in the fuel, decrease the neutron leakage probability because of the denser core, and load a larger mass of fuel in the same core volume.

In this paragraph, the fuel volume fraction of the S-PRISM size B&B core is decreased by 1%, from 34.1% to 33.1%. The gap volume fraction is decreased by 0.3%, and the coolant volume fraction is increased by 1.3%. The original and modified volume fractions are provided in Table 7.4. The new HM density is 4.93 g per $cm^3$of core. The analysis is performed for the S-PRISM size B&B core having a power of 1600 MW_{th}, and using the improved shuffling scheme.

Table 7.4: Original and Modified S-PRISM Size B&B Core Volume Fractions

	Original	Modified
Fuel	34.1%	33.1%
Gap	11.4%	11.0%
Structural material	26.6%	26.6%
Coolant	28.0%	29.3%

Due to the extensive time required to determine the equilibrium core characteristics, it has not been possible to simulate an equilibrium cycle having a minimum k_{eff} equal to unity. The closest simulation performed yielded a minimum k_{eff} value of 0.99837±0.00072 corresponding to a discharge burnup of 402 GWd/tHM – 41.2% FIMA. Interpolating the results obtained for the several simulations performed with the modified volume fractions, it is estimated that the maximum achievable burnup is somewhere between 375 and 385 GWd/tHM. It is also observed that by changing the targeted discharge burnup the improved shuffling scheme is not anymore optimized: the burnup reactivity swing becomes more than twice larger than for the reference core.

It is concluded that the achievable discharge burnup is very sensitive to the HM density in the core. When designing a breed and burn core, the fuel volume fraction and fuel density are the key parameters to achieve a high discharge burnup. This confirms the behavior observed in Section 5.3.4 for the different type of fuels and at the end of Section 7.3.1 when comparing the neutron balance of metallic fuel with difference zirconium weight fraction – i.e. different HM weight fractions.

7.3.3 Fuel recycling process

The performance of the 1600 MW_{th} S-PRISM size B&B core is assessed in this section, using the AIROX-like process instead of the melt-refining process. In Section 2.2 the AIROX-like and melt-refining processes were presented. The melt-refining has been preferred so far because of the larger amount of fission products removed from the fuel and its compatibility with metallic fuel. Using a different fuel recycling process for which different fractions and different isotopes are removed can yield significantly different performance. With fewer fission products in the core, fewer neutrons will be lost, the spectra will be slightly harder and the maximum achievable burnup will be increased. With the AIROX-like process a significantly smaller fraction of fission products are removed from the fuel than with the melt-refining.

Initially, the improved shuffling scheme described in Table 7.2 for the S-PRISM size B&B core operating with the melt-refining process is used. The target discharge burnup has been decreased, but it has not been possible to achieve a sustainable breed and burn mode. By slightly modifying the shuffling scheme and using the one described in Table 7.5, it has been found possible to achieve an equilibrium mode, where the minimum value of the multiplication factor is equal to ~1.001 at both BOEC and EOEC, with a discharge burnup of 399 GWd/tHM – 40.6% FIMA versus 45.2% FIMA when using the melt-refining process. The burnup reactivity swing is only 0.2%, approximately half the β_{eff} value and the radial power peaking factor is 2.96; this is 5% larger than with melt-refining fuel recycling.

By using the AIROX-like process – where only the volatile and gaseous fission products are removed from the fuel, instead of the melt-refining – where in addition to the volatile and gaseous fission products a significant fraction of the lanthanides is removed from the fuel, it is possible to sustain the breed and burn mode of operation in the S-PRISM size B&B core, but the maximum achievable burnup is decreased by approximately 5% FIMA.

Table 7.5: Improved Shuffling Scheme for AIROX-like Process in the S-PRISM Size B&B Core

Radial zone…	is moved to radial location…
16	15
15	14
14	13
13	12
12	11
11	10
10	5
5	4
4	3
3	2
2	6
6	7
7	8
8	9
9	1
1	discarded

7.4 Assembly-level model performance

In order to verify that the cylindrical model of the core is a good enough approximation of the real core, an assembly-level model is analyzed in this section. All the results presented in the previous sections of this chapter pertain to the S-PRISM size B&B core modeled using 16 concentric cylindrical zones. Each radial zone is made of three axial homogenized compositions, the volume fractions of which have been provided in Table 7.4 – left column. The GEMs and control assemblies are smeared into the volume fractions. In reality, the control rods assemblies are located close to the core center in order to maximize their reactivity worth and the GEMs are located in the outer core region. In addition, only 16 fuel batches with averaged compositions are used, while in reality the fuel composition inside a batch is not uniform. Those simplifications can result in an underestimated axial neutron leakage probability and biased core performance.

In the assembly-level model studied in this section, each fuel, GEM and control assembly is modeled individually with three axial zones. Each of the three axial zones is made of a homogenized composition. The control assemblies are assumed to be completely withdrawn from the core; they are represented by only sodium. The volume fractions of the fuel assemblies and the GEMs are provided in Table 7.6. The number of fuel assemblies initially assumed, 445, cannot be split into 16 fuel batches and in order to model the core with the same number of fuel assemblies in each batch, the following modifications are made:

- the number of fuel batches is reduced to 15 (formerly 16);
- the total number of fuel assemblies is increased to 450;
- the number of control rods assemblies is increased to 13 (formerly 12);
- the shield is now composed of 84 assemblies (formerly 78);
- the active core diameter is increased to 183.54 cm (formerly 182.36 cm).

Table 7.6: Volume Fractions for the Assembly-level S-PRISM Size B&B Core Model

	Fuel assembly	GEM
Fuel	35.44%	-
Gap	11.81%	-
Structural material	25.37%	18.05%
Coolant	27.38%	81.95%

Due to symmetry considerations, only one sixth of the core is modeled. The general core layout and the volume fractions modeled in MCNP5 are provided in Figures 7.10 and 7.11. There are 84 full or partial length fuel assemblies modeled in MCNP5, for a total of 252 depletion zones and 252 fuel compositions. The fuel batches layout is shown in Figure 7.10. The assemblies filled in black and brown are, respectively, the primary and secondary control systems. The assemblies filled in white with a dark dot are the GEMs assemblies.

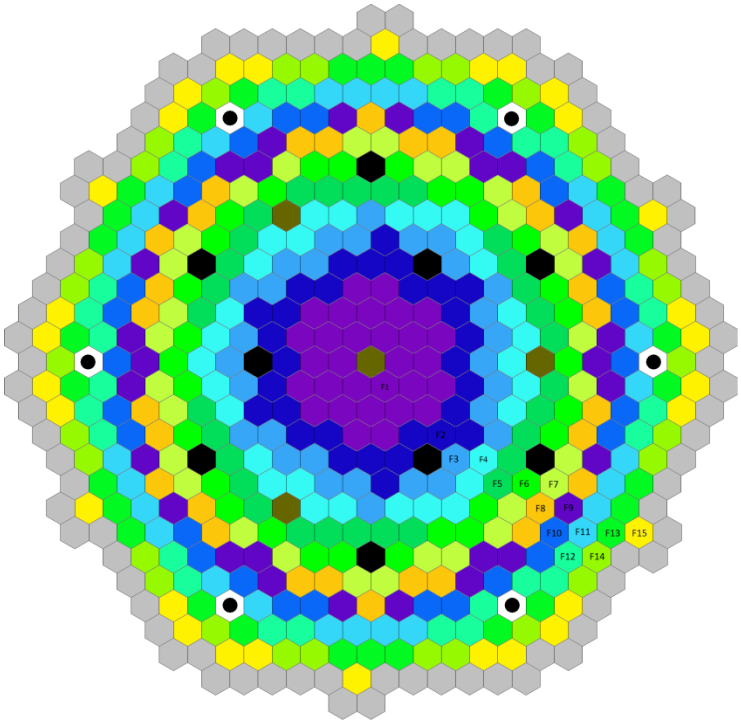

Figure 7.10: Full core layout with the 15 fuel batches, control systems and GEMs – the reflector is in grey

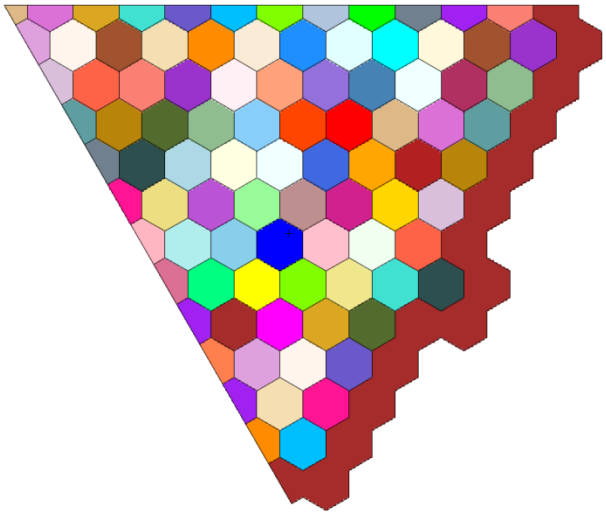

Figure 7.11: Sixth core model with MCNP5 – shield is in dark red

Since the number of fuel batches and assemblies has been changed, the performance of this core needs to be assessed with both the assembly-level and cylindrical models. The core power is taken to be 1200 MW_{th}, and the shuffling scheme is described in Table 7.7. The equilibrium core characteristics are obtained for a targeted discharge burnup of 395 GWd/tHM. It took only 1.5 days to obtain the results for the cylindrical model, while it took more than a week to obtain the same results for the assembly-level model, due to the much larger number of depletion zones.

Table 7.7: Improved Shuffling Scheme for the Assembly-level Model with 15 Fuel Batches

Radial zone…	is moved to radial location…
15	14
14	13
13	12
12	11
11	10
10	9
9	4
4	3
3	2
2	5
5	6
6	7
7	8
8	1
1	discarded

The evolution of k_{eff} is compared in Figure 7.12 for the two core models. Most of the values are within one standard deviation of each other and the trends are identical for the two models: the initial k_{∞} increase is due to plutonium build-up in the low burnup assemblies and is followed by a decrease due to the increasing neutron leakage probability. Overall, the k_{eff} values of the cylindrical model are slightly larger than those of the assembly-level model.

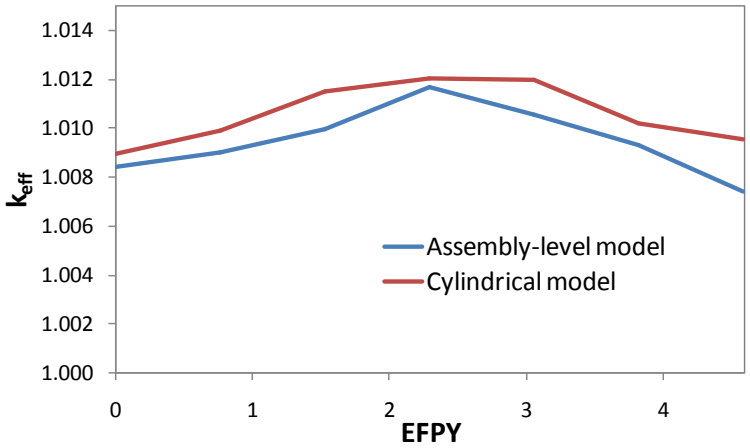

Figure 7.12: k_{eff} evolution for the S-PRISM size B&B core for the assembly-level and cylindrical models with 15 fuel batches

The two models studied show a good agreement. Some important characteristics are compared in Table 7.8. The axial leakage probability is found to be larger by +0.35% for the assembly-level model, justifying the difference observed in k_{eff} values. The plutonium isotopes inventory, heavy metal inventory and fission product inventories are almost identical. The other notable differences are the peak power density and radial power peaking factor, which are found smaller for the cylindrical model: the values obtained for the cylindrical model are the averaged values of the 30 assemblies composing a fuel batch. However, the magnitude of these two differences is less important than in Section 6.1.3 for the large B&B core, because of the larger number of radial zones used for the S-PRISM size B&B cylindrical core model – 15 instead of 8.

The axially averaged burnup of the fuel assemblies and the radial power distribution at BOEC and EOEC are provided in Figures 7.13 and 7.14. When comparing the average burnup and power fraction of each fuel batch between the cylindrical model and the assembly-level model, very little difference is found. Tables 7.9 and 7.10 provide the burnup and power fraction values for each batch, as well as the relative difference. The average batch burnup values agree within 0.15% FIMA, and the batch power fractions absolute errors are all within 0.5% of the total power.

Table 7.8: General Characteristics Comparison between the Cylindrical and Assembly-level S-PRISM Size B&B Core Models

Model	Cylindrical	Assembly-level
Average discharge burnup [GWd/tHM]	394.6	395.3
Cycle length [years]	4.59	
Average power density [W/cm^3]	79.72	
Peak power density [W/cm^3]	277.3	286.9
Radial power peaking factor	2.79	3.04
Burnup reactivity swing %Δk	0.31%	0.43%
Conversion Ratio	1.105	1.104
Axial leakage probability at BOEC/EOEC [%]	7.60%/7.56%	7.94%/7.94%
Radial leakage probability at BOEC/EOEC [%]	1.47%/1.78%	1.41%/1.73%
Average core BU at BOEC/EOEC [% FIMA]	11.14%/13.84%	11.19%/13.87%
^{239}Pu at BOEC/EOEC [tons]	3.67/3.99	3.65/3.97
^{240}Pu at BOEC/EOEC [tons]	0.75/0.88	0.75/0.88
^{241}Pu at BOEC/EOEC [tons]	0.067/0.082	0.068/0.083
HM at BOEC/EOEC [tons]	67.92/65.86	67.76/65.72
FP at BOEC/EOEC [tons]	3.33/5.15	3.34/5.16

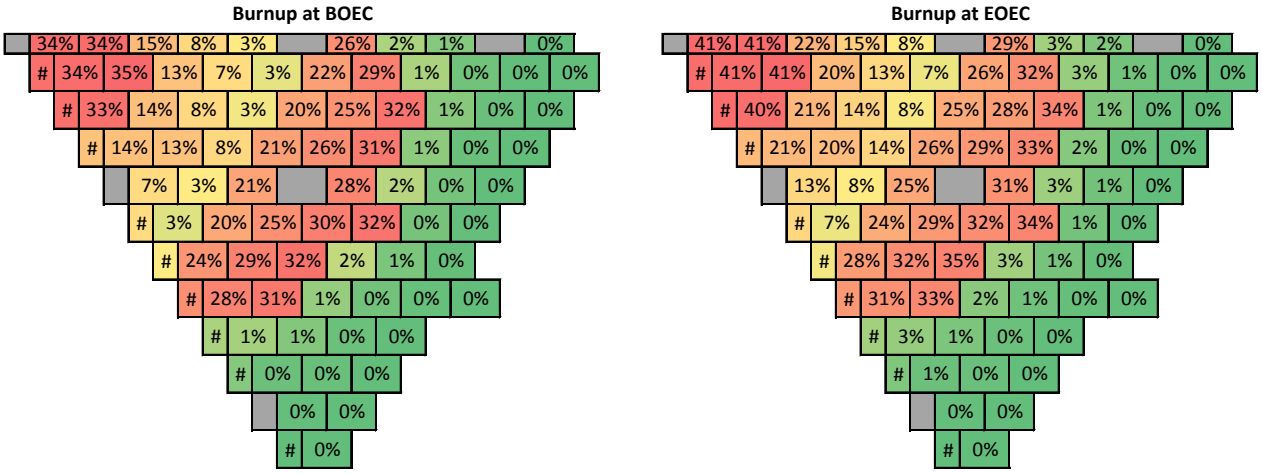

Figure 7.13: Axially averaged burnup – % FIMA – at BOEC and EOEC in each fuel assembly

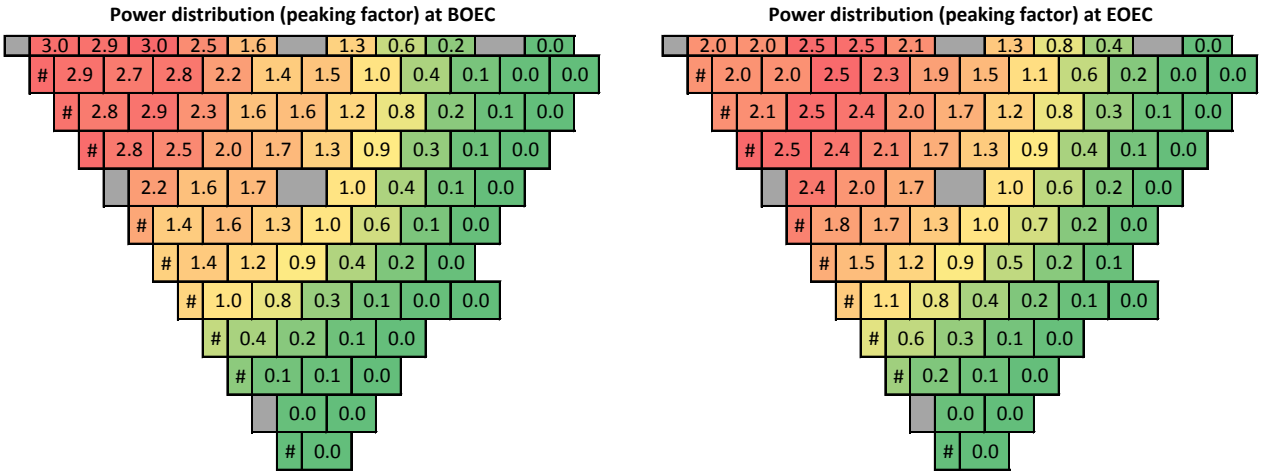

Figure 7.14: Power distribution at BOEC and EOEC in each fuel assembly

Table 7.9: Batch Burnup Comparison for the S-PRISM Size B&B Core between the Assembly-level Model and the Cylindrical Model

Burnup	Assembly-level		Cylindrical		Absolute error	
Radial batch	BOEC	EOEC	BOEC	EOEC	BOEC	EOEC
1	33.9%	40.5%	33.9%	40.4%	-0.02%	-0.09%
2	13.6%	20.8%	13.5%	20.7%	-0.11%	-0.11%
3	7.6%	13.6%	7.4%	13.5%	-0.14%	-0.15%
4	3.0%	7.5%	2.9%	7.4%	-0.12%	-0.14%
5	20.8%	25.2%	20.7%	25.2%	-0.09%	-0.03%
6	25.2%	28.8%	25.2%	28.8%	-0.08%	0.03%
7	28.9%	31.7%	28.8%	31.7%	-0.06%	0.03%
8	31.8%	33.9%	31.7%	33.9%	-0.09%	0.04%
9	1.6%	3.0%	1.6%	2.9%	-0.05%	-0.10%
10	0.8%	1.6%	0.8%	1.6%	-0.01%	-0.04%
11	0.4%	0.8%	0.4%	0.8%	-0.01%	-0.01%
12	0.2%	0.4%	0.2%	0.4%	0.01%	-0.01%
13	0.1%	0.2%	0.1%	0.2%	0.00%	0.01%
14	0.0%	0.1%	0.0%	0.1%	0.00%	0.00%
15	0.0%	0.0%	0.0%	0.0%	0.00%	0.00%

Table 7.10: Batch Power Fraction Comparison for the S-PRISM Size B&B Core between the Assembly-level Model and the Cylindrical Model

Power fraction	Assembly-level		Cylindrical		Absolute error	
Radial batch	BOEC	EOEC	BOEC	EOEC	BOEC	EOEC
1	19.0%	13.6%	18.6%	13.5%	-0.42%	-0.13%
2	18.7%	16.6%	18.6%	16.5%	-0.06%	-0.05%
3	14.6%	15.5%	14.6%	15.5%	-0.02%	-0.01%
4	9.9%	12.7%	9.8%	12.7%	-0.02%	0.00%
5	10.9%	11.0%	10.9%	11.2%	-0.02%	0.13%
6	8.7%	8.9%	9.0%	9.1%	0.25%	0.16%
7	6.9%	7.1%	7.1%	7.2%	0.21%	0.13%
8	5.1%	5.4%	5.4%	5.6%	0.22%	0.20%
9	2.9%	4.0%	2.8%	3.7%	-0.08%	-0.25%
10	1.7%	2.4%	1.6%	2.3%	-0.05%	-0.10%
11	0.9%	1.4%	0.9%	1.3%	-0.01%	-0.02%
12	0.5%	0.8%	0.4%	0.7%	-0.02%	-0.07%
13	0.2%	0.3%	0.2%	0.4%	0.02%	0.02%
14	0.1%	0.2%	0.1%	0.2%	0.00%	-0.01%
15	0.0%	0.1%	0.0%	0.1%	0.00%	0.01%

It is found that the results obtained with the cylindrical model are consistent with those obtained with the finer assembly-level model. Since the computation time required to determine the equilibrium characteristics of the assembly-level model is five times larger than for the cylindrical model, it is preferable to keep performing the S-PRISM size B&B core studies using the cylindrical model. However, it is important to remember that due to the averaged volume fraction used with the cylindrical model, the neutron leakage probability is slightly underestimated, and that the peak power density is underestimated by a few percents.

7.5 Control systems analysis

The performance of the two control assemblies systems of the S-PRISM size B&B core is assessed in this section. The primary and secondary control systems are made of nine and four assemblies, respectively. The "stuck rod criterion" [57] for each control system is that it must provide sufficient shutdown margin with only one of the two control systems activated and with the control assembly with the largest reactivity worth not inserted. The control assemblies having the highest reactivity worth are those located near the core center, where the neutron flux and importance function are the largest. The reactivity worth of each control assembly is first estimated at each step of the equilibrium cycle, and then the reactivity worth of the whole control system – primary or secondary – is estimated using the above defined safety criteria condition. The shutdown margin should be estimated at cold condition and would require changing many core parameters: fuel temperature, coolant density, dimensions of the core... Due to the complexity of realistically changing all those parameters, the shutdown margins are estimated at operating temperature. According to the DOE handbook [57], a shutdown margin larger than 1% reactivity is required. A thorough analysis of the control systems should be performed along with the study of the reactivity coefficients.

The study is performed for the 1200 MW_{th} S-PRISM size B&B core at equilibrium with the fuel being discharged at 395 GWd/tHM. The model used is a modified cylindrical model, as illustrated by Figure 7.15, in which the control assemblies have been discretely modeled. The volume fractions of the 15 radial fuel zones, provided in Table 7.11, have been modified accordingly. The performance of the modified cylindrical model is found identical to the performance of the same core modeled with the simple cylindrical model – without the discrete control assemblies. The shuffling scheme used to determine the equilibrium uncontrolled k_{eff} evolution, shown in Figure 7.16, is based in the shuffling scheme described in Table 7.2. Since there are only 15 radial zones, the depleted uranium is inserted in zone 15 rather than 16; the rest of the shuffling scheme is identical.

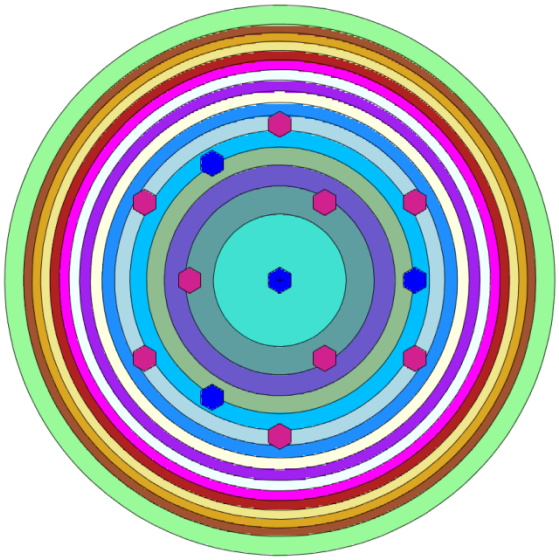

Figure 7.15: Modified cylindrical model layout. Primary control system is in purple, secondary control system is in blue.

Table 7.11: Core Volume Fractions of the Modified Cylindrical Model

Fuel	35.0%
Gap	11.7%
Structural material	25.2%
Coolant	28.2%

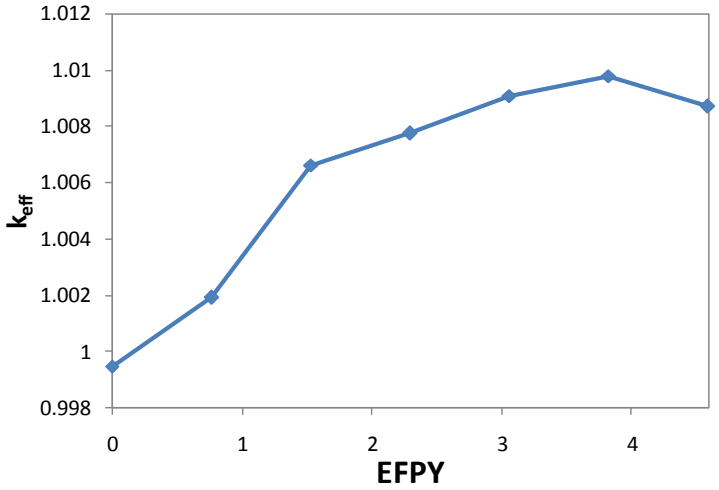

Figure 7.16: Uncontrolled k_{eff} evolution at equilibrium

7.5.1 Initial design: B_4C control rods

The control rods used in the S-PRISM design [28] and the ABR design [27] are made of boron carbide, B_4C. The natural composition of boron is 19.9 at% ^{10}B and 80.1 at% ^{11}B, but the capture cross-section of ^{10}B being larger, boron is commonly enriched in ^{10}B up to 90 at% [9]. The control rods used in the S-PRISM size B&B core are assumed to be made of B_4C with boron enriched at 80 at% in ^{10}B. Only 90% of the B_4C nominal density, 2.52 g/cm^3, is used since it is a ceramic material and it is challenging to fabricate B_4C pellets having the theoretical density. The control assemblies have the same dimensions as the regular fuel assemblies and are filled with seven rods of B_4C cladded with 4 mm of HT-9. The control assembly volume fractions are given in Table 7.12.

Table 7.12: Control Assembly Volume Fractions

Absorber volume fraction	52.9%
HT-9 volume fraction	29.0%
Coolant volume fraction	18.1%

When only one control assembly of the primary control system is inserted, the average assembly worth during the equilibrium cycle is found to be 960 pcm for the inner row assemblies and 365 pcm for the outer row assemblies. For the secondary system, the average worth for the control assembly located at the core center is 1450 pcm and is 508 pcm for the outer row control assemblies.

The reactivity worth of the primary control system are summarized in Table 7.13, and shown in Figure 7.17, when (a) all the control assemblies are inserted and when (b) all the control assemblies but one of the inner row are inserted. It increases from 6272 pcm at BOEC to 6676 pcm at EOEC for (a) and from 4524 pcm at BOEC to 4795 pcm at EOEC for (b). The reactivity worth increase of the primary control system is due to the power distribution change. During the equilibrium cycle the power fraction in the two innermost fuel zones decreases while it increases for the third and fourth innermost fuel zones – it does not change anywhere else – increasing the neutron flux in those zones: the reactivity worth of the control assemblies is increasing. It is

found that the primary control system successfully meets the safety criteria scenario, with a minimum shutdown margin of ~3800 pcm.

Table 7.13: Reactivity Worth of the Primary Control System when (a) all Assemblies are Inserted and (b) All Assemblies but the Highest Reactive One are Inserted

Time [EFPY]	0	0.76	1.53	2.29	3.06	3.82	4.59
Reference k_{eff}	0.99948	1.00192	1.00663	1.00775	1.00909	1.00978	1.00871
Reactivity worth for (a) in pcm	6272	6241	6421	6563	6625	6688	6676
Reactivity worth for (b) in pcm	4524	4433	4621	4682	4684	4816	4795

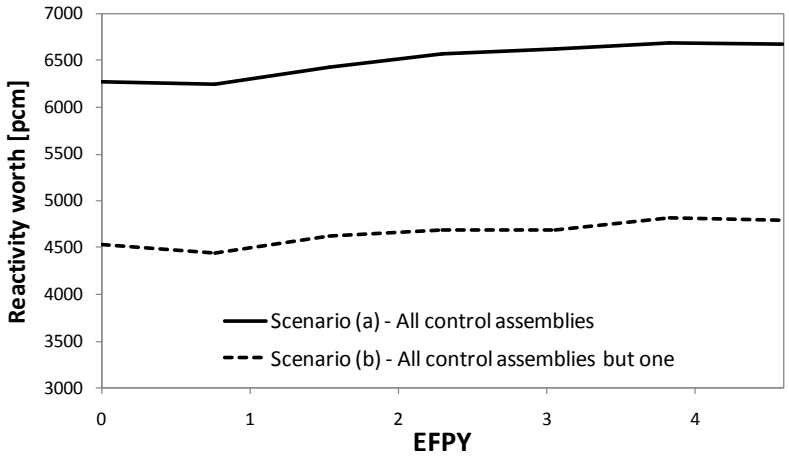

Figure 7.17: Reactivity worth evolution of the primary control system during an equilibrium cycle

The reactivity worth of scenarios (a) and (b) for the secondary control system are summarized in Table 7.14 and presented in Figure 7.18. When all the control assemblies are inserted, the secondary control system features acceptable shutdown margin. The total reactivity worth of the secondary control system ranges from 3889 pcm at BOEC to 3251 pcm at EOEC. When the central control assembly is not inserted, the shutdown margin becomes less than 900 pcm at EOEC, and the reactivity worth of the secondary system is only about 1800 pcm. The shutdown margin is calculated as being the reactivity difference between the k_{eff} value of the shutdown reactor and unity (critical reactor). Since those results pertain to hot conditions, the real shutdown margin is even smaller, below the 1% reactivity (1000 pcm) criteria acceptable and the secondary control system needs to be modified by using a different control rod material, using a larger number of control assemblies, or changing the location of the control rods.

Table 7.14: Reactivity Worth of the Secondary Control System when (a) all Assemblies are Inserted and (b) all Assemblies but the Highest Reactive One are Inserted

Time [EFPY]	0	0.76	1.53	2.29	3.06	3.82	4.59
Reference k_{eff}	0.99948	1.00192	1.00663	1.00775	1.00909	1.00978	1.00871
Reactivity worth for (a) in pcm	3889	3552	3664	3454	3355	3393	3251
Reactivity worth for (b) in pcm	1671	1658	1895	1833	1872	1866	1832

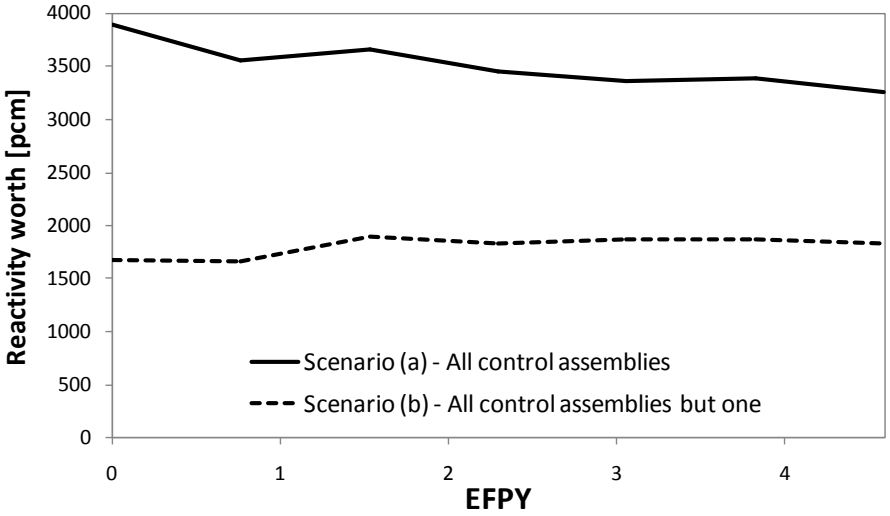

Figure 7.18: Reactivity worth evolution of the secondary control system during an equilibrium cycle

7.5.2 Initial design: HfH_x control rods

Control rods made of HfH_x have been recently studied as a possible alternative to B_4C control rods in fast reactors by Iwasaki & Konashi [58]. They claim that when the H to Hf atom ratio is larger than 1.5, the reactivity worth of the HfH_x control rod is larger than the worth of B_4C control rods enriched with 80 wt% ^{10}B. Another advantage is that several hafnium isotopes have a large neutron capture cross-section – ^{177}Hf, ^{178}Hf and ^{179}Hf – and therefore the absorbing material depletion will take longer to occur. It takes three neutron captures in ^{177}Hf, two in ^{178}Hf and one in ^{179}Hf to produce ^{180}Hf that has a small capture cross-section. The number of excess neutrons to be absorbed by the control assemblies to make k_{eff}=1 in the B&B cores being very small, the control rod depletion is not expected to be significant, both for B_4C or HfH_x control rods. The main reason for studying HfH_x control rods is the potentially larger reactivity worth than with B_4C control rods.

The maximum H to Hf atom ratio is limited by the internal hydrogen pressure. The highest acceptable ratio, 1.8, is assumed for this study with an effective density of 11.1 g/cm^3. The same volume fractions as in Table 7.12 are assumed. For those $HfH_{1.8}$ control assemblies, only the reactivity worth of scenario (b) is studied for both control systems. It is found in Table 7.15 that the primary control system reactivity worth is about 4750 pcm, while it is only 1850 pcm for the secondary control system. Those values are ~2.3% larger than for the 80 at% ^{10}B enriched B_4C control systems and do not provide an acceptable shutdown margin for the secondary control system.

Table 7.15: Reactivity Worth of the Primary and Secondary Control Systems Made of $HfH_{1.8}$ when (b) All Assemblies but the Highest Reactive One are Inserted

Time [EFPY]	0	0.76	1.53	2.29	3.06	3.82	4.59
Reference k_{eff}	0.99948	1.00192	1.00663	1.00775	1.00909	1.00978	1.00871
Primary system [pcm]	4563	4531	4809	4722	4864	4921	4942
Secondary system [pcm]	1740	1683	1844	1886	1979	1851	1927

7.5.3 Improved layout

The locations of the secondary control assemblies are modified in order to increase their reactivity worth. The improved layout is shown in Figure 7.19. The central control assembly has not been relocated, but the three other control assemblies have been moved closer to the core center, where the highest neutron flux is occurring. Despite this location change, the equilibrium core characteristics, in particular k_{eff}, are unchanged. Since the primary control system has not been modified, its performance is unchanged.

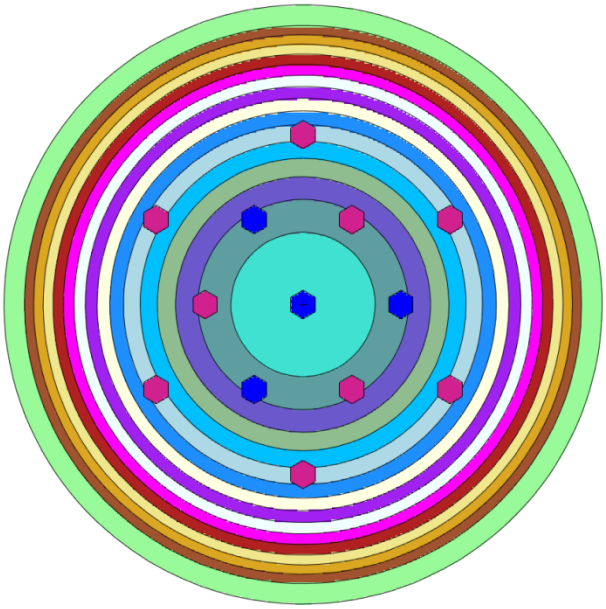

Figure 7.19: Improved secondary control system layout. Primary control system is in purple, secondary control system is in blue.

The control assemblies studied in this section are identical to the B_4C control assemblies studied in Section 7.5.1. The reactivity worth of the secondary control system is found to be approximately 3875 pcm. The reactivity worth values for each step of the equilibrium cycle are given in Table 7.16. The reactivity worth of the secondary system has been more than doubled compared to the initial design and is now performing 85% as well as the primary control system, made of more assemblies. The smallest shutdown margin of the secondary control system is found to be 2930 pcm.

Table 7.16: Reactivity Worth of the Improved Secondary Control System Made of B_4C when (b) All Assemblies but the Highest Reactive One are Inserted

Time [EFPY]	0	0.76	1.53	2.29	3.06	3.82	4.59
Improved secondary control system layout [pcm]	3843	3825	3954	3927	3865	3927	3794
Improved to initial layout worth ratio	2.30	2.31	2.09	2.14	2.06	2.10	2.07
Improved secondary to primary worth ratio	0.85	0.86	0.86	0.84	0.83	0.82	0.79

This primary and secondary control systems analysis has been performed for an equilibrium cycle having an excess reactivity of about 1%. It has been found that the shutdown

margins of both systems are acceptable and are featuring a minimum margin value of approximately 3%. Based on those results, it is expected to be possible controlling the S-PRISM size B&B core with the improved control system, as long as the uncontrolled excess reactivity is not larger than 2%. In this case, the shutdown margin will be about 2%.

7.6 Model improvements

In Section 7.4, the cylindrical model used to represent the S-PRISM size B&B core has been compared to an assembly-level model and proven to yield acceptable results. This comparison validated the model itself, but not the underlying approximations used to simulate the fuel cycle. Approximations that can have a significant effect on the core maximum achievable burnup are:

- All fuel elements are instantly recycled at EOEC. With a discrete recycling, the amount of fission products in the core will be larger and the parasitic neutron absorption might decrease the multiplication factor. The cooling of the fuel elements being reprocessed will enable ^{241}Pu to decay, and also decrease the core k_{eff}.
- The same sodium density, corresponding to 800K, is used for all the axial fuel zones. In the real system, the coolant inlet temperature at the bottom of the core is assumed to be 668 K and to rise progressively to 853 K at the top of the core. The practical sodium density is larger than assumed at the bottom of the core and smaller at the top. This will affect the axial neutron leakage probability.
- Due to the computation capability limitations, the core has been modeled with only three axial zones. Modeling the real core more accurately with a larger number of axial will change the equilibrium core composition and possibly the axial neutron leakage probability and core k_{eff}.

Those three improvements are implemented for the 1200 MW_{th} S-PRISM size B&B core described in Section 7.4 at equilibrium operating with the melt-refining fuel recycling and an average discharge burnup of 40.4% FIMA.

7.6.1 Discrete fuel recycling

The decision whether or not a fuel element is to be recycled should be based on the accumulated DPA in the cladding since the last fuel re-fabrication and should not be recycling at every EOEC. In this section and the followings, the fuel batches are to be recycled when the peak cladding DPA reaches 200, the currently accepted value for HT-9 alloy. Table 7.17provides the peak DPA accumulation in a fuel batch as it is shuffled across the core, where it resides for 15 cycles. It also gives the peak accumulated DPA when no recycling is performed and when the fuel is recycled before reaching 200 DPA. It is assumed that the fuel recycling is occurring while the reactor is operating for one cycle with the fuel not recycled and the fuel recovered from the recycling facility; the cooling time corresponding to the recycling is equal to 4.59 years – one equilibrium cycle.

Table 7.17: DPA Accumulation Without and With Fuel Recycling Before Reaching 200 DPA

Cycle #	Radial location	DPA per cycle	Accumulated DPA	Accumulated DPA (recycling)
1	15	2.3	2.3	2.3
2	14	4.9	7.2	7.2
3	13	6.5	13.6	13.6
4	12	13.7	27.3	27.3
5	11	16.2	43.6	43.6
6	10	26.6	70.2	70.2
7	9	43.7	113.9	113.9 (recycled at EOEC)
8	4	106.5	220.4	106.5 (recycled at EOEC)
9	3	132.5	352.9	132.5 (recycled at EOEC)
10	2	144.6	497.5	144.6 (recycled at EOEC)
11	5	89.5	587.0	89.5
12	6	80.9	667.9	170.4 (recycled at EOEC)
13	7	66.8	734.6	66.8
14	8	49.4	784.1	116.2 (recycled at EOEC)
15	1	143.4	927.4	143.4

When the fuel is discharged at 40.4% FIMA, it has been recycled six times. On average, the fuel elements are recycled when the peak accumulated DPA reaches ~130 and the average accumulated DPA is only 105 due to the axial power peaking factor. At EOEC, the six fuel batches that need recycling – 40% of the core volume – are discharged and sent to the recycling facility. Since the core is at equilibrium, the fuel batches recycled during the previous cycle are substituted to the six batch just discharged. All the fuel batches – nine in the core and six refabricated by the recycling facility – are shuffled according to the shuffling scheme and reloaded in the core. At equilibrium, there is constantly 40% of the core nominal fuel volume being recycled and the total fuel volume required to operate the B&B core with this mode of operation represents 140% of the core volume.

With this partial fuel shuffling and fuel management it is found that at equilibrium the core k_{eff} is approximately 215 pcm smaller than for the scenario where all the fuel batches are instantly recycling. The mass of fission products in the fuel is 8% larger when the partial fuel recycling is used and accounts for ~65% of the difference. The decay of ^{241}Pu during fuel recycling accounts for ~35% of the difference. At BOEC, there are 3.60 tons of fission products in the core for the partial fuel recycling, while there are only 3.33 tons for the full and instantaneous recycling. The evolution of k_{eff} for those two scenarios is compared in Figure 7.19. No notable difference can be observed between the two scenarios concerning the radial power distribution and axially averaged k_∞ distribution.

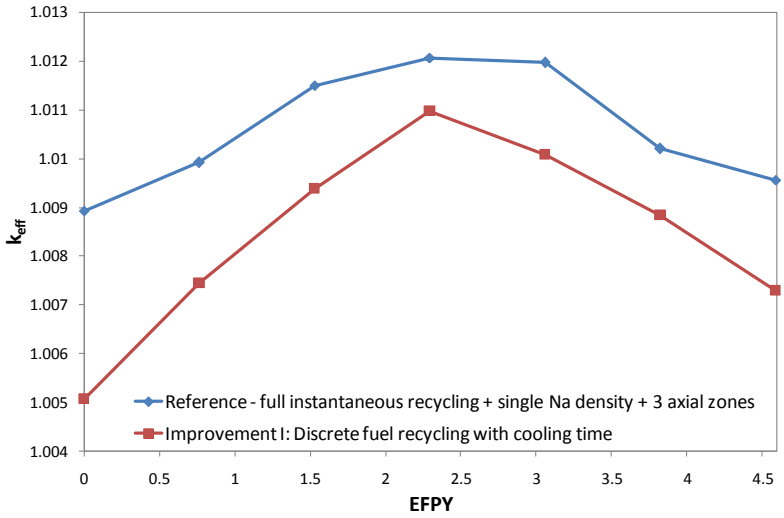

Figure 7.19: k_{eff} evolution comparison for the S-PRISM size B&B core with full instantaneous fuel recycling and discrete fuel recycling (including cooling)

7.6.2 Axial dependence of the sodium density

The model improved in Section 7.6.1 with the discrete fuel recycling is further improved by modifying the sodium temperatures and densities. The sodium temperature in the bottom and radial shield, inlet coolant cavity, grid plate and lower end plug is supposed to be the same as the inlet sodium temperature, 668 K. The outlet coolant temperature is 853 K, and is assumed to be the same as the sodium temperature in the upper plug and upper reflector. To simplify the determination of the coolant axial density, it is assumed that the coolant temperature is linearly rising along the fuel pin. The sodium temperatures and densities used are given in Table 7.18 for the S-PRISM size B&B core prior and after this improvement.

Table 7.18: Sodium Temperatures and Densities Before and After Improvement

	Before improvement		After improvement	
	Temperature [K]	ρ [g/cm^3]	Temperature. [K]	ρ [g/cm^3]
Bottom core components	800	0.8283	668	0.8587
Upper core components	800	0.8283	853	0.8161
Fuel - bottom	800	0.8283	699	0.8516
Fuel - middle	800	0.8283	761	0.8374
Fuel - top	800	0.8283	822	0.8232

The evolution of k_{eff} at equilibrium is shown in Figure 7.20 for the two S-PRISM size B&B core models studied in this section: (a) with partial fuel recycling, single sodium density at 800 K and three axial depletion zones; and (b) with partial fuel recycling, axially dependant sodium density and three axial depletion zones. Most of the values for the two models compared are within one standard deviation of each other. It is found that the axial neutron leakage probability across the top of the core is increased by 1.9% – from 3.80% to 3.87% – due to the lower sodium density, and the axial leakage probability across the bottom of the core is decreased by 1.7% – from 3.79% to 3.72%. The total neutron leakage probability is about equal for the two

models and the core characteristics at equilibrium are not changed when using axially dependant sodium densities.

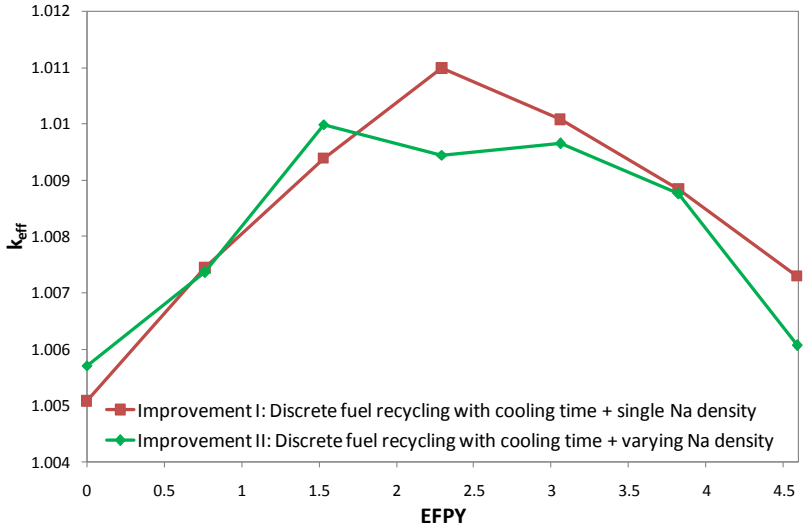

Figure 7.20: k_{eff} evolution comparison for the S-PRISM size B&B core with single sodium density and with axially dependant sodium density

7.6.3 Finer axial meshing

The last improvement made to the S-PRISM size B&B core model is the number of axial zones used. Due to the computation capability available, the number of axial zones has always been limited to three. With a larger number of axial zones, the axial fuel composition variation will be better accounted for. The model (b) studied in the previous section is improved by splitting the three axial depletion zones into nine axial zones of equal length. The sodium temperatures and densities in the fuel are adapted using a linear interpolation of the temperature; the values for each of the nine axial fuel zones are given in Table 7.19. The core model (c) is now composed of 135 depletion zones and it takes approximately one week on 15 processors to obtain the equilibrium characteristics.

Table 7.19: Axial Sodium Temperatures and Densities for the Nine Axial Fuel Zones

Axial zone	Temperature [K]	ρ [g/cm^3]
1 - Bottom	678	0.8563
2	699	0.8516
3	719	0.8469
4	740	0.8421
5	761	0.8374
6	781	0.8327
7	802	0.8279
8	822	0.8232
9 - Top	843	0.8185

The evolution of k_{eff} is shown in Figure 7.21 for the S-PRISM size B&B core models (b) and (c). Again, the k_{eff} values at each step of the equilibrium cycle are within one standard deviation of each other. On average, the k_{eff} values of model (b) are ~50 pcm larger than for model (c). This difference is less significant than the difference due to the partial fuel recycling instead of the full instantaneous fuel recycling difference, but is more important than the difference resulting from the axially dependant sodium density. Due to the significant larger computation time required to determine the equilibrium characteristics with 9 axial zones, it is preferable to perform the simulations with only three axial zones, until a final set of parameters is chosen for the S-PRISM size B&B core, discussed in Section 7.8.

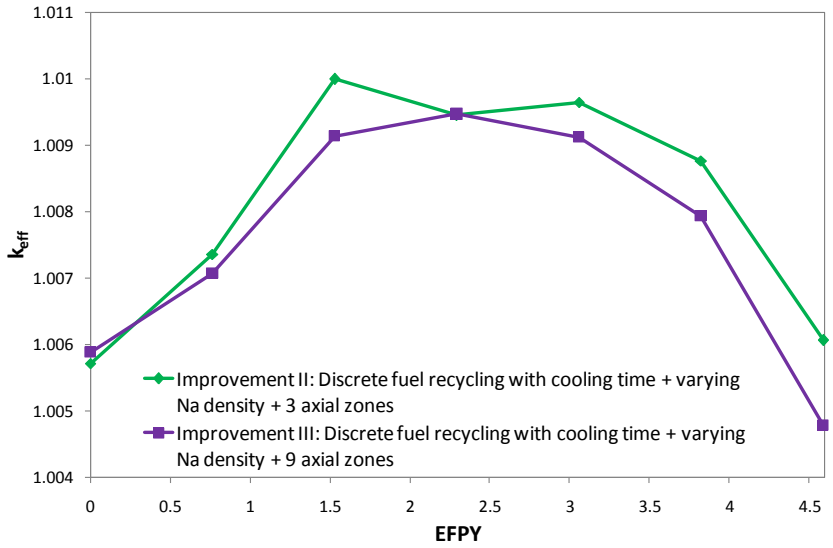

Figure 7.21: k_{eff} evolution comparison for the S-PRISM size B&B core with 3 and 9 axial fuel zones – both with discrete fuel recycling and axially dependant sodium density

7.7 Thermal hydraulic validation

A simple thermal hydraulic analysis of the S-PRISM size B&B core is performed in this section in order to determine the maximum achievable power, based on the radial power peaking factor and the number of fuel pin per assembly, without exceeding the thermal hydraulics constraints described in Section 2.6.1. The radial power peaking factor is assumed to be 2.75 and the axial power distribution used is the one obtained with the simple shuffling scheme for the core studied in Section 7.1.1. The axial power peaking factor is about 1.3 and is occurring in the middle section of the fuel assemblies. The cladding and fuel peak temperatures are reached at the top of the active fuel zone, where the coolant temperature is the highest.

The coolant volume fraction inside an assembly having a P/D ratio of 1.106 is 25.9%. The cladding volume fraction is 22.0% and the remaining 52.1% are occupied by the fuel (75%) and the gap (25%). In order to estimate the maximum practical core power, different numbers of fuel rods per assembly are studied: with fewer fuel rods having a larger diameter, the pressure drop due to friction is decreased, and the coolant velocity across the core can be increased. The results are provided in Table 7.20.

Table 7.20: Thermal Hydraulic Performance of the S-PRISM Size B&B Core for a Radial Power Peaking Factor of 2.75

Parameters	Case 1	Case 2	Case 3
p/d	1.106	1.106	1.106
Fuel rod pitch [mm]	9.06	11.48	13.24
Fuel rod diameter [mm]	8.20	10.38	11.97
Fuel rods per assembly	**271**	**169**	**127**
Clad thickness [mm]	0.661	0.837	0.966
Coolant volume fraction	25.9%	25.9%	25.9%
Cladding volume fraction	21.99%	21.99%	21.99%
Reynolds number	9.64E+04	1.35E+05	1.58E+05
Pressure drop due to friction [MPa]	0.87	0.85	0.77
Core pressure drop [MPa]	1.00	1.00	0.93
Coolant velocity [m/s]	10.39	11.7	12.00
Maximum core power [MW_{th}]	**1751.8**	**1972.7**	**2021.6**
Maximum inner cladding temp. [°C]	**604.5**	**625.0**	**641.7**
Max. fuel temperature [°C]	699.0	833.0	945.6

By decreasing the number of fuel rods per assembly to 127, it is possible to decrease the pressure drop such that the power becomes constrained by the maximum coolant velocity. The maximum practical power is 2000 MW_{th}. Although the maximum cladding and fuel temperature are not exceeded, the cladding temperature is only a few degrees below the maximum acceptable value. With 271 fuel rods per assembly it is found that the maximum practical power is 1750 MW_{th}. This corresponds approximately to the highest core power used for the studies performed in this chapter, 1677 MW_{th}. For the improved shuffling scheme, it has been found in Section 7.4 that the radial power peaking factor is 3.0. The maximum practical powers for cases 1 and 2 become 1600 MW_{th} and 1850 MW_{th}, respectively.

It is concluded that it is feasible to establish a breed and burn mode of operation in a core that could fit within the S-PRISM pressure vessel and operate this core at, at least, the nominal S-PRISM power level of 1000 MW_{th}.

7.8 Final design performance

The various modeling and simulation improvements made in this chapter to analyze the S-PRISM size B&B core are refined in this section in order to better represent the real core behavior. The dimensions of the core, fuel assemblies and fuel rods, and the number of fuel, control and GEMs assemblies are not modified. However, the volume fractions, temperature, material densities and shuffling assumptions are modified according to the various results obtained in Sections 7.3 and 7.6. The core model used and the associated fuel cycle assumptions are fully described in Section 7.8.1. The results pertaining to this final design study are discussed in Section 7.8.2.

7.8.1 Core and fuel cycle description

The general core layout is shown in Figure 7.22 and the dimensions, volume fractions and temperatures are given in Table 7.21. The active fuel zone is modeled with 15 radial zones and 9 axial zones of equal volume. In reality, the core is made of 450 fuel assemblies, 13 control assemblies and 6 GEM assemblies. All the assemblies have the same pitch, duct thickness and inter-duct gap: 161.42 mm, 3.94 mm and 4.32 mm, respectively. The fuel assemblies are made of 271 fuel rods, having an outer diameter of 8.196 mm and a cladding thickness of 0.559 mm, wrapped with a 1.422 mm in diameter wire. The P/D ratio of the fuel rods inside the assembly is equal to 1.106. The active fuel height is 142.24 cm and the equivalent radius is 183.54 cm. In order to accommodate the fission gas released from the fuel during irradiation, the plenum height is taken to be the same as the active fuel height. The upper reflector and lower and upper plug volume fractions used for the previous models have been modified in order to be consistent with the fuel rod geometry: the plugs and reflector are the prolongation of the fuel rod and are made of HT-9. The volume fractions assumed for these zones are 28% Na and 72% HT-9.

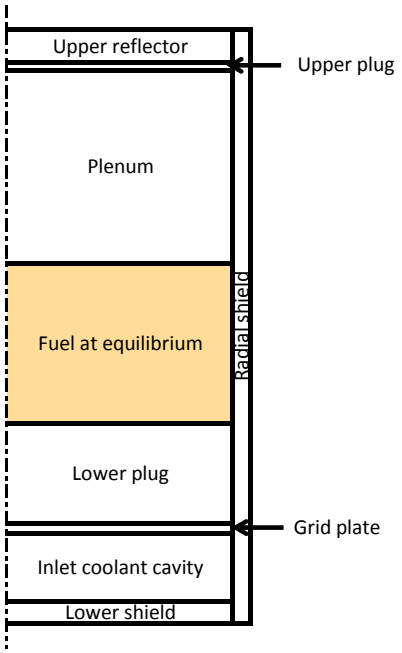

Figure 7.22: Layout of the final S-PRISM size B&B core design

The temperature gradient and sodium density along the fuel rods have been provided in Table 7.19 for the nine axial zones. The cladding material (HT-9) density is estimated at the average cladding temperature, 683 K, obtained from the thermal hydraulics study discussed in Section 7.7. The fuel is the ternary metallic fuel U-TRU-Zr with 6 wt% zirconium. Using the phase diagram of U-Zr, and following the methodology described in Section 2.4, the nominal fuel density is found to be 17.04 g/cm^3, and the smear density is taken to be 0.75. It has been found in Section 7.7 that with a core power of 1600 MW_{th}, it is possible to accommodate a radial power peaking factor as high as 3 so that 1600 MW_{th} is used for the final core design. The initial mass of heavy metal in the core is 81.98 tons and the specific power density is 19.52 W/g of HM.

Table 7.21: Dimensions, Volume Fractions and Material of the Final S-PRISM Size B&B Core Design

Region	Height (cm)	Thickness (cm)	Material (Volume %)	T [K]
Upper reflector	30.48	183.54	28% Na - 72% HT9	853
Upper end plug	2.54	183.54	28% Na - 72% HT9	853
Plenum	142.24	183.54	50% Na - 26.55% HT9	853
Fuel at equilibrium	142.24	183.54	34% Fuel - 26.55% HT9 - 28.12% Na	668 to 853
Lower end plug	90.42	183.54	28% Na - 72% HT9	668
Grid plate	5.18	183.54	50% Na - 50% HT9	668
Coolant inlet	60	183.54	78% Na - 22% HT9	668
Lower shield	20	183.54	43.1% B_4C - 29.7% HT9 - 27.2% Na	668
Radial shield	522.69	13.59	43.1% B_4C - 29.7% HT9 - 27.2% Na	668

The equilibrium core characteristics are determined using the equilibrium module described in Section 2.5.4 and the shuffling scheme described in Table 7.7. The maximum achievable cladding DPA is taken to be 400 DPA, twice the proven value for HT-9. It is assumed that in the near future ferritic martensitic steels, oxide dispersion strengthened (ODS) alloy or a different clad material will be able to sustain this value. Based on the results previously obtained in Section 7.4 for the selected shuffling scheme, it is estimated that only the third and seventh innermost fuel batches will need to be recycled at EOEC. The fuel is recycled using the melt-refining process described in Section 1.2.2 and is cooled for the same length as an equilibrium cycle. For this final design study, it is assumed that 1% of the actinides are lost during the fuel recycling process. Since the fuel is recycled twice, the heavy metal loss of the fuel will be slightly smaller than 2% of the initial amount of heavy metal. During the regular operation of the reactor, it is assumed that 75% of the gaseous fission products are diffusing trough the fuel and are released into the fission gas plenum. This assumption has been discussed in Section 2.3.

7.8.2 Core characteristics at equilibrium

It is found possible to achieve a sustainable breed and burn mode of operation for the final S-PRISM size B&B core design, with an average discharge burnup of 43.4% FIMA – 424.5 GWd/tHM. The uranium utilization factor for the breed and burn mode of operation being equal to the fuel burnup, it is more than 70 times larger than for a once-trough LWR operating at 50 GWd/tHM with 4.5% enriched uranium – 0.6% – and more than 16 times larger than for the S-PRISM size conventional core operating with a radial blanket and with an infinite-batch fuel management scheme – 2.77% – analyzed in Section 4.3.The above mentioned burnup accounts for the mass of heavy metal lost during the fuel recycling operations – with a burnup lower than the discharge burnup:

- 0.85% of the initial HM mass is lost during the first recycling with an average burnup of 15.2% FIMA;

- 0.65% of the initial HM mass is lost during the second recycling with an average burnup of 34.6 % FIMA;
- The rest of the fuel is discharged from the reactor with an average burnup of 43.7% FIMA.

With the 15 fuel batches management scheme, an equilibrium cycle lasts 3.97 years. The evolution of k_{eff} during a cycle is shown in Figure 7.23. At BOEC k_{eff} is almost constant because the plutonium build-up in the second, third and fourth fuel batches – having a burnup below 20% FIMA – is balanced by the consumption of plutonium in the innermost fuel batch, having the highest burnup. As the burnup increases in the second fuel batch, its k_∞, which was initially increasing, starts decreasing, making the core k_{eff} decreasing. The radial distribution of the axially averaged k_∞ and burnup in each of the 15 fuel batches is shown in Figure 7.24 at BOEC and EOEC. The k_{eff} decrease is also induced by the increasing neutron leakage probability discussed below along with the power distribution evolution. The radial power distribution and the net leakage probability for each fuel batch are provided at BOEC and EOEC in Figures 7.25 and 7.26, respectively

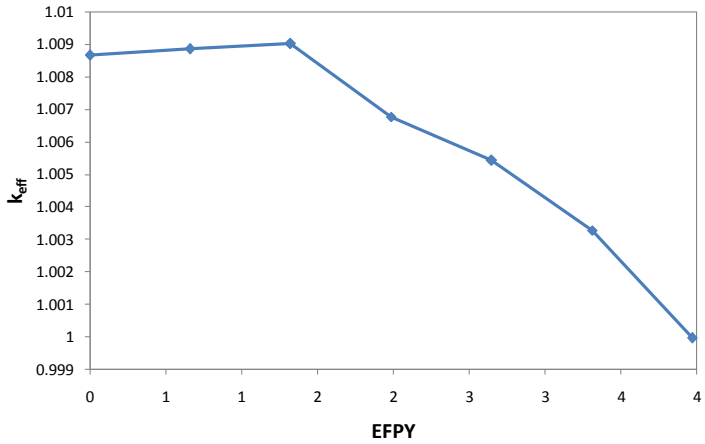

Figure 7.23: Evolution of k_{eff} during the equilibrium cycle for the final S-PRISM size B&B core design with an average discharge burnup of 43.4% FIMA

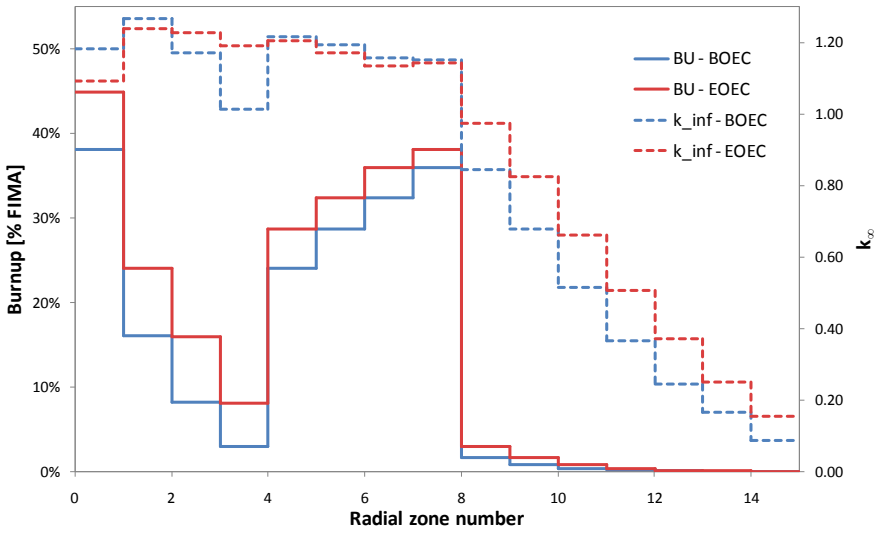

Figure 7.24: Burnup and k_∞ radial distribution at BOEC and EOEC for the final S-PRISM size B&B core design

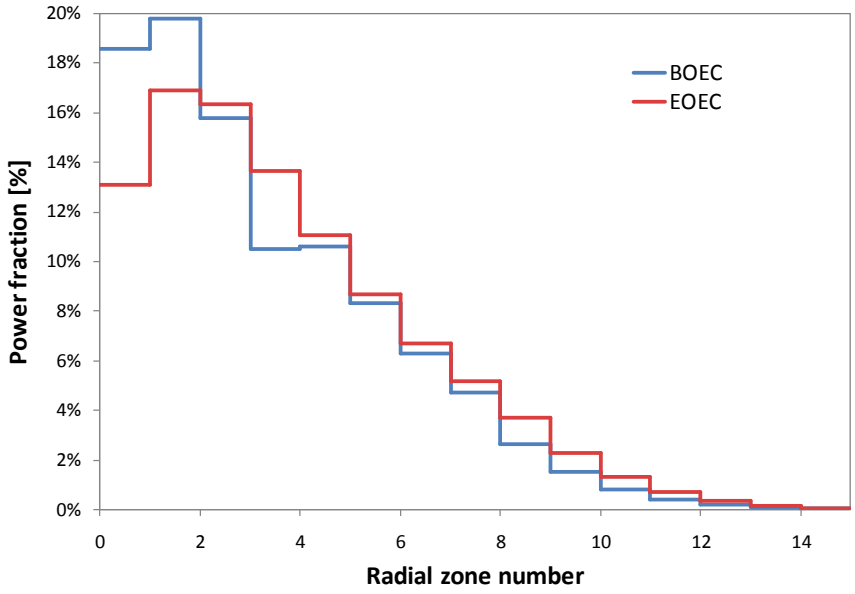

Figure 7.25: Radial power distribution at BOEC and EOEC for the final S-PRISM size B&B core design

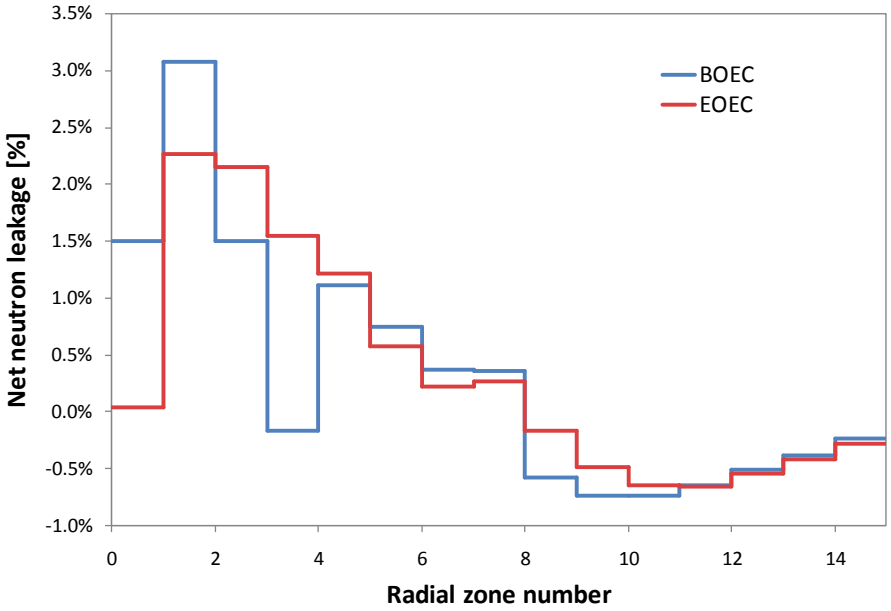

Figure 7.26: Net neutron leakage probability at BOEC and EOEC for the final S-PRISM size B&B core design

From BOEC to EOEC, the k_∞ of the innermost fuel batch is decreasing and its power fraction is strongly decreasing. When the second innermost batch burnup reaches ~20% FIMA, its k_∞ also starts decreasing making its power fraction drop. The fourth fuel batch sees its k_∞ increasing from 1.0 at BOEC to almost 1.2 at EOEC and therefore its power fraction is increasing by +3.5%. At BOEC, the fourth fuel batch generates a smaller power fraction than the fifth fuel batch despite the larger neutron flux, because it has a significantly lower k_∞. The radial power peaking factor reaches 2.97 at BOEC in the second fuel batch. The peak power density is 417.7 W/cm^3, also achieved at BOEC.

Due to the power distribution outward shift, the axial/radial neutron leakage probabilities are increasing from 6.94%/1.11% at BOEC to 7.10%/1.48% at EOEC. The burnup reactivity swing being only 0.9%, the increasing leakage probability represents more than 58% of it. Table 7.22 summarizes the important characteristics of the final S-PRISM size B&B core at BOEC and EOEC. The conversion ratio provided in this table is the ratio between the number of transuranium atoms in the entire core, at the end and beginning of an equilibrium cycle.

The peak DPA accumulated during a cycle and the cumulative peak DPA accumulated since last fuel reconditioning is provided in Table 7.23 for each fuel batch. At EOEC the third and seventh fuel batches are discharged from the reactor to be recycled. When the third batch is recycled, its average burnup is 15.15% FIMA and the peak DPA accumulated in the cladding is 366. When the seventh batch is recycled, its average burnup is 34.6% FIMA, and the peak DPA accumulated is 404. If it appears that 404 DPA is not acceptable, it will be necessary to recycle the sixth fuel batch instead of the seventh having a peak DPA of 342 at EOEC. This different batch recycling will not affect the equilibrium core characteristics since those two batches are located near each other. The peak accumulated DPA of the discharged fuel at 43.7% FIMA is 207 when the seventh batch is recycled, and would be 269 if the sixth batch was to be recycled instead.

Table 7.22: Summary of Some Characteristics for the Final S-PRISM Size B&B Core Design at Equilibrium

Characteristic	Value
Average discharge burnup [% FIMA]	43.40%
Cycle length [years]	3.97
Average power density [W/cm^3]	106.3
Peak power density [W/cm^3]	417.7
Radial power peaking factor	2.97
Burnup reactivity swing [%Δk]	0.90%
Conversion Ratio	1.105
Axial leakage probability at BOEC/EOEC [%]	6.94%/7.10%
Radial leakage probability at BOEC/EOEC [%]	1.11%/1.48%
Average core BU at BOEC/EOEC [% FIMA]	12.5%/15.6%
^{239}Pu at BOEC/EOEC [tons]	3.815/4.141
^{240}Pu at BOEC/EOEC [tons]	0.797/0.933
^{241}Pu at BOEC/EOEC [tons]	0.074/0.090
TRU at BOEC/EOEC [tons]	4.76/5.26
HM at BOEC/EOEC [tons]	71.66/69.30
FP at BOEC/EOEC [tons]	5.42/7.58

Table 7.23: Peak DPA Accumulation in Each Fuel Batch

Cycle #	Fuel batch #	Peak DPA/cycle	Accumulated peak DPA
1	15	2.16	2.16
2	14	3.94	6.10
3	13	6.52	12.62
4	12	10.34	22.96
5	11	16.13	39.08
6	10	24.37	63.46
7	9	35.24	98.69
8	4	121.48	220.18
9	3 (recycled at EOEC)	145.89	366.07
10	2	163.01	163.01
11	5	99.32	262.33
12	6	79.49	341.82
13	7 (recycled at EOEC)	62.25	404.06
14	8	48.35	48.35
15	1	158.63	206.98

Based on to the preliminary results presented in Section 2.4 regarding the fuel swelling with burnup, no make-up fuel has been added during fuel recycling. It was expected that the fuel swelling due to soluble and non-soluble fission products would be almost balanced by the fuel shrinkage due to consumption of the HM atoms. By using the fuel swelling methodology discussed in Section 2.4 for the fuel batches recycled at equilibrium, it is found that the fraction

volume increase per percent burnup for the third and seventh fuel batches is -0.0029% and -0.0275%, respectively. Multiplying those values with the average burnup of the batches, it is found that the volume of the third batch is decreased by less than 0.05% after recycling, while it is decreased by about 1% for the seventh fuel batch. For such small volume changes, it is acceptable to use a simplified melt-refining process where no make-up fuel is added. However, if the actinides losses due to fuel recycling are larger than the 1% assumed, make-up fuel should be added to the melt.

7.9 Conclusions

It was found feasible to establish a breed and burn mode of operation in a core that can fit within the S-PRISM reactor vessel; this core can deliver at least the 1000 MW_{th} called for the S-PRISM design. The maximum achievable burnup with the breed and burn mode of operation for the S-PRISM size B&B core has been found to be 45% FIMA for the improved shuffling scheme, with the same assumptions as in Chapters 4 and 6. This maximum burnup is ~21% smaller than the burnup achievable for the large B&B core, discussed in Chapter 6, due to the increased neutron leakage probability and slightly lower heavy metal density. This is however approximately equal to the achievable burnup in a conventional S-PRISM size fast reactor – 45.2% FIMA, without blanket and operating with an infinite-batch fuel management, studied in Section 4.3. It has also been found that the core excess reactivity can easily be controlled by the control assemblies systems and they are providing comfortable shutdown margin as long as the uncontrolled excess reactivity does not become larger than ~2000 pcm.

Throughout this chapter, it has also been found that the maximum achievable burnup of the core has little sensitivity to the number of axial depletions zones, to the axially dependant sodium density or to the power density used, as long as those parameters remain in a reasonable range. The achievable burnup is however very sensitive to the heavy metal density of the core and somewhat sensitive to the fuel recycling process used. Using a partial fuel recycling rather than an instantaneous total fuel recycling had a small effect, which will be mostly dominated by the heavy metal losses associated to the recycling process used.

When using an improved set of modeling and simulation assumptions for the S-PRISM size B&B core – in particular accounting for the partial fuel recycling and recycling losses, the maximum achievable burnup, equal to the uranium utilization factor, has been found to be 43.4% FIMA. The uranium utilization factor is more than 70 times larger than for a traditional LWR operating at 50 GWd/tHM with 4.5% enriched uranium – 0.6% – and 16 times larger than for the S-PRISM size conventional core operating with a radial blanket and with an infinite-batch fuel management scheme – 2.77%. Although no waste analysis has been performed, it is expected that the fuel discharged from the S-PRISM size B&B core will feature slightly impaired characteristics as compared to the fuel discharged at 55% FIMA from the large B&B core and analyzed in Section 6.2.2.

The deployment of the S-PRISM size B&B cores is constrained by the same yet unresolved issues as the large B&B core. Those are (a) the cladding maximum sustainable DPA, (b) the feasibility of the fuel reconditioning process, (c) the feasibility of refabricating fuel with very high burnup and (d) the feasibility of cooling the core when the power distribution is radially shifting.

Chapter 8

Breed and Burn Feasibility for Alternative Core Designs

The performance of the breed and burn mode of operation has been extensively studied in the two previous chapters for cores cooled with sodium and using uranium based metallic fuel. The objective of the work presented in this section is to assess the feasibility of achieving a breed and burn mode of operation for alternative core design concepts.

The alternative designs explored in this section are:

- Uranium based metallic fuel with lead based – LBE and PbLi – coolants and HT-9 cladding;
- Thorium based metallic fuel with sodium coolant and HT-9 cladding;
- Thorium based metallic fuel with sodium coolant and SiC cladding;
- Thorium based metallic fuel with helium coolant and SiC cladding;
- Uranium based nitride fuel with sodium coolant and HT-9 cladding.

The analysis is performed using the 0-D neutron balance approach described in Section 5.1. In Sections 6.4.1 and 7.2 it has been found that the neutron balance performed with a 0-D unit cell is yielding consistent results for a simple shuffling scheme, although for complex shuffling schemes the accuracy of this method is not as reliable. However, embarking upon a thorough space-dependent study of all those designs would require a significant amount of time, while using the neutron balance method with a 0-D unit cell provides a good first assessment of the system performance with a limited amount of time and lowered difficulty.

8.1 Core cooled with lead based alloys: LBE and PbLi

Lead based alloys are the main coolant alternative to sodium, the coolant usually used in fast reactors. Since lead based alloys do not chemically react with air and water, there is no need to use a secondary coolant loop to isolate the primary coolant from the steam generator, significantly decreasing the cost of the reactor cooling system. In addition, the neutron leakage probability with lead based coolant, for the same core dimensions, is smaller than with sodium

because of the larger macroscopic scattering cross-section. However, lead is more corrosive and erosive than sodium and can provoke early failure of the fuel rods, when lead chemistry is not adequately controlled.

8.1.1 Thermal hydraulic / neutronics trade-off study

Thermal hydraulics performance of lead-bismuth eutectic (LBE) and lead-lithium are studied in this section. The maximum velocity of lead based alloys is limited by the erosion rate of the protective oxide layer formed on the cladding. Oxidation of iron and/or other additives to the clad, such as Si or Al, forms a protective layer on the cladding, the stability of which can be controlled by oxygen pressure. Erosion of this layer will reduce the cladding thickness and may, eventually, cause it to fail. The commonly accepted velocity limit for lead base coolants is 2 to 3 m/s [46], but improved alloys, such as is currently under development by Prof. Ballinger et al. at MIT may enable increasing the velocity to up to 6 m/s [47]. In order to determine the maximum achievable heat removal capacity and achievable power, the maximum velocity is taken to be 6 m/s and the maximum pressure drop 1 MPa. The thermo-physical properties of LBE and PbLi are provided in Appendix C and the main properties of LBE, PbLi and sodium are compared in Table 8.1 at 800 K.

Table 8.1: Comparison of the Main Thermo-physical Properties of Na, LBE and PbLi at 800 K

Coolant	Na	LBE	PbLi
Density [g/cm^3]	0.828	10.013	9.569
Specific heat [J/kg.K]	1.26E+03	146.5	187.7
Dynamic viscosity [N.s/m^2]	2.27E-04	1.30E-03	1.10E-03
Thermal conductivity [W/m.K]	62.9	14.9	17.6
Thermal expansion coefficient [K^{-1}]	2.82E-04	1.38E-04	1.24E-04

The thermal hydraulic analysis is performed for LBE and PbLi at different P/D ratio and different number of fuel rods per assembly in the large B&B core described in Section 2.1.2 and studied in Chapter 6. The radial power peaking factor is assumed to be 1.7. The assembly dimensions are taken to be the same as used for the large B&B core thermal hydraulic analysis performed in Section 6.6. The results are provided along with the volume fractions inside an assembly in Table 8.2 for LBE and in Table 8.3 for PbLi. For all the configurations analyzed the core power is limited by the maximum coolant pressure drop. The coolant velocity ranges from 2.3 m/s to almost 4.5 m/s, depending on the number of fuel rods per assembly.

Due to the large pressure drop, the attainable power is 2.6 times smaller with LBE and 2.1 times smaller with PbLi than with sodium for a same P/D ratio. In order to achieve the same core power level with lead based coolant as with sodium coolant, it is necessary to increase the P/D ratio of the LBE and PbLi systems. When the P/D ratio is changed, the core dimensions – height and radius – are not changed, but the fuel rod dimensions are changed. By increasing the P/D ratio to 1.30 for the LBE coolant and to 1.24 for the PbLi coolant and decreasing the number of fuel rods per assembly to 91, it is possible to increase the maximum core power up to 3600 MW_{th} for both lead based alloys. With the increased P/D ratios, the HM loading is decreased by 45% for the LBE cooled core and by 39.5% for the PbLi cooled core, compared to the sodium cooled core. For the PbLi cooled core, when using 91 fuel rods per assembly, the maximum acceptable temperature in the cladding is exceeded by 3 degrees. For a same P/D ratio, it is observed that

PbLi enables removing 26% more heat from the core then LBE, enabling increasing the core power by the same fraction. This is due to the higher specific heat and lower dynamic viscosity of PbLi.

Table 8.2: Thermal Hydraulic Performance of the LBE Cooled Large B&B Core with a Radial Power Peaking Factor of 1.7

Parameters	Case 1	Case 2	Case 3	Case 4	Case 5	Case 6
p/d ratio	**1.1**	**1.2**	**1.3**	1.3	1.3	1.3
Fuel rod pitch [mm]	9.06	9.06	9.06	11.48	13.24	15.64
Fuel rod diameter [mm]	8.24	7.55	6.97	8.83	10.19	12.03
Fuel rods per assembly	271	271	271	**169**	**127**	**91**
Clad thickness [mm]	0.667	0.611	0.564	0.715	0.824	0.974
Coolant volume fraction	25.0%	37.0%	46.3%	46.3%	46.3%	46.3%
Cladding volume fraction	22.3%	18.7%	16.0%	16.0%	16.0%	16.0%
Fuel volume fraction	39.5%	33.2%	28.3%	28.3%	28.3%	28.3%
LBE velocity [m/s]	2.33	3.05	3.76	4.07	4.25	4.44
Maximum power [MW_{th}]	**1029**	**1991**	**3072**	**3325**	**3472**	**3627**
Max. inner cladding temp. [°C]	**584**	**589**	**594**	**605**	**615**	**631**
Max. fuel temperature [°C]	608	634	664	758	847	991

Table 8.3: Thermal Hydraulic Performance of the PbLi Cooled Large B&B Core with a Radial Power Peaking Factor of 1.7

Parameters	Case 1	Case 2	Case 3	Case 4	Case 5	Case 6
p/d ratio	**1.1**	**1.24**	**1.3**	1.24	1.24	1.24
Fuel rod pitch [mm]	9.06	9.06	9.06	11.48	13.24	15.64
Fuel rod diameter [mm]	8.24	7.31	6.97	9.26	10.68	12.61
Fuel rods per assembly	271	271	271	**169**	**127**	**91**
Clad thickness [mm]	0.667	0.592	0.564	0.749	0.864	1.021
Coolant volume fraction	25.0%	41.0%	46.3%	41.0%	41.0%	41.0%
Cladding volume fraction	22.3%	17.6%	16.0%	17.6%	17.6%	17.6%
Fuel volume fraction	39.5%	31.1%	28.3%	31.1%	31.1%	31.1%
PbLi velocity [m/s]	2.4	3.43	3.88	3.77	3.96	4.18
Maximum power [MW_{th}]	**1298**	**3038**	**3882**	**3339**	**3507**	**3702**
Max. inner cladding temp. [°C]	**591**	**603**	**609**	**618**	**632**	**653**
Max. fuel temperature [°C]	614	657	683	739	820	954

When increasing the P/D ratio, the parasitic neutron capture in the coolant and the neutron leakage probability are enhanced, worsening the neutron economy of the core. In order to determine the P/D ratio yielding the same neutron leakage probability in a LBE cooled core than a sodium cooled core having P/D=1.11, the large B&B core leakage is analyzed.

In Section 6.3.1, it had been found that for the simple shuffling scheme, the minimum discharged burnup required to sustain the breed and burn mode of operation for this sodium cooled large B&B core is 20.4% FIMA. The k_{eff} values and neutron leakage probabilities are given in Table 8.4. The k_{eff} values and neutron leakage probabilities are re-estimated when

substituting LBE to sodium, using the volume fractions and fuel composition of the sodium cooled core. The leakage probabilities and k_{eff} values for the modified core are shown in Table 8.5. It is found that, for the same P/D ratio, the leakage probability is almost 25% smaller (-1.1%) with LBE than with sodium. In addition, the k_{eff} values with LBE are 2.8% larger than with sodium; this is because the LBE spectrum is harder and yields a larger reproduction factor. The equilibrium fuel composition used for estimating the LBE cooled core performance is that obtained with sodium coolant; in reality the amount of fissile material at equilibrium will be smaller in the LBE cooled core than in the sodium cooled core.

Table 8.4: k_{eff} and Leakage Probabilities for the Large Sodium Cooled B&B Core at Equilibrium with P/D =1.11 – 20.4% FIMA

Time [EFPY]	0.00	0.51	1.03	1.54	2.05
k_{eff}	0.99934	1.01286	1.02538	1.03369	1.04217
Axial leakage	3.82%	3.74%	3.76%	3.71%	3.61%
Radial leakage	0.65%	0.66%	0.67%	0.69%	0.69%
Total leakage	4.47%	4.40%	4.43%	4.40%	4.30%

Table 8.5: k_{eff} and Leakage Probability for the Large LBE Cooled B&B Core at Equilibrium with P/D=1.11 – 20.4% FIMA – where the Sodium has been Replaced with LBE

Time [EFPY]	0.00	0.51	1.03	1.54	2.05
k_{eff}	1.0288	1.04127	1.05336	1.06238	1.07218
Axial leakage	2.92%	2.89%	2.84%	2.82%	2.82%
Radial leakage	0.46%	0.47%	0.47%	0.50%	0.49%
Total leakage	3.38%	3.35%	3.31%	3.32%	3.31%

The P/D ratio of the large B&B core at equilibrium in which sodium has been replaced by LBE is progressively increased until its average neutron leakage probability becomes equal to the neutron leakage probability of the sodium cooled core with P/D=1.11. It is found that with P/D=1.3 the total neutron leakage probability is 4.66%; similar to the leakage probability of the sodium cooled core with P/D=1.11. The resulting k_{eff} values of the LBE cooled core with P/D=1.3 are given in Table 8.6. It is observed that k_{eff} is significantly smaller than in Table 8.4, while the leakage probability is about the same. This indicates that the minimum discharge burnup required to sustain the breed and burn mode in the LBE cooled large B&B core having P/D=1.3 is larger than 20.4% FIMA.

Table 8.6: k_{eff} and Leakage Probability for the Large LBE Cooled B&B Core at Equilibrium with P/D=1.3 – 20.4% FIMA – where the Sodium has been Replaced with LBE

Time [EFPY]	0.00	0.51	1.03	1.54	2.05
k_{eff}	0.95496	0.96854	0.97992	0.99066	1.00107
Axial leakage	3.90%	3.83%	3.73%	3.82%	3.73%
Radial leakage	0.82%	0.85%	0.89%	0.87%	0.88%
Total leakage	4.72%	4.68%	4.62%	4.69%	4.61%

8.1.2 Minimum required burnup

In the previous section it has been found that when using 271 fuel rods per assembly with P/D=1.3, it is possible to operate the LBE cooled large B&B core at 3000 MW_{th} with an average neutron leakage probability approximately equal to the sodium cooled large B&B core – P/D=1.11 – leakage probability. It has also been found possible to achieve 3000 MW_{th} with the PbLi cooled large B&B core for a P/D ratio of 1.24 – and 271 fuel rods per assembly. The leakage probability has not been calculated for this core and in this section it is assumed to be 4.66%, the same as for the LBE cooled core. The PbLi coolant is made of lithium enriched to 99 wt% in ^{7}Li because ^{7}Li has significantly lower capture cross-section than ^{6}Li.

The minimum required burnup is determined for those two cores – LBE and PbLi cooled – by performing the depletion analysis and neutron balance in a 0-D unit cell and using the above mentioned neutron leakage probability, 4.66%. The burnup reactivity swing is assumed to be 4.4%: an average of 2.2% of the neutrons is lost in the control systems. The methodology has already been discussed in Section 5.1.2 and applied in Sections 6.4 and 7.2. The average power density used for the depletion is 112.5 W/cm^3 and the volume fractions used are given in Table 8.7. The fuel characteristics are the same as presented for the large B&B core in Section 2.1.2. During operation, 75% of the fission gases are removed from the fuel and approximately every 10 years the fuel is instantaneously recycled with the melt-refining without recycling loss. The evolution of k_∞ with burnup is shown in Figure 8.1 and the corresponding neutron balance is shown for the LBE and PbLi cooled large B&B cores in Figure 8.2.

Table 8.7: Unit Cell Fuel Volume Fraction – Inter-Duct Gap and Duct Wall are not Accounted for

P/D	1.24	1.30
Fuel (U-Zr10)	31.1%	28.0%
Gap (empty)	10.4%	9.3%
Structural material (HT9)	17.6%	16.4%
Coolant (PbLi/LBE)	41.0%	46.3%

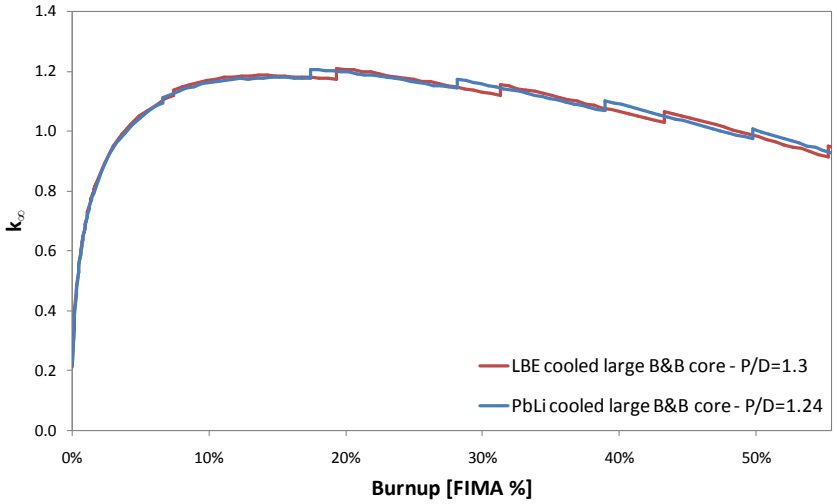

Figure 8.1: k_∞ evolution for the LBE cooled core with P/D=1.30 and the PbLi cooled core with P/D=1.24 – 0-D unit cell

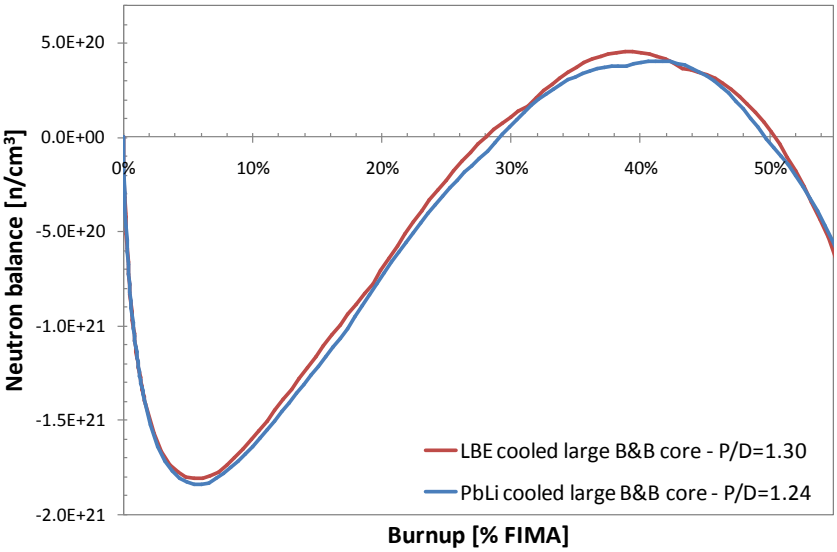

Figure 8.2: Neutron balance for the LBE cooled core with P/D=1.30 and the PbLi cooled core with P/D=1.24

The k_{eff} evolutions for the LBE and PbLi cooled cores are very similar apart for the burnup at which the fuel recycling is occurring. The fuel recycling is occurring every ~10 years in both cores, but the mass of HM being smaller in the LBE cooled core because of the larger P/D ratio, the burnup accumulates faster and fewer fuel recycling are occurring than for the PbLi cooled core. It is observed that despite this difference, the neutron balance, per unit of fuel volume, is almost identical for the two cores. This suggests that the neutronics behavior of the LBE cooled core having a P/D ratio of 1.3 and of the PbLi cooled core having a P/D ratio of 1.24 is similar. For both cores, the minimum burnup required to sustain the breed and burn mode of operation is around 29% FIMA. At this burnup, there are 335.5 kg of ^{239}Pu per cubic meter in the PbLi cooled core, while there are only 299.0 kg of ^{239}Pu per cubic meter in the LBE cooled core. The ^{239}Pu to HM fraction is 10.8 wt% for both cores. The spectrum being slightly harder in the LBE cooled core than in the PbLi cooled core, a smaller mass of fissile plutonium is required to achieve a similar k_{eff}.

8.1.3 Comparison with sodium-cooled B&B core

The results obtained in the previous section for the LBE cooled core with P/D=1.3 are compared with the results obtained for the sodium cooled core with P/D=1.11 in Section 6.4.1. For the sodium cooled system, the neutron leakage has been found to be 4.40% and the fraction of neutrons absorbed in the control elements is assumed to be 2.2%. With this set of assumptions, it has previously been found that the minimum required burnup to sustain the breed and burn mode in the sodium cooled large B&B core is 20.4% FIMA.

Since the P/D ratio of the LBE cooled core has been increased to 1.3 and the macroscopic absorption cross-section of LBE is larger than for sodium, the parasitic neutron capture in the LBE is larger. The evolution of k_∞ for the two cores is shown in Figure 8.3. On average k_∞ is approximately 2% larger for the sodium cooled core than for the LBE cooled core, significantly affecting the neutron balance, shown in Figure 8.4. The neutron balance has been performed

assuming the same fraction of neutrons – 2.2%, absorbed in the control system and a neutron leakage probability of 4.40% for the sodium cooled core and 4.66% for the LBE cooled core. The minimum required burnup for the LBE cooled core with P/D=1.30 had been found to be approximately 28% FIMA in the previous section. Compared to the sodium cooled core, it is observed that the number of neutrons that need to be absorbed in the depleted uranium to make its k_∞ larger than unity is larger for the LBE cooled core than for the sodium cooled core and the amount of excess neutrons left in the fuel of the LBE cooled core after sustaining the breed and burn mode is not sufficient to spawn an additional core. If the fraction of neutrons lost by leakage and in the control systems can be decrease below 4%, then it will be possible to spawn one additional core from the LBE cooled core.

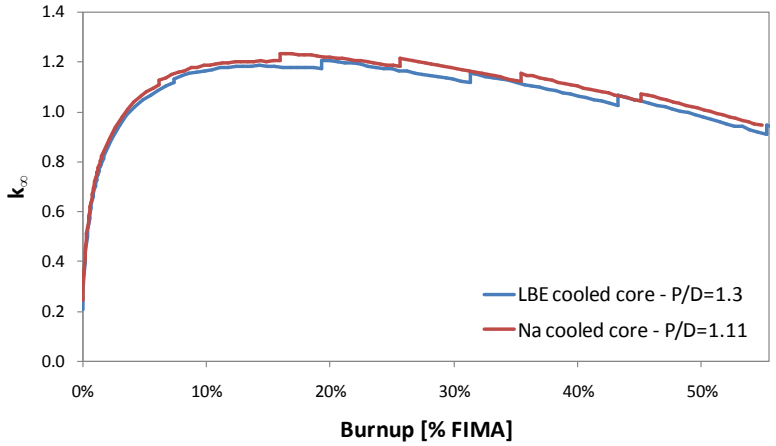

Figure 8.3: k_∞ evolution for the LBE cooled core with P/D=1.3 and Na cooled core with P/D=1.11

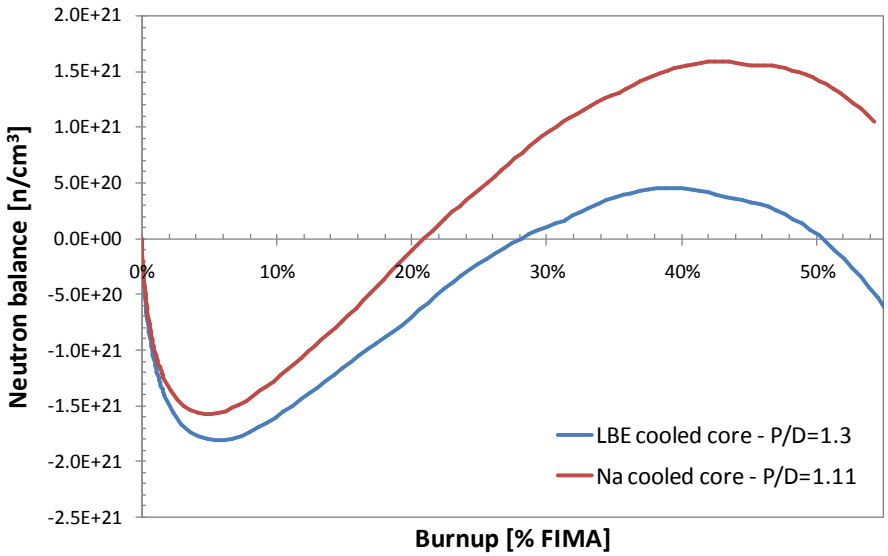

Figure 8.4: Neutron balance for the LBE cooled core with P/D=1.30 and for the sodium cooled core with P/D=1.11

In summary, in order to achieve an acceptable thermal hydraulic performance in the lead alloy cooled core, the P/D ratio needs to be larger than for sodium cooled core, impairing the neutron economy. It is however possible to sustain the breed and burn mode of operation with a discharged burnup anywhere between ~28% FIMA and ~50% FIMA. In addition to the absence of a secondary coolant loop, the LBE cooled core requires a significantly smaller mass of fissile material to make the core critical. The evolution of the plutonium mass for the two cores studied is compared in Figure 8.5. When the unit cell becomes critical (k_∞=1.0) the burnups in the sodium cooled and the LBE cooled cores are 3.46% FIMA and 3.83% FIMA, respectively, and the mass of fissile plutonium is 323 g/cm^3 and 238 g/cm^3, respectively. Relative to the total HM mass, this fissile plutonium weight fraction is about 6.25% for both cores. The initial mass of heavy metal and enriched uranium – or TRU recovered from the LWR UNF – required to initially make the reactor critical is ~26% smaller for the LBE cooled core than for the sodium cooled core.

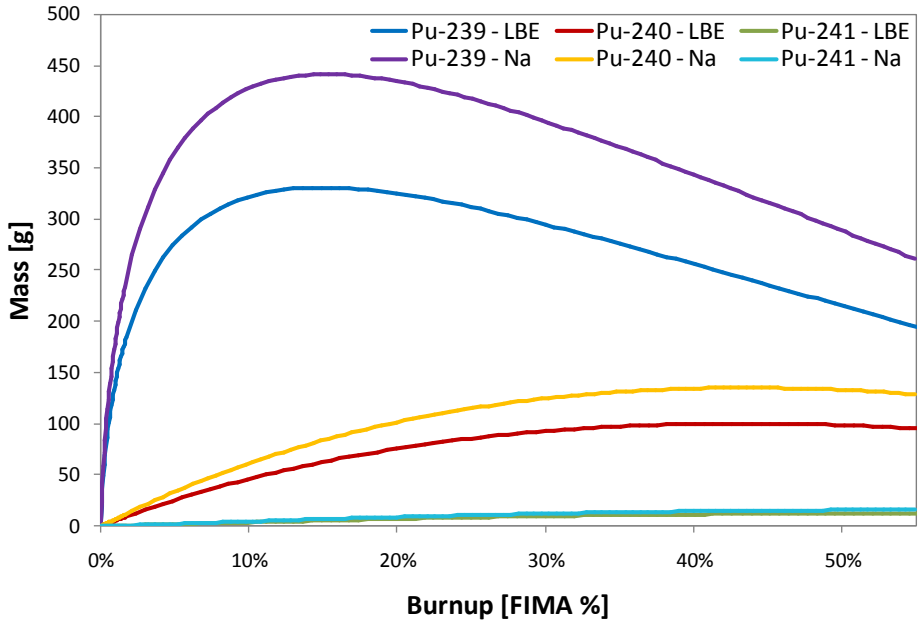

Figure 8.5: Plutonium isotopes mass evolution for the LBE and sodium cooled cores for a unit cell of 1000 cm^3

8.2 Thorium based metallic fuel

The feasibility of establishing a breed and burn mode of operation in thorium fueled fast reactor core is assessed using the zero-dimensional neutron balance methodology for various cladding materials and coolants. Metallic thorium fuel has already been examined in Section 3.2.3. Its density is 11.65 g/cm^3 and it is made of 100% ^{232}Th. The volume fractions and smear density used for the metallic thorium based 0-D unit cell than are those used for the uranium based metallic fuel studied in Section 8.1. The initial heavy metal density is decreased from 5.35 g/cm^3 for the uranium based cell to 4.37 g/cm^3 for the thorium based cell, both using the same P/D ratio of 1.11. Also the same are the simulation assumptions: continuous removal of 75 of the fission gases and instantaneous fuel recycling every ~10 years with the melt-refining. Although the melt-refining process is not compatible with thorium, if this study shows that thorium features

attractive performance, it will be justified to embark upon developing a recycling process for thorium fuel without actinides separation. The neutron leakage probability and the fraction of neutrons lost in the control system are assumed to be 2% and 1%, respectively.

8.2.1 HT-9 structural material with sodium coolant

In this paragraph the coolant and structural material are the same as for the uranium based unit cell: sodium and HT-9. The only difference is the type of fuel and its density. The k_∞ evolution for the thorium based and uranium based metallic fuels are compared in Figure 8.6. For the thorium fuel, the maximum value reached is 1.1 while it is 1.2 for the uranium fuel. The primary fissile isotope of the thorium chain is ^{233}U and is ^{239}Pu for the ^{238}U chain. For the same fast spectrum, the reproduction factor of ^{233}U is ~15% smaller than of ^{239}Pu, making the maximum value of the thorium system k_∞ smaller and significantly impairing the neutron economy. Since thorium is not alloyed with zirconium, the neutron slowing down is smaller and the spectrum is slightly harder, resulting in a reproduction factor for the thorium fueled core only 8.5% smaller than for the uranium fueled core. The neutron balance is shown in Figure 8.7.

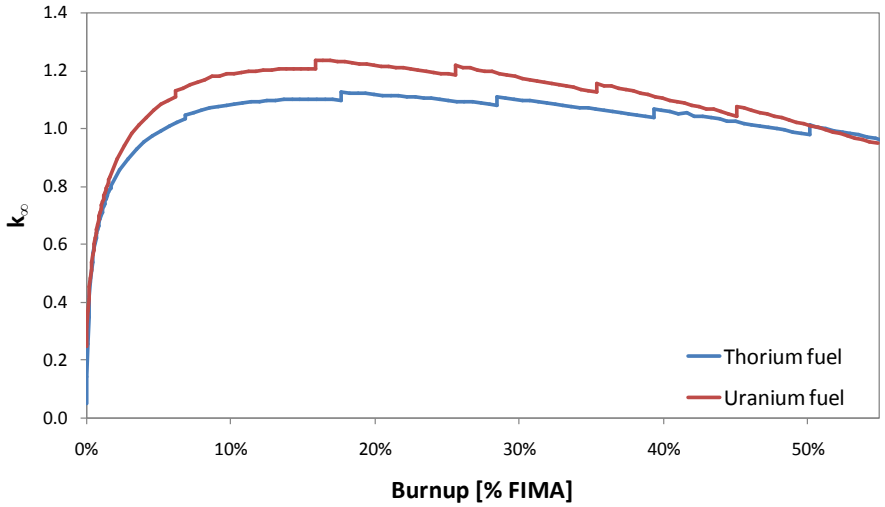

Figure 8.6: k_∞ evolution for the thorium based and uranium based metallic fuels in a unit cell

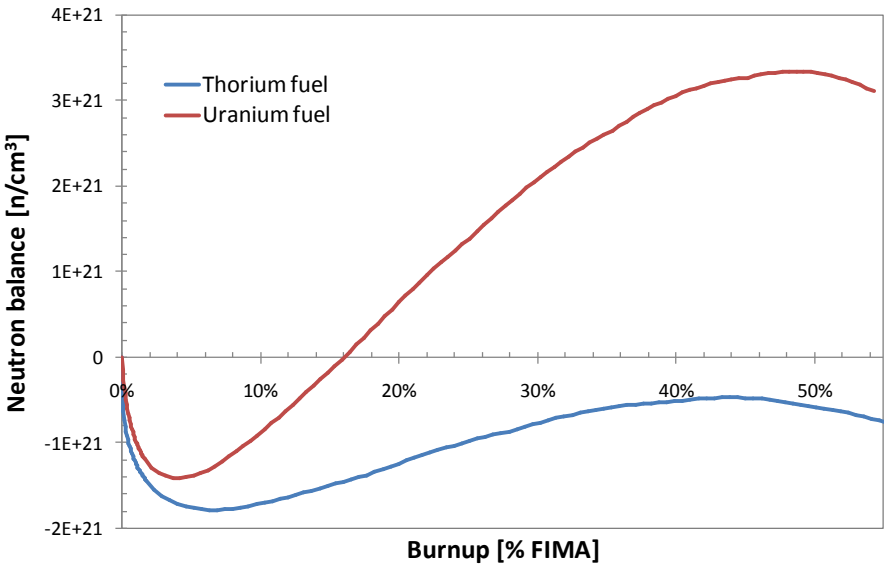

Figure 8.7: Neutron balance for the thorium based and uranium based metallic fuels in a unit cell

The assumed neutron losses being significantly smaller than the practical values assumed in the previous section, the minimum burnup required to sustain the breed and burn mode using uranium fuel is ~16% FIMA instead of 20.4% FIMA reported in Section 6.3.1. Despite of the optimistic assumptions, it is not found possible to sustain the breed and burn mode of operation with the thorium based metallic fuel, sodium coolant and HT-9 cladding. This is due to the 8% smaller k_{eff} values of thorium fuel.

8.2.2 SiC structural material with sodium coolant

In order to improve the neutron economy of the thorium fuel, the HT-9 cladding is replaced with silicon carbide, SiC. Its density is assumed equal to the nominal density, 3.21 g/cm^3. As the neutron capture in the SiC cladding is smaller than in the HT-9 cladding, k_∞ is somewhat higher, as shown in Figure 8.8. Due the presence of lighter elements in the cladding, the neutron spectrum, shown in Figure 8.9, is softened; for a same burnup level, the SiC/Th core contains ~10% more fissile material than the HT-9/Th core. The two strong deeps in the SiC spectrum at ~50 keV and ~200 keV are due to the two main resonances of the ^{28}Si elastic scattering cross-section. Table 8.8 provides the ^{233}U concentration, the unit cell k_∞ and the fuel reproduction factor for the HT-9/Th and SiC/Th cores compared at 10.3% and 20.0% FIMA. The parasitic neutron absorption represents 2.5% in the HT-9 cladded core, while it is only 0.2% in the SiC cladded core. The fuel reproduction factor is smaller with SiC because of the softer spectrum, but due to the significantly smaller parasitic neutron capture in the cladding, its k_∞ is larger than for the HT-9/Th core.

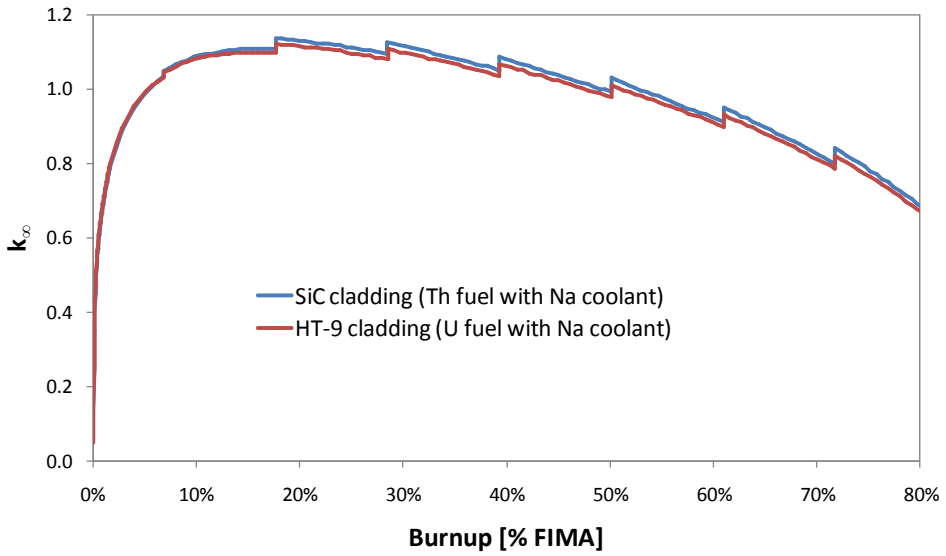

Figure 8.8: k_∞ evolution for the SiC cladded and HT-9 cladded thorium fuel in a unit cell cooled with sodium

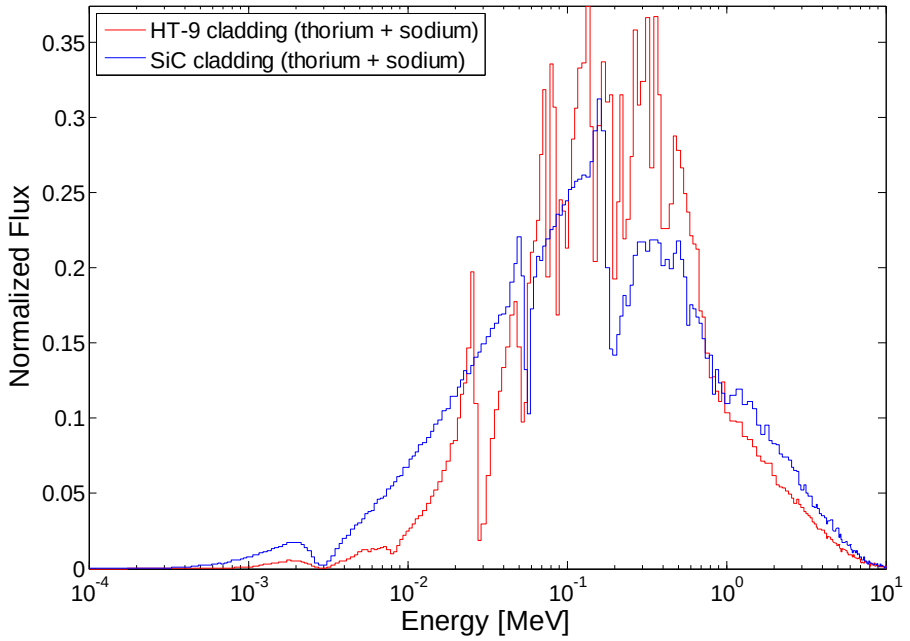

Figure 8.9: Spectra comparison between SiC cladded and HT-9 cladded thorium fuel in a unit cell cooled with sodium

Table 8.8: Comparison of the ^{233}U Concentration, Core k_∞ and Fuel Reproduction Factor between the HT-9 Cladded Core and the SiC Cladded Core at 10.3% and 20.0% FIMA

	10.3% FIMA		20.0% FIMA	
	HT-9	SiC	HT-9	SiC
^{233}U density [g/cm^3]	0.321174	0.349884	0.3143	0.3472
Core k_∞	1.08417	1.0908	1.11676	1.12895
Fuel η	1.1114	1.0921	1.14510	1.13214

Despite the higher k_∞ and slightly improved neutron balance shown below in Figure 8.12, replacing the HT-9 cladding with SiC cladding is not sufficient to make the breed and burn mode sustainable with thorium based metallic fuel and sodium coolant. Only 1.94E+20 additional neutrons per cm^3 of fuel are required to sustain the breed and burn mode. It is possible to establish the B&B mode of operation by feeding the core with slightly enriched fuel. When the fissile material is obtained from fertile material breeding, at least two neutrons are required to produce a sustainable fission: one for breeding, one for fissioning. When the fissile material is directly fed into the reactor, only one neutron is required for fissioning. Therefore, one needs to feed the core with 1.94+20 fissile ^{233}U atoms per cm^3 of fuel. Enriching thorium with 0.64 wt% ^{233}U would be sufficient. If enriching it with ^{239}Pu, lower enrichment will be required since ^{239}Pu produces more neutrons per fission than ^{233}U.

8.2.3 Helium coolant with SiC structural material

The sodium coolant is replaced with helium coolant, improving the neutron economy because helium does not capture and does not effectively slow down the neutrons. Several reactor designs [22, 59] using SiC cladding with helium coolant are already existing. The core performance is assessed by replacing the sodium with helium at a pressure of 70 atm and a temperature of 700 K. The helium density at this pressure and temperature is calculated to be 4.88 kg/m^3.

The evolution of k_∞, shown in Figure 8.10, is very similar to the k_∞ evolution for the core with SiC cladding and sodium coolant. Overall the values are approximately 1.0% larger. As Helium has a significantly smaller atomic density than sodium and a smaller scattering cross-section, its spectrum, shown in Figure 8.11, is slightly harder than for the sodium cooled core. Compared to the sodium cooled core with SiC cladding, the helium cooled core features:

- 2% lower mass of fissile material at a given burnup;
- 0.9% larger fuel reproduction factor;
- 1.2% larger k_∞;
- a parasitic neutron absorption 0.3% smaller due to the null helium capture cross-section.

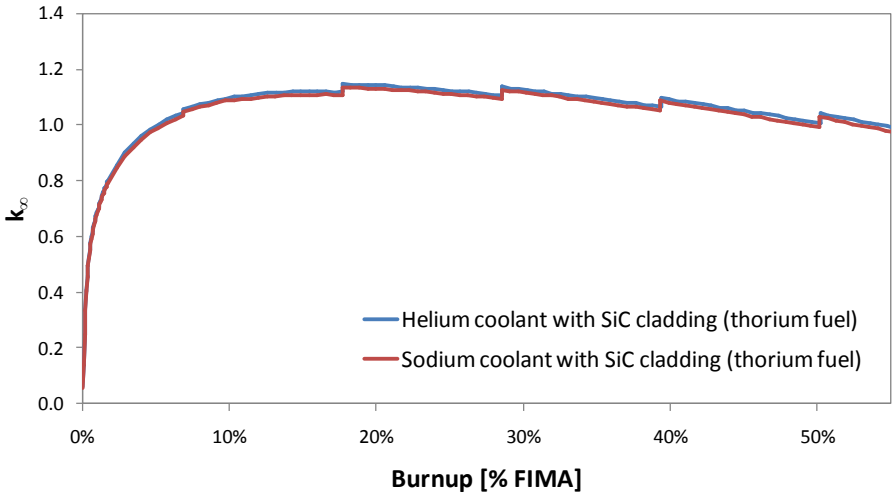

Figure 8.10: k_∞ evolution for the selium cooled and sodium cooled thorium fuel in a unit cell cooled with SiC cladding

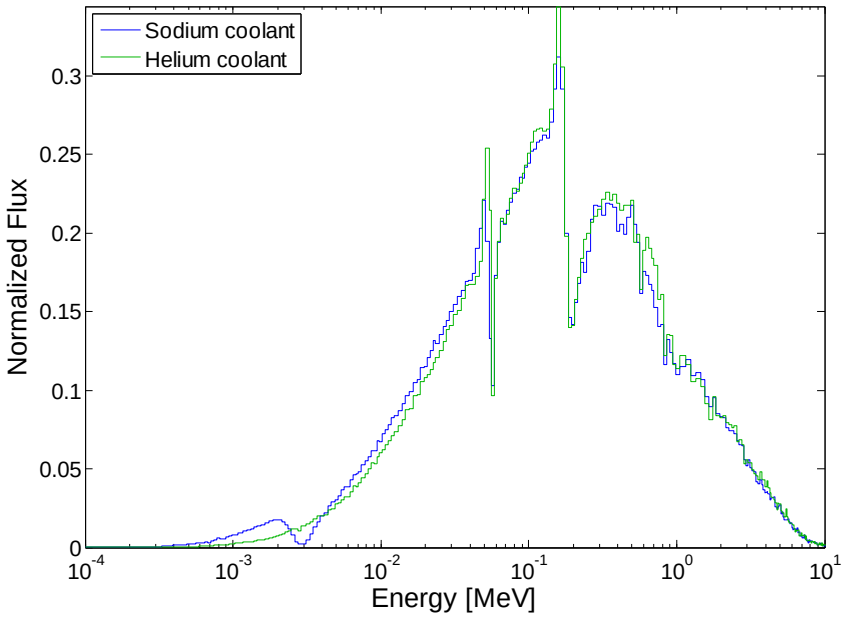

Figure 8.11: Spectra comparison in the sodium cooled and in the helium cooled cores made of thorium fuel and SiC cladding

The neutron balance is represented in Figure 8.12 and shows that it is possible to sustain a breed and burn mode of operation with pure ^{232}Th feed. The minimum required burnup is approximately 39% FIMA. However, the 3% neutron loss (2% leakage, 1% in the control system) assumed is not realistic. With the large B&B core cooled with LBE, it was not possible to achieve a leakage lower than 3% and helium is a worst neutron reflector than sodium. In a real helium cooled core the neutron leakage probability will be larger than for the sodium cooled core, the neutron leakage probability of which has been used in this section. It is found that the maximum leakage probability for which the breed and burn mode can be sustained with the Th/SiC/He core is 2.5%, at 46% FIMA.

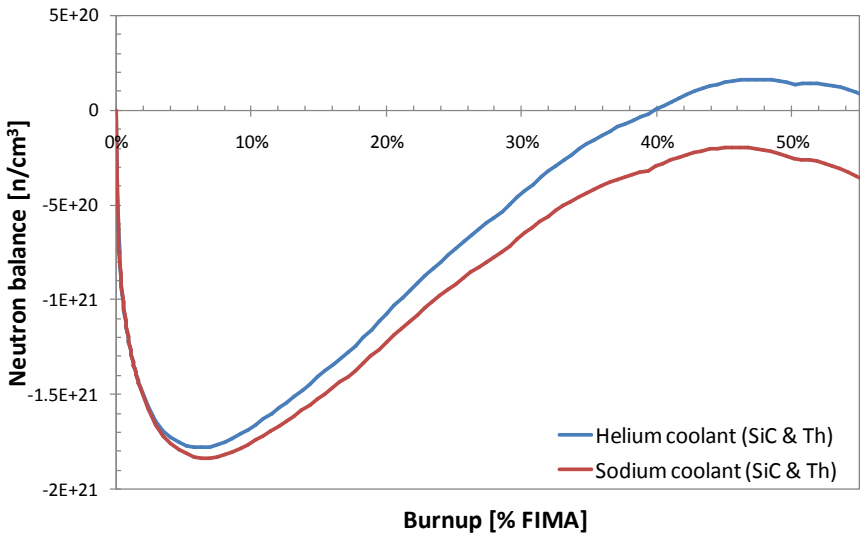

Figure 8.12: Neutron balance for the helium cooled and sodium cooled cores with SiC cladding and thorium fuel

8.3 Nitride fuel

In the breed and burn mode feasibility study performed in Section 5.3.4, it has been found that only nitride fuel could provide slightly impaired performance as compared with the uranium based metallic fuel. However, the assumptions made for the nitride fuel analysis were inaccurate and not practical. In this section, those assumptions are refined and the feasibility to establish the breed and burn mode is analyzed. According to [39, 60, 61], it is possible to fabricate uranium nitride pellets having up to 90% of the theoretical density, 14.32 g/cm^3. In addition, uranium nitride swells less with burnup than metallic fuel and the assumed smear density is 80%. Since the neutron capture cross-section of ^{14}N is larger than ^{15}N, the nitride is enriched to 99 at% of ^{15}N. The cladding and coolant volume fractions are the same as for the metallic uranium fuel, but the fuel and gap volume fractions are changed due to the different smear density. The volume fractions used are provided in Table 8.9.

Table 8.9: Volume Fractions of Nitride Fuel for the Unit Cell Study

	U-Zr	UN
Fuel	37.48%	39.97%
Gap (empty)	12.49%	9.99%
Structural material (HT9)	21.99%	21.99%
Coolant (Na)	28.05%	28.05%

The evolution of k_∞ for the metallic uranium and uranium nitride (UN) fuels is compared in Figure 8.13. The k_∞ values in the UN fuelled core are ~4% smaller because of the softer spectrum due to the neutron slowing down by nitrogen atoms. The spectrum is shown at 20% FIMA burnup in Figure 8.14 for the two cores. Due to the softer spectrum and despite the smaller k_∞ values, the UN fuelled core features a 10.3% larger fissile to HM atomic ratio than the U-Zr fuelled core. It is also observed that the parasitic neutron absorption is reduced by about 0.7%

when using UN fuel instead of U-Zr because of the significantly lower macroscopic capture cross-section of nitrogen compared to zirconium, in a fast spectrum.

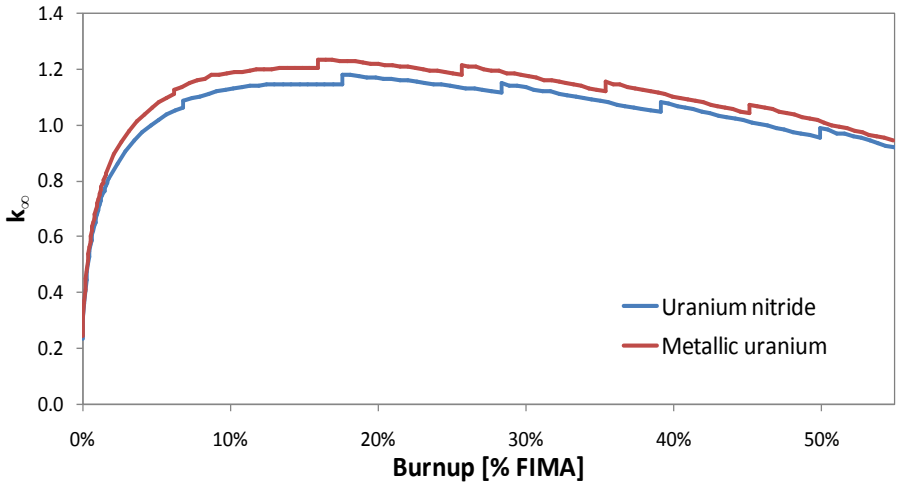

Figure 8.13: k_∞ evolution for uranium nitride and metallic uranium fuels in a unit cell cooled with sodium and cladded with HT-9

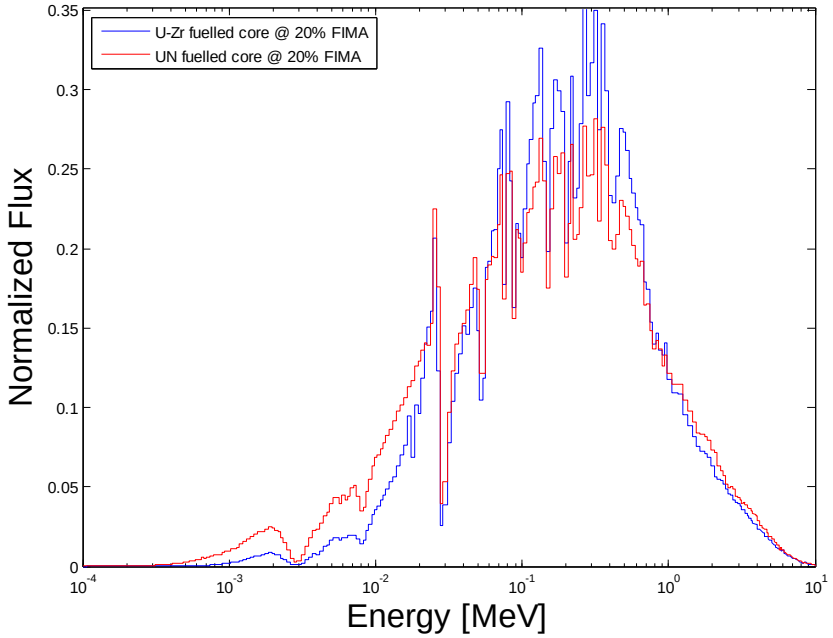

Figure 8.14: Spectra comparison between the metallic uranium fuel and the uranium nitride fuel at 20% FIMA

The neutron balance is performed for the UN fuelled core, assuming the same neutron leakage probability, 4.40%, and the same fraction of neutron absorbed in the control systems, 1%, as found for the U-Zr fueled large B&B core in Section 8.1.1. The results are compared in Figure 8.15 for the two cores. The minimum required burnup for the U-Zr fuelled core is ~19% FIMA while it is ~33% FIMA for the UN fuelled core. It is possible to sustain the breed and burn mode in a large B&B core with UN fuel, as long as the fraction of neutrons lost by leakage or absorbed

in the control systems is smaller than 5.6%. It is however unpractical to spawn additional cores from a UN fueled B&B core due to the very small excess neutrons left after sustaining the breed and burn mode in the first core.

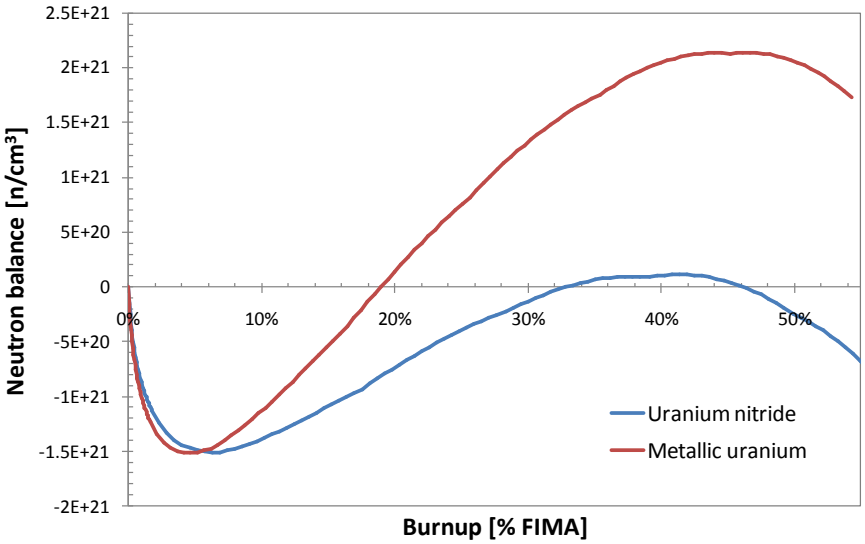

Figure 8.15: Neutron balance for the metallic uranium fuelled and uranium nitride fueled cores with HT-9 cladding and sodium coolant

8.4 Conclusions

The feasibility to sustain the breed and burn mode of operation in the following alternative core designs was assessed in this chapter: (a) LBE and PbLi cooled metallic fuelled cores; (b) metallic thorium fuelled core; and (c) uranium nitride fuelled cores. The assessment was based on the neutron balance method. The reliability of this method is not perfect and has already been discussed in Section 7.2.

It was found that with lead based alloys, it is possible to achieve the same thermal hydraulic performance as in a sodium cooled core having P/D=1.11 by increasing the P/D ratio to 1.24 for PbLi coolant and to 1.30 for LBE coolant. With the increased P/D ratios, the neutron economy is impaired but it is possible to sustain the breed and burn mode with a minimum discharge burnup of 28% FIMA. For the sodium cooled core, the minimum discharge burnup is 20.4% FIMA. The two main advantages of lead based alloys it that there is no need for a secondary coolant loop and that the mass of fissile material initially required to make the reactor critical is decreased by ~26%, compared to a sodium cooled system of same size.

The best performance obtained with thorium based metallic fuel has been achieved with SiC cladding and helium coolant. Replacing the sodium with helium and the HT-9 with SiC enabled slightly improving the neutron balance and even makes the breed and burn mode of operation sustainable when the fraction of neutron lost by leakage and in the control systems is smaller than 2.5%. It is, however, unlikely that a realistic helium cooled thorium fueled reactor could be designed to have such a good neutron economy. Therefore, it appears impossible to practically sustain the breed and burn mode of operation with thorium based metallic fuel, without using enriched fuel feed.

The last finding of this chapter is the possibility to sustain be breed and burn mode of operation with nitride fuel enriched with 99 at% ^{15}N. When assuming a realistic neutron leakage probability and a realistic fraction of neutrons lost in the control systems, the minimum required burnup is estimated to be 33% FIMA. This is significantly larger than for the uranium based metallic fuel, 20.4% FIMA. Moreover, the number of excess neutrons left in the fuel after sustaining the breed and burn mode is far too small to enable spawning new cores. It is not possible either to design a S-PRISM size B&B core, such as studied in Chapter 7, with nitride fuel because of the larger neutron leakage probability than in the large B&B core studied in Chapter 6.

Although it has not been studied, it is likely possible to improve the neutron economy of the uranium based metallic fuel by using a SiC cladding and helium coolant. However, the challenges faced by the design of helium cooled fast reactors and the lack of experimental data and technology for SiC make this option impractical in the near future.

Chapter 9

Conclusions

The primary objective of this study was to estimate the maximum fuel utilization that is achievable using fast reactors that are designed to operate with fuel reconditioning when the fuel reaches its radiation damage constraint. The primary function of the fuel reconditioning is to relieve the pressure of the gaseous fission products, replace the cladding and reduce radiation damage effects in the fuel. That is, the fuel recycling processes considered cannot be used for the separation of actinides from most of the fission products and to extract plutonium or any other actinide from the fuel. Hence, these recycling processes are highly proliferation resistant and, hopefully, less expensive than processes traditionally considered for used fuel recycling. With the fuel reconditioning, the maximum discharge burnup is dictated by the reactivity of the fuel and is not limited by the material damage constraints. A couple of fuel management strategies were examined: a multi-batch fuel management and a breed and burn mode of operation. The two recycling processes examined are an AIROX-like process and the melt-refining process.

9.1 Multi-batch refueling

9.1.1 Conventional fast reactors

Table 9.1 compares the cumulative discharge burnup and fuel utilization attainable in a 1200 MW_{th} fast reactor core (S-PRISM size) and in a large 3000 MW_{th} fast reactor core against those attainable using a once-through LWR. The results quoted for the fast reactors are upper bound estimates as they assume infinite number of batches and ignore loss of actinides during the fuel reconditioning process. All the reactors inter-compared use enriched uranium. The fast reactors either use or do not use depleted uranium radial blanket.

Table 9.1: Discharge Burnup and Uranium Utilization for LWR and for a Medium and Large Size Conventional Fast Reactors

Reactor type	Fuel management	Average discharge burnup [enriched fuel/blanket]	Uranium utilization…	relative to LWR
LWR	4 batches	5.10%	0.61%	1
Large FR - radial reflector	infinite-batches	58%	2.63%	4.3
S-PRISM size FR - radial reflector	infinite-batches	45.90%	1.84%	3.0
Large FR - radial blanket	infinite-batches	65.3%/39.7%	4.76%	7.8
S-PRISM size FR - radial blanket	infinite-batches	52.4%/16.7%	2.77%	4.5

It has been found that the maximum discharge burnup is achieved in the fast reactor designs having a radial blanket. For the S-PRISM size and large fast reactors operating with enriched fuel the maximum achievable burnups are 52.4% FIMA and 65.3% FIMA, respectively. These burnups correspond to a uranium utilization that is 4.6 times and 7.9 times larger, respectively, than of a conventional once-trough LWR operating at 50 GWd/tHM. In addition to offering a significant improvement over the LWR uranium utilization, all the discharged fuel characteristics of the fast reactors, per unit of energy generated, were found more favorable than the characteristics of the fuel discharged from a conventional LWR. The achievable burnup in the S-PRISM size and large conventional fast reactors represent approximately 71% and 88% of the theoretical maximum achievable burnup in an infinite core when the majority of the solid fission products are not separated; i.e., when using fuel reconditioning.

9.1.2 Breed and burn reactors

With the breed and burn mode of operation hereby proposed, all the uranium mined can be used as fuel. Hence, the uranium utilization in this mode of operation is, ignoring losses, the fraction of the fuel fissioned; that is, the fuel discharge burnup in FIMA. After the initial enriched fuel loading, only depleted or natural uranium is needed to sustain the fission chain reaction.

The maximum fuel utilization and maximum achievable burnup are constrained by the fuel reactivity due to accumulation of fission products. Table 9.2 summarizes the maximum discharge burnup and achievable fuel utilization for the S-PRISM size and large B&B reactors at equilibrium, using the melt-refining process. The results quoted pertain to 15 fuel batches for the S-PRISM size B&B reactor and 8 fuel batches for the large size B&B reactor.

Table 9.2: Discharge Burnup and Uranium Utilization for the Medium Size and Large B&B Reactors

Reactor	Fuel management	Average discharge burnup	Uranium utilization…	…relative to LWR
Large B&B reactor	8 batches	57%	57%	93.4
S-PRISM size B&B reactor	15 batches	43.4%	43.4%	71.1

At equilibrium, the maximum attainable burnup has been found to be 43.4% FIMA for the S-PRISM size B&B reactor and 57% FIMA for the large B&B reactor. These maximum

achievable burnups are ~15% smaller than for the conventional fast reactors that are reloaded with enriched fuel and assumed to operate using an infinite-batch fuel management scheme. The uranium utilization of the large and S-PRISM size B&B reactors relative to the conventional fast reactors and LWR is provided in Table 9.3. Despite of the lower discharge burnup, the uranium utilization with the B&B mode of operation is higher 16-fold for the S-PRISM size reactor and 12-fold for the large reactor. Compared to a conventional LWR, the B&B reactors uranium utilization is higher by 71-fold and 93-fold for, respectively, the S-PRISM size and large B&B reactors. Due to the higher thermal efficiency of fast reactors, the amount of electrical energy generated by the S-PRISM size and large B&B reactors per unit of uranium mined is, respectively, 85 times and 112 times larger than for a once through LWR. The characteristics of the fuel discharged from the B&B fast reactors at 55% FIMA are compared to the LWR discharged fuel, per unit of electricity generate in Table 9.4. The fuel discharged from the S-PRISM size B&B fast reactor at 43.4% FIMA is expected to feature somewhat smaller improvements because of the lower discharge burnup.

Table 9.3: B&B Reactors Uranium Utilization Relative to Conventional FR and LWR

Uranium utilization relative to…	Large B&B reactor	S-PRISM size B&B reactor
Conventional FR (multi-batch)	12	15.7
OT LWR (50 GWd/tHM) per unit thermal energy generated	93.4	71.1
OT LWR (50 GWd/tHM) per unit electric energy generated	112.1	85.3
Energy content of the US DU stockpiles (550000 tons) [10^3 GWeD]	~125000	~96000

Table 9.4: B&B Reactor Discharge Fuel Characteristics Relative to LWR Discharge Fuel per GWeD

	B&B reactor at 55% FIMA
TRU mass	40%
Inventory of ^{237}Np and its precursors	10%
TRU decay heat 1 year after discharge	12%
TRU&FP radiotoxicity 1 year after discharge	28%
Neutron emission rate 1 year after discharge	7%

For the breed and burn mode of operation to be sustainable, the fuel must reach a minimum burnup to ensure that sufficient fissile material has been bred in the fertile fuel feed elements. The minimum theoretical required burnup is estimated for an infinite core to be 13% FIMA. This is somewhat larger than the maximum permissible burnup in a HT-9 clad metallic fuel without fuel reconditioning. Practically, it is found that for a S-PRISM size (1200 MW_{th}) B&B core and for a large (3000 MW_{th}) B&B core the minimum required burnup is, respectively, 31% FIMA and 20% FIMA. These values are very sensitive to the neutron leakage probability; using a less leaky core will enable decreasing the minimum required burnup.

By discharging the fuel from the large B&B reactor when it reaches its minimum required burnup, it is possible to spawn new B&B reactors without using any additional enriched fuel. The effective doubling time of the large B&B reactor is estimated to be 14 years. The corresponding

capacity annual growth rate is ~3.85%. No enriched fuel needs be provided to the expanding fleet of B&B reactors with the exception of the igniters required for the Mother reactors. This annual capacity growth rate is larger than in most of the socio-economic scenarios envisioned by the IIASA.

The mass of ^{235}U or TRU required to fabricate the initial igniter has not been carefully optimized in this work. It was found that by using a higher concentration of fissile fuel loaded in shorter fuel rods it is possible to design the igniter to have a smaller mass than when using lower enrichment full-length igniter fuel rods. It is also possible to decrease the igniter mass by more than 25% when a lead based alloy is substituted for sodium. The thermal hydraulic performance of lead based alloys was found inferior to sodium; it is necessary to increase the core P/D ratio to achieve the same core power. This impairs the neutron economy. With the two approaches identified capable of reduction of the fissile material requirements, it may not be possible to operate the large B&B core with the spawning mode of operation, but it is possible to establish and sustain the breed and burn mode.

The minimum burnup required for sustaining the B&B mode of operation is very sensitive to the neutron spectrum and, hence, to the fuel type and density. The best fuel type identified is a U-Zr alloy; the smaller the Zr content the lower can be the minimum required burnup. The minimum required burnup is slightly larger for UN fuel, with nitrogen enriched to ^{15}N. It is not possible to establish the B&B mode of operation with oxide fuel, carbide fuel or inert matrix dispersion fuel due to the lowered heavy metal density and its dilution with lighter elements. With thorium fuel it is not possible to establish a breed and burn mode of operation due to the low reproduction factor of ^{233}U as compared to that of ^{239}Pu.

The successful development of the B&B reactors and of the associated fuel recycling technologies could provide a great measure of energy security and energy cost stability during the next centuries. Beyond the deployment of the first generation of B&B reactors, no enriched fuel, enrichment facility or actinide separation facility will be required to support the B&B fleet, while still being possible to sustain a 3.85% capacity annual growth rate with a uranium utilization factor possibly exceeding 40% and, possibly, close to 50%. The 560 tons of plutonium estimated to be contained in the United States UNF, as of 2010, could provide the enriched fuel for at least 83 GWe of B&B reactors, corresponding to ~83% of the 2009 US nuclear energy capacity. The 550000 depleted uranium tons stockpiles already accumulated in the US represents from 96000 to 125000 TWeD (10^3 GWeD) when used in the B&B reactors. This energy value is equivalent to at least seven centuries of the total 2009 supply of electricity in the USA [62] – all sources of electricity included.

9.2 Future directions and challenges

Before the B&B reactors and fuel cycle hereby proposed can be deployed, several challenges need to be addressed and additional studies need to be performed.

A thorough analysis of the B&B cores reactivity coefficients should be performed in order to determine whether or not the core meets the inherent safety criteria such as those defined by Wade & Chang in [63] for liquid metal cooled fast reactors. Since the S-PRISM size B&B reactor has a smaller core volume and higher neutron leakage probability, it is expected that its coolant temperature and void reactivity coefficients will be less positive than for the large B&B reactor, improving its inherent safety. Although it was found that the control systems are offering a

comfortable shutdown margin at hot condition, the analysis should be repeated in order to assess the shutdown margins at cold condition – the most reactive state of the reactor. The effect of the control assemblies depletion on their reactivity worth need be determined as well. Detailed safety analysis need be performed by simulating different accident and transient scenarios.

Technology-wise, the first challenge to be faced is the development of a cladding material able to sustain very high DPA. Several ODS alloys and ferritic martensitic steels are being developed and, hopefully, at least one of them will be able to sustain at least 600 DPA and a fast fluence of ~1.2E+24 n/cm^2. Due to the lack of fast neutrons irradiation facilities capable of irradiating a material to such a high DPA level, the qualification of those materials may take decades and delay the deployment of advanced fast reactors. A related challenge is the development of fuel materials and/or designs able to achieve ~30% peak burnup without applying excessive stress on the clad via swelling. Smear factors smaller than 75% may have to be used to accommodate the fuel swelling. In addition, it may be necessary to vent the gaseous fission products from the fuel since increasing the fission gas plenum volume by a factor of three (proportional to the increase in the discharge burnup) may not be practical.

Another important challenge to be addressed is the feasibility and performance assessment of the fuel recycling process. The melt-refining process has been demonstrated during the EBR-II project only for low burnup (~10% FIMA) fuel [32] and not at commercial scale. The performance of this process may be impaired when used to treat very high burnup fuel because of the significantly larger amount of fission products in the fuel. In particular, the lanthanides are removed by oxidation with the zirconia crucible. But the oxide layer formed on the wetted crucible surface passivates the crucible and limits the amount of lanthanide that can oxidize with the crucible. This issue can be solved by melting the fuel several times in different crucibles, but that will also increase the heavy metal losses and recycling cost. The melt-refining material losses during the EBR-II project were significantly larger than those assumed during this study: up to 10% instead of 1%. It is necessary to re-assess the performances of the melt-refining process for very high burnup fuel and modify the process in order to decrease the material losses. The modified melt-refining process does not have to remove lanthanides; reactivity-wise they will not impair the feasibility and performance of the B&B mode of operation.

A related technological challenge is the prevention of chemical interaction between the recycled fuel and the clad. The recycled fuel contains significant amount of fission products some of which are chemically reactive with the HT-9 constituents. It may be necessary to separate the recycled fuel from the HT-9 clad by coating or lining the inner clad surface by a protection layer that is resistant to chemical attack by the fission products.

Bibliography

1. IEA/NEA, *Projected Costs of Generating Electricity - 2010 Edition*. 2010. p. 218.
2. IAEA. *Nuclear´s Great Expectations*. 2008 [cited 2010 June]; Available from: http://www.iaea.org/NewsCenter/News/2008/np2008.html.
3. DOE/EIA, *Annual Energy Review 2008*. 2009.
4. IIASA, *GGI Scenario Database v2.0*. 2009.
5. US-DOE, *Audit Report: Potential Uses for Depleted Uranium Oxide*. 2009, DOE. p. 15.
6. WNA. *Uranium and Depleted Uranium*. 2009 [cited 2010 June]; Available from: http://www.world-nuclear.org/info/inf14.html.
7. Albright, D., *Plutonium and highly enriched uranium, 1996 : world inventories, capabilities, and policies*, ed. W. Walker, et al. 1997, Solna, Sweden : Oxford ; New York ; Oxford University Press.
8. Fuel-Trac, *Spent Fuel / Reprocessing*, in *Nuclear Industry Status Reports*. 1999.
9. IAEA, *Fast Reactor Database 2006 Update*, in *IAEA TECDOC Series*. 2006, IAEA. p. 450.
10. Feinberg, S.M. *Discussion Comment*. in *ICPUAE*. 1958. Geneva, Switzerland.
11. Atefi, B., *An Evaluation of the Breed/Burn Fast Reactor Concept*, in *Department of Nuclear Engineering*. 1979, Massachusetts Institute of Technology. p. 295.
12. Fischer, G.J. and R.J. Cerbone, *The fast-mixed spectrum reactor - Interim report - Initial feasibility study*. January 1979, Brookhaven National Laboratory.
13. Feoktistov, L.P., *An analysis of a concept of a physically safe reactor*, in *Preprint IAE-4605/4*. 1988.
14. Teller, E., M. Ishikawa, and L. Wood, *Completely automated nuclear reactors for long-term operation*. 1996. 12 p.
15. Toshinsky, G.I., *LMFBR Operation in the Nuclear Cycle without Fuel Reprocessing*, in *Advanced reactors safety 1997*, American Nuclear Society, Editor. 1997: Orlando, Florida, USA.
16. Sekimoto, H. and K. Ryu, *A new reactor burnup concept CANDLE*, in *Physor 2000*. 2000, American Nuclear Society: Pittsburgh.
17. Su'ud, Z. and H. Sekimoto, *Preliminary design study of the ultra long life fast reactor.* Nuclear Engineering and Design, 1993. **140**(2): p. 251-260.
18. Song, H., Y.I. Kim, and Y.I. Kim. *Ultra Long Life Core Using Direct Refabrication Concept*. in *Korean Nuclear Society Autumn Meeting*. 2006. Gyeongju, Korea.

19. Kim, T.K. and T.A. Taiwo, *Feasibility Study of Ultra-long Life Fast Reactor Core Concept*, in *Physor 2010*, American Nuclear Society, Editor. 2010: Pittsburgh, Pennsylvania, USA.
20. Driscoll, M., et al., *Engineering and Physics Optimization of Breed and Burn Fast Reactor Systems*. 2005, Massachusetts Institute of Technology.
21. Gilleland, J., et al., *Novel Reactor Designs to Burn Non-Fissile Fuels.* 2008.
22. GA. *Energy Multiplier Module*. 2010; Available from: http://www.ga.com/energy/em2/.
23. Greenspan, E. *Multi-Recycling of Spent Fuel with Low Proliferation Risk*. in *ICENES 98*. 1998. Herzelia, Israel.
24. Monti, L., *Validation of the ENHS Core Neutronics Design*. 2005, Universita degli Studi di Bologna.
25. Ikegami, T. *Core Characteristics of Fast Reactor Cycle with Simple Dry Pyrochemical Processing*. in *INES-2*. 2006. Yokohama, Japan.
26. Ellis, T., et al. *Traveling-Wave Reactors: A Truly Sustainable and Full-Scale Resource for Global Energy Needs*. in *ICAPP'10*. 2010. San Diego, CA, USA.
27. Kim, T.K., et al., *Core design studies for a 1000 MWth Advanced Burner Reactor.* Annals of Nuclear Energy, 2009. **36**(3): p. 331-336.
28. Dubberley, A.E., et al., *SuperPrism Oxide and Metal Fuel core Designs*, in *ICONE 8*. 2000: Baltimore, MD, USA.
29. Hofman, G.L., *Assessment of Low Zr Metallic Fuel Alloys*, in *Global 2009*. 2009: Paris, France.
30. Majumdar, D., et al., *Recycling of nuclear spent fuel with AIROX processing*, in *Other Information: PBD: Dec 1992*. 1992. 67 p.
31. Lee, J.S., et al., *Research and Development Program of KAERI for DUPIC (Direct Use of Spent PWR Fuel in CANDU Reactors).* 1993.
32. Hesson, J.C., M.J. Feldman, and L. Burris, *Description and Proposed Operation of the Fuel Cycle Facility for the Second Experimental Breeder Reactor (EBR-II)*, in *Reactor Technology*. 1963. p. 193.
33. Petroski, R., B. Forget, and C. Forsberg, *Neutronic Evaluation of Breed-and-Burn Reactor Fuel Types Using an Infinite-Medium Depletion Approximation*, in *Physor 2010*, American Nuclear Society, Editor. 2010: Pittsburgh, Pennsylvania, USA.
34. Richter, K. and H. Blank, *Fabrication processes and characterization of LMFBR carbide and nitride fuels and fuel pins*, in *Technical committee meeting on advanced fuel for fast breeder reactors: Fabrication and properties and their optimization*. 1987: Vienna, Austria. p. 58-67.
35. Savchenko, A., et al., *Dispersion type zirconium matrix fuels fabricated by capillary impregnation method.* Journal of Nuclear Materials, 2007. **362**(2-3): p. 356-363.
36. Foster, J.P. and U.P. Nayak, *Direct observation of fuel-cladding mechanical interaction (FCMI) in mixed-oxide fast reactor fuel pins.* Journal of Nuclear Materials, 1981. **101**(3): p. 295-313.
37. Crawford, D., D. Porter, and S. Hayes, *Fuels for sodium-cooled fast reactors: US perspective.* Journal of Nuclear Materials, 2007. **371**(1-3): p. 202-231.
38. Dollins, C.C. and M. Jursich, *Fission gas release from oxide fuels at high burnups.* Journal of Nuclear Materials, 1982. **105**(2-3): p. 269-275.
39. Tanaka, K., et al., *Fission gas release and swelling in uranium-plutonium mixed nitride fuels.* Journal of Nuclear Materials, 2004. **327**(2-3): p. 77-87.

40. Lee, C.B., D.H. Kim, and Y.H. Jung, *Fission gas release and swelling model of metallic fast reactor fuel.* Journal of Nuclear Materials, 2001. **288**(1): p. 29-42.
41. Hofman, G.L., L.C. Walters, and T.H. Bauer, *Metallic fast reactor fuels.* Progress in Nuclear Energy, 1997. **31**(1-2): p. 83-110.
42. LANL, *MCNP — A General Monte Carlo N-Particle Transport Code, Version 5*, X-5 Monte Carlo Team. 2003.
43. Milošević, M., E. Greenspan, and J. Vujic, *Effects of Uncertainties in Lead Cross Section Data in Monte Carlo Analysis of Lead Cooled and Reflected Reactors*, in *M&C + SNA 2007*, American Nuclear Society, Editor. 2007: Monterey, California, USA.
44. ORNL, *ORIGEN 2.2 - Isotope Generation and Depletion Code*. 2002.
45. Moore, R.L., et al., *MOCUP: MCNP-ORIGEN2 Coupled Utility Program*, INEL, Editor. 1995.
46. Zhang, J. and N. Li, *Review of the studies on fundamental issues in LBE corrosion.* Journal of Nuclear Materials, 2008. **373**(1-3): p. 351-377.
47. Ballinger, R.G., *Personal Communication*. 2010.
48. Suspuglas, A. and E. Greenspan, *Implementation of the ENHS Thermal Hydraulic Optimization Code for Recent ENHS Design Improvement*. 2005.
49. Gaiduchenko, A., *Thermophysical properties of irradiated uranium-zirconium fuel.* Atomic Energy, 2008. **104**(1): p. 5-10.
50. Hong, S.G., E. Greenspan, and Y.I. Kim, *The Encapsulated Nuclear Heat Source (ENHS) Reactor Core Design.* Nuclear technology., 2005. **149**(1): p. 22.
51. Tsai, H., et al., *Behavior of mixed-oxide fuel elements during an overpower transient*. 1992. 24 p.
52. Leggett, R.D. and L.C. Walters, *Status of LMR fuel development in the United States of America*. 1992. 10 p.
53. Gluekler, E.L., *U.S. advanced liquid metal reactor (ALMR).* Progress in Nuclear Energy, 1997. **31**(1-2): p. 43-61.
54. Sekimoto, H., K. Ryu, and Y. Yoshimura, *CANDLE: The New Burnup Strategy.* Nuclear science and engineering : the journal of the American Nuclear Society., 2001. **139**(3): p. 306.
55. Petroski, R., *Direct Use of Depleted Uranium As Fuel in a Traveling-Wave Reactor.* American Nuclear Society, 2009. **101**: p. 741-742.
56. US-DOE, *Annual Transuranic Waste Inventory Report - 2009*. 2009, U.S. Department of Energy. p. 812.
57. Not, A., *DOE fundamentals handbook: Nuclear physics and reactor theory*. 1993. (121 p).
58. Iwasaki, T. and K. Konashi, *Development of Hydride Absorber for Fast Reactor -- Application of Hafnium Hydride to Control Rod of Large Fast Reactor.* Journal of nuclear science and technology., 2009. **46**(8): p. 874.
59. PBMR. *Pebble Bed Modular Reactor*. 2010; Available from: http://www.pbmr.com/.
60. Matthews, R.B., et al., *Fabrication and testing of uranium nitride fuel for space power reactors.* Journal of Nuclear Materials, 1988. **151**(3): p. 345-345.
61. Muta, H., et al., *Thermal and mechanical properties of uranium nitride prepared by SPS technique.* Journal of Materials Science, 2008. **43**(19): p. 6429-6434.
62. EIA, *EIA-860 Database*. 2009.
63. Wade, D.C. and Y.I. Chang, *The integral fast reactor (IFR) concept: Physics of operation and safety*. 1987. Pages: 27.

64. Masdelesvalls, E., et al., *Lead–lithium eutectic material database for nuclear fusion technology*. Journal of Nuclear Materials, 2008. **376**(3): p. 353-357.

Appendixes

Appendix A

IMOCUP scripts

The IMOCUP program is made of three scripts, provided below. A detailed description of the role of these scripts is given in the IMOCUP manual.

1. **mcnpIMO script**

It is executed with:

```
mcnpIMO ${t} inp.${t} mctal.${t} outp.${t} mpo.${t} fmt nct
```

Code:

```
#!/bin/bash
# mcnpIMO - updated 2 july 2010 with new RX rate - mpo files sorted by numeric
order
t=$1
input=$2
mc=$3
out=$4
mp=$5
fmt=$6
nct=$7
#t=1

# The purpose is to generate the exact same MPO files as thoses generated by
mcnpPRO, but using a different layout of the mctal file.
# The same features have to be available (eg. "$" sign is not yet
available...)

awk -v step=$t -v mpo=$mp '
# File counter
FNR==1&&NR!=FNR{fi++}
# Load in the NCT matrix the nct file (fourth file) contents
fi==3{nct[$1]=$0;next}
# Second file treatment (mctal)
# Save the values of the flux in "fluxTal"
fi==1&&$0~/begin IMOCUP fluxes/{f1=1;next}
```

```
fi==1&&f1==1&&$1~/^vals/{f1=2;next}
fi==1&&f1==2&&$1~/^tfc/{f1=0;next}
fi==1&&f1==2{for(i=1;i<=NF;i+=2)fluxTal[++c5]=$i}
# Save the values of the flux in "rxrateTal"
fi==1&&$0~/begin IMOCUP reaction rates/{f2=1;next}
fi==1&&f2==1&&$1~/^vals/{f2=2;next}
fi==1&&f2==2&&$1~/^tfc/{f2=0;next}
fi==1&&f2==2{for(i=1;i<=NF;i+=2)rxrateTal[++c6]=$i}
fi==1{next}
# Treatment of the last file (outp)
NR!=FNR&&$0~/print table 60/{cr7=1;next}
NR!=FNR&&cr7==1{if($1~/total/){cr7=0;next}if($1~/^[0-
9]/){matTable[$2]=$3;atDens[$2]=$4;volume[$2]=$6}}
NR!=FNR{next}

# Load in memory all the materials defined in the problem (only first line is
required because of the way ORIGEN works)
$1!~/^[0-9]/{c10=0}
$0~/^m[0-9]/{m=substr($1,2,length($1)-
1);if(substr(m,1,1)==0)m=substr(m,2,length(m)-1);mater[m]=$2;c10=1}
c10==1{allIso[m" "$(NF-1)]=$NF}
# Analyses the tallies
$0~/begin IMOCUP fluxes/{fl=1;next}
$0~/end IMOCUP fluxes/{fl=0;next}
fl==1{i=1;
  if($0~/^f/)i++
  for(i;i<=NF;i++)
    zo[++c1]=$i
}
$0~/begin IMOCUP reaction rates/{f2=1;next}
$0~/end IMOCUP reaction rates/{f2=0;next}
f2==1&&$1!~/^[Ff][0-9]/{
  go=0;gsub(/\)/," ",$0);gsub(/\(/," ",$0)
  for(i=1;i<=NF;i++){
    if(go>=2){
      nombreRX[mater[mat]]=go-1
      if($i~/^[0-9]|^-[0-9]/)
        rxrate[++rr]=$i
      if($i~/^\$$/)
        dollar[mater[mat]]=1
    }
    if(go>=1){go++}
    if(go==0&&$i~/^[0-9]/){
      go++;
      t1=$(i+1);
      if(t1~/^0/)t1=substr(t1,2,length(t1)-1);
      matal[++c3]=t1;
      mat=t1;
  }}
}
# Generate the MPO files
END{
for(zone=1;zone<=c1;zone++){
  c7=0
  print "."step > mpo"."zone
  # to be changed:
  print 1 >> mpo"."zone
```

```
  print " "zo[zone]"  "matTable[zo[zone]]"  "fluxTal[zone]"
"atDens[zo[zone]]"  "volume[zo[zone]] >> mpo"."zone
  print "  "c3 >> mpo"."zone
  for(iso=1;iso<=c3;iso++){
    print "  "nct[mater[matal[iso]]],allIso[matTable[zo[zone]]"
"mater[matal[iso]]] >> mpo"."zone
    print "   "nombreRX[mater[matal[iso]]]" ",dollar[mater[matal[iso]]] >>
mpo"."zone
    for(rx=1;rx<=nombreRX[mater[matal[iso]]];rx++){
      tvar=rxrate[++c7]
      rxName="unknown"
# This is where the known reactions are defined
      if(tvar~/^102/)rxName="SNG"
      else if(tvar~/^16/)rxName="SN2N"
      else if(tvar~/^17/)rxName="SN3N"
      else if(tvar~/^(1[89])|(20)/)rxName="SNF"
      else if(tvar~/^107/)rxName="SNA"
      else if(tvar~/^-2/)rxName="SNAB"
      else if(tvar~/^-6/)rxName="SNF"
      else if(tvar~/^21/)rxName="SNF"
      printf("%1.12s %1.6E %1.12s\n","
"rxName,rxrateTal[++c4]/fluxTal[zone],"0.000000") >> mpo"."zone }
  }
}
}
' $input $mc $out $nct
```

2. origenIMO script

It is executed with:

```
origenIMO ${t} skeleton mpo.${t} moi ocf runIMO O2_lib
```

Code:

```
#!/bin/bash
# origenIMO
st=$1
skeleton=$2
mpo=$3
moi=$4
ocf=$5
run=$6
lib=$7
st2=`expr $st + 1`

# The first role of this module is to generate the TAPE4.INP and
# TAPE5.INP files from the skeleton file specified by the user
# and the mpo file for every depletion zone.

liste=`ls $mpo.[0-9]* | awk 'BEGIN{FS="."}{print $3}'`
for zoN in $liste
do
# Need to update the script below to detect the presence of the "$"sign (and
do the corresponding work)
awk '
```

```
FNR!=NR&&FNR==1{c1=0;fil++}
fil==2{z++;for(i=1;i<=NF;i++)xslib[i" "z]=$i;next}
FNR!=NR&&$1~/^[iI][nN][pP]$/{if($3>0)liadd=1}
FNR==NR&&FNR==3{vol=$NF}
FNR==NR&&$1~/^[0-9]*\.[0-9]*[a-
z]$/{listI[++c3]=$2;atomD[$2]=$3;iso=$2;if(length(orlist[d1+1]"
"$2)>70)d1++;orlist[d1+1]=orlist[d1+1]" "$2;c1=1;next}
FNR==NR&&c1==1{c1++}
FNR==NR&&c1==2&&$1~/^SN2N$/{sn2n[iso]=$2}
FNR==NR&&c1==2&&$1~/^SN3N$/{sn3n[iso]=$2}
FNR==NR&&c1==2&&$1~/^SNF$/{snf[iso]=$2}
FNR==NR&&c1==2&&$1~/^SNA$/{sna[iso]=$2}
FNR==NR&&c1==2&&$1~/^SNG$/{sng[iso]=$2}
FNR==NR&&c1==2&&$1~/^SNAB$/{snab[iso]=$2}
fil==1&&FNR==1{
  for(i=1;i<=3;i++)print "  -1"
  for(i=1;i<=d1;i++)print "  LPU   "orlist[i]
  print "  LPU   "orlist[d1+1]" -1"}
fil==1&&$1~/^LIB$/{
  for(i=6;i<=8;i++)
    if($i>=0)lib[++c2]=$i
    else if($i<0)lib[++c2]=-$i}
fil==1&&$1~/^STP$/{print;nextfile}
fil==1{print;next}

END{
li=1;
if(lib[li]!=0){
for(i=1;i<=c3;i++){
  go=1
   for(k=1;k<=z;k+=1){
    if(xslib[1" "k]==lib[li]&&xslib[2" "k]==listI[i]){
      go=0;
      cat[listI[i]]=li;
      if(sng[listI[i]]>0)xslib[3" "k]=sprintf("%1.3E",sng[listI[i]]);
      if(sn2n[listI[i]]>0)xslib[4" "k]=sprintf("%1.3E",sn2n[listI[i]]);
      if(sna[listI[i]]>0)xslib[5" "k]=sprintf("%1.3E",sna[listI[i]]);
      if(snf[listI[i]]>0)xslib[6" "k]=sprintf("%1.3E",snf[listI[i]]);
      print xslib[1" "k],xslib[2" "k],xslib[3" "k],xslib[4" "k],xslib[5"
"k],xslib[6" "k],xslib[7" "k],xslib[8" "k],xslib[9" "k]}
}}}
#
li=2;
if(lib[li]!=0){
for(i=1;i<=c3;i++){
  go=1
   for(k=1;k<=z;k+=1){
    if(xslib[1" "k]==lib[li]&&xslib[2" "k]==listI[i]){
      go=0;
      cat[listI[i]]=li;
      if(sng[listI[i]]>0)xslib[3" "k]=sprintf("%1.3E",sng[listI[i]]);
      if(sn2n[listI[i]]>0)xslib[4" "k]=sprintf("%1.3E",sn2n[listI[i]]);
      if(sn3n[listI[i]]>0)xslib[5" "k]=sprintf("%1.3E",sn3n[listI[i]]);
      if(snf[listI[i]]>0)xslib[6" "k]=sprintf("%1.3E",snf[listI[i]]);
      print xslib[1" "k],xslib[2" "k],xslib[3" "k],xslib[4" "k],xslib[5"
"k],xslib[6" "k],xslib[7" "k],xslib[8" "k],xslib[9" "k]}
}}}
```

```
#
li=3;
if(lib[li]!=0){
for(i=1;i<=c3;i++){
  go=1
   for(k=1;k<=z;k+=1){
    if(xslib[1" "k]==lib[li]&&xslib[2" "k]==listI[i]){
      go=0;
      cat[listI[i]]=li;
      if(sng[listI[i]]>0)xslib[3" "k]=sprintf("%1.3E",sng[listI[i]]);
      if(sn2n[listI[i]]>0)xslib[4" "k]=sprintf("%1.3E",sn2n[listI[i]]);
      if(sna[listI[i]]>0)xslib[5" "k]=sprintf("%1.3E",sna[listI[i]]);
      print xslib[1" "k],xslib[2" "k],xslib[3" "k],xslib[4" "k],xslib[5"
"k],xslib[6" "k],xslib[7" "k],xslib[8" "k],xslib[9" "k]
    k++;
    print xslib[1" "k],xslib[2" "k],xslib[3" "k],xslib[4" "k],xslib[5"
"k],xslib[6" "k],xslib[7" "k],xslib[8" "k],xslib[9" "k]}
}}}

# List the isotopes used and their number of moles
if(liadd==1){
  for(i=1;i<=c3;i++)print
cat[listI[i]],listI[i],sprintf("%1.6E",atomD[listI[i]]*vol*10/6.02214),"0 0.0"
}
print 0}
' ${mpo}.$zoN ${skeleton}.$zoN $lib > ./moi_files/${moi}.${zoN}.${st}.inp

# Copy the source composition to the TAPE4 file
cp ./moi_files/${ocf}.${zoN}.${st} ./TAPE4.INP

# Execute ORIGEN2.2
./$run ./moi_files/${moi}.${zoN}.${st} $lib
mv ./moi_files/${moi}.${zoN}.${st}.pch ./moi_files/${ocf}.${zoN}.${st2}

done
```

3. compIMO script

It is executed with:

```
compIMO ${t} mpo.${t} inp ocf
```

Code:

```
#!/bin/bash

# compIMO

st=$1
mpo=$2
inp=$3
ocf=$4
#mpo=mpo.1
st2=`expr $st + 1`

cp ${inp}.$st INP.TPS
liste=`ls $mpo.[0-9]* | awk 'BEGIN{FS="."}{print $3}'`
```

```
for zoN in $liste
do

awk '
FNR==1{fil++}
FNR==NR{for(i=2;i<NF;i+=2)mol[$i]=$(i+1)}
fil==1{next}

fil==2&&FNR==3{vol=$NF;cell=$1;mat=$2;next}
fil==2&&$1~/[0-9]*\.[0-9]*[a-z]/{cor[$1]=$2;next}
fil==2{next}

fil==3&&FNR==1{for(i in cor)molTOT+=mol[cor[i]]}
#fil==3&&$1==cell&&$2==mat&&c1!=1{$3=sprintf("%1.6E",molTOT/vol*6.023/10);c1=1
}
fil==3&&$1!~/^[0-9]/{c2=0}
fil==3&&$1~"^m"mat"$"{c2=1;
  if(cor[$2]!=0){
    printf("%-5.5s %1.10s  %1.6E\n",$1,$2,mol[cor[$2]]/vol*6.023/10);next}
  print;next}
fil==3&&c2==1&&cor[$1]!=0{
    print "      "$1" ",sprintf("%1.6E",mol[cor[$1]]/vol*6.023/10);next}
fil==3{print}
#END{printf("%3.3s %3.3s %1.6E\n",cell,mat,molTOT/vol*6.023/10) > "INP.TOT"}
END{printf("%3.3s %3.3s\n",cell,mat) > "INP.TOT"}
' ./moi_files/${ocf}.${zoN}.${st2} ${mpo}.${zoN} INP.TPS > INP.TPS2

#cat INP.TOT

awk -v tot="`cat INP.TOT`" '
BEGIN{split(tot,tra," ")}
FNR==NR&&$1~/^[a-z]/{c1=0}
FNR==NR&&$1~("^m"tra[2]"$"){c1=1;total+=$3;next}
FNR==NR&&c1==1{total+=$2;print total > "afac";next}
FNR!=NR&&$1==tra[1]&&$2==tra[2]{$3=sprintf("%1.6e",total)}
FNR!=NR{print}
' INP.TPS2 INP.TPS2 > INP.TPS
\rm INP.TPS2 INP.TOT
done
mv INP.TPS ${inp}.${st2}
```

Appendix B

Core pressure drop calculation

The core pressure drop and coolant velocity in the core are correlated and are obtained using the analytical approach described below. The pressure drop can be decomposed into several terms:

- **Contraction at grid plate**

$$\Delta P_1 = 0.5\left(1 - \frac{A_u^{GRPL}}{A_u^{CELL}}\right)\frac{\rho(\mathrm{T_{IN}})(\mathrm{V_{GRPL}})^2}{2} \qquad \text{(Eq. B.1)}$$

A_u^{GRPL} is the unit flow area at grid plate
A_u^{CELL} is the unit cell area in core region
$\rho(T_{IN})$ is the coolant density at inlet temperature
V_{GRPL} is the coolant velocity at grid plate

- **Expansion after grid plate**

$$\Delta P_2 = \left(1 - \frac{A_u^{GRPL}}{A_u^{GP-FR}}\right)^2\frac{\rho(\mathrm{T_{IN}})(\mathrm{V_{GRPL}})^2}{2} \qquad \text{(Eq. B.2)}$$

A_u^{GP-FR} is the unit flow area between grid plate and fuel rods

- **Contraction at fuel rods**

$$\Delta P_3 = 0.5\left(1 - \frac{A_u^{FLCO}}{A_u^{GP-FR}}\right)\frac{\rho(\mathrm{T_{IN}})(\mathrm{V_{CORE}})^2}{2} \qquad \text{(Eq. B.3)}$$

A_u^{FLCO} is the unit flow area in the core region
V_{CORE} is the coolant velocity in the core

- **Friction along fuel rods, including the wire wraps pressure drop** (>85% of the total pressure drop)

$$\Delta P_4 = f \frac{H_{core} + H_{plenum}}{D_{H,rod}} \frac{\rho(\mathrm{T_{AVE}})(\mathrm{V_{CORE}})^2}{2} \qquad \text{(Eq. B.4)}$$

H_{core} and H_{plenum} are the core and fission gas plenum height
$D_{H,rod}$ is the fuel rod hydraulic diameter
$\rho(T_{AVE})$ is the coolant density at average coolant temperature

The expression of the friction coefficient f is:

$$f = \frac{C_{fbt}}{Re^{0.18}} \qquad \text{(Eq. B.5)}$$

Where,

$$C_{fbt} = \left(0.8063 - 0.9022 \log_{10}\left(\frac{H}{D}\right) + 0.3526 \left(\log_{10}\left(\frac{H}{D}\right)\right)^2 \left(\frac{P}{D}\right)^{9.7} \left(\frac{H}{D}\right)^{1.78-2.0\left(\frac{P}{D}\right)}\right) \qquad \text{(Eq. B.6)}$$

This equation is valid for pitch-to-diameter ratio, P/D, from 1.025 to 1.42 and H/D from 8 to 50.

- **Friction in upper support**

$$\Delta P_5 = f \frac{H_{support}}{D_{H,USUP}} \frac{\rho(\mathrm{T_{OUT}})(\mathrm{V_{USUP}})^2}{2} \qquad \text{(Eq. B.7)}$$

$H_{support}$ is the upper support height
V_{USUP} is the coolant velocity in the upper support
$D_{H,USUP}$ is the hydraulic diameter in upper support

- **Expansion at upper support**

$$\Delta P_6 = \left(1 - \frac{A_u^{FLCO}}{A_u^{USUP}}\right)^2 \frac{\rho(\mathrm{T_{OUT}})(\mathrm{V_{CORE}})^2}{2} \qquad \text{(Eq. B.8)}$$

A_u^{USUP} is the unit flow area in the upper support
$\rho(T_{OUT})$ is the coolant density at outlet coolant temperature
V_{USUP} is the coolant velocity in the upper support

- **Expansion at top of core**

$$\Delta P_7 = \left(1 - \frac{A_u^{USUP}}{A_u^{CELL}}\right)^2 \frac{\rho(\mathrm{T_{OUT}})(\mathrm{V_{USUP}})^2}{2} \qquad \text{(Eq. BS.9)}$$

The total pressure drop is the sum of ΔP_1 to ΔP_7. The maximum coolant mass flow is determined from the estimate of the core pressure drop, using the coolant thermo-physical properties, provided in Appendix C for sodium, lead-bismuth and lead-lithium.

Appendix C

Coolant thermo physical properties

The thermo-physical properties of liquid sodium, lead-bismuth and lead-lithium are provided in this appendix. The sodium and lead-bismuth properties have been obtained from [48] and the lead-lithium properties have been obtained from [64].

For all the formulas provided in this appendix, T is the temperature in Kelvin.

C.1 Sodium thermo-physical properties

C.1.1 Density

For 371 K < T < 2503.7 K:

$$\rho = 219 + 275.32\left(1 - \frac{T}{2503.7}\right) + 511.58\left(1 - \frac{T}{2503.7}\right)^{0.5} \qquad \text{(Eq. C.1)}$$

C.1.2 Thermal expansion coefficient

The instantaneous volumetric thermal expansion is tabulated in Table A.1.

Table A.1: Thermal expansion coefficient of liquid sodium

Temperature [K]	$\alpha_p * 10^4 [K^{-1}]$
400	2.41
500	2.5
600	2.6
700	2.71
800	2.82
900	2.95
1000	3.1
1100	3.26
1200	3.45

1300	3.66
1400	3.9
1500	4.2
1600	4.55
1700	4.98
1800	5.52
1900	6.23

C.1.3 Dynamic viscosity

For 371 K < T < 2503.7 K, in Pa.s:

$$\ln(\eta) = -6.4406 - 0.3958 * \ln(T) + \frac{556.835}{T} \quad \text{(Eq. C.2)}$$

C.1.4 Thermal conductivity

For 371 K < T < 1500 K, in W/m.K:

$$k = 124.67 - 0.11381 * T + 5.5226 * 10^{-5} * T^2 - 1.1842 * 10^{-8} * T^3 \quad \text{(Eq. C.3)}$$

C.1.5 Specific heat

In kJ/kg.K:

$$c_p = 1.6582 - 8.479 * 10^{-4} * T + 4.4541 * 10^{-7} * T^2 - 2992.6 * T^{-2} \quad \text{(Eq. C.4)}$$

A.2 Lead-bismuth thermo-physical properties

C.2.1 Density

For 473 K < T < 1273 K, in kg/m^3:

$$\rho = 10740 - 1.38 * (T - 273.15) \quad \text{(Eq. C.5)}$$

C.2.2 Thermal expansion coefficient

For 473 K < T < 1273 K, in K^{-1}:

$$\beta = \frac{1}{8055.759 - T} \quad \text{(Eq. C.6)}$$

C.2.3 Dynamic viscosity

For 400 K < T < 1173 K, in kg/m.s:

$$\mu = 4.9 * 10^{-4} * \exp\left(\frac{760.1}{T}\right) \quad \text{(Eq. C.7)}$$

C.2.4 Thermal conductivity

For 421 K < T < 973 K, in W/m.K:

$$k = 12.4119 - 3.37233 * 10^{-2} * T + 7.75802 * 10^{-5} * T^2 - 3.94661 * T^3 \quad \text{(Eq. C.8)}$$

C.2.5 Specific heat

For 400 K < T < 973 K, the LBE specific heat is constant and equal to 146.51 J/kg.K.

C.3 Lead-lithium thermo-physical properties

C.3.1 Density

For 510 K < T < 880 K, in g/cm^3:

$$\rho = 10.52 * (1 - 113 * 10^{-6} * T) \quad \text{(Eq. C.9)}$$

C.3.2 Thermal expansion coefficient

For 510 K < T < 880 K, in K^{-1}:

$$\beta = 1.124 * 10^{-4} + 1.505 * 10^{-8} * T \quad \text{(Eq. C.10)}$$

C.3.3 Dynamic viscosity

For 510 K < T < 625 K, in Pa.s:

$$\mu = 1.87 * 10^{-4} * \exp\left(\frac{11640}{RT}\right) \quad \text{(Eq. C.11)}$$

C.3.4 Thermal conductivity

For 510 K < T < 625 K, in W/m/K:

$$\lambda = 1.95 + 19.6 * 10^{-3} * T \quad \text{(Eq. C.12)}$$

C.3.5 Specific heat

For 510 K < T < 800 K, in J/g.K:

$$c_p = 0.195 - 9.116 * 10^{-6} * T \quad \text{(Eq. C.13)}$$